

High resolution paleoclimatic study using corals

Thesis submitted to

Indian Institute of Technology, Gandhinagar, India



for the degree of

Doctor of Philosophy

in

Earth Sciences

by

Harsh Raj

supervised by

Dr. Ravi Bhushan

Physical Research Laboratory,

Ahmedabad, India

July, 2020



भौतिक अनुसंधान प्रयोगशाला
Physical Research Laboratory

Dedicated
to
my parents

DECLARATION

I declare that this written submission represents my ideas in my own words and where others' idea or words have been included, I have adequately cited and referenced the original sources.

I also declare that I have adhered to all principles of academic honesty and integrity and have not misrepresented or fabricated or falsified any idea/data/fact/source in my submission. I understand that any violation of the above will be cause for disciplinary action by the Institute and can also evoke penal action from the sources which have thus not been properly cited or from whom proper permission has not been taken when needed.

Date:

Name: Harsh Raj
(Roll No: 15330001)



Indian Institute of Technology Gandhinagar,
Gandhinagar, Gujarat-382355

CERTIFICATE

This is to certify that this thesis titled “High resolution paleoclimatic study using corals” submitted by Mr. Harsh Raj (Roll No. 15330001) to the Indian Institute of Technology Gandhinagar, is a record of bona fide research work carried out under my supervision and has not been submitted elsewhere for a degree. I have read this dissertation and in my opinion, it is fully adequate, in scope and quality, for the degree of Doctor of Philosophy.

Date:

Dr. Ravi Bhushan
Geoscience Division,
Physical Research Laboratory,
Ahmedabad, India.
(Thesis Supervisor)

Thesis Approval

The thesis entitled

High resolution paleoclimatic study using corals

by

Harsh Raj

(Roll No: 15330001)

is approved for the degree of

Doctor of Philosophy

Examiner

Examiner

Supervisor

Chairman

Date: _____

Place: _____

Acknowledgment

It is my immense pleasure to express my gratitude towards everyone who has contributed directly or indirectly to the amazing journey of my PhD research. Interactions and support from many individuals helped me in carrying out this research work. Without their help and encouragement it would not have been possible to complete this thesis work.

Primarily, I wish to convey my deepest gratitude to my supervisor, Dr. Ravi Bhushan, for his continuous support during my PhD. Working with him was a great learning experience. He taught me to carry out research with a positive attitude even in adverse scenarios. I am thankful to him for giving me the freedom to explore new ideas and experiments. His guidance and supervision has helped me to develop as a researcher. Discussions with him along with his encouraging words were really helpful in carrying out and completing this research work.

I would also like to express my sincere gratitude to my DSC members, Dr. M G Yadava and Dr. Neeraj Rastogi for their helpful discussions and critical comments. I would like to thank Dr. Sanjeev Kumar for his help with stable isotopic analysis and discussions. I would also like to thank Dr. A K Sudheer for his support and suggestions during trace element analysis. I am thankful to Dr. R D Deshpande, Prof. S K Singh, Prof. J S Ray, Dr. Arvind Singh, Dr. A D Shukla, Dr. Vineet Goswami, Dr. Amzad Laskar and Mr. R A Jani for their valuable inputs and comments during area seminar. Their suggestions were always constructive. I sincerely thank Dr. M G Yadava, Dr. Neeraj Rastogi and Dr. Vineet Goswami for their contribution towards improving this thesis. I am thankful to our director, dean and academic committee for their support during my PhD tenure. I am grateful to the academic committee for critically reviewing my research work and providing fruitful inputs. I am also grateful to all the professors for their informative lectures during the course work. I am thankful to Mr. Hugo van Staveren for sharing his knowledge about handling AMS. I am also thankful to Prof. AJT Jull for enhancing my knowledge of radiocarbon and AMS. I convey my gratitude to Dr. Rajneesh Bhutani and (Late) Dr. PK Sarkar for their valuable teachings that motivated me to pursue research.

I am extremely thankful to Ministry of Earth Sciences (MoES) for funding the GEOTRACES project under which this work was carried out. I am grateful to the Ministry of Environment and Forest (MoEF) and local authorities for granting permission for collection of corals. I thank Dr. P M Mohan, Pondicherry University for his support during the field. Coral sampling would not have been possible without the help of R Kaila, Sikander, Upasana, Chandana, Chinmay,

Nitesh, Muruganantham, Romi, and Ankur. I am really grateful to R Kaila for his technical support during coral cutting. I thank Manan for his support in the AMS lab. I am grateful to Sangeeta for her help during stable isotope measurements. I would also like to acknowledge the support and help of staff members of PRL library, computer center, administration, account section, workshop, CMG, purchase and stores during this period.

Life during this thesis work would have been mundane without my PRL colleagues. To begin with, I would like to express my sincere appreciation to my cubicle mates Romi and Partha for being a great company and I will cherish the time shared with them. I am thankful to Romi for her enormous help during final formatting of this thesis. I wish to express my heartfelt thanks to my buddies Oza and Ashish for always being there for me. Their ‘jokes’ and ‘shayari’ were always ready to lighten up the mood. I thank all the Chemistry department members, Upasana, Chandana, Chinmay, Muruganantham, Anil, Satish, Venky, Subha, Atinder, Damu, Nitesh, Ankur, Shivam, Mahesh, Priyanka, Abhishek, Nisha, Sanjit, Sanjukta, Rahul, Jaldhi, Ramsha, Payal, Ishita, Deep, Akshay, and Riya for their kind support, cooperation and encouragement during my PhD tenure. Their friendliness and cooperative attitude made me feel at home. I am thankful to Pravinbhai and Rashmikhbai for their kind support during the laboratory work. I am grateful to my batch mates, Naman, Arthy, Balbeer, Subir, Archita, Mishraji, Nidhi, Shefali, Kaustubh, Rahul, Akanksha, Shivangi, Richa, Ranadeep, and Varun for a memorable and happy stay at PRL. I thoroughly enjoyed their company. I would also like to express my gratitude to Kiran, Bivin, Ikshu, Niharika, Anirban, Shrema, Shraddha, and Jinia for their support and motivation.

I am thankful to Harshita Raj, Ashwin Kumar and Binu Kumar for making the life outside the lab enjoyable. I want to thank my family for their immense love and care. I am thankful to my late grandfather Shri Sant Prasad who instilled in me a sense of respect towards academia. Most importantly, I am grateful to my parents, Subhadra Kumari and Kumar Rajesh. They have always believed in me and encouraged me to follow my dream. They have been the source of strength and this work would not have been possible without their unending support.

Although I tried, it is almost impossible to mention everyone who has contributed to this journey of research in some or other way. I am thankful to everyone of them who helped complete this thesis work.

-Harsh Raj

Abstract

Corals are important natural archives of environmental records that can provide continuous, long term, high resolution proxy data. Coral records provide insight to the processes governing variability in the sea surface conditions, which can be helpful in understanding the climatic and oceanic changes. This work primarily focuses on the corals from the northern Indian Ocean to understand changes in sea surface conditions recorded in them by studying different geochemical and isotopic proxies. Samples of *Porites* corals were collected from the Lakshadweep and the Andaman islands. These samples were investigated for their stable oxygen and carbon isotopes, Sr/Ca ratios and radiocarbon composition.

The Lakshadweep and the Andaman corals show mean annual growth rate 14.7 ± 4.8 mm/yr and 9.4 ± 2.4 mm/yr respectively. Both corals show a decline in their annual growth rate towards present, which could be related to thermal stress on these coral due to the warming Indian Ocean.

The bimonthly stable oxygen and carbon isotope record from the Lakshadweep show seasonal variability. There exists inter-colony variability in the oxygen isotope values of Lakshadweep corals. This suggests that oxygen isotopic composition of fossil corals from the region should be carefully analysed to decipher past sea surface conditions. The Lakshadweep corals oxygen isotope were used to determine the seawater oxygen isotope of the region. It is observed that period of depleted seawater oxygen isotope corresponds to enhanced Indian rainfall period. It indicates that Lakshadweep coral records can potentially provide information about enhanced Indian monsoon rainfall period. The reconstructed seawater oxygen isotopic values along with available coral oxygen isotope records from literature were used to determine a $\delta^{18}\text{O}$ -SST relation, and the derived relation can be used to reconstruct past changes sea surface temperature variability. The Lakshadweep corals oxygen isotope values of monsoon period record sea surface temperature variations more robustly when compared to summer period. The carbon isotope values of Lakshadweep coral shows depletion during monsoon period. It is observed that $\delta^{13}\text{C}$ variability in Kadmat coral is not only modulated by photosynthesis, but some other processes that contribute to the observed $\delta^{13}\text{C}$ variability.

Paired Sr/Ca and $\delta^{18}\text{O}$ (oxygen isotope) measurement on the Andaman coral was carried out. It was found that coral Sr/Ca values show good correlation with sea surface temperature, but $\delta^{18}\text{O}$ showed weak correlation with sea surface temperature. This indicates significant

contribution of seawater $\delta^{18}\text{O}$ variability to coral $\delta^{18}\text{O}$ variations. Using paired Sr/Ca and $\delta^{18}\text{O}$ measurements, seawater $\delta^{18}\text{O}$ changes were calculated. Both sea surface temperature and rainfall influence the seawater $\delta^{18}\text{O}$ of the region. A linear correlation between monsoon rainfall and coral derived seawater $\delta^{18}\text{O}$ value of corresponding period is observed. Such a correlation can be used to understand past monsoon rainfall. Long term running average value of Andaman coral $\delta^{18}\text{O}$ values show depletion (enrichment) when NINO 3.4 region in east central tropical Pacific Ocean shows warmer (cooler) conditions, suggesting SST conditions in NINO 3.4 region influences the sea surface conditions in the Andaman region. The carbon isotope of Andaman coral shows a good correlation with outgoing longwave radiation values over the region, implying that it is mainly modulated by photosynthesis process in coral.

First radiocarbon records of corals from these islands are reported, which provides important insight on the oceanic conditions prevailing in these regions. These radiocarbon records suggests that the Lakshadweep region is influenced by upwelled waters, whereas surface waters in the northern Andaman region are less influence by upwelling as it is relatively stratified due to fresh water input from rivers. The coral radiocarbon records were used to determine air-sea CO_2 exchange rate over these regions. The air-sea CO_2 exchange rate over the Lakshadweep region is calculated to be $13.4 \pm 2.1 \text{ mol m}^{-2} \text{ yr}^{-1}$, whereas for the northern Andaman region it is $8.8 \pm 1.3 \text{ mol m}^{-2} \text{ yr}^{-1}$. It is observed that air-sea CO_2 exchange rates over the northern Indian Ocean show positive correlation with wind speed. The calculated net regional CO_2 flux from the Lakshadweep region is about 2.5 Tg C yr^{-1} and for northern Andaman region it is $-0.3 \text{ Tg C yr}^{-1}$. This shows that the Lakshadweep region acted as a source of atmospheric CO_2 but the Andaman region behaved like sink for atmospheric CO_2 . The pre-bomb radiocarbon record from the Andaman coral (1948-1951) yields reservoir age correction (ΔR) value of $-138 \pm 61 \text{ yr}$, which is the lowest reported for the northern Indian Ocean. The ΔR values reported from the Andaman basin shows significant variation, wherein southern Andaman ΔR value is higher than that of the northern Andaman and the Bay of Bengal. As the northern Andaman basin receives more freshwater flux as compared to the southern Andaman, such differences in reservoir age could be observed. The obtained ΔR value will be useful for radiocarbon dating of marine samples from the northern Indian Ocean.

Contents

List of Figures.....	vii
List of Tables	x
List of Abbreviations	xi
Chapter -1 Introduction	1
1.1. Introduction.....	2
1.2. Corals: Marine Archives of Past Climate	2
1.3. Northern Indian Ocean.....	4
1.4. Geochemical and Isotopic Proxies in Corals	7
1.4.1. Stable Oxygen Isotope Proxy in Corals	8
1.4.2. Stable Carbon Isotope Proxy in Corals	10
1.4.3. Strontium to Calcium Ratio in Corals.....	11
1.4.4. Radiocarbon in Corals.....	13
1.5. Scope of the Study	16
1.6. Objectives of the Study	17
Chapter-2 Methodology.....	18
2.1. Methodology	19
2.2. Regional Setting.....	19
2.2.1. Lakshadweep Islands	19
2.2.2. Andaman Islands.....	20
2.3. Coral Sampling	21
2.4. Stable Isotope Measurements	26
2.5. Sr/Ca Ratio Measurements	27
2.6. Radiocarbon Measurements.....	30
Chapter-3 Environmental Signatures in Stable Isotopic Composition of Kadmat Coral	39
3.1. Introduction.....	40
3.2. The Growth Rate of Kadmat Coral.....	42
3.3. Inter-Colony Variability in $\delta^{18}\text{O}$	44
3.4. Kadmat Coral $\delta^{18}\text{O}$ Record.....	47
3.5. Lakshadweep Coral $\delta^{18}\text{O}$ -SST Relation	51
3.6. $\delta^{13}\text{C}$ Record of the Kadmat Coral	55
3.7. Inferences	58

Chapter-4 Significance of Sr/Ca Ratio and Stable Isotope Composition of Landfall Coral for Paleoclimate Reconstruction	59
4.1. Introduction.....	60
4.2. The Growth Rate of Landfall Coral	61
4.3. 2012-2017: Monthly Records	63
4.3.1. Paired Sr/Ca and $\delta^{18}\text{O}$ Record	64
4.3.2. Seawater $\delta^{18}\text{O}$ Variability in Andaman	72
4.3.3. $\delta^{13}\text{C}$ Variability in Landfall Coral	75
4.4. 1949-2011: Bimonthly Records	76
4.5. Annual Oxygen Isotope Variations in Landfall and Kadmat Coral.....	79
4.6. Inferences	81
Chapter-5 Marine Reservoir Correction and Air-sea CO₂ Exchange Rates Based on Radiocarbon Records from Kadmat and Landfall Corals	82
5.1. Introduction.....	83
5.2. $\Delta^{14}\text{C}$ Values of Kadmat and Landfall Coral	84
5.3. Coral records from the Indian Ocean.....	88
5.4. Marine Reservoir Age Correction for the Andaman Basin	89
5.5. Landfall Corals Radiocarbon Record between 1948-1951	90
5.6. Air-Sea CO ₂ Exchange Rates over the Indian Ocean based on Corals.....	95
5.7. Air-Sea CO ₂ Exchange Rate and Wind Speed.....	97
5.8. Air-Sea CO ₂ Exchange Rate and surface water chemistry	100
5.9. Estimation of Net CO ₂ Flux.....	102
5.10. Inferences	104
Chapter-6 Summary and Conclusion	105
6.1. Summary and Conclusion	106
6.2. Future Scope of the Study.....	109
Appendix A	111
Appendix B	112
Appendix C	113
Appendix D	114
Geochemical and isotopic data	116
References.....	133
List of Publications	149

List of Figures

Figure 1.1: Coral core section along with X-radiograph of the coral showing density banding (right panel)	4
Figure 1.2: Surface circulation in the northern Indian Ocean during winter and summer season (after Shankar et al. 2002). WICC, West India Coastal Current; EICC, East India Coastal Current; WMC, Winter Monsoon Current; SMC, Summer Monsoon Current.....	6
Figure 1.3: Depth profile of radiocarbon concentration in ocean water of the Arabian Sea and the Bay of Bengal from GEOSECS expedition (Stuiver and Ostlund 1983)	14
Figure 2.1: (a) Sampling location in the northern Indian Ocean with black rectangles marking region of the Lakshadweep and the Andaman Islands; (b) Location of Kadmat Island in the Lakshadweep archipelago; (c) Location of Landfall Island in the northern Andaman Island	23
Figure 2.2: Image of a massive coral colony in the shallow waters of the Lakshadweep Islands	24
Figure 2.3: Image of underwater drilling of a Porites coral to obtain a coral core	24
Figure 2.4: X-radiograph of Porites coral core raised from (a) the Kadmat Island in the Arabian Sea and (b) the Landfall Island in the Andaman Sea.....	25
Figure 2.5: Sr/Ca ratio values of coral standard (PRL-C) measured during coral sample analysis in ICP-OES	30
Figure 2.6: (a) Image of the AURiS facility at Physical Research Laboratory;(b) Schematic of the 1 MV Accelerator Mass Spectrometer showing its components. Carousel accommodates sample targets and Ion source generates negative ion beam from sample targets, LE Magnet injects negative ion beam to the accelerator where ions are accelerated and stripping occurs. After stripping, positive ion beam is further accelerated and then analysed by HE Magnet where abundant isotopes are measured in Faraday cups. The rare isotope moves along the beam path where it is analysed by ESA and RI Magnet to suppress interferences and is finally detected in the GIC detector	32
Figure 2.7: Isotopic ratios of New Oxalic acid standard (Ox-II) measured during the performance test of the AURiS.....	34
Figure 2.8: Comparison of measured radiocarbon parameters obtained by AURiS with their consensus values.	35
Figure 2.9: Pressure record of reactors (R1-R7) showing five steps of the graphitization process.....	37
Figure 2.10: Radiocarbon values of (a) VIRI-R and (b) PRL-C (in-lab coral standard) measured during coral sample analysis in AURiS.....	38
Figure 3.1: Mean monthly variability in Sea Surface Temperature (ERSSTv5) of Lakshadweep and All India rainfall (www.tropmet.res.in) value for period 1966-2014....	40
Figure 3.2: Stable oxygen and carbon isotopic composition of Kadmat coral.....	42
Figure 3.3: Annual growth rate of Kadmat coral from 1977-2014	43
Figure 3.4: Average annual growth rate and water depth of Porites corals analysed from the Lakshadweep region.....	44

Figure 3.5: Disequilibrium offset between oxygen isotope of Clam (Chakraborty and Ramesh 1993) and Porites corals from Lakshadweep for the period 1984-1988; (Kv = Kavaratti, Bg = Bangaram, Kd = Kadmat)	46
Figure 3.6: (a) Linear correlation between bimonthly $\delta^{18}O$ values of Kadmat coral and SST (ERSSTv5) values of the Lakshadweep region; (b) mean bimonthly SST (ERSSTv5) and $\delta^{18}O$ values of Kadmat coral for the period of 1977-2014	47
Figure 3.7: Correlation between seasonal minima $\delta^{18}O$ and difference between seasonal maxima and minima $\delta^{18}O$	48
Figure 3.8: $\delta^{18}O_{sw}$ values derived from Kadmat corals oxygen isotopic record.....	49
Figure 3.9: Correlation between Kadmat coral derived $\delta^{18}O_{sw}$ and sea surface salinity of the region	49
Figure 3.10: Four-year running mean values of $\delta^{18}O_{sw}$ from the Lakshadweep region and All India Rainfall value (www.tropmet.res.in), showing co-occurrence of periods of enhanced rainfall and depleted $\delta^{18}O_{sw}$ values.....	50
Figure 3.11: (a) $\Delta\delta^{18}O$ values of Lakshadweep corals (Kavaratti and Bangaram) between 1984-1991 and (b) mean of the two corals $\Delta\delta^{18}O$ values	52
Figure 3.12: Linear correlation between ΔSST and $\Delta\delta^{18}O$ of Porites from Lakshadweep archipelago. Seasonal extreme values (●) are used for SST calibration and interpolated data (○) are plotted in between the extreme values	53
Figure 3.13: Observed and calculated ΔSST variability along with the residual values for calculated ΔSST values	54
Figure 3.14: Observed ΔSST and calculated ΔSST values using Kadmat coral.....	55
Figure 3.15: Depletion of $\delta^{13}C$ values of Kadmat coral during monsoon period.....	57
Figure 4.1: Growth rate of Landfall coral between 1949-2017.....	63
Figure 4.2: Geochemical records of the Landfall coral showing seasonality in Sr/Ca, $\delta^{18}O$ and $\delta^{13}C$ values between 2012-2017.....	64
Figure 4.3: Linear correlation between the Landfall coral Sr/Ca values and sea surface temperature of the region.....	65
Figure 4.4: Linear correlation between slope and intercept of Sr/Ca-SST relation of Porites corals from Indian Ocean	67
Figure 4.5: Difference between observed monthly SST and reconstructed monthly SST using coral Sr/Ca values.....	68
Figure 4.6: (a) Mean monthly values of sea surface temperature (SST) and Sr/Ca ratio of Landfall coral, (b) mean monthly values of outgoing longwave radiation (OLR) and $\delta^{13}C$ of Landfall coral, (c) mean monthly values of All India Rainfall and reconstructed $\Delta\delta^{18}O_{sw}$	71
Figure 4.7: Correlation of reconstructed $\Delta\delta^{18}O_{sw}$ with (a) rainfall and (b) coral Sr/Ca ratio for time period between June and October	73
Figure 4.8: Correlation of reconstructed $\Delta\delta^{18}O_{sw}$ with (a) rainfall and (b) coral Sr/Ca ratio for time period between November and May	74
Figure 4.9: Monthly $\delta^{13}C$ values of the Landfall coral and outgoing longwave radiation (OLR) values over the region.....	76
Figure 4.10: Bimonthly $\delta^{18}O$ and $\delta^{13}C$ record of the Landfall coral between 1949-2011.....	77
Figure 4.11: Linear correlation between SST variability and temperature component of Landfall $\delta^{18}O$ values between 1949-2011	78

Figure 4.12: Ten year running mean values of coral $\delta^{18}\text{O}$ and ONI (Ocean Nino Index) values.....	79
Figure 4.13: A long term depleting trend in annual $\delta^{18}\text{O}$ values of Landfall and Kadmat coral	80
Figure 5.1: Atmospheric radiocarbon values from the northern hemisphere (Hua et al. 2013), showing bomb radiocarbon peak.....	83
Figure 5.2: $\Delta^{14}\text{C}$ values of (a) Landfall and (b) Kadmat coral along with surface water $\Delta^{14}\text{C}$ values measured during GEOSECS, WOCE and PRL expeditions	85
Figure 5.3: $\Delta^{14}\text{C}$ values of Kadmat coral, Landfall coral, Gulf of Kutch coral (Chakraborty et al. 1994), Thane tree ring (Chakraborty 1993) and northern hemisphere atmosphere (Hua et al. 2013)	87
Figure 5.4: Coral radiocarbon records from the Indian Ocean (inset: map of coral sites in the Indian Ocean).....	88
Figure 5.5: Map of north-eastern Indian Ocean with reservoir age correction values from Landfall Island (this study), Chilika lake, Stewart sound (Dutta et al. 2001) and Nicobar Island (Southon et al. 2002) (Inset: Study location marked by rectangle in northern Indian Ocean)	95
Figure 5.6: Air-sea CO_2 exchange rates in the northern Indian Ocean along with colour contours of average wind speed (m s^{-1}) (COADS, Slutz et al. 1985). \blacktriangle represents coral based air-sea CO_2 exchange rates ($\text{mol m}^{-2} \text{yr}^{-1}$) from this study and Chakraborty et al. (1994). \blacklozenge represents CO_2 air-sea exchange rates ($\text{mol m}^{-2} \text{yr}^{-1}$) estimated by Dutta and Bhushan (2012).....	97
Figure 5.7: Relationship between air-sea CO_2 exchange rate and wind speed. Air-sea CO_2 exchange rates were calculated from gas transfer velocity (or piston velocity) using equation (1) in Druffel et al. (1989). Lines represent empirically derived relationship between wind speed and air-sea CO_2 exchange rates. Datapoints are bomb radiocarbon based estimates of air-sea CO_2 exchanges rates in northern Indian ocean region along with tropical Indian ocean and world ocean values	99
Figure 5.8: Colour contours of (a) Alkalinity ($\mu\text{Eq kg}^{-1}$), (b) Total carbon or DIC ($\mu\text{mol kg}^{-1}$), (c) $p\text{CO}_{2\text{sw}}$ of seawater (μatm) over the northern Indian Ocean (Takahashi et al 2014) along with the air-sea CO_2 exchange rates. \blacktriangle represents coral based CO_2 air-sea exchange rates ($\text{mol m}^{-2} \text{yr}^{-1}$) from this study and Chakraborty et al (1994). \blacklozenge represents CO_2 air-sea exchange rates ($\text{mol m}^{-2} \text{yr}^{-1}$) estimated by Dutta and Bhushan (2012)	101
Figure 6.1: Plot showing calculation of ΔR values in two steps using measured radiocarbon age and known age of the pre-bomb surface marine samples (http://calib.org/deltar). Step 1 (represented by line 1) is determining ^{14}C age corresponding to the known age of the pre-bomb marine sample using marine calibration curve. Step 2 (represented by line 2) is subtracting the marine calibration curve based ^{14}C age from the measured ^{14}C age of the pre-bomb marine sample.....	113

List of Tables

<i>Table 1.1: Commonly studied geochemical and isotopic proxies in corals</i>	<i>7</i>
<i>Table 2.1: Stable oxygen and carbon isotopic analysis of MMB and NBS-18 standards.....</i>	<i>27</i>
<i>Table 2.2: Operating conditions of ICP-OES for Sr/Ca ratio measurements in coral samples</i>	<i>29</i>
<i>Table 2.3: Radiocarbon reference standard measured values.....</i>	<i>36</i>
<i>Table 3.1: Pearson correlation coefficient between Lakshadweep corals $\Delta\delta^{18}O$ values and sea surface temperature values; (Kv = Kavaratti, Bg = Bangaram).....</i>	<i>52</i>
<i>Table 4.1: Sr/Ca-SST calibration obtained for Porites corals from Indian Ocean region.....</i>	<i>66</i>
<i>Table 5.1: Results of ^{14}C analysis in Landfall coral skeleton between 1948-1951</i>	<i>92</i>
<i>Table 5.2: Reservoir age correction (ΔR) values of pre-bomb marine samples from the Andaman Basin.....</i>	<i>93</i>
<i>Table 5.3: Air to sea CO_2 net flux estimates based on coral radiocarbon record from the northern Indian Ocean region.....</i>	<i>103</i>
<i>Table 6.1: Stable Isotopic composition of Kadmat coral</i>	<i>116</i>
<i>Table 6.2: Sr/Ca ratios and stable isotopic composition of top 65 mm of Landfall coral</i>	<i>120</i>
<i>Table 6.3: Stable isotopic composition of Landfall coral below the top 65 mm</i>	<i>122</i>
<i>Table 6.4: Radiocarbon values of Kadmat coral samples.....</i>	<i>130</i>
<i>Table 6.5: Radiocarbon values of Landfall coral samples.....</i>	<i>130</i>

List of Abbreviations

AGE	:Automated Graphitization Equipment
AMS	:Accelerator Mass Spectrometer
AURiS	:Accelerator Unit for Radioisotope Studies
CHS	:Carbonate Handling System
COADS	:Comprehensive Ocean Atmosphere Data Set
DIC	:Dissolved Inorganic Carbon
EA	:Elemental Analyser
EICC	:East India Coastal Current
ENSO	:El Niño-Southern Oscillation
ERSSTv5	:Extended Reconstructed Sea Surface Temperature, Version 5
GEOSECS	:Geochemical Ocean Sections program
HIRS	:High-resolution Infrared Radiation Sounder
ICP-AES	:Inductively Coupled Atomic Emission Spectrometer
ICP-MS	:Inductively Coupled Plasma Mass Spectrometer
ICP-OES	:Inductively Coupled Plasma Optical Emission Spectrometer
IOD	:Indian Ocean Dipole
IRMS	:Isotopic Ratio Mass Spectrometer
ITCZ	:Inter Tropical Convergence Zone
MMB	:Makrana Marble
NAO	:North Atlantic Oscillation
OLR	:Outgoing Longwave Radiation
ONI	:Ocean Nino Index
RMSR	:Root Mean Square Residual
RSD	:Relative Standard Deviation
SMC	:Summer Monsoon Current
SSS	:Sea Surface Salinity
SST	:Sea Surface Temperature
TIMS	:Thermal Ionization Mass Spectrometer
WICC	:West India Coastal Current
WMC	:Winter Monsoon Current
WOCE	:World Ocean Circulation Experiment program

Chapter -1

Introduction

1.1. Introduction

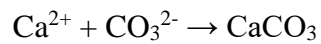
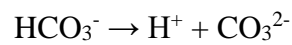
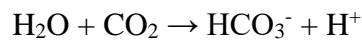
The Earth, our home planet, has a long history of changing climate affecting the life and ecosystem sustaining on it. During the era of human civilisation, climate has been a driving factor affecting social and economic state. It has long been of immense interest to predict the dynamic course of climate to avoid unforeseen dire situations. Investigations of climate history helps in understanding past conditions and can be important in estimating future course of climate change. However, the instrumental records of climate are limited to several decades back in time and also are spatially limited. In view of this, natural archives of climate proxy records can expand the instrumental record in both space and time. The climate parameters obtained from these climate proxy records can be used to assess climate models used for future predictions. Comparison of proxy based paleoclimate observations with model based simulations can provide much needed insight about past climatic variability and processes governing it.

Corals are one such natural archive that provide crucial high-resolution information about climate indices like sea surface temperature, sea surface salinity, ocean water circulation, upwelling, rainfall and air-sea gas exchange. As a source of a wide array of proxy records, multi-proxy investigations of corals can provide better understanding of past climate conditions. The seasonal to annual proxy records from corals provide glimpse of oceanic and atmospheric behaviour at timescales that are relevant to society. Several investigations on corals in the past have revealed crucial information about the past climate and its variability (Cole et al. 2000, Tudhope et al. 2001, Druffel et al. 2007, Abram et al. 2008, Wu et al. 2018), attesting the potential of coral based paleoclimate studies. This research work focuses on studying the geochemical proxy records of corals from the northern Indian Ocean to obtain high resolution record of surface ocean conditions. These records are studied to understand the information that they can provide about the sea surface conditions in the northern Indian Ocean and to identify signatures of Indian monsoon in these records.

1.2. Corals: Marine Archives of Past Climate

Corals living in shallow marine environments are one such natural archive that record the sea surface conditions. These marine organisms are very sensitive to the changes in the environment where they are living. Corals mainly thrive in shallow waters with warm temperatures, normal ocean salinity and lower sediment load. Their sensitivity to temperature limits them majorly to dwell in shallow waters within temperate and tropical latitudes. Corals

are marine invertebrate animals belonging to Scleractinia group in subclass of Zoantharia (Druffel 1997). Structurally, corals consist of a cylindrical shaped individual entity called polyp overlying a basal disc and underlying an oral disc with mouth opening at the centre. The oral disc has tentacles attached to it that are equipped with nematocysts used for collection of food and defence. Corals have ability to fix DIC (Dissolved Inorganic Carbon) and calcium ions from seawater to form their calcium carbonate skeleton, leading to a rapid precipitation of calcium carbonate in the form of metastable aragonite in a portion of polyp tissue called calcioblast . Following reactions take place during skeletal calcium carbonate precipitation:



Skeletogenesis in corals involves an exchange of ions between seawater and calcifying fluid in calcioblast. H^+ ions from the calcifying fluid are exchanged with Ca^{2+} ions, raising pH and Ca^{2+} saturation in calcifying fluid relative to seawater. Seawater DIC and metabolic sourced DIC is transferred to the calcioblast by diffusion of CO_2 and/or HCO_3^- pumping (McCulloch et al. 2017). These processes relatively raise pH and CaCO_3 saturation of calcifying fluid than seawater, leading to precipitation of calcium carbonate. The corals are mainly classified into two groups: hermatypic and ahermatypic corals. The ahermatypic type corals do not form reefs, whereas the hermatypic corals form reefs. The hermatypic corals generally host endosymbiotic algae called zooxanthellae. The zooxanthellae reside within the endoderm of the polyp tissue and impart vibrant colours to the corals. Photosynthetic activities of these zooxanthellae enhance above skeletogenesis reactions by providing energy and carbon. Scleractinia corals grow in various forms like branching, tabulated, massive, foliaceous or encrusting shape. These massive hermatypic corals are generally studied for paleoclimate reconstruction. Their massive structure is resistant to wave action allowing them to grow uninterrupted for a few hundred years providing long continuous high-resolution climate proxy records. The skeleton of these corals can provide crucial information about physical and chemical conditions prevalent in surrounding waters during their growth. The discovery of annual banding in corals' carbonate skeleton by Knutson et al. (1972) opened the scope for exploring vast information of past climatic history stored in corals. These annual density bands in corals are analogous to tree rings in dendrochronology. Hudson et al. (1976) suggested that coral density bands can be used to cross date different corals just like tree rings to extend record back in time. The density bands

are observed when X-radiograph of thin (5-10 mm) coral skeleton slice is obtained along its vertical growth axis. Figure 1.1 shows a coral core cut section along with its X-radiograph exhibiting light and dark density bands

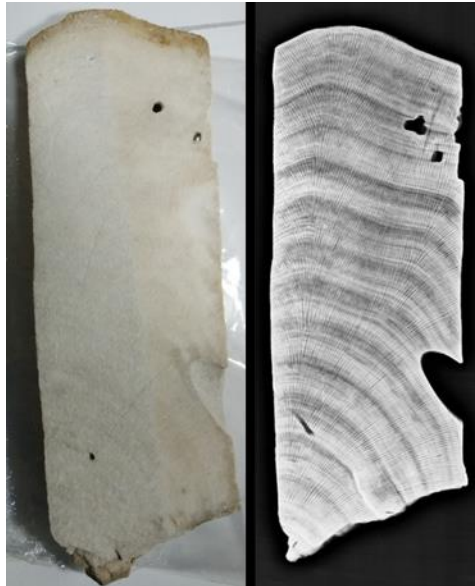


Figure 1.1: Coral core section along with X-radiograph of the coral showing density banding (right panel)

Barnes and Lough (1993) explained the mechanism and significance of density band formation in corals. These annual density bandings are characteristic of massive corals and advantageous for paleoclimate study. The annual bands in corals aid in controlling the sampling resolution and establishing chronology of coral proxy data. Apart from characteristics like high resolution records and chronological control on proxy data, corals also provide a multitude of proxy records providing diverse range of environmental information. The geochemical and isotopic investigations of corals have provided valuable records of past variabilities in climatic and oceanic parameters such as, sea surface temperature, salinity, pH, upwelling, ocean circulation, rainfall, air-sea CO₂ exchange (Cember 1989, Cole and Fairbanks 1990, Druffel and Griffin 1993, Gagan et al. 1998, Grumet et al. 2004, Wei et al. 2009).

1.3. Northern Indian Ocean

Unlike the Pacific and the Atlantic oceans, the Indian Ocean is a unique basin which is landlocked at its northern front. The presence of Asian landmass at northern end of the Indian ocean rapidly heats up relative to the Indian ocean during the boreal summer. This differential heating of land and ocean leads to a pressure gradient which drives the seasonal reversal of winds called monsoon. Monsoon winds carry moisture from the ocean and bring precipitation

to the Indian sub-continent. Indian monsoon system plays an important role in driving the socio-economic conditions of large population residing on the Indian subcontinent. The monsoon generates seasonal variations in ocean currents and regulates various physical processes of the region. The eastern side of the northern Indian Ocean is known as the Bay of Bengal, which receives large fluxes of freshwater through rivers due to monsoon rainfall. On the other hand, the western side of the northern Indian Ocean, known as the Arabian Sea, experiences strong upwelling due to monsoonal winds. Due to significant differences in fresh water supply, a strong salinity contrast has been observed between both oceanic basins. During the winter season water from the eastern Bay of Bengal flows westward to the Arabian Sea via winter monsoon surface current. A branch of this winter monsoon current flows into the eastern Arabian Sea as west Indian coastal current. The winter monsoon current brings low salinity water of Bay of Bengal origin to the Arabian Sea. This low salinity water spreads along the western coast by the west India coastal current (Figure 1.2). During the summer season, water moves from the western Arabian Sea to the eastern Bay of Bengal via summer monsoon current (Shankar et al. 2002). The Lakshadweep and the Andaman Islands located respectively in the Arabian Sea and the Bay of Bengal are among the major coral reef locations in the northern Indian Ocean. Corals growing in these regions can record changes pertaining to several natural processes in their geochemical and isotopic composition and provide crucial information about past changes in monsoon and sea surface conditions.

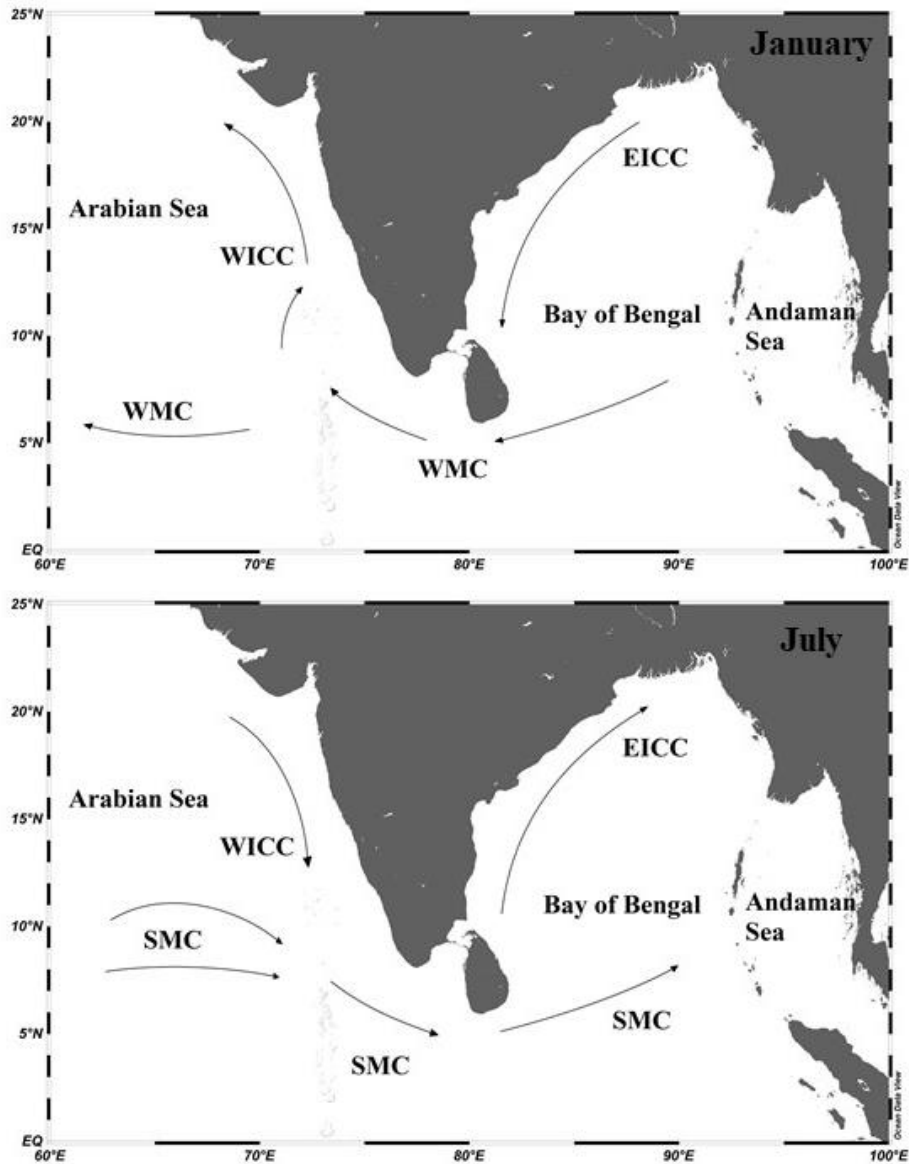


Figure 1.2: Surface circulation in the northern Indian Ocean during winter and summer season (after Shankar et al. 2002). WICC, West India Coastal Current; EICC, East India Coastal Current; WMC, Winter Monsoon Current; SMC, Summer Monsoon Current

1.4. Geochemical and Isotopic Proxies in Corals

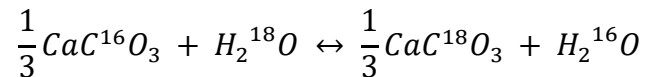
Several investigations on geochemical and isotopic compositions of corals have established different climate proxies. Table 1.1 lists a few commonly studied geochemical proxies in corals for paleoclimatic investigations.

Table 1.1: Commonly studied geochemical and isotopic proxies in corals

Proxy type	Tracer	Environmental parameter	References
Stable isotopes	^{18}O	Sea surface temperature, rainfall, salinity	Fairbanks and Dodge 1979, McConnaughey 1989a,b, Cole and Fairbanks 1990, Cole et al. 2000, Le Bec et al. 2000, Morimoto et al. 2002, Felis et al. 2003
	^{13}C	Insolation, zooplankton level	Fairbanks and Dodge 1979, Felis et al. 1998, Grottoli and Wellington 1999, Rosenfeld et al. 2003, Gagan et al. 2015, Watnabe et al. 2017
Trace elements	Sr/Ca	Sea surface temperature	Beck et al. 1992, Gagan et al. 1998, Marshall and McCulloch 2001, Pfeiffer et al. 2009, Delong et al. 2011,
	Mg/Ca	Sea surface temperature	Mitsuguchi et al. 1996, Wei et al. 2000, Watnabe et al. 2001
	Ba/Ca	Upwelling, riverine outflow	Shen et al. 1992, McCulloch et al. 2003
Radiogenic isotopes	^{14}C	Upwelling, seawater circulation, air-sea CO_2 exchange	Cember 1989, Druffel and Griffin 1993, Grumet et al. 2004, Hua et al. 2005, Guilderson et al. 2009

1.4.1. Stable Oxygen Isotope Proxy in Corals

As ^{18}O abundance in oceanic carbonate deposits varies as a function of temperature, Urey (1947) proposed that it can be useful in determining seawater paleotemperature. The isotopic exchange reaction between carbonate and water is shown as:



If the exchange happens at equilibrium, the equilibrium constant (K) can be expressed as:

$$K = \frac{([\text{CaC}^{18}\text{O}_3]/[\text{CaC}^{16}\text{O}_3])^{1/3}}{([\text{H}_2^{18}\text{O}]/[\text{H}_2^{16}\text{O}])}$$

Further, this equilibrium constant can also be written as:

$$K = \left(\frac{R_c}{R_w}\right) = \alpha_w^c$$

Where, R is ratio of heavy to light isotope in a phase (c = carbonate; w = water) and α is isotope fraction factor. The fractionation factor denotes the isotopic fraction that occurs during a physio-chemical reaction, and varies inversely with temperature (Kim O'Neil 1997). Epstein et al. (1953) reported an inverse relationship between temperature at which marine carbonate shells precipitated and their oxygen isotopic composition. The reported equation is as follows:

$$T = 16.5 - 4.3(\delta) + 0.14(\delta)^2$$

Where, T is seawater temperature and δ is the difference of the oxygen isotopic composition between sample with respect to a reference gas (in units of per mil). These δ values are corrected for the isotopic composition of water. When this equation is approximated as linear (ignoring δ^2 term as it is very small), the slope values of 4.3 in the relationship implies that for every 1 °C rise in water temperature, the oxygen isotope value of precipitated carbonate decreases by 0.23 ‰. Epstein et al. (1951) reported that organisms like molluscs and brachiopods precipitate carbonate in isotopic equilibrium with seawater, while echinoderms and corals do not due to physiological effects. McConnaughey (1989a,b) suggested that the kinetic isotopic effect during hydration and hydroxylation of CO_2 during skeletogenesis in corals causes the observed deviations from carbonate-seawater isotopic equilibrium. The disequilibrium implies that the precipitation occurs faster than equilibration of oxygen isotope between CaCO_3 and H_2O in the calcioblast. Although, corals precipitate carbonate with depleted oxygen isotopic values than expected from equilibrium precipitation, the depletion is

observed to be constant among a genus. Weber and Woodhead (1972) studied 44 genera of corals and observed that despite the isotopic disequilibrium their oxygen isotopic composition varies as a function of temperature. Following this pioneering study, oxygen isotope in corals became one of the most commonly studied geochemical proxies. Many investigations have been carried out on oxygen isotopic composition of corals to show that it can reconstruct past sea surface temperatures (Fairbanks and Dodge 1979, Wellington et al. 1996, Linsley et al. 1999, Cole et al. 2000, Pfeiffer and Dullo 2006). Coral oxygen isotope values are also a function of surface seawater oxygen isotopic composition apart from the temperature. Cole and Fairbanks (1990) observed that oxygen isotopic records of corals from western equatorial Pacific reflect the changes in surface seawater oxygen isotopic composition due to rainfall over the region. Intense rainfall over a region can alter the salinity and oxygen isotopic composition of surface waters which in turn gets recorded by the corals. Le Bec et al. (2000) showed that oxygen isotope record of Fiji coral is driven by sea surface temperature on seasonal scale, however, on an interannual timescale it is affected by sea surface salinity of the region. Morimoto et al. (2002) also showed that oxygen isotope values of corals from western Pacific reflect changes in oxygen isotope of seawater and can be used to reconstruct paleosalinity. The coral oxygen isotope composition is thus an important proxy for past temperature, salinity and rainfall reconstruction. Such records can be very useful in deriving crucial information about past climate and associated changes.

Apart from SST and seawater composition, the growth rate of corals have also been observed to affect the oxygen isotopic composition of coral skeleton. This leads to variations in coral oxygen isotopic composition and SST relationship among colonies of the same species or within an individual coral itself. Due to variations in growth rate, lateral variation in oxygen isotopic composition in coral along the surface is present (McConnaughey 1989a). McConnaughey (1989a) suggested that kinetic behaviour during skeletogenesis leads to significant variations, where rapidly growing skeletons show stronger depletion as compared to slowly growing skeleton. This led to a common practice of sampling corals along major growth axis to avoid such variability. Even after following such careful sampling practice some studies have reported inter-colony variabilities (Linsley et al. 1999, Felis et al. 2003, Suzuki et al. 2005) in mean oxygen isotopic values of corals. Felis et al. (2003) observed inter-colony variability of about 1.28‰ between corals from the Red Sea. They showed that growth-rate related kinetic effect greatly contribute to such inter-colony variability with significant variability observed in corals having growth rates lower than 6 mm yr⁻¹. However, after

correcting for growth rate variations, inter-colony variation of 0.43 ‰ was obtained in mean oxygen isotope value. Linsley et al. (1999) also reported inter colony variability of 0.4 ‰ among corals from Clipperton atoll in the Pacific. Using cultured *Porites* corals, Suzuki et al. (2005) reported inter-colony variability of 1 ‰ in their oxygen isotopic ratios. In sum, these observations imply that paleoclimatic reconstructions using coral oxygen isotopic composition should be carried out with caution particularly when investigating multiple coral colonies.

Oxygen isotopic records from corals have provided crucial insights into different climatic phenomena such as, El Nino Southern Oscillation (ENSO), Indian Ocean Dipole (IOD), North Atlantic Oscillation (NAO) and Indian monsoon. Abram et al. (2008) constructed corals oxygen isotope based Indian Ocean Dipole index and observed that the frequency and strength of the IOD has been increasing during the twentieth century. Using coral oxygen isotopes, Charles et al. (1997) observed that the interannual variability of western equatorial Indian Ocean is linked to equatorial Pacific. Cole et al. (2000) reported that the tropical Pacific forces decadal variability in western Indian Ocean. Using coral oxygen isotope records, Pfeiffer and Dullo (2006) observed significant sea surface cooling due to the Indian monsoon. Further, these records suggest significant correlation with ENSO, hinting at influence of ENSO-like variability in the Indian Ocean. Based on a 115 years long coral oxygen isotope record off Kenyan coast, Nakamura et al. (2011) suggested that climate in the region is dominated by IOD rather than ENSO. Felis et al. (2000) studied 245 years long coral record and observed that both NAO and ENSO contributed to the middle east climate variability. However, such long records are not available from the Indian Ocean region, making investigations of past climate variability over the Indian region difficult.

1.4.2. Stable Carbon Isotope Proxy in Corals

In addition to stable oxygen isotopic measurements, carbonates also provide an additional parameter: stable carbon isotopic composition. The stable carbon isotopes in corals can provide some crucial information about their depositional environment. But unlike oxygen isotope records, quantification of carbon isotopic variations is complicated by several processes. Kinetic effects during carbonate precipitation in corals simultaneously depletes both oxygen and carbon isotopes, however, metabolic effects cause carbon isotopes to deviate from this kinetic behaviour (McConnaughey 1989a,b). In case of fast-growing corals, metabolic effect can be masked by kinetic effects (McConnaughey 1989b). Physiological factors such as, photosynthesis, respiration and heterotrophy greatly influences the coral carbon composition.

Photosynthesis by zooxanthellae preferentially fixes lighter carbon isotope, enriching the heavier carbon isotopes in the corals' internal carbon pool and skeleton (McConnaughey 1989a). Further, respiration by coral adds lighter isotopes to the calcification reservoir (Swart 1983). Since corals calcification occurs mainly during period of photosynthesis, McConnaughey et al. (1997) observed that photosynthesis related variability dominates respiration related changes in carbon isotope in reef corals. Heterotrophic feeding on zooplankton by corals can also influence their skeletal carbon isotopic composition (Felis et al. 1998, Grottoli and Wellington 1999). Zooplanktons are depleted in heavier carbon isotope (^{13}C) and thus feeding on them will deplete corals carbon isotopic composition. Further, it has been observed that heterotrophy in *Porites* accounts for a small percentage of daily carbon budget (Grottoli et al. 2006). Gagan et al. (1994) also showed that mass spawning activity by corals can enrich their ^{13}C . Therefore, multiple physiological processes in conjunction can modulate corals carbon isotope.

Apart from physiological factors, environmental parameters can also modulate corals carbon isotopes. Changes in carbon isotopic composition of seawater DIC can be recorded by corals (Felis et al. 1998, Dassie et al. 2013). Dassie et al. (2013) reported that ^{13}C depletion in atmospheric CO_2 is reflected in surface water DIC which is recorded by corals. Watanabe et al. (2017) could identify seasonal upwelling events using carbon isotopes of coral from Gulf of Oman. As upwelled waters are depleted in ^{13}C , upwelling events leads to depletion in corals carbon isotopic composition. Variation in light availability to corals greatly influences their carbon isotopic composition as it has the potential to affect coral photosynthetic activity. Therefore, any changes in cloudiness, insolation, turbidity and/or water depth can also be recorded by corals (Fairbanks and Dodge 1979, Grottoli and Wellington 1999, Rosenfeld et al. 2003). Coral carbon isotopic compositions can also record large phytoplankton blooms, as phytoplankton preferentially uptakes lighter carbon (^{12}C) subsequently enriching ^{13}C in corals (Abram et al. 2003). As several environmental parameters influence coral carbon isotopic composition, obtaining paleoclimatic information from coral stable carbon isotopic records becomes complex. Nevertheless, coral stable carbon isotopes provides a useful additional proxy which can deliver qualitative information about past insolation/cloudiness and surface water conditions.

1.4.3. Strontium to Calcium Ratio in Corals

The Sr/Ca ratio in corals is another commonly analysed geochemical proxy which is used to reconstruct past sea surface temperature variations. Unlike stable oxygen isotope, Sr/Ca ratio

is not affected by salinity and provides more robust and reliable temperature estimates. Strontium is strongly bounded in the coral carbonate skeleton (Mitsuguchi et al 2001, Corregge 2006). Sr/Ca ratio in coral skeleton varies with temperature at which coral carbonate precipitates. Kinsman and Holland (1969) reported that the Sr/Ca distribution coefficient between precipitated aragonite and seawater varies inversely with temperature. Distribution coefficient (D_{Sr}^A) of Sr/Ca for aragonite can be represented as:

$$D_{Sr}^A = \left(\frac{(Sr/Ca)_{aragonite}}{(Sr/Ca)_{seawater}} \right)$$

Weber (1973) found that in a given genus of coral, skeletal concentration of Sr is inversely correlated with seawater temperature. They also reported a “genus effect” due to which Sr concentrations between coral genus varies despite similar environmental conditions. Smith et al. (1979) also observed that Sr/Ca ratios in corals’ aragonite skeleton varies as function of temperature, however, they reported that Sr/Ca distribution coefficient in corals differ from that of inorganically precipitated aragonite due to some biological process. Weber (1973) suggested some influence of coral growth rate on Sr content of coral skeleton, however, Smith et al. (1979) did not observe a direct influence of growth rate on coral Sr/Ca ratios. Later, Beck et al. (1992) applied Sr/Ca-SST relationship from a modern coral to reconstruct seasonal SST from a fossil coral. They demonstrated that measurement of coral Sr/Ca ratio using high precision Thermal Ionization Mass Spectrometry could provide monthly resolved SST estimates with accuracy better than 0.5 °C.

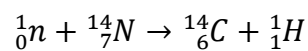
Further, they also suggested that coupling coral Sr/Ca ratio with oxygen isotopic data can provide crucial information about sea surface oxygen isotope values by removing the temperature component from the coral oxygen isotope signal. Subsequently, many studies followed on reconstructing past climate using Sr/Ca ratios in corals (Beck et al. 1992, Gagan et al. 1998, Corrège et al. 2000, Linsley et al. 2000).

De Villiers et al. (1994) reported that growth rate influences the Sr/Ca in corals. In contrast, a multitude of studies have also suggested no influence of growth rate on coral Sr/Ca ratios (Shen et al. 1996, Gagan et al. 1998, Allison and Finch 2004). The mechanism of trace element incorporation in corals is not completely understood but physiology appears to play an important role in their uptake. Despite the role of physiology in Sr uptake in coral aragonite, if a single species is used and sampled along the major growth axis then the obtained Sr/Ca ratios

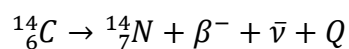
vary as a function of temperature (Marshall and McCulloch 2002). Using an Ion Microprobe, Allison and Finch (2004) observed large small-scale heterogeneities in coral Sr/Ca values. They suggested that such heterogeneities can be reduced by decreasing the sampling resolution. The seawater Sr and Ca concentrations also affects coral Sr/Ca ratios. Due to the large oceanic residence time of Sr and Ca, it is generally assumed that the Sr/Ca ratio of seawater has remained constant for past few thousands of years. However, some studies have shown that seawater Sr/Ca in modern ocean can be variable (De Villiers et al. 1994, Shen et al. 1996), compromising the accuracy of reconstructed SST. Nevertheless, various studies have demonstrated that coral Sr/Ca ratio is a robust paleothermometer (Gagan et al. 1998, Corrège et al. 2000, Marshall and McCullouch 2001, Pfeiffer et al. 2009, Delong et al. 2011, Sagar et al. 2016, Murty et al. 2018).

1.4.4. Radiocarbon in Corals

Radiocarbon (^{14}C) is one of the naturally occurring isotope of carbon which is radioactive and has a half-life of 5730 years. Its natural abundance on earth is very low, about one atom for every 10^{12} ^{12}C atoms. ^{14}C is mainly produced in upper atmosphere as a result of interaction between cosmic ray produced thermal neutrons and nitrogen atoms. This interaction can be represented by following reaction:



where, n is the neutron and H is the proton. Mean production rate of radiocarbon in atmosphere is around $1.57 \text{ atoms cm}^{-2} \text{ s}^{-1}$ (Key 2001). Radiocarbon decays by emitting β -particles at energy of 156 keV. This decay converts carbon into stable nitrogen atom:



where, $\bar{\nu}$ is antineutrino and Q is beta decay energy. The cosmogenic radiocarbon atoms produced in the atmosphere immediately reacts with atmospheric oxygen and subsequently converts to carbon dioxide molecules, further dispersing into other carbon reservoirs (hydrosphere and biosphere). Apart from age determination of objects, radiocarbon can be used as a potential tracer in identifying pathways and rates of carbon exchange between these reservoirs. During early 1950s and 1960s, artificial radiocarbon (bomb radiocarbon) was introduced in the atmosphere due to nuclear weapons testing (Hua et al 2013). As a result, the atmospheric radiocarbon concentration doubled by 1963-1964 and has been decreasing since then due to exchange between atmosphere and other carbon reservoirs: ocean and biosphere.

This bomb radiocarbon has been effectively used for studying ocean circulation and air-sea CO₂ exchange processes (Stuiver 1980, Broecker 1985, Druffel 1989, Cember 1989, Chakraborty et al. 1994, Bhushan et al. 2000).

Corals living in shallow marine waters record the temporal changes in sea surface DIC radiocarbon values. This bomb radiocarbon signature embedded in corals can be useful in providing information about natural processes affecting the surface waters of the region (Druffel and Griffin 1993, Grumet et al. 2004, Hua et al. 2005, Guilderson et al. 2009). Radiocarbon concentration of DIC in ocean surface water depends on radiocarbon concentrations of atmosphere and oceanic sub-surface waters. Since ocean sub-surface waters remain isolated from atmosphere for hundreds of years before shoaling up, their radiocarbon concentrations are generally lower than that of the atmosphere. Figure 1.3 shows depth profile of radiocarbon concentrations in Bay of Bengal and Arabian Sea waters measured during the GEOSECS expedition (Stuiver and Ostlund 1983). It is clearly observed that deeper ocean waters are depleted in radiocarbon as compared to surface ocean waters.

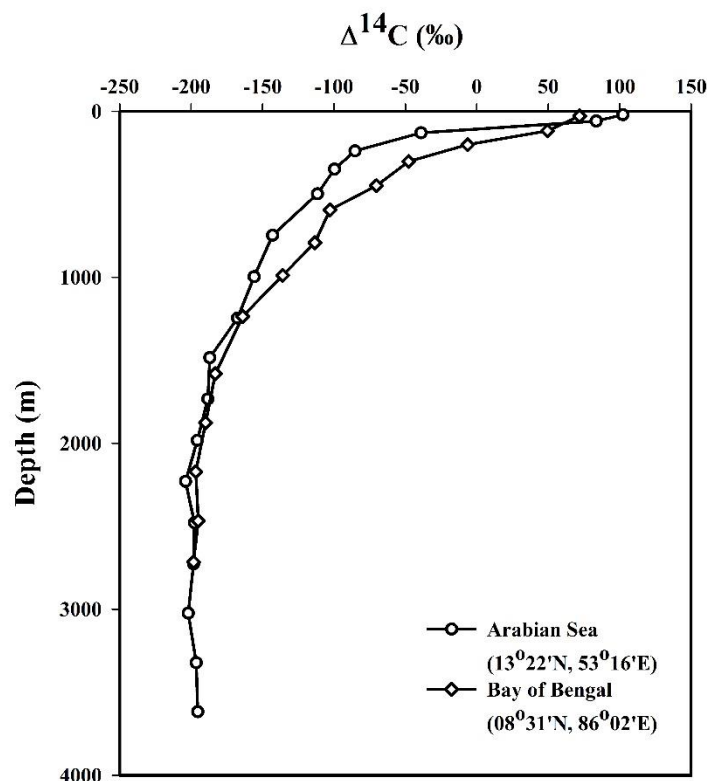


Figure 1.3: Depth profile of radiocarbon concentration in ocean water of the Arabian Sea and the Bay of Bengal from GEOSECS expedition (Stuiver and Ostlund 1983)

Combination of air-sea CO₂ exchange and upwelling, reduces the ¹⁴C activity of the surface ocean reservoir as compared to that of the atmosphere, leading to a reservoir effect (Stuiver and Polach 1977, Alves et al. 2018). This causes an offset between radiocarbon age of marine samples and corresponding atmospheric age of that time; such offset is called the reservoir age (R) (Stuiver and Braziunas 1993). Variations in regional R from the global average R value is called reservoir effect correction (ΔR). Using the marine calibration curve, the radiocarbon age corresponding to calendar year of sample growth or collection provides the global average R value for that time. Mathematically, subtracting this global average R value from measured radiocarbon age of marine samples yield ΔR (Stuiver and Braziunas 1993, Reimer and Reimer 2017, Alves et al. 2018). ΔR values are important in radiocarbon dating since they are applied to radiocarbon ages before calibration to correct for local reservoir effects. As reservoir age values vary due to ocean circulation, upwelling and freshwater fluxes, they also help in understanding the oceanography of a region.

Carbon dioxide (CO₂) is one of the important greenhouse gases, which has been increasing in the atmosphere rapidly since the industrialization. The atmosphere is a dynamic and homogenous reservoir with least amount of carbon that makes it very sensitive to the changes in carbon cycle (Alves et al. 2018). Understanding the sources and sinks is crucial. Chakraborty et al. (2020) (Krishnan et al. 2020), showed that since 1980s the terrestrial ecosystem over Indian region has been a sink of carbon. Dutta and Bhushan (2012) observed that in late 1990s the northern Indian Ocean has been a source of CO₂. The ocean is a bigger reservoir of carbon which overall acts as a sink for carbon. However, some oceanic regions can behave as a source of carbon. It is important to know the CO₂ fluxes and exchange rates between the major reservoirs to better understand the carbon cycling. The bomb radiocarbon inventory in ocean is mainly controlled by the air-sea CO₂ exchange rate and lateral and vertical movements of oceanic waters. Air-sea CO₂ exchange rates can be obtained using the bomb radiocarbon inventory of seawater, changes in atmospheric and surface-ocean radiocarbon abundances (Stuiver 1980, Bhushan et al. 2000, Dutta & Bhushan 2012). The tree ring radiocarbon data provides a history of atmospheric radiocarbon variations (Murphy et al. 1997, Hua et al. 2000, Chakraborty et al. 2008, Hua et al. 2013), whereas corals can provide radiocarbon record of surface ocean (Druffel et al. 1978, 1983, 2002, Cember et al. 1989, Chakraborty et al. 1994, Hua et al. 2005). Estimates of air-sea CO₂ exchange rates can be useful in deriving net CO₂ flux and better understand carbon cycling over a region.

1.5. Scope of the Study

The primary aim of this research work is to study the geochemical proxy records of corals from the northern Indian Ocean which can help to understand and reconstruct the past changes in climate and sea surface conditions.

Some earlier investigations from the northern Indian Ocean provided valuable observations that helped in building a basic understanding of coral proxy records of the region. Chakraborty and Ramesh (1993) showed that corals (*Porites*) from Lakshadweep Islands faithfully record seasonal SST changes of the region in their oxygen isotopic composition. The SST change in the region results due to vertical mixing of subsurface waters induced by monsoonal winds and thus, oxygen isotopic values of Lakshadweep corals can provide useful information about past monsoonal variations. Chakraborty & Ramesh (1997) showed that $\delta^{18}\text{O}$ and $\delta^{13}\text{C}$ records of Lakshadweep corals reflect monsoonal seasonality over the region. Ahmad et al. (2011) observed an ENSO related periodicity of about 5 years in the oxygen isotopic record of Lakshadweep corals. Later, Ahmad et al. (2014) found a decline of 10-15% in calcification rate of *Porites* coral from the Lakshadweep region. Interestingly, these investigations reported different $\delta^{18}\text{O}$ -SST calibration equation, which demands attention towards coral $\delta^{18}\text{O}$ -SST relationship for using Lakshadweep corals for paleoclimatic studies. Although, the above discussed investigations showed that the Lakshadweep corals record monsoon induced SST cooling, they did not observe the influence of monsoon rainfall on Lakshadweep coral isotopic records (Chakraborty & Ramesh 1997, Ahmad et al. 2011). Based on a study on Oman corals, Tudhope et al. (1996) observed that oxygen isotope record of these corals corresponding to northeast monsoon period correlate with annual rainfall anomalies in India. Chakraborty (2020) suggested that oxygen isotope composition corals from the northern Indian Ocean, mainly from the Lakshadweep region can potentially provide information about Indian monsoon rainfall.

In the Andaman Sea region, Allison et al. (1996) studied few *Porites* cores from close to the southern Thailand margin and observed that calcification rate influences the oxygen isotopic composition of corals. Rixen et al. (2011) analysed a *Porites* from Port Blair, Andaman Islands and suggested that observed oxygen and carbon isotope variability in coral is produced by monsoon driven reversal of surface ocean circulation. Unlike the Lakshadweep region, the Andaman Sea is influenced by large freshwater flux, therefore proxies like stable oxygen isotopes in corals from the region can be greatly influenced by isotopic composition of

seawater. A careful multi-proxy investigation is required to better understand the variability of coral proxy records in the region and their relationship with monsoon.

Chakraborty et al. (1994) analysed radiocarbon composition of corals from Gulf of Kutch (Arabian Sea) to calculate air-sea CO₂ exchange rates over the region. Such information is useful for studying oceanic uptake of CO₂. However, Lakshadweep and Andaman regions lack such high-resolution seawater DIC radiocarbon records. Coral radiocarbon records from these regions can be useful in determining air-sea CO₂ exchange rates over them. Additionally, coral radiocarbon records of pre-bomb period can also provide valuable information about local reservoir corrections, crucial for reliable radiocarbon dating of marine samples.

1.6. Objectives of the Study

In order to better understand the environmental processes recorded by coral geochemical proxies from the northern Indian Ocean, several coral cores were collected from the Lakshadweep and Andaman islands. Geochemical analyses of these coral cores were carried out with following aims:

- To assess the $\delta^{18}\text{O}$ -SST relation in Lakshadweep corals and their ability to capture SST variability.
- To identify the monsoon signature in the Lakshadweep corals stable isotopic records.
- To understand the variability of geochemical proxies of Andaman corals and their relationship with environmental parameters like SST and rainfall.
- To determine air-sea CO₂ exchange rates over the Andaman and Lakshadweep regions.
- To find reservoir age correction values for the northern Andaman region.

Chapter-2

Methodology

2.1. Methodology

India has a coastline of approximately 8000 km; however, the coral reefs are concentrated mainly in four different regions: Andaman and Nicobar, Lakshadweep, Gulf of Kutch and Gulf of Mannar. The total area occupied by Indian coral reefs is nearly 2383 km² (Bahuguna et al. 2013). About 199 species of scleractinian corals of 37 genera have been reported from Indian coral reefs (Pillai 1996). Among these, 72.8 % constitute hermatype corals and the rest are ahermatype corals (Muley et al. 2000). *Porites* is among the dominant genera of massive corals found in Indian waters (Pillai 2010). Among massive type Scleractinia corals, *Porites* is the most common genus analysed for paleoclimate studies (Lough 2010). A relatively higher growth rate of about 1-2 cm yr⁻¹ for these corals makes them easier to obtain high resolution records. This work aims to analyse geochemical proxies of live *Porites* corals from the Indian region for paleoclimate study. In this work, two coral cores were analysed, one each from the Lakshadweep and Andaman islands. Stable oxygen and carbon isotopic compositions, radiocarbon concentrations and Sr/Ca ratio were studied in these coral cores.

Establishing the new AMS (Accelerator Mass Spectrometer) lab at PRL was part of this thesis work. Protocol for high precision measurements of Sr/Ca ratios in corals in our lab was also established during the course of thesis work. This chapter discusses the regional setting of the study area and techniques applied for sampling and geochemical analyses of studied coral cores.

2.2. Regional Setting

2.2.1. Lakshadweep Islands

Lakshadweep Archipelago, situated in the Arabian Sea about 200-400 km off the south-western coast of peninsular India comprises group of 36 small islands with an accumulated area of 32 km², (James, 2011) (Figure 2.1). It is located in the northern part of Chagos-Maldives-Laccadive submarine ridge, which extends for over 2350 km along a north-south direction in the northern Indian Ocean. The Lakshadweep islands are divided into 3 groups of islands, namely Amindivi, Laccadive and Minicoy group. In this archipelago, all of the islands have coral reefs, mostly atoll and platform type reefs. More than 100 coral species have been identified in waters close to Lakshadweep islands (Pillai & Jasmine, 1989). *Porites* is among the dominant genus in Lakshadweep coral reefs. The northern Indian Ocean experiences monsoon each year, which is a seasonal reversal of winds that bring rainfall over the region.

The region receives both southwest and northeast monsoons, amounting to about 80% of annual rainfall of the region (Sreekesh, 2016). The SST in Lakshadweep region attains its maxima and minima during the months of May and August, respectively. The decrease in SST is accompanied by onset of the summer monsoon. The monsoonal wind induces vertical mixing in subsurface waters, cooling the SST of the region by 3-4 °C. Paul and Ramamirtham (1963) reported Sea Surface Salinity (SSS) in the Lakshadweep Sea ranging between 34.2 - 36.2 during the winter season. Low surface water salinity was observed by Varkey et al. (1979) in the Lakshadweep Sea. They suggested significant freshwater incursion from the Bay of Bengal into the Arabian Sea, with maximum invasion during the January-February period.

2.2.2. Andaman Islands

The Andaman Islands are situated in north-eastern part of the Indian Ocean (Figure 2.1). The Andaman archipelago is bounded by the Bay of Bengal to the west and Andaman Sea to the east. The Andaman and Nicobar islands are major coral reef areas of the India Ocean with rich diversity. These islands are home to 89 different genera with 135 different coral species including massive type corals like *Porites* (Pillai 1996). Indian monsoon system is a major climatic phenomenon that influences this region. Indian monsoon is caused by seasonally reversing wind patterns that flow due to differential heating of the Indian sub-continent and the Indian Ocean. These winds bring the important monsoon rainfall over the Indian subcontinent. The mean annual rainfall over the Andaman region is about 290 cm. The Andaman receives a major fraction of rainfall during monsoon season which consists of about 60 % of its annual rainfall (Kumar et al. 2012). Monsoon brings freshwater into the Bay of Bengal through rainfall and Himalayan rivers discharge reducing its surface salinity and stratifies the surface layer, inhibiting vertical mixing in the region (Rao and Sivakumar 2003). Irrawaddy river is a major river that drains into the Andaman Sea. The large amount of summer monsoonal runoff from Irrawaddy decreases sea surface salinity of the northern Andaman Sea which reduces southwards. The sea surface temperature values of the Andaman Sea on a monthly scale show double oscillation with two maxima and two minima each year (Rengarajan and Marichamy 1972). The maxima correspond to hot dry periods and the minima occurs during summer and winter monsoon periods. The sea surface salinity changes in the Andaman region follows a similar trend to SST variations (Rengarajan and Marichamy 1972).

2.3. Coral Sampling

Field trips for sampling corals from the Lakshadweep and Andaman islands were conducted in 2015 and 2018, respectively. Initially, field survey was carried out to identify large massive type *Porites* corals in the sampling areas. Live *Porites* coral with height more than 1 m were identified. The coral cores were then drilled from the identified *Porites* coral heads. An underwater coral drill was used with the help of SCUBA (Self-Contained Underwater Breathing Apparatus) divers for drilling coral cores from various locations (Figure 2.3). Drilling was carried out from central part of the coral head top in order to obtain maximum number of annual density bands. In the Lakshadweep archipelago, coral was sampled from Kadmat Island (11°15'N, 72°46'E) at water depth of around 1.8 m (Figure 2.1b). In the Andaman region, coral was sampled from Landfall Island (13°39'N, 93°02'E) at water depth of around 5.3 m (Figure 2.1c). All necessary precautions were taken to ensure that the coral drilling is carried out parallel to the growth axis of corals from top of their heads. Subsequently, cylindrical shaped cores with a diameter of 8 cm were retrieved. The coral core raised from Kadmat Island was 95 cm long and the core from Landfall Island was 126 cm long. The coral core pieces were properly marked and transported back to the laboratory in Ahmedabad for further analyses. A thin slice of 8-10 mm thickness was cut out from the cylindrical coral cores. X-radiograph of these slices were taken to observe the density bands, which defined the further sampling strategy. The X-radiograph of both corals show alternating high- and low-density bands (Figure 2.4). Before sub-sampling the corals for geochemical analyses, the cut sections of the core were treated with 30% H₂O₂ solution to remove the organic material from the carbonate. The core sections were then sonicated and thoroughly cleaned with Milli-Q water to further remove any adhering particles. Cleaned sections were then kept in an oven at 50°C for drying. After drying, the sub-sampling of core sections was carried out using a hand held dentist drill and an automatic micro-drill (M/S New Wave Research). During the initial phase of work, a handheld dentist drill was used for drilling out the samples. After procuring the micro-drill, high resolution samples were extracted. Coral samples from both the cores were micro-drilled along their major growth axis. The handheld drilling allowed sampling at intervals of about 1.5 – 2 mm, and the automated drill improved sampling the interval to a higher 0.7 mm resolution. The typical coral sample requirements for stable isotopic analyses is less than 400 µg. For analysis of Sr/Ca ratios, typically less than 1 mg of coral powders are required. Therefore, drilling of samples for stable isotope and Sr/Ca ratio measurements were carried out at monthly and bimonthly resolution (depending on annual growth band length).

For radiocarbon measurements using PRL (Physical Research laboratory) AMS facility (AURiS: Accelerator Unit for Radioisotopic Studies), about 10 mg of carbonate powder was needed for optimised analysis. Thus, drilling of radiocarbon samples were carried out at relatively lower resolution of about 1-2 sample per year. The sampling for radiocarbon measurements was carried out along the same sampling transect as that for Sr/Ca and stable isotope analyses.

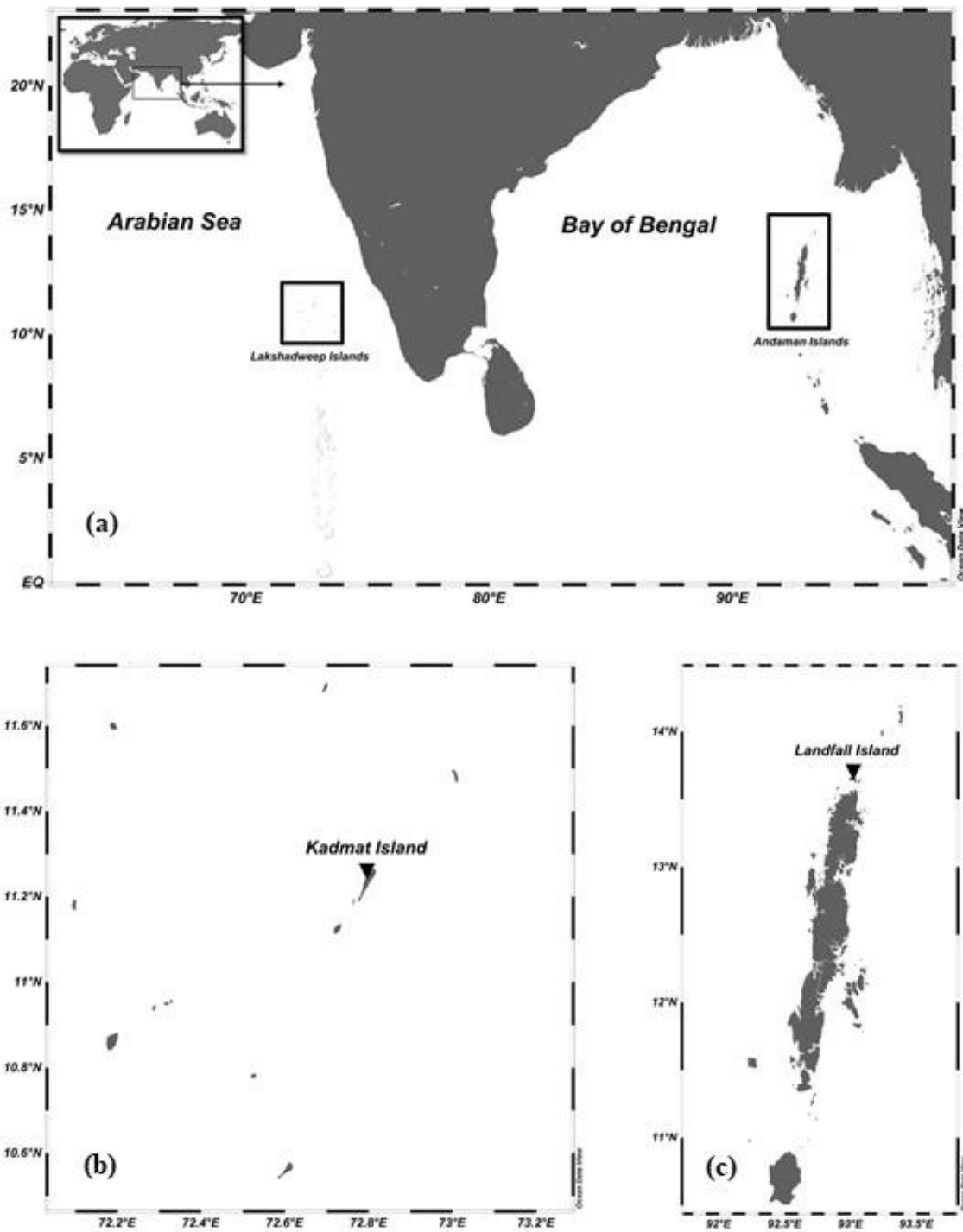


Figure 2.1: (a) Sampling location in the northern Indian Ocean with black rectangles marking region of the Lakshadweep and the Andaman Islands; (b) Location of Kadmat Island in the Lakshadweep archipelago; (c) Location of Landfall Island in the northern Andaman Island



Figure 2.2: Image of a massive coral colony in the shallow waters of the Lakshadweep Islands



Figure 2.3: Image of underwater drilling of a Porites coral to obtain a coral core

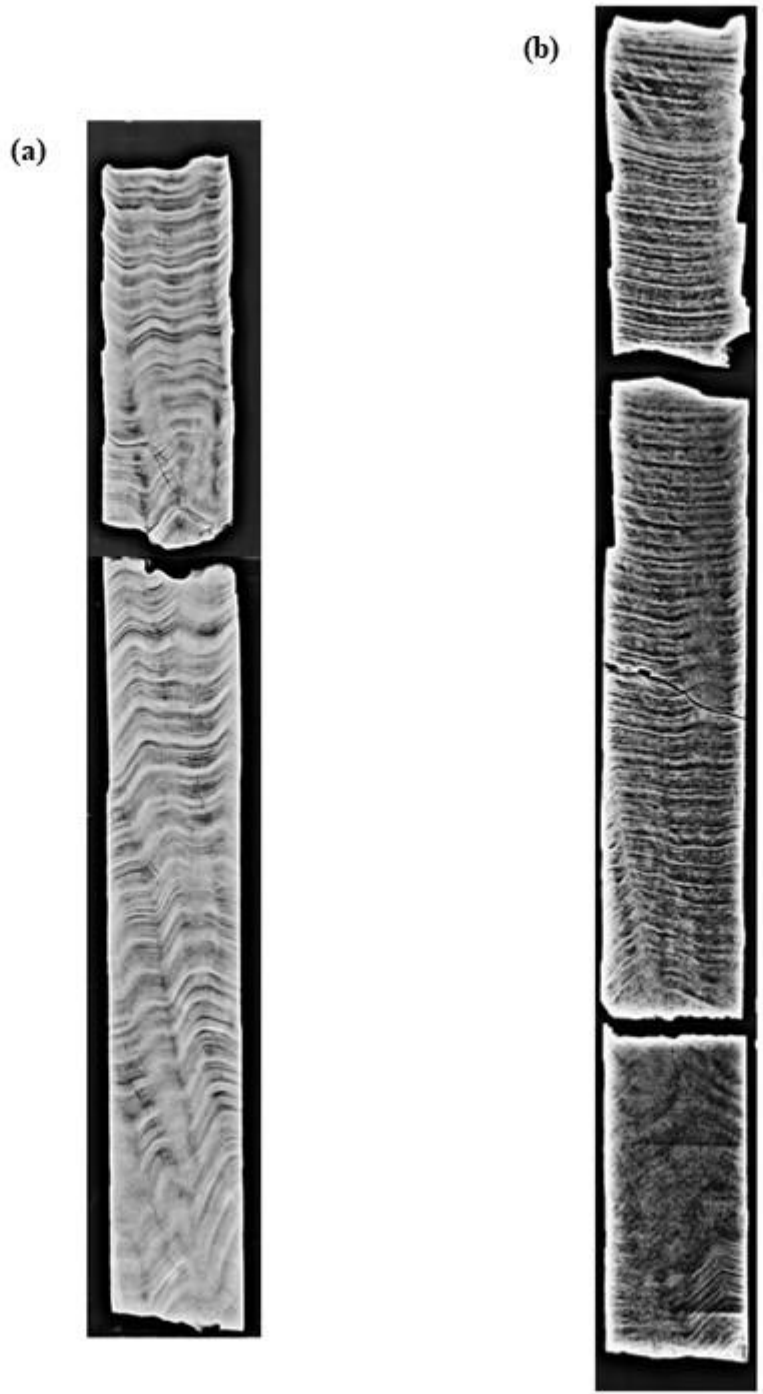


Figure 2.4: X-radiograph of Porites coral core raised from (a) the Kadmat Island in the Arabian Sea and (b) the Landfall Island in the Andaman Sea

2.4. Stable Isotope Measurements

Oxygen isotope composition in carbonate varies due to change in temperature (Urey 1947). This temperature dependence of oxygen isotope composition of carbonate is because the fractionation factor of oxygen isotope (in $\text{CaCO}_3\text{-H}_2\text{O}$ system) varies as a function of temperature (Kim O'Neil 1997). Epstein et al (1951,1953) had reported relation between temperature and oxygen isotope composition of marine (carbonate) shells. The oxygen isotope values of corals skeleton has also been studied and observed to be temperature dependent (Weber and Woodhead 1972, Fairbanks and Dodge 1979, Wellington et al. 1996, Pfeiffer and Dullo 2006). However, coral oxygen isotope composition is also influenced by isotopic signature of seawater (Cole and Fairbanks 1990, Druffel 1997, Gagan et al 2000). Therefore, corals oxygen isotope retains information of both SST and seawater oxygen isotope variations. The coral carbon isotope composition is influenced by both kinetic and metabolic effects (McConnaughey 1989a,b). It is mainly modulated by physiological factors such as, photosynthesis, respiration and heterotrophy (McConnaughey 1989a, Grottoli and Wellington 1999). Environmental factors influencing the seawater DIC change can also be recorded in corals carbon isotope composition (Felis et al. 1998, Dassie et al. 2013, Watanabe et al. 2017). Therefore, both oxygen and carbon stable isotope values of corals skeleton are important for paleoclimatic studies as they provide information of past sea surface conditions.

All oxygen and carbon stable isotopic measurements were carried out at the geosciences division, Physical Research Laboratory, Ahmedabad, India. Kadmat coral samples were analysed using Delta Plus Advantage Mass Spectrometer coupled with a Kiel carbonate device. The Landfall samples were analysed using Delta V Mass Spectrometer coupled with Gasbench II. Each instrument requires very small amount of carbonate samples for isotopic analyses. For isotopic measurements using the Delta V Mass Spectrometer around 200 - 400 μg of carbonate sample is required. Using a Delta Plus Advantage Mass Spectrometer only about 100 μg carbonate sample is required for analysis. In both devices 100% ortho-phosphoric acid is used to generate CO_2 gas from carbonate samples. A Kiel Carbonate device uses a moisture trap to remove H_2O from the gas to be analysed. The Gasbench II device uses Nafion trap for H_2O removal from the analyte gas. In both mass spectrometers, extracted and cleaned CO_2 gas is firstly ionised. These ions are then analysed based on their mass by charge ratio to obtain the relative stable isotopic abundances of samples. Results of stable oxygen and carbon isotopic measurements are reported in terms of δ notations, which denotes deviation of stable isotope

ratio of sample from VPDB international standard in per mil units (‰). Following are the formulas to calculate $\delta^{18}\text{O}$ and $\delta^{13}\text{C}$ values:

$$\delta^{18}\text{O} = \left(\frac{\left(\frac{^{18}\text{O}}{^{16}\text{O}} \right)_{\text{sample}}}{\left(\frac{^{18}\text{O}}{^{16}\text{O}} \right)_{\text{standard}}} - 1 \right) \times 1000$$

$$\delta^{13}\text{C} = \left(\frac{\left(\frac{^{13}\text{C}}{^{12}\text{C}} \right)_{\text{sample}}}{\left(\frac{^{13}\text{C}}{^{12}\text{C}} \right)_{\text{standard}}} - 1 \right) \times 1000$$

The analytical precision of measurements was established by measuring several standards of known isotopic values along with the coral samples. During all the measurements analytical error was less than 0.1‰ for $\delta^{18}\text{O}$ and $\delta^{13}\text{C}$ values. The mean values of repeated analyses of the international standard (NBS-18) and lab standard (MMB) during the course of analyses are given in the Table 2.1.

Table 2.1: Stable oxygen and carbon isotopic analysis of MMB and NBS-18 standards

	$\delta^{18}\text{O}_{\text{VPDB}} \pm \sigma$ (‰)	$\delta^{13}\text{C}_{\text{VPDB}} \pm \sigma$ (‰)
<u>MMB</u>		
Measured value (n=25)	-10.7 ± 0.1	4.0 ± 0.1
Recommended value	-10.7	3.9
<u>NBS-18</u>		
Measured value (n=20)	-23.1 ± 0.1	-4.9 ± 0.1
Recommended value	-23.01	-5.01

2.5. Sr/Ca Ratio Measurements

The Sr/Ca ration in corals changes as a function of temperature of seawater in which it is growing (Beck et al 1992). The amount of Sr co-precipitates with aragonite is dependent on

temperature, as distribution coefficient of Sr/Ca between aragonite-seawater decreases with increase in temperature (Kinsman and Holland 1969). Although Sr/Ca distribution coefficient of corals differ from that of inorganically precipitated aragonite, the Sr/Ca ratio in corals varies as a function of temperature (Smith et al 1979). Therefore, Sr/Ca ratio in corals can provide valuable information about past SST changes (Marshall and McCullouch 2001, Pfeiffer et al. 2009, Sagar et al. 2016, Murty et al. 2018).

Sr/Ca ratio measurement protocols were set up at Physical Research Laboratory. Top 65 mm of Landfall coral was drilled at resolution of 0.7 mm interval. This length corresponds to 6 years (2012-2018), with average growth rate of 8.6 mm yr⁻¹ during this period and yielded average of 13 samples per year. One of the main challenges of coral Sr/Ca analysis is low dependence of Sr/Ca on temperature and thus, high-precision measurements are required to obtain reliable data for paleoclimatic studies. Typically, Sr/Ca ratios obtained in corals range from 8.5 to 9.5 mmol/mol. The slope of coral Sr/Ca-SST relationship generally ranges between 0.04 – 0.08 mmol/mol °C⁻¹ (Corrège 2006). Therefore, in order to discern changes of 0.5 °C in SST, typical Sr/Ca analytical precisions of 0.3% or better are required. Such precisions have been achieved earlier using Thermal Ionization Mass Spectrometry (TIMS) (Beck et al. 1992), Inductively Coupled Plasma Mass Spectrometry (ICP-MS) (Le Cornec and Corrège, 1997) and Inductively Coupled Atomic Emission Spectrometry (ICP-AES) (Schrag et al. 1999). The Sr/Ca ratios in coral samples were measured using Thermo Scientific iCAP 7000 Inductively Coupled Plasma Optical Emission Spectrometer (ICP-OES) as it was able to provide required precision with fast measurements.

For Sr/Ca measurements, about 0.5 mg of each coral sample was dissolved in 10 ml of 0.4 N nitric acid (HNO₃). 0.4 N Nitric acid was prepared from 65% (Merck suprapur grade) HNO₃ and Milli-Q water. Dissolved coral sample solutions were further diluted using prepared 0.4 N nitric acid to achieve desired concentrations as per the analytical requirements. Mono-element Calcium and Strontium standards were used to make calibration standard solutions. Along with these, a check standard solution was prepared by dissolving an in-lab coral standard powder (PRL-C) in 0.4 N nitric acid. The Ca concentrations of check standard solution and coral samples were kept within a similar range.

In ICP based measurements, most of the scatter in elemental ratios is due to variations in the plasma and sample introduction system. Measuring elemental ratios removes the high frequency variability caused by plasma and sample introduction which affect all the elements

(Schrage et al. 1999). Some long-term drift in the data can be removed by measuring a Sr and Ca reference solution in proportions similar to the coral skeleton in between samples (Schrage et al. 1999). A correction factor is then calculated for each sample by averaging the reference solution bracketing the sample and comparing with the true value of the reference solution. Similarly, a reference solution was prepared and analysed between coral samples for its Sr/Ca ratio and correction factor was accordingly applied to each sample. Instrumental operating parameters for the high-precision measurement of Sr/Ca are provided in Table 2.2

Table 2.2: *Operating conditions of ICP-OES for Sr/Ca ratio measurements in coral samples*

Parameters	Value
RF Power	1150 W
Coolant Gas flow	12.0 L/min
Auxiliary gas flow	0.50 L/min
Nebulizer flow	0.60 L/min
Pump speed	50 rpm
Flush pump speed	70 rpm
Exposure time	5 sec
Replicates	3

Our in-house coral standard (PRL-C) was also run at regular intervals. The measurements were performed at 407 nm and 373 nm lines for Sr and Ca respectively. The obtained analytical precision for Sr/Ca analyses was 0.25% RSD (relative standard deviation) or 0.02 mmol/mol (1σ) (Figure 2.5).

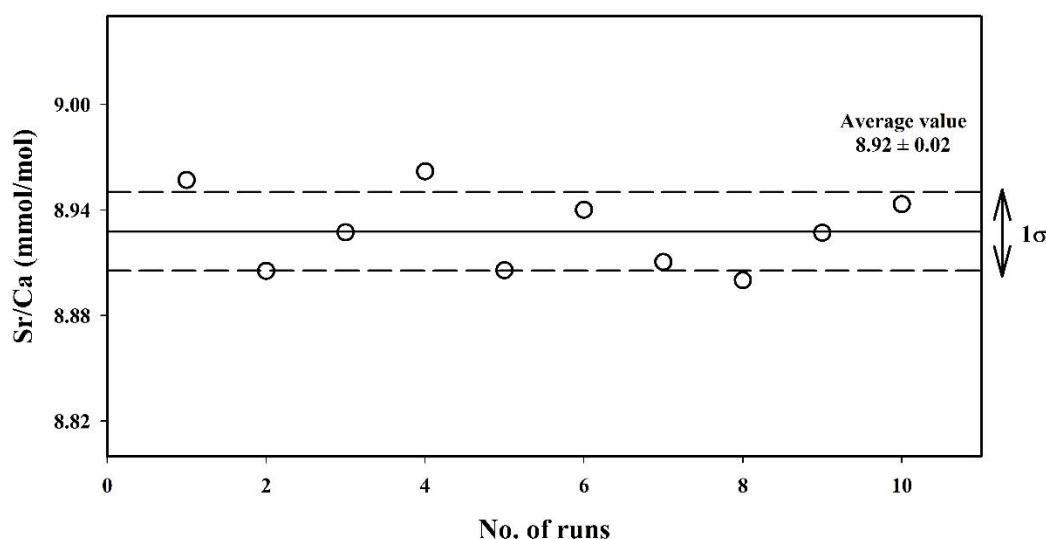


Figure 2.5: Sr/Ca ratio values of coral standard (PRL-C) measured during coral sample analysis in ICP-OES

In shallow water corals (e.g. *Porites*) both Sr/Ca ratio and $\delta^{18}\text{O}$ provide proxy record of sea surface temperature. Coral Sr/Ca reflect changes in SST only but coral $\delta^{18}\text{O}$ varies as a function of both SST and $\delta^{18}\text{O}$ of seawater. $\delta^{18}\text{O}$ is a useful proxy of temperature for regions where $\delta^{18}\text{O}$ of seawater is relatively constant through the year (Grottoli and Eakin 2007). But in region where $\delta^{18}\text{O}$ value of seawater is highly variable, Sr/Ca ratio could be a better SST proxy as it is relatively more stable (Correge 2006). The Bay of Bengal and the Andaman region receives freshwater fluxes from riverine discharge and rainfall during monsoon, which changes the salinity in the region. Therefore, $\delta^{18}\text{O}$ record of Landfall Island (Andaman) coral should reflect both SST and $\delta^{18}\text{O}$ of seawater (salinity) variation of the region. In such cases, coral Sr/Ca ratio can be a more reliable proxy of SST. Landfall coral samples were analysed for both $\delta^{18}\text{O}$ and Sr/Ca ratio.

2.6. Radiocarbon Measurements

Radiocarbon measurements of all samples were done at the Accelerator Mass Spectrometer (AMS) laboratory at Physical Research Laboratory (PRL), Ahmedabad, India. The PRL AMS facility was installed during my PhD tenure. A significant part of this research work included establishing the state of the art AMS facility at PRL, and setting up related protocols for its tuning and sample measurements. The facility constitutes of a sample preparation unit and an AMS unit for cosmogenic radionuclide measurements. Low-energy AMS systems, compared to high-energy ones are cost effective as they require relatively little maintenance and

manpower. In addition to the ^{14}C measurements, they are capable of measuring ^{10}Be , ^{26}Al , ^{129}I and actinides (Synal 2009). The 1 MV tandetron Accelerator Mass Spectrometer procured from HVEE (High Voltage Engineering Europa, B.V., Netherlands) (Klein et al. 2006) was named as PRL-Accelerator Unit for Radioisotope Studies (PRL-AURiS). PRL-AURiS is composed of several parts: Negative ion source, low-energy (LE) bouncer-injector magnet, Tandetron accelerator, high-energy (HE) magnet, electrostatic analyser (ESA), rare isotope (RI) magnet, and gas ionisation chamber (GIC) detector (Figure 2.6).

The ion-source (SO-110) can accommodate 50 sample targets in the carousel and uses Cs for sputtering target material producing 35keV negative ions. By applying suitable DC voltage pulses between the ion source at ground level and the 120° Bouncer-Injector (BI) magnet (radius 455mm), energy of the negative ions can be varied and hence different isotopes of interest can be introduced sequentially in the 1 MV Tandetron accelerator for stripping using argon gas. DC pulses (at $\sim 100\text{Hz}$) are associated with blanking unit (fast switching steerer) located between injector magnet and accelerator which gives settling time to bouncing voltages that helps in reducing uncertainty arising from beam instabilities (Klein et al 2004). Based on durations of the bouncer settings of respective pulses, the abundant isotopes are injected into the accelerator for short time as compared to the rare isotopes. Stripping process breaks molecule and removes electron from the ions producing positive ion states (Jacob et al 2000). Beam emerging from the accelerator is a positive ion beam and it is analysed by a 90° High-Energy (HE) magnet (radius 850mm) which directs abundant stable isotope(s) into offset Faraday cup(s) for ratio measurements. The maximum mass-energy product for low energy and high energy magnets is 9.8 and 63 AMU·MeV respectively. Out of the two Faraday cups, one is moveable and has an internal slit system which monitors variability in terminal voltage and keeps the beam position stable using a feedback control. The rare isotope beam is further analysed by a 120° Electrostatic Analyser (ESA, radius 650mm) and passes through a 20° Rare Isotope (RI, radius 850mm) magnet. Finally residual energy (E_{res}) vs. energy loss (ΔE) for the rare isotope, along with traces of unwanted ions, is measured in a gas-filled dual-anode ionisation chamber detector which is isolated from the vacuum line by a 75nm thick silicon nitride foil. PRL-AURiS was successfully installed in October 2016 and has been tuned for measurements of ^{14}C , ^{10}Be and ^{26}Al . AMS can efficiently measure both $^{14}\text{C}/^{12}\text{C}$ and $^{14}\text{C}/^{13}\text{C}$ ratios in samples and standards.

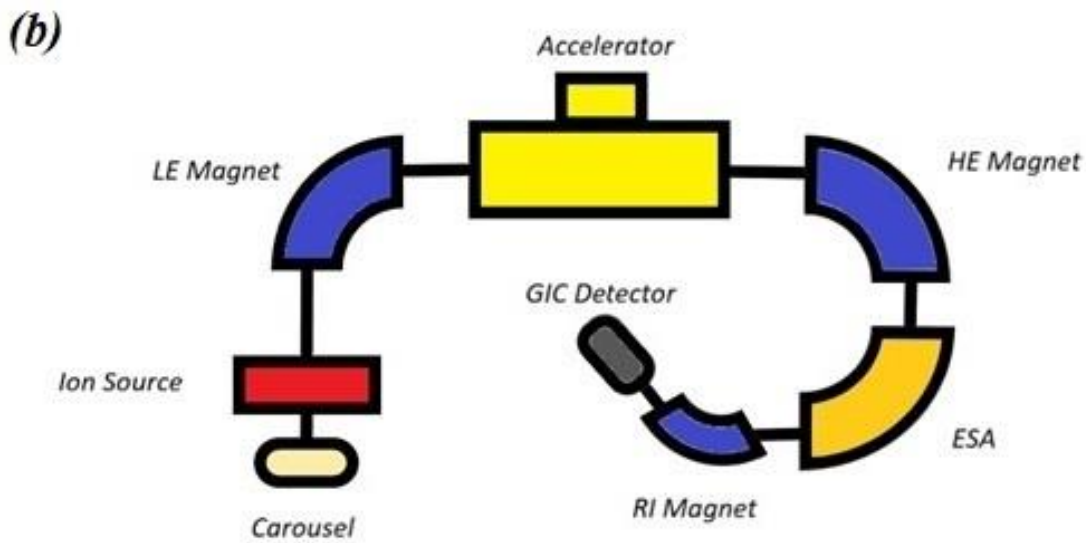


Figure 2.6: (a) Image of the AURiS facility at Physical Research Laboratory; (b) Schematic of the 1 MV Accelerator Mass Spectrometer showing its components. Carousel accommodates sample targets and Ion source generates negative ion beam from sample targets, LE Magnet injects negative ion beam to the accelerator where ions are accelerated and stripping occurs. After stripping, positive ion beam is further accelerated and then analysed by HE Magnet where abundant isotopes are measured in Faraday cups. The rare isotope moves along the beam path where it is analysed by ESA and RI Magnet to suppress interferences and is finally detected in the GIC detector

For ^{14}C measurements, charge state $^{14}\text{C}^{2+}$ is used for measurement, as it has higher stripping efficiency at 1 MV with 44% transmission. Additionally, the $^{13}\text{CH}^{2+}$ molecules are not stable enough permitting lower stripper gas density for measurements (Chamizo et al. 2008, Jacob et al. 2000). However, ions like $^7\text{Li}^+$ having similar mass/charge ratio to that of $^{14}\text{C}^{2+}$ pass through kinematic filters and interferes with $^{14}\text{C}^{2+}$ signals. Such interferences can be reduced by fine tuning the instrument as their trajectories slightly differ from that of ^{14}C and using the detector energy resolution (Chamizo et al. 2008). During the performance test, AURiS demonstrated high-precision measurements with low background levels (Bhushan et al. 2019a). Figure 2.7 shows performance test result on New Oxalic Acid standard (Ox-II) yielding relative standard deviation (RSD) for $^{13}\text{C}/^{12}\text{C}$ ratio measurements within $\pm 0.8\%$ and for $^{14}\text{C}/^{12}\text{C}$ deviation within $\pm 2.2\%$. To test sample preparation unit, several radiocarbon reference materials (IAEA-C1, IAEA-C2, FIRI-E and VIRI-U) made available from the International Radiocarbon Inter-comparison exercises (Rozanski et al. 1992, Boaretto et al. 2002, Scott et al. 2010) were processed in the laboratory and analysed.

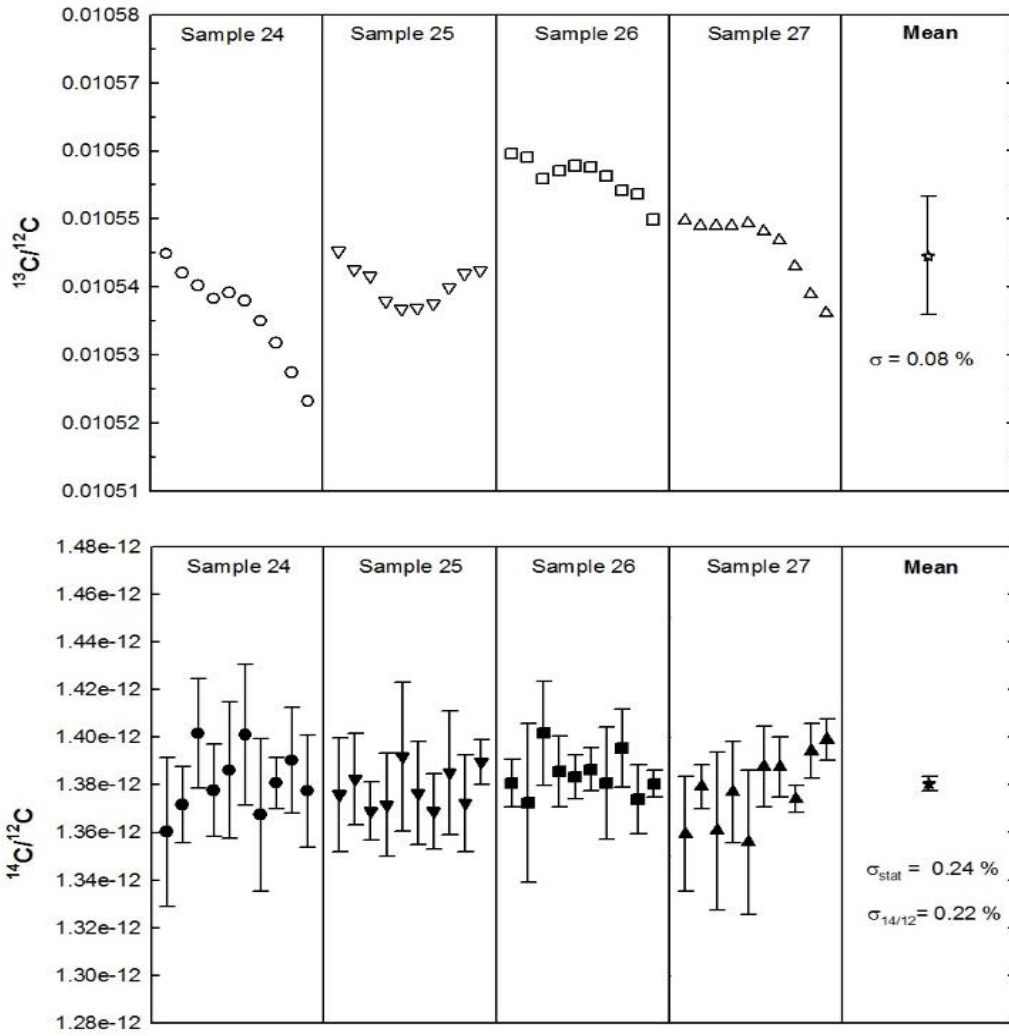


Figure 2.7: Isotopic ratios of New Oxalic acid standard (Ox-II) measured during the performance test of the AURiS

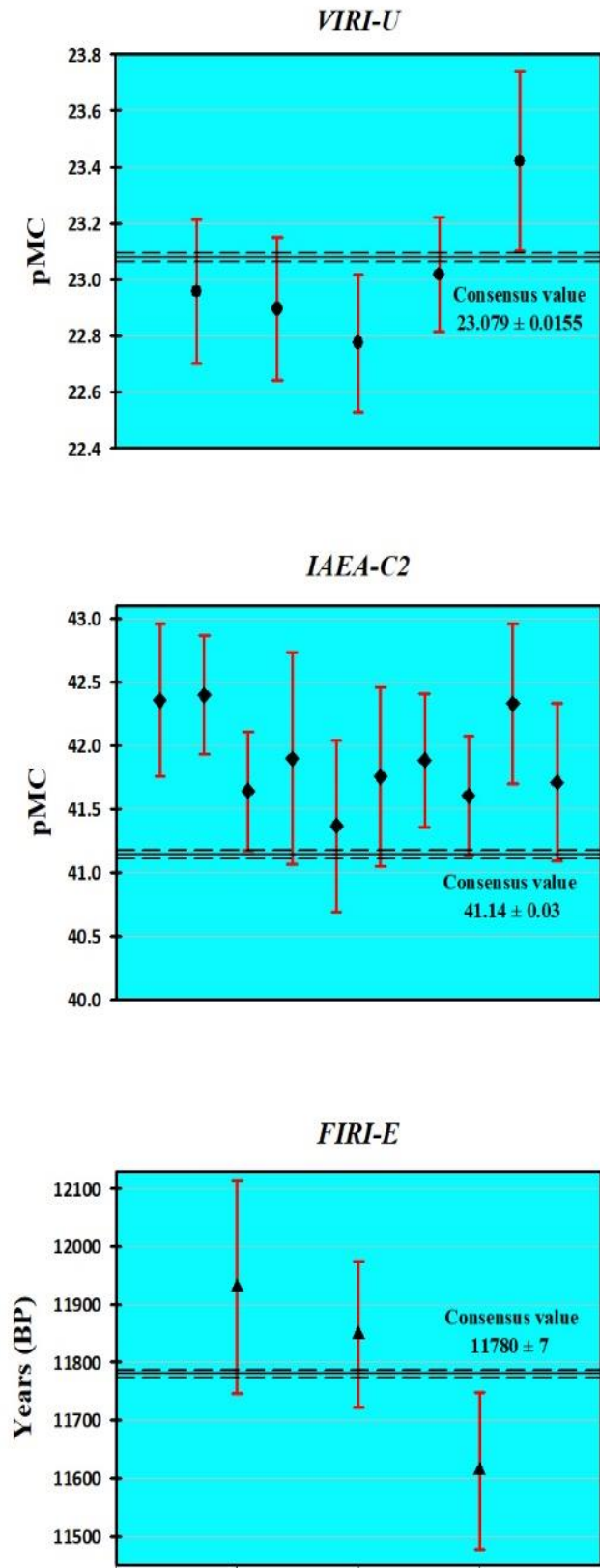


Figure 2.8: Comparison of measured radiocarbon parameters obtained by AURiS with their consensus values.

An AGE3 (Automated Graphitization Equipment) system was used to convert sample carbon into graphite (Wacker et al. 2010, Wacker et al. 2013). The measured values by PRL-AURiS are provided in Table 2.3. A comparison in Figure 2.8 shows that PRL-AURiS values are similar and well within the acceptable limits of the consensus values for the intercomparison samples. We used IAEA-C1 and anthracite to check an overall background contribution sourced from both the machine and the sample preparation process. The low $^{14}\text{C}/^{12}\text{C}$ ratios ($< 2.00 \times 10^{-15}$) of processed blank samples indicates a minute contamination during sample preparation process. Nevertheless, it shows that presently PRL-AURiS can detect ^{14}C in 51,000 yr BP old samples, with better sample preparation process and minimal contamination.

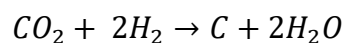
Table 2.3: Radiocarbon reference standard measured values

Reference	Material	Unit	Consensus ^{14}C value	PRL-AURiS ^{14}C Value*
IAEA-C1	Marble	pMC	0.00 (0.02)** \pm 0.02	0.14 \pm 0.04
IAEA-C2	Travertine	pMC	41.14 \pm 0.03	41.89 \pm 0.36
FIRI-E	Humic acid	years (BP)	11780 \pm 7	11800 \pm 160
VIRI-U	Humic acid	pMC	23.079 \pm 0.0155	23.13 \pm 0.25

*Average of multiple measurements

**Background sample, weighted mean is indicated in parentheses

The radiocarbon measurements of coral samples were based on aliquots of around 10 mg of coral powder, taken in the airtight 12 ml glass vials with Butyl septum cap. These vials were put in the Carbonate Handling System (CHS) end of the AGE3 system, and flushed with He (Helium) gas to remove atmospheric air. Further, ortho-Phosphoric acid (H_3PO_4) was added to the vials to liberate CO_2 from the coral samples. Extracted CO_2 gas was flushed to the AGE3 system using a stream of He gas. Additional moisture was removed from analyte CO_2 by Phosphorus pentoxide water trap. The CO_2 gas was then adsorbed on the Zeolite trap of the AGE3 system. After CO_2 loading on Zeolite trap, it was heated to release trapped CO_2 into the AGE3 system reactor in which CO_2 reduces to graphite in presence of Fe powder (4-5 g) and H_2 gas. The graphitization is a complex process, but in simple terms it can be represented by Bosch reaction



The sample graphitization inside the reactor takes place in these steps: (1) Fe preheating in presence of air, (2) flushing and cleaning with H_2 , (3) loading CO_2 to reactors, (4) chemical

reaction, and (5) argon flushing. Figure 2.9 shows these five steps of graphitization process in a pressure-time plot.

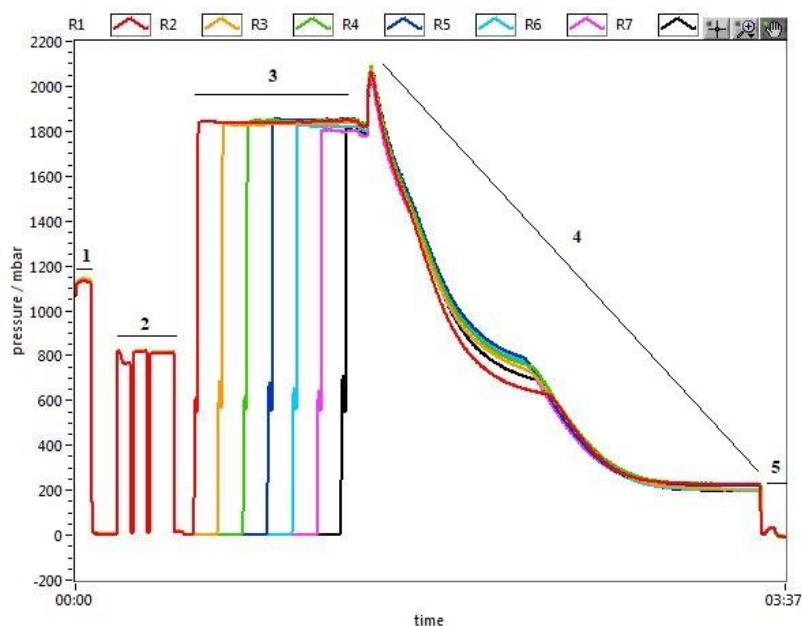


Figure 2.9: Pressure record of reactors (R1-R7) showing five steps of the graphitization process

Carbonate standards were also prepared following the same procedures. Organic standards like Oxalic acids (Ox I, Ox II) were processed using Elemental Analyser (EA) part of the AGE system. Organic standard equivalent to 1000 μg of carbon was tightly packed in tin capsules and combusted in presence of oxygen inside EA oxidation column. The generated gas mixture was carried to the reduction column of EA by Helium (carrier gas). The excess O_2 from the gas mixture was trapped in the reduction column. Further, CO_2 was separated from N_2 and H_2O by passing it through a gas separation column. These gases then proceed through the Zeolite trap of the AGE system, trapping the CO_2 . Further thermal heating releases the trapped CO_2 to the reactor in the AGE system. Finally, the graphitization process in the reactor was completed following the above mentioned five step procedure.

As corals are modern samples, they contain relatively high amounts of radiocarbon in their carbonate material. Therefore, reference standards with high radiocarbon contents were analysed along with the coral samples. A reference standard called VIRI-R which is a Murex shell from Tel Dor archaeological site (Scott et al. 2010) along with our in-lab coral standard (PRL-C) were used for this purpose. All sample and standard targets were analysed for 10 cycles with 10000 counts in each cycle. This counting strategy enable us to achieve analytical

precisions of better than 5%. The coral radiocarbon values are generally expressed in terms of pMC and $\Delta^{14}\text{C}$, following conventions of Stuiver and Poach (1977). Detailed steps to calculate these parameters from raw AMS data are given in Appendix A. The in-lab coral standard (PRL-C) yielded a mean radiocarbon value 111.3 ± 0.5 pMC. The average radiocarbon value obtained for VIRI-R standard is 73.8 ± 0.5 pMC (Figure 2.10), matching well with its consensus value of 73.338 ± 0.037 pMC (Scott et al. 2010). Multiple runs of these standards during the course of analysis show good precision (0.7% RSD) and accuracy ($< 1\%$) for radiocarbon measurements.

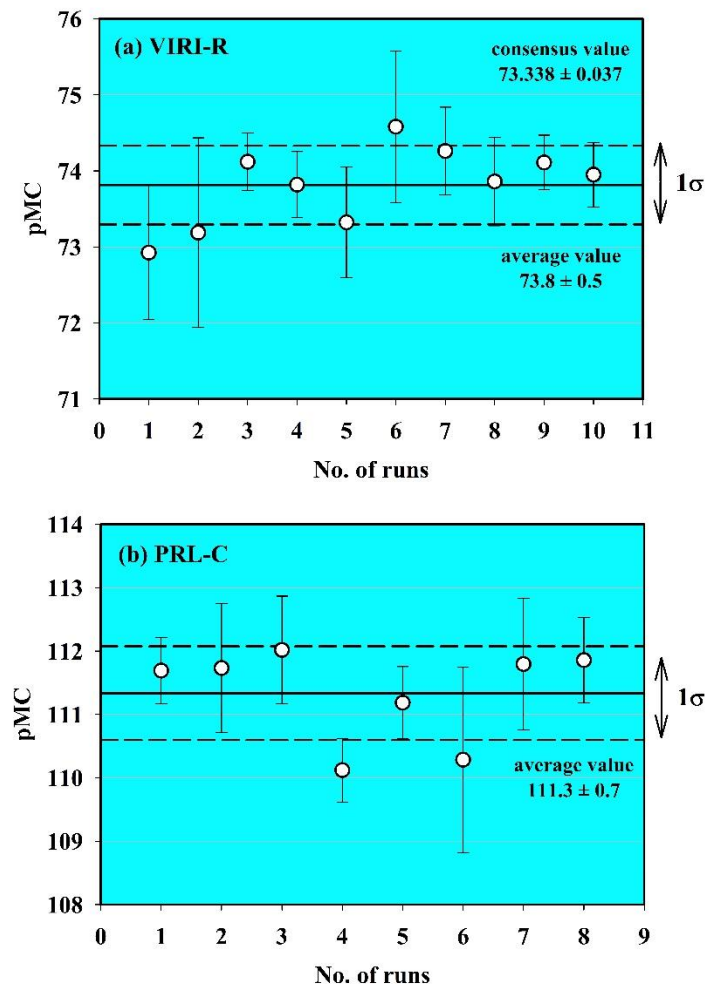


Figure 2.10: Radiocarbon values of (a) VIRI-R and (b) PRL-C (in-lab coral standard) measured during coral sample analysis in AURiS

Chapter-3
Environmental Signatures in Stable Isotopic
Composition of Kadmat Coral

3.1. Introduction

The proxy records derived from corals provide us with valuable information on environmental conditions. These shallow marine corals are natural archives of past sea surface temperature, sea surface salinity, rainfall, and many other environmental parameters. Coral records give useful insight into various natural processes and teleconnections in the recent warming world. Coral reefs are distributed mainly in the shallow regions of tropical to the sub-tropical ocean, including the northern Indian Ocean. The northern Indian Ocean experiences monsoon phenomena each year, which influences its sea surface conditions. The northern Indian Ocean turns into the warmest region in the global ocean during April and May, just before the start of monsoon (Shenoi et al. 1999). The warm pool of the Indian Ocean moves northwards from the Equator after February along with the ITCZ (Inter Tropical Convergence Zone). The core of this warm pool can be observed in the Lakshadweep Sea during May when Sea Surface Temperature (SST) rises above 30 °C. With the onset of monsoon, the Lakshadweep region experiences a decline of 2-3 °C in sea surface temperature from May to August (Figure 3.1). This cooling of SST results due to monsoonal wind-induced vertical mixing of subsurface waters (Chakraborty and Ramesh 1993).

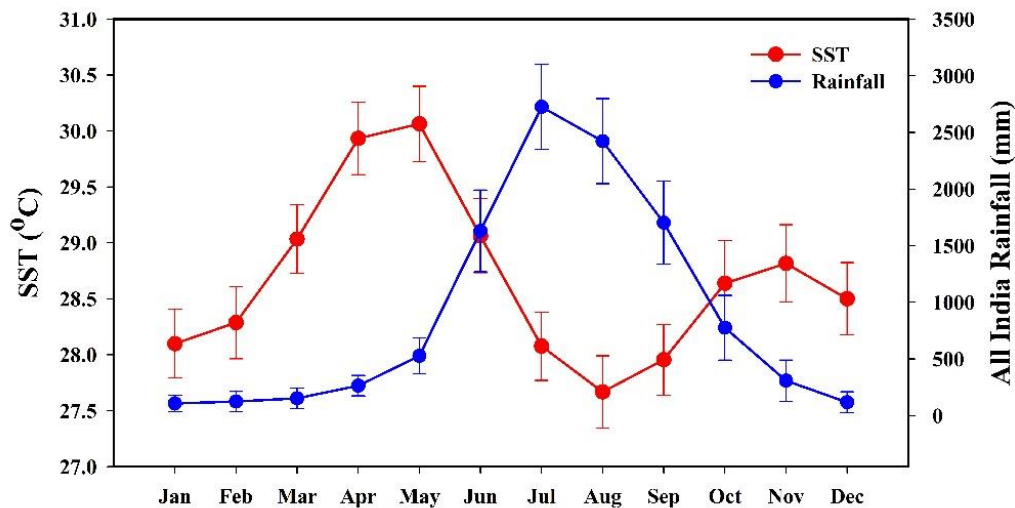


Figure 3.1: Mean monthly variability in Sea Surface Temperature (ERSSTv5) of Lakshadweep and All India rainfall (www.tropmet.res.in) values for period 1966-2014

As the Islands of Lakshadweep have coral colonies growing in shallow waters, they can record signatures of this SST changes. Few investigations on the *Porites* corals from the Lakshadweep Islands have shown that corals can record the monsoon induced SST changes in their oxygen isotopic composition (Chakraborty and Ramesh 1993,1997, Ahmad et al. 2011, Ahmad et al.

2014). These investigations of *Porites* corals stable isotope composition and suggested that $\delta^{18}\text{O}$ values from Lakshadweep coral can be used to reconstruct past SST records. But the obtained $\delta^{18}\text{O}$ -SST relation for corals was different in these investigations. Therefore, a better understanding of the $\delta^{18}\text{O}$ -SST relationship of Lakshadweep corals is required.

Along with temperature, seawater $\delta^{18}\text{O}$ value changes also influence the coral $\delta^{18}\text{O}$ record. Apart from changing SST in the Lakshadweep region, the monsoon also brings rainfall to the Indian region, which could influence the coral $\delta^{18}\text{O}$ values. Previous investigations did not observe monsoon rainfall signatures in coral $\delta^{18}\text{O}$ records (Chakraborty and Ramesh 1997, Ahmad et al. 2011). Gopalakrishna et al. (2005) observed salinity changes in the Lakshadweep Sea and found freshening of surface seawater during the winter season (December-January) and suggested that rainfall during monsoon season introduces excess freshwater into the Bay of Bengal. In the following winter season, the advection of this low saline water from the Bay of Bengal to the Lakshadweep Sea by EICC (East Indian Coastal Current) and WMC (Winter Monsoon Current) reduces the salinity of the Lakshadweep surface waters. Thus, although monsoon rainfall may not directly influence the surface seawater $\delta^{18}\text{O}$ values of the Lakshadweep Sea, it can indirectly modulate it through the advection of low saline water from the Bay of Bengal. These rainfall signatures influencing the surface waters of the region could be recorded in the Lakshadweep corals and need to be explored. The $\delta^{13}\text{C}$ record of Lakshadweep coral also reflects the monsoon seasonality (Chakraborty and Ramesh 1997). The $\delta^{13}\text{C}$ values of *Porites* skeleton deposited during the monsoon period were found to be relatively depleted (Chakraborty and Ramesh 1997, Ahmad et al. 2014), whereas other *Porites* from the Lakshadweep Islands show relative enrichment during the monsoon period (Ahmad et al. 2011). This contrasting observation suggests that more investigation is required to better understand carbon isotope variability in the Lakshadweep corals in terms of the various processes governing these changes.

Therefore, to better understand the $\delta^{18}\text{O}$ and $\delta^{13}\text{C}$ variability in the Lakshadweep corals and analyse the monsoon signature in their records, a *Porites* coral core was collected from the Kadmat Island in the Lakshadweep archipelago at the water depth of 1.8 m. The length of the Kadmat coral core was 95 cm, where top 55 cm of the coral showed clear annual bands but bands were not clearly visible in lower 40 cm. A total of 295 samples were micro-drilled from the top 555 mm length of the coral. The drilling was carried out using a hand-held dentist drill, which allowed a sampling resolution of about 8 samples per year. As mentioned earlier, the coral samples were analysed for stable oxygen and carbon isotopic compositions using the

Delta Plus Advantage Isotopic Ratio Mass Spectrometer (IRMS) coupled with Kiel carbonate device. Figure 3.2 shows the stable oxygen and carbon isotopic composition of analysed samples. The Kadmat coral isotopic record spans 37 years between 1977-2014. The chronology was assigned using coral $\delta^{18}\text{O}$ values. The coral $\delta^{18}\text{O}$ minima and maxima values were tied to the bimonthly period with the highest and lowest SST. Remaining data points were interpolated to a bimonthly scale between these two anchor points using QAnalyseries software (Kotov and Pälke, 2018).

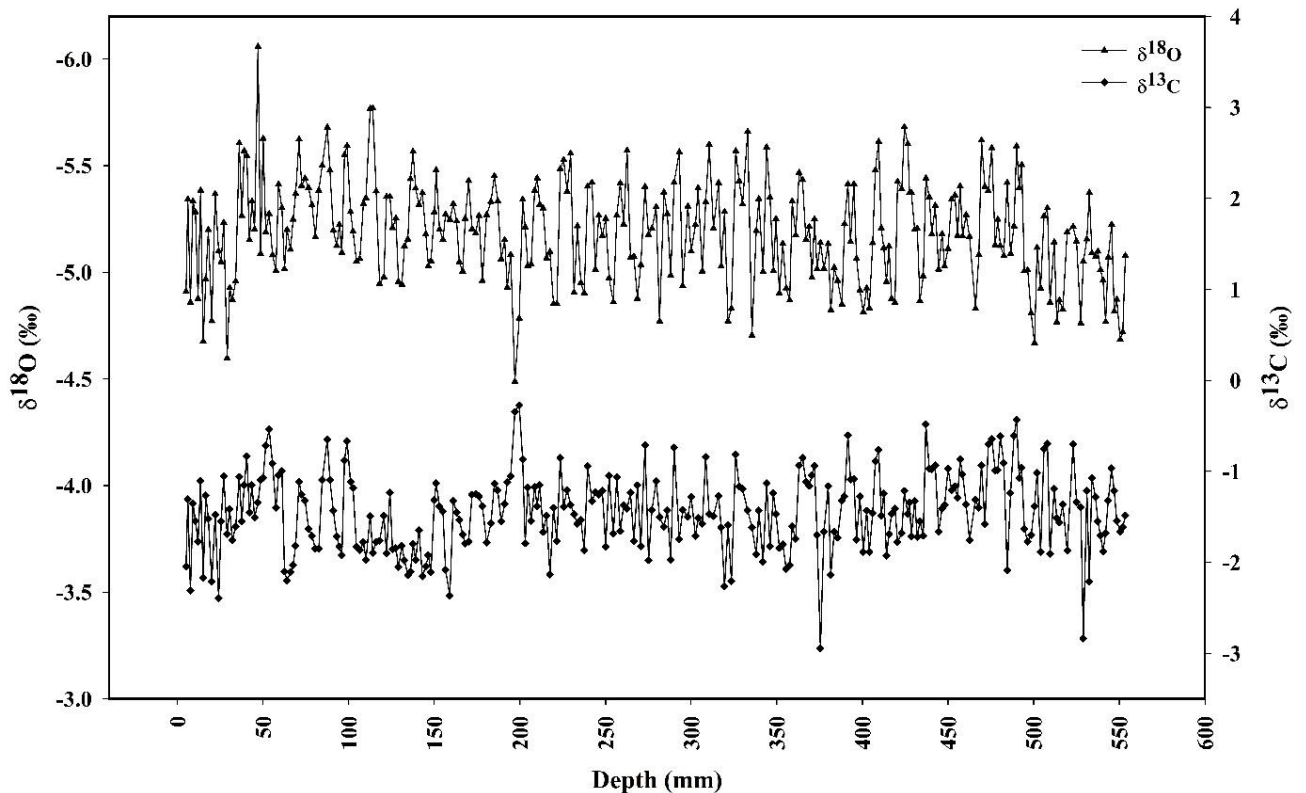


Figure 3.2: Stable oxygen and carbon isotopic composition of Kadmat coral

3.2. The Growth Rate of Kadmat Coral

The alternate high- and low-density bands of Lakshadweep coral corresponds to monsoon and non-monsoon season, respectively. During the monsoon season due to ensuing rainfall, cloudiness, enhanced turbidity, and sediment suspension, corals experience stressed growth conditions and thus secrete high-density skeletal bands (Chakraborty and Ramesh 1997; Ahmad et al. 2014). Low-density skeletal band growths are observed during the non-monsoon season when the stress-inducing factors for coral growth are absent. The average annual growth

rate of Kadmat coral was about 14.7 ± 4.8 mm/yr (mean \pm SD) (Figure 3.3) for the period of 1977-2014, which is well within the observed range of growth rate for *Porites* from Indo-Pacific region (Scoffin et al. 1992; Lough and Barnes 2000; Felis et al. 2003). This obtained growth rate is also similar to that reported for other *Porites* corals from the Lakshadweep region (Chakraborty and Ramesh 1997; Ahmad et al. 2011; Sagar et al. 2016). When the growth rate of Lakshadweep corals is compared with their water depth, it is observed that deeper corals show a relatively slower growth rate (Figure 3.4). The light intensity decreases with water depth (Fairbanks and Dodge 1979), which in turn can reduce the photosynthetic activity in corals. Photosynthesis enhances the growth rate in corals (Lough and Barnes 2000, Sun et al. 2008); therefore, shallow-water corals in Lakshadweep, on average, show higher growth rates. It is observed that the Kadmat corals have shown a long term decreasing trend since 1988. Ahmad et al. (2014) also reported a decrease in the growth rate of a coral from Lakshadweep between 1996-2003. They suggested that such a decrease in growth rate could be due to temperature stress, ocean acidification, and/or local pollution. Sagar et al. (2016) analysed a Lakshadweep coral record spanning between 1981-2008 and reported that the Lakshadweep region is under thermal stress condition. This suggests that temperature stress might be responsible for such a decline in the growth rates of Lakshadweep corals.

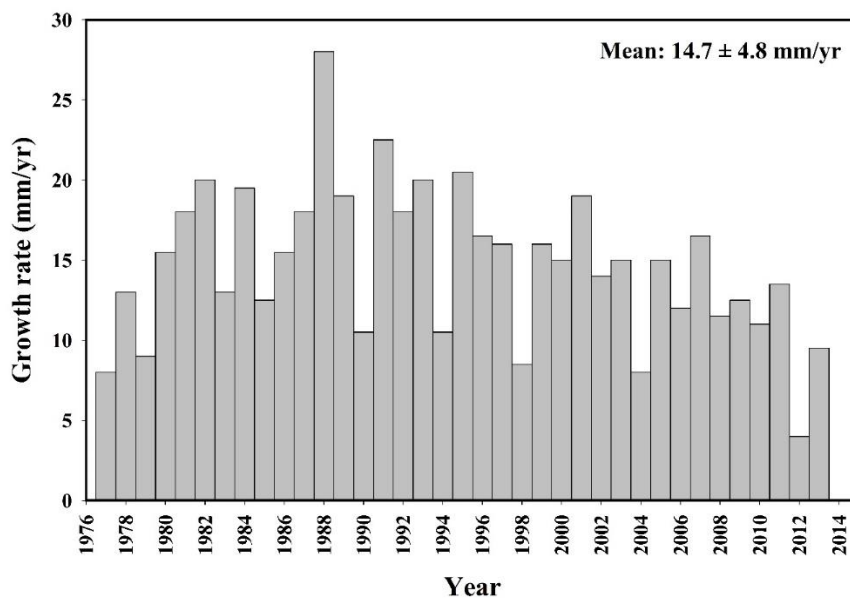


Figure 3.3: Annual growth rate of Kadmat coral from 1977-2014

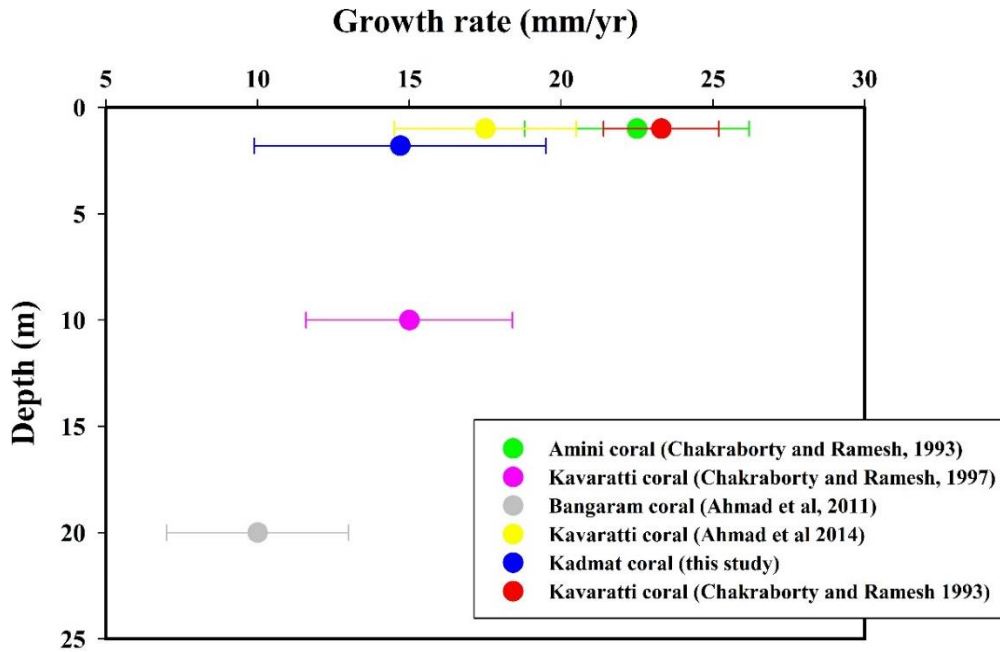


Figure 3.4: Average annual growth rate and water depth of *Porites* corals analysed from the Lakshadweep region

3.3. Inter-Colony Variability in $\delta^{18}\text{O}$

Corals precipitate carbonate lower in $\delta^{18}\text{O}$ value during coralline skeleton formation as compared to carbonate precipitated in equilibrium with seawater due to kinetic fractionation (McConnaughey, 1989a, b). This depletion is known as disequilibrium offset. Bimonthly stable oxygen isotope value of Kadmat coral ranged between -4.5 to -6.1 ‰ with an average of -5.2 ± 0.2 ‰ (mean \pm SD). The lowest $\delta^{18}\text{O}$ value was observed during May-June 2010, which is the warmest period between 1977-2014. The highest $\delta^{18}\text{O}$ value was observed in 1999, corresponding to the monsoon season. $\delta^{18}\text{O}$ record of a coral from Kavaratti reported by Chakraborty and Ramesh (1997) varies between -4.7 to -5.8 ‰ and show the average value of -5.2 ± 0.2 ‰ (mean \pm SD). Bangaram Island *Porites* coral $\delta^{18}\text{O}$ records from Ahmad et al. (2011) ranges between -4.0 to -4.9 ‰ with an average of -4.4 ± 0.2 ‰ (mean \pm SD). The Bangaram coral shows relatively higher mean $\delta^{18}\text{O}$ values. Inter-colony variability in mean $\delta^{18}\text{O}$ values are also reported in corals records from other regions, however, this inter-colony variability value of 0.8 ‰ is higher than that reported for *Porites* from the eastern Pacific Ocean and Red Sea regions (Linsley et al. 1999, Felis et al. 2003). According to slope of -0.22 ‰ $^{\circ}\text{C}^{-1}$ for biogenic carbonate precipitations (Epstein et al. 1953), this difference of about 0.8 ‰ between mean $\delta^{18}\text{O}$ values of these corals corresponds to a temperature difference of 3.6 $^{\circ}\text{C}$. In terms of salinity, 0.8 ‰ amounts to about 5.7 difference in SSS, considering the slope of SSS-

seawater $\delta^{18}\text{O}$ relation for the Arabian Sea (Deshpande et al. 2013). These three corals (from Kadmat, Kavaratti and Bangaram) were collected from the top 20m of water column. In Lakshadweep, the top 50 m of the Arabian Sea water column is almost isothermal, and in shallow regions, the water column is homogenous up to sediment-water interface (Varkey et al. 1979). Therefore, SST and SSS cannot yield such differences in mean $\delta^{18}\text{O}$ values of *Porites* corals growing in shallow depths at margins of Lakshadweep Islands. The coral growth rate is another factor that affects their isotopic compositions. The slow-growing corals show relatively higher $\delta^{18}\text{O}$ values when compared to fast-growing ones (McConnaughey 1989b). Felis et al. (2003) observed that mean coral $\delta^{18}\text{O}$ values show a good inverse correlation with the growth rates in corals growing at a rate of less than 6 mm yr⁻¹. However, the growth rates of these Lakshadweep corals are similar and greater than 10 mm yr⁻¹, which discards the growth rate as the primary factor behind the observed variability.

Chakraborty and Ramesh (1993) established a disequilibrium offset in *Porites* coral by calculating the difference between $\delta^{18}\text{O}$ values of contemporaneous coral and giant clam (*Tridacna Maximus*) samples from the same region. As giant clams precipitate $\delta^{18}\text{O}$ in equilibrium with seawater, they can be used to estimate disequilibrium offset in coral growing in the same area. They reported the disequilibrium offset value for *Porites* coral from Lakshadweep to be -4.5 ± 0.2 ‰. Using another contemporaneous set of coral and clam from Lakshadweep, Rajan (2013) observed mean disequilibrium offset value for *Porites* coral to be -4.1 ± 0.2 ‰.

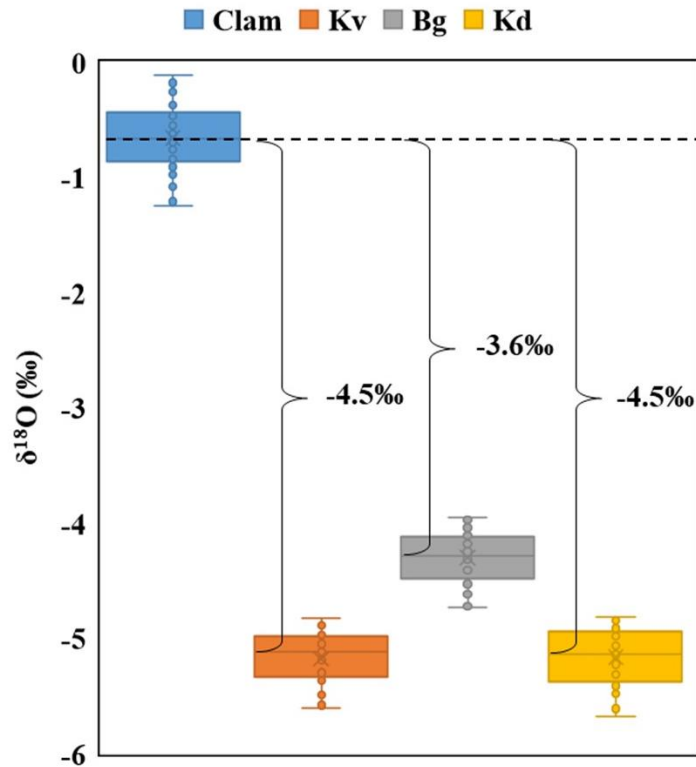


Figure 3.5: Disequilibrium offset between oxygen isotope of Clam (Chakraborty and Ramesh 1993) and *Porites* corals from Lakshadweep for the period 1984-1988; (Kv = Kavaratti, Bg = Bangaram, Kd = Kadmat)

Figure 3.5 shows the average $\delta^{18}\text{O}$ values of clam studied by Chakraborty and Ramesh (1993) and three Lakshadweep corals (Kadmat, Kavaratti and Bangaram) for the same duration of 1984-1988. It is observed that the differences between clam and coral $\delta^{18}\text{O}$ values are not same, supporting the observation that variability in disequilibrium offset exists between *Porites* colonies in Lakshadweep. Due to this inter-colony variability in coral $\delta^{18}\text{O}$ values, paleoclimatic interpretations based on Lakshadweep coral $\delta^{18}\text{O}$ records should be done cautiously. Further, the previously reported SST- $\delta^{18}\text{O}$ relationship for *Porites* coral from Lakshadweep (Chakraborty and Ramesh 1993; Ahmad et al. 2011, Ahmad et al. 2014) doesn't take care of this inter-colony variability. Therefore, application of this relationship when applied to other Lakshadweep coral records can yield erroneous results.

3.4. Kadmat Coral $\delta^{18}\text{O}$ Record

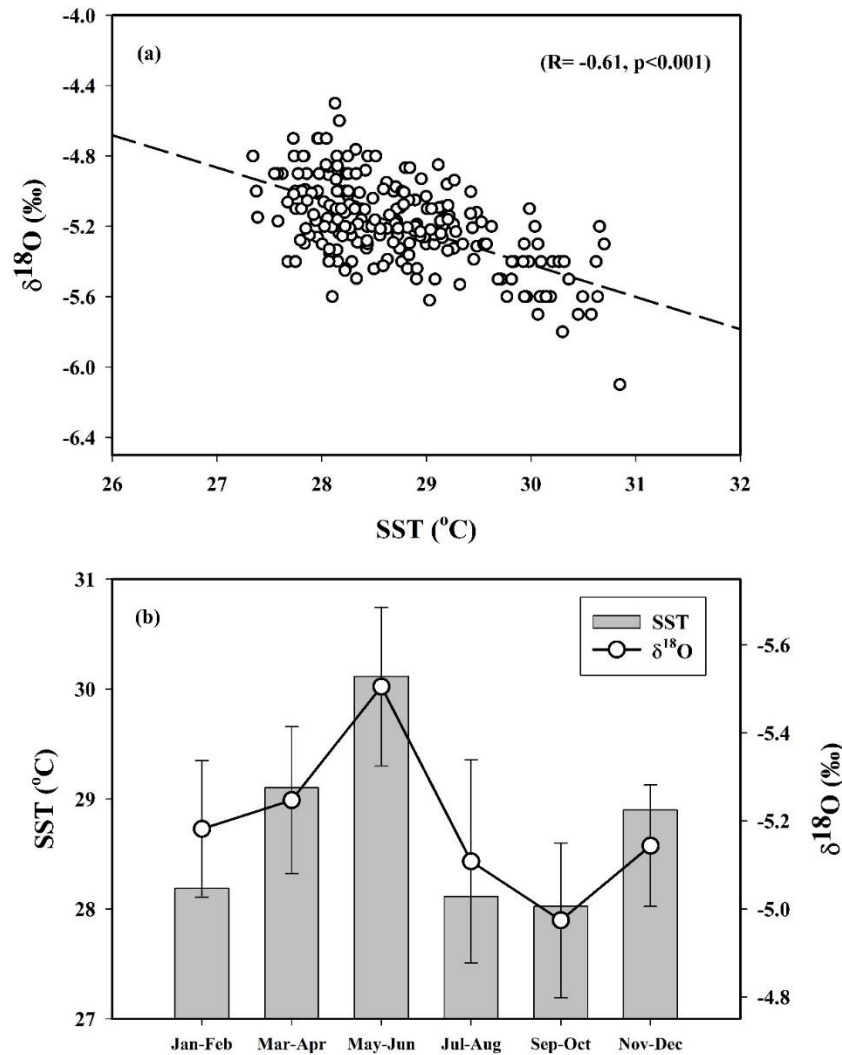


Figure 3.6: (a) Linear correlation between bimonthly $\delta^{18}\text{O}$ values of Kadmat coral and SST (ERSSTv5) values of the Lakshadweep region; (b) mean bimonthly SST (ERSSTv5) and $\delta^{18}\text{O}$ values of Kadmat coral for the period of 1977-2014

The bimonthly $\delta^{18}\text{O}$ values of Kadmat coral show a significant relationship with SST of the region (Figure 3.6), suggesting the modulation of $\delta^{18}\text{O}$ records by SST of *Porites* in Lakshadweep, similar to observations of Chakraborty and Ramesh (1997) and Ahmad et al. (2011). The observed summer monsoon cooling of SST is due to the monsoonal wind-induced vertical mixing of subsurface seawaters (Chakraborty and Ramesh 1993). The bimonthly Kadmat coral $\delta^{18}\text{O}$ values show average seasonality of 0.6‰. Comparison of seasonal minima $\delta^{18}\text{O}$ values with differences between maxima and minima $\delta^{18}\text{O}$ values of each year, yields a significant positive correlation ($R = 0.57$, $p < 0.001$) (Figure 3.7). This correlation could be because the y-axis value (the difference between maxima and minima $\delta^{18}\text{O}$ value) is a function

of the x-axis value (minima $\delta^{18}\text{O}$). However, it has also been observed that maxima and minima $\delta^{18}\text{O}$ values show a positive correlation with each other, suggesting that warm summer SST relates to relatively warmer monsoon SST. Thus, the observed correlation in Figure 3.7 might not exist just because the y-axis value is a function of the x-axis value. Overall, the data suggests that a warm summer SST is followed by increased monsoonal cooling of SST in the region.

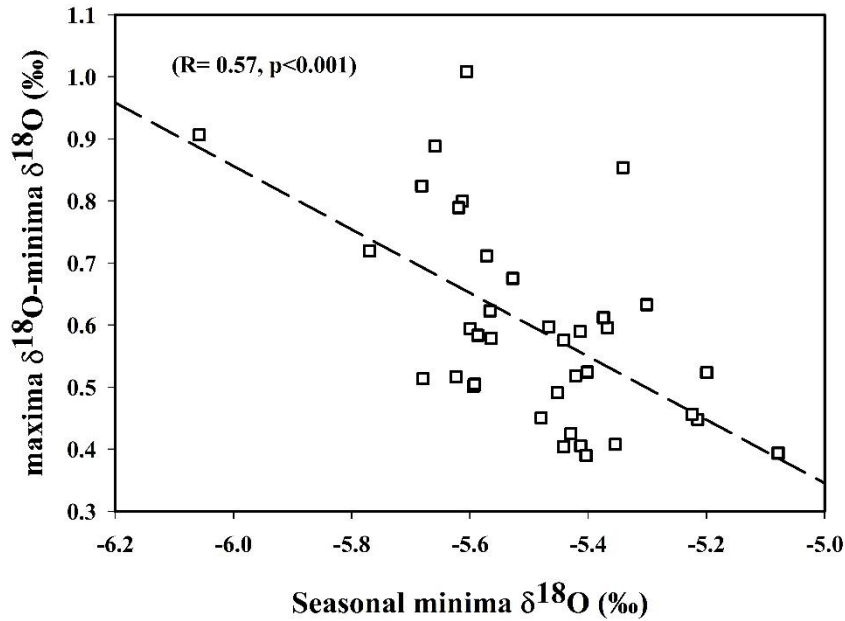


Figure 3.7: Correlation between seasonal minima $\delta^{18}\text{O}$ and difference between seasonal maxima and minima $\delta^{18}\text{O}$

To establish a reliable coral $\delta^{18}\text{O}$ -SST relationship, it is crucial to have information about seawater $\delta^{18}\text{O}$ values. However, an in-situ long term record of seawater $\delta^{18}\text{O}$ values from the Lakshadweep region is not available. These values can be derived with the help of following equation given by Chakraborty and Ramesh (1993)

$$SST = 3 - 4.68 \times (\delta^{18}\text{O}_c - \delta^{18}\text{O}_{sw}) \quad (1)$$

This equation was obtained using *Porites* coral with mean $\delta^{18}\text{O}$ of -5.2 ‰ given by Chakraborty and Ramesh (1993). As this mean value is similar to that of Kadmat coral, it suggests that there is no inter-colony variability between these two corals. Thus, the above equation can be applied to Kadmat coral. By using observed SST values (ERSSTv5, Huang et al. 2017) and measured coral $\delta^{18}\text{O}$ values in the equation, $\delta^{18}\text{O}$ value of seawater ($\delta^{18}\text{O}_{sw}$) can be obtained. The obtained $\delta^{18}\text{O}_{sw}$ values vary between -0.23 to 0.88 ‰ with a mean $\delta^{18}\text{O}_{sw}$ value of 0.32 ± 0.19 ‰ (Figure 3.8).

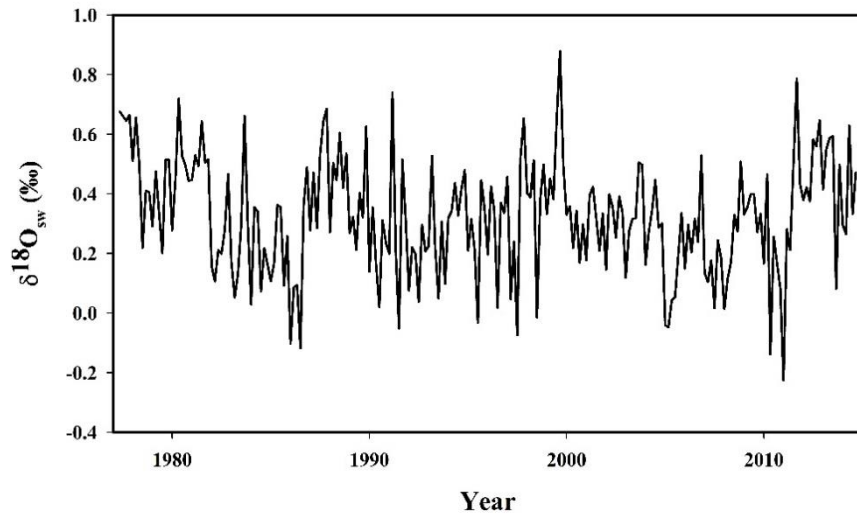


Figure 3.8: $\delta^{18}O_{sw}$ values derived from Kadmat corals oxygen isotopic record

Bimonthly $\delta^{18}O_{sw}$ values of chronology tie-points (SST maxima and minima) were compared with corresponding SSS (EN.4, Good et al. 2013) values of the region. The observation points to a weak correlation between $\delta^{18}O_{sw}$ and the SSS ($r = 0.23$, $p < 0.05$) (Figure 3.9). The slope and intercept of the $\delta^{18}O_{sw}$ -SSS relationship is similar to that observed by Deshpande et al. (2013) for the Arabian Sea surface waters. The reported scatter in $\delta^{18}O_{sw}$ -SSS relation for salinity above 34 is similar to that observed in this study and could explain the weak correlation in the Lakshadweep coral derived $\delta^{18}O_{sw}$ -SSS.

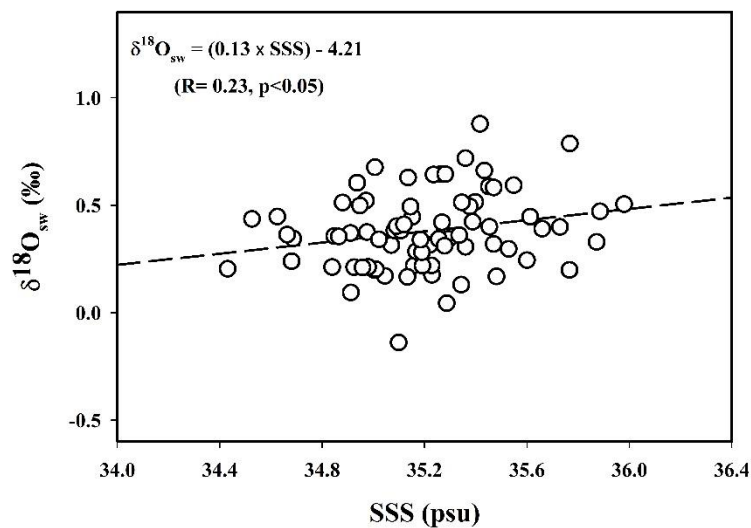


Figure 3.9: Correlation between Kadmat coral derived $\delta^{18}O_{sw}$ and sea surface salinity of the region

Mean bimonthly record of $\delta^{18}\text{O}_{\text{sw}}$ for the period 1977-2014 show the lowest value during the winter period. During winters, the East Indian Coastal Current and Winter Monsoon Current transports low salinity waters from the Bay of Bengal to the Lakshadweep Sea. Increased rainfall during monsoon season contributes to the enhanced freshening of the Bay of Bengal surface waters which causes subsequent freshening of the Lakshadweep waters in the following winter season (Gopalakrishna et al. 2005). Varkey et al. (1979) also observed that the maximum incursion of low salinity waters from the Bay of Bengal to the Arabian Sea occurs during January-February. Thus, the observed lower mean monthly value of $\delta^{18}\text{O}_{\text{sw}}$ around winter could be due to the low saline water incursion from the Bay of Bengal. As the intensity of Indian monsoon rainfall appears to influence the degree of freshening of Lakshadweep Sea, the obtained $\delta^{18}\text{O}_{\text{sw}}$ values were compared with rainfall values (All India Rainfall values, www.tropmet.res.in). No significant correlation was observed when bimonthly values are compared. Chakraborty and Ramesh (1997) and Ahmad et al. (2011) had compared rainfall with coral $\delta^{18}\text{O}$ value but did not observe any significant correlation.

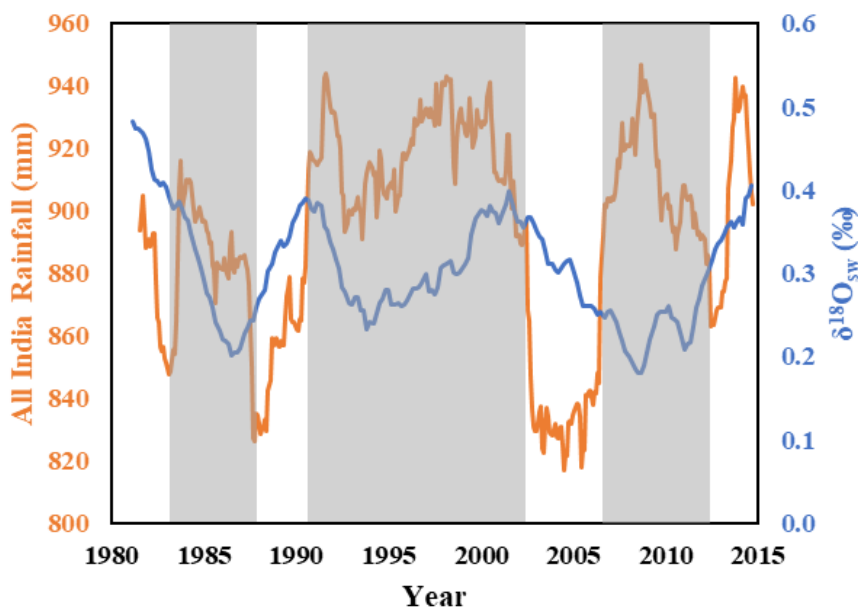


Figure 3.10: Four-year running mean values of $\delta^{18}\text{O}_{\text{sw}}$ from the Lakshadweep region and All India Rainfall value (www.tropmet.res.in), showing co-occurrence of periods of enhanced rainfall and depleted $\delta^{18}\text{O}_{\text{sw}}$ values

To understand variations in oxygen isotopic composition of the Lakshadweep Sea on interannual timescale, a long term four-year running average was obtained from Kadmat coral derived $\delta^{18}\text{O}_{\text{sw}}$ values. The four-year running average of derived $\delta^{18}\text{O}_{\text{sw}}$ values show a cyclic trend. Comparison of the averaged $\delta^{18}\text{O}_{\text{sw}}$ with similar four-year running average value of monthly All India Rainfall, suggested that periods of increased rainfall correspond to lower

$\delta^{18}\text{O}_{\text{sw}}$ values (Figure 3.10). This data comparison suggests that a long period of enhanced rainfall over the Indian region leads to the relative freshening of the Lakshadweep surface waters. Significant rainfall over India occurs during the summer monsoon period, which brings freshwater flux to the Bay of Bengal. During the ensuing winter, this less saline water is advected to the Lakshadweep region (Gopalakrishna et al. 2005), decreasing the Lakshadweep $\delta^{18}\text{O}_{\text{sw}}$ values. Therefore, during the enhanced rainfall period, the Lakshadweep records show relatively lower $\delta^{18}\text{O}_{\text{sw}}$ values. Although, seasonal rainfall variation does not correlate with the Lakshadweep $\delta^{18}\text{O}_{\text{sw}}$ values, the interannual monsoon rainfall variation influences the $\delta^{18}\text{O}_{\text{sw}}$ value of the Lakshadweep region. Therefore, apart from influencing the sea surface temperature, monsoon also affects the seawater isotopic composition of the Lakshadweep region on an interannual timescale.

3.5. Lakshadweep Coral $\delta^{18}\text{O}$ -SST Relation

Based on previous discussions, it was noted that coral $\delta^{18}\text{O}$ values from the Lakshadweep region show inter-colony variability due to varying disequilibrium offset. This disequilibrium offset contributes to the intercept of the coral $\delta^{18}\text{O}$ -SST relation making it unfit to be applied to other corals from the region, as it varies with different coral colonies. To remove such an offset difference between corals and make it easier to compare, mean centered $\delta^{18}\text{O}$ ($\Delta\delta^{18}\text{O}$) values of corals can be used (see Appendix B). Linsley et al. (1999) analysed multiple coral cores from Clipperton atoll and suggested that mean centered coral $\delta^{18}\text{O}$ values provide a more accurate understanding of the coral record. Therefore, mean centered coral $\delta^{18}\text{O}$ values were used for obtaining $\delta^{18}\text{O}$ -SST relation in Lakshadweep corals. The SST data used in this calculation is obtained from ERSSTv5 dataset, which represents SST data over a $2^\circ \times 2^\circ$ grid. A coral record from one single species could be affected by local signatures and could lead to variability in their isotopic signature. Averaging multiple coral core records thus would better represent regional or larger scale SST variability (Levy et al. 2006). Hence, Kavaratti and Bangaram coral records for the overlapping period (1984-1991) were considered to assess the SST- $\delta^{18}\text{O}$ relationship for *Porites* corals in the Lakshadweep region (Figure 3.11).

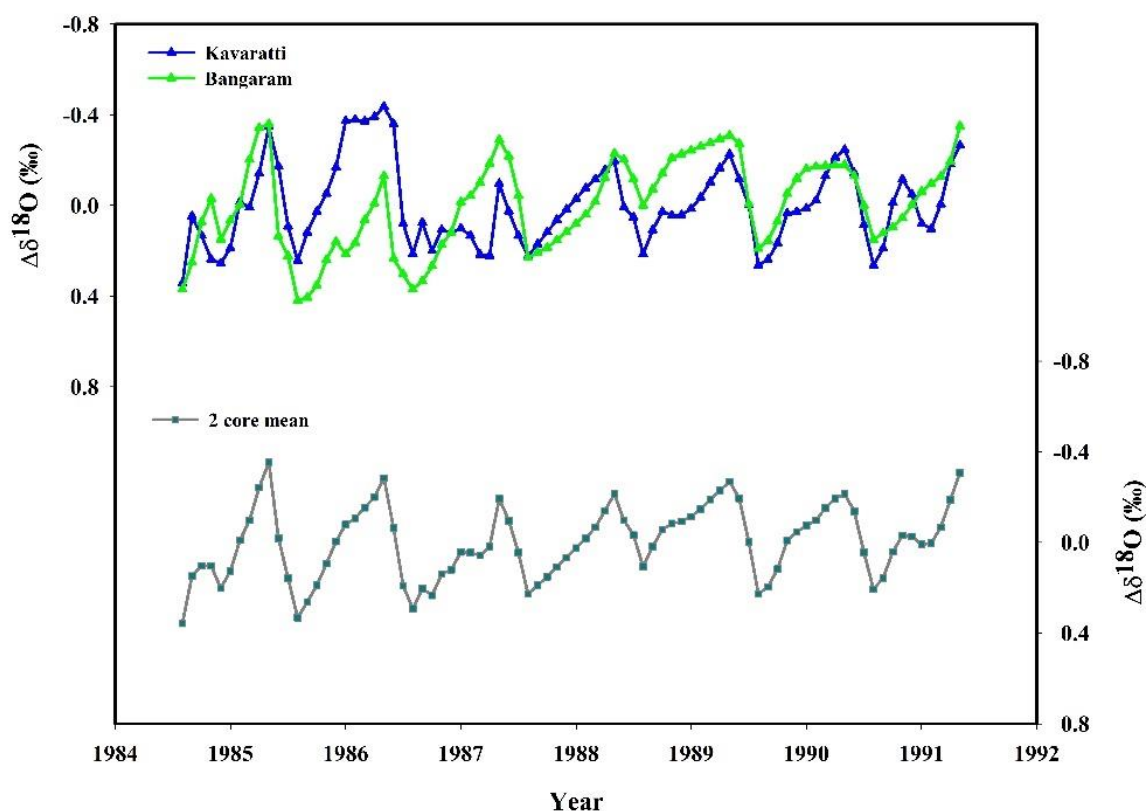


Figure 3.11: (a) $\Delta\delta^{18}\text{O}$ values of Lakshadweep corals (Kavaratti and Bangaram) between 1984-1991 and (b) mean of the two corals $\Delta\delta^{18}\text{O}$ values

Both coral records show similar seasonality of -0.5‰ , recording SST cooling of about 2.5°C between May and August. Individually, both corals $\Delta\delta^{18}\text{O}$ values show good correlation with SST values. However, the mean $\Delta\delta^{18}\text{O}$ value of two cores show a better correlation with SST for the region when compared to individual coral values (Table 3.1). Thus, a mean of multiple coral oxygen isotope records is a better representative of the seasonal SST variations.

Table 3.1: Pearson correlation coefficient between Lakshadweep corals $\Delta\delta^{18}\text{O}$ values and sea surface temperature values; (Kv = Kavaratti, Bg = Bangaram)

	Kv $\Delta\delta^{18}\text{O}$	Bg $\Delta\delta^{18}\text{O}$	2 core mean	ERSSTv5
Kv $\Delta\delta^{18}\text{O}$	1			
Bg $\Delta\delta^{18}\text{O}$	0.40	1		
2 core mean	0.82	0.85	1	
ERSSTv5	-0.60	-0.68	-0.77	1

In the absence of a continuous record of in-situ $\delta^{18}\text{O}_{\text{sw}}$ measurements from the Lakshadweep coral reefs, the bimonthly $\delta^{18}\text{O}_{\text{sw}}$ values derived from the Kadmat coral can be assumed to be representative of the $\delta^{18}\text{O}_{\text{sw}}$ value of the Lakshadweep region. The mean centered seawater $\delta^{18}\text{O}$ values were calculated from derived average bimonthly $\delta^{18}\text{O}_{\text{sw}}$ values of the Kadmat coral. These values were subtracted from coral $\Delta\delta^{18}\text{O}$ values, and the resultant $\Delta\delta^{18}\text{O}$ values defining seasonal maxima and minima were regressed against the corresponding ΔSST (mean centered SST) values to obtain the calibration equation (Gagan et al. 1998; Suzuki et al. 1999; Corrège et al. 2004). $\Delta\delta^{18}\text{O}_{\text{sw}}$ values applied for May was 0.0 ‰ and for August was -0.1‰.

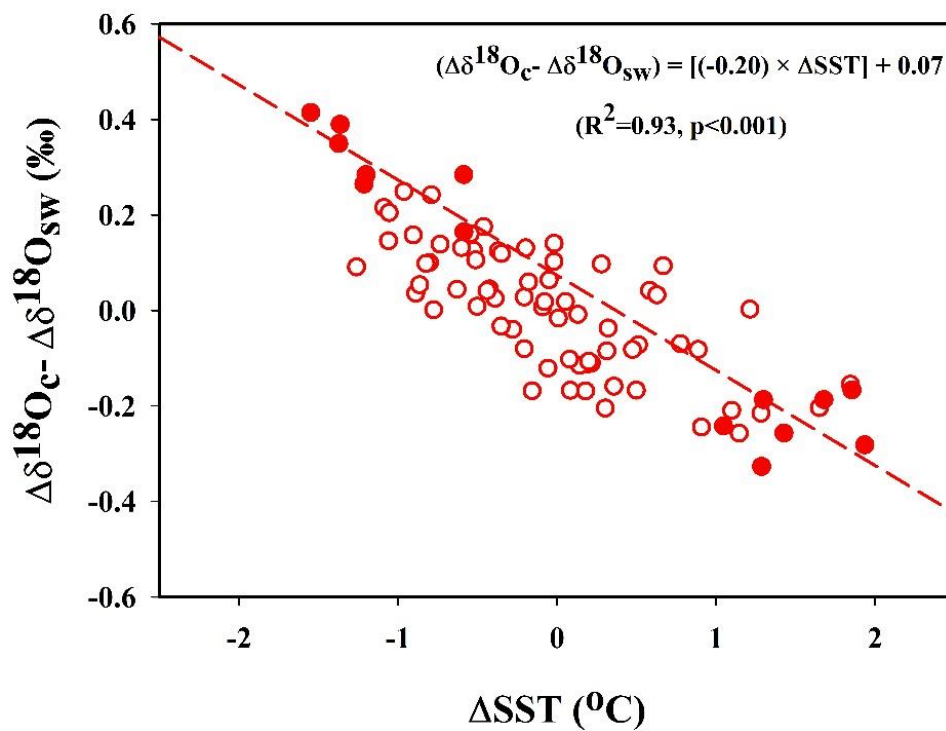


Figure 3.12: Linear correlation between ΔSST and $\Delta\delta^{18}\text{O}$ of *Porites* from Lakshadweep archipelago. Seasonal extreme values (●) are used for SST calibration and interpolated data (○) are plotted in between the extreme values

$\Delta\delta^{18}\text{O}$ and ΔSST show a good linear correlation with a slope of $-0.20\text{‰ }^{\circ}\text{C}^{-1}$ (Figure 3.12), which is within the range of reported slope values for *Porites* coral (Grottoli and Eakin 2007; Shimamura et al. 2005). Thus, past sea surface temperature variability of the Lakshadweep region can be reconstructed using the derived calibration equation:

$$(\Delta\delta^{18}\text{O}_c - \Delta\delta^{18}\text{O}_{\text{sw}}) = [(-0.20) \times (\Delta\text{SST})] + 0.07 \quad (2)$$

The above derived calibration equation was applied to the mean value of two cores to estimate the monthly SST variability. It is observed that the calculated SST variability is very close to

the observed SST variability. The difference between calculated and observed SST variability varies between -0.9 to 1.4°C with a mean value of $0.3 \pm 0.5^{\circ}\text{C}$. Considering only the maxima and minima values, the difference reduces in the range of -0.7 to 0.7°C with a mean value of $0.0 \pm 0.4^{\circ}\text{C}$. The RMSR (root mean square residual) for monthly values is 0.59°C (Figure 3.13), and for extreme values, it is 0.36°C .

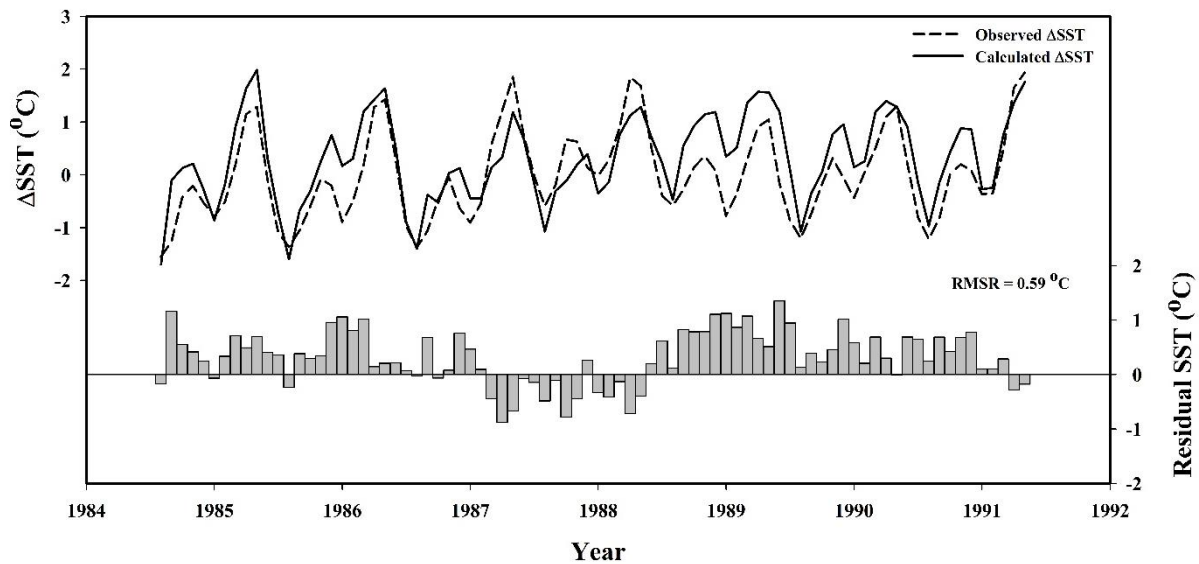


Figure 3.13: Observed and calculated ΔSST variability along with the residual values for calculated ΔSST values

The error of 0.1‰ and 0.2‰ associated with $\Delta\delta^{18}\text{O}$ values of coral and seawater respectively results in uncertainty of 1.1°C in calculated ΔSST values. This uncertainty can be further decreased by using *in-situ* observations of seawater $\delta^{18}\text{O}$ variations. It is observed that coral $\delta^{18}\text{O}$ values for August show significant relation with ERSST values ($R^2=0.66$, $p<0.05$). However, no significant relation was observed between coral $\delta^{18}\text{O}$ values and ERSST values for the month of May. Sagar et al. (2016) had reported that Sr/Ca signal of Lakshadweep corals get damped due to thermal stress introduced during summer months with SST greater than maximum monthly mean values. In the late twentieth century, loss of $\delta^{18}\text{O}$ signal in a western Indian Ocean coral to record SST changes due to environmental stress was observed by Dammasa et al. (2006). The maximum monthly mean for the Lakshadweep region is around 30.1°C , and SST in 1987, 1988, and 1991 for the month of May were above the maximum monthly mean value. These very warm summer period could lead to stress in the coral and affect its growth. Such extreme warm conditions may influence the actual SST signal recorded by corals. This suggests that the regional SST variations are recorded more robustly in coral $\delta^{18}\text{O}$ values during monsoon season when compared to $\delta^{18}\text{O}$ values of summer months. When

the above calibration equation is applied to the Kadmat coral values, it is observed that RMSR for reconstructed Δ SST maxima values were higher than that of reconstructed Δ SST minima values (Figure 3.14). This implies that monsoon season reflects SST more accurately as compared to the summer season.

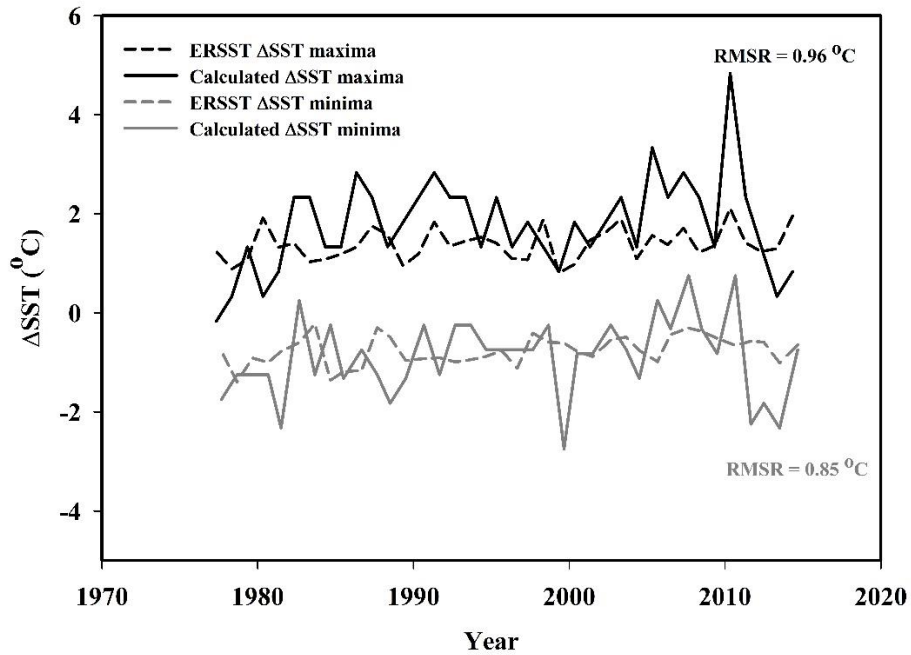


Figure 3.14: Observed Δ SST and calculated Δ SST values using Kadmat coral

3.6. $\delta^{13}\text{C}$ Record of the Kadmat Coral

The coral $\delta^{13}\text{C}$ record for the Kadmat varies between -0.3 and -2.9 ‰. The $\delta^{13}\text{C}$ record shows some seasonality with a mean value of -1.5 ± 0.4 ‰. This mean value is comparable to that reported for the Kavaratti coral record (Chakraborty and Ramesh 1997). It is observed that the Kadmat coral $\delta^{13}\text{C}$ record shows that $\delta^{13}\text{C}$ values are lower during the monsoon period when $\delta^{18}\text{O}$ values are higher (Figure 3.15). However, during the monsoon period of 1999, both $\delta^{13}\text{C}$ and $\delta^{18}\text{O}$ values show simultaneous enrichments, which could be ascribed to reduced growth rates due to stress conditions during that period. The $\delta^{13}\text{C}$ depletion in the Lakshadweep coral during the monsoon period has also been observed in earlier investigations (Chakraborty and Ramesh 1997; Ahmad et al. 2014). However, Ahmad et al. (2011) reported relatively higher $\delta^{13}\text{C}$ values in high-density bands formed during the monsoon season of the Lakshadweep coral. The carbon isotopic composition of the coral skeleton can be influenced by a variety of physiological and environmental factors. The $\delta^{13}\text{C}$ variability in the corals is often linked to the light availability for photosynthesis in corals (Grottoli and Wellington 1999; Rosenfeld

2003; Gagan et al. 2015). The photosynthesis activity by zooxanthellae fixes lighter carbon isotope, leaving the internal DIC pool enriched in heavier carbon isotope. This subsequently leads to coral skeleton carbonate becoming higher in $\delta^{13}\text{C}$ value (McConnaughey 1989a,b). On the other hand, respiration by corals depletes the skeletal $\delta^{13}\text{C}$ value (Swart 1983). Additionally, $\delta^{13}\text{C}$ value of seawater DIC, heterotrophic feeding, and mass spawning can also influence coral $\delta^{13}\text{C}$ values (Gagan et al. 1994; Felis et al. 1998; Dassie et al. 2013). In Lakshadweep during monsoon season, increased upwelling brings nutrient-rich deeper water with lower $\delta^{13}\text{C}$ value to the surface, which increases biological productivity in the Arabian Sea, and could further reduce $\delta^{13}\text{C}$ value of surface waters (Chakraborty and Ramesh 1997). During monsoon, sediment suspension and sedimentation in Lakshadweep waters increases, which in turn reduces the light availability for photosynthesis (Suresh and Matthew 1993). Additionally, increased cloudiness during monsoon also reduces the light reaching to corals for photosynthesis. All these conditions could result in the observed depletion of $\delta^{13}\text{C}$ values in the Kadmat coral during monsoon season. To check the influence of photosynthesis on the Kadmat coral carbon isotopic composition, its $\delta^{13}\text{C}$ values were compared with outgoing longwave radiation (OLR) values (HIRS OLR, Lee et al. 2007) over the region. The mean bimonthly $\delta^{13}\text{C}$ values of Kadmat coral shows the highest value during the May-June period, whereas mean bimonthly OLR maxima occur during the January-February period. The $\delta^{13}\text{C}$ values do not show any correlation with the OLR values over the region. This suggests that the observed $\delta^{13}\text{C}$ variability in the Kadmat coral is not simply modulated by photosynthesis, but some other factors like upwelling, heterotrophy, or some physiological process might also be contributing to the observed $\delta^{13}\text{C}$ variability. Unlike the Kadmat coral and other *Porites* $\delta^{13}\text{C}$ records from the Lakshadweep region (Chakraborty and Ramesh 1997, Ahmad et al. 2014), Ahmad et al. (2011) observed relative enrichment in $\delta^{13}\text{C}$ values of a *Porites* from the Bangaram islands during monsoon. The Bangaram *Porites* belongs to deeper depth (20 m) compared to other corals where relatively less light is available. The effect of light intensity in forcing $\delta^{13}\text{C}$ value of deeper corals is less, and the influence of kinetic effect is more in $\delta^{13}\text{C}$ variability of deeper coral (Rosenfeld et al. 2003). Thus, the observed enrichment in $\delta^{13}\text{C}$ value of the Bangaram coral during monsoon season might be due to the kinetic effect as corals grow slowly in the Lakshadweep region during monsoon season.

Chakraborty and Ramesh (1997) and Ahmad et al. (2011) also reported a long term negative trend/shift in $\delta^{13}\text{C}$ values of the *Porites* corals. A long term decreasing trend is also observed in the Kadmat coral $\delta^{13}\text{C}$ record, however, the slope is very low compared to that observed by

Chakraborty and Ramesh (1997). Such a decreasing trend could be due to processes like the Suess effect in atmospheric CO₂ (Dassie et al. 2013) or due to the changing growth rate of the coral (McConnaughey 1989a). At present, it is difficult to determine the exact cause for such depletion.

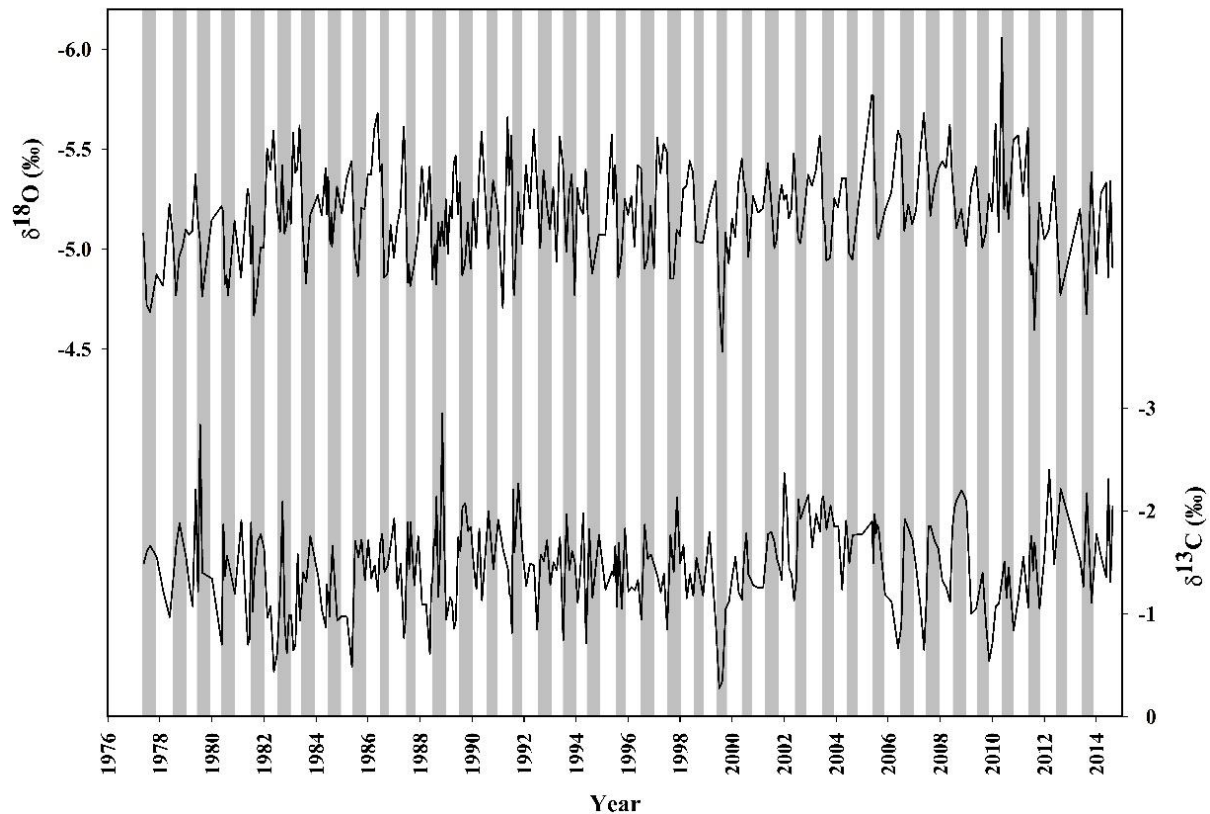


Figure 3.15: Depletion of $\delta^{13}\text{C}$ values of Kadmat coral during monsoon period

This study demonstrates that the coral isotopic records from the Lakshadweep region are influenced by monsoon on both seasonal and interannual scales. The four-year running average of seawater $\delta^{18}\text{O}$ value derived from Lakshadweep coral can be used in identifying periods of enhanced Indian rainfall. There exists inter-colony variability in the Lakshadweep corals, which makes it problematic to reconstruct past SST. Although it is difficult to determine exact SST values from fossil coral $\delta^{18}\text{O}$ values, the SST variability (ΔSST) could be obtained by using mean centered $\delta^{18}\text{O}$ ($\Delta\delta^{18}\text{O}$) values of corals in calibration equation derived here along with the observed monthly average $\Delta\delta^{18}\text{O}_{\text{sw}}$ values. On a seasonal scale, it is observed that $\delta^{18}\text{O}$ values of monsoon month record SST change more faithfully as compared to summer month records. Monsoon also appears to influence the $\delta^{13}\text{C}$ record of Lakshadweep corals as $\delta^{13}\text{C}$ values of the monsoon period mostly show depleted values.

3.7. Inferences

The Kadmat coral showed an average growth rate of 14.7 ± 4.8 mm/yr between 1977-2014. In Lakshadweep, it is observed that coral growing in relatively deeper water show a lower growth rate compared to shallow water corals, which could be related to reduced light availability at deeper depths. Kadmat coral show a decline in growth rate towards the present, suggesting stressed condition for coral growth in recent times. It is observed that the *Porites* corals from the Lakshadweep islands exhibit inter colony variability in $\delta^{18}\text{O}$ values. Therefore, the oxygen isotopic records from the Lakshadweep corals should be carefully interpreted for paleoclimatic studies. Kadmat coral $\delta^{18}\text{O}$ values were used to reconstruct seawater $\delta^{18}\text{O}$ values. On the seasonal scale, the lowest mean $\delta^{18}\text{O}_{\text{sw}}$ value is obtained during winter, which is in agreement with the observation of freshening of Lakshadweep surface waters during the winter season. The four-year running mean value of derived $\delta^{18}\text{O}_{\text{sw}}$ show periods of depletion coinciding with a period of enhanced All India Rainfall, suggesting that the Lakshadweep corals efficiently record rainfall signatures in their isotopic trends and can be used to identify periods of enhanced rainfall. By using mean centered monthly $\delta^{18}\text{O}$ records from Lakshadweep corals and Kadmat coral derived $\delta^{18}\text{O}_{\text{sw}}$ values, a calibration equation was derived. The derived calibration equation could be used to reconstruct past SST variability. It was observed that Lakshadweep coral $\delta^{18}\text{O}$ values corresponding to monsoon month record the regional SST variations more robustly as compared to $\delta^{18}\text{O}$ values of summer months. Kadmat coral $\delta^{13}\text{C}$ record show depletion during the monsoon period. It is observed that $\delta^{13}\text{C}$ variability in Kadmat coral is not only modulated by photosynthesis, but other processes might also be contributing to the observed $\delta^{13}\text{C}$ variability.

Chapter-4
**Significance of Sr/Ca Ratio and Stable Isotope
Composition of Landfall Coral for Paleoclimate
Reconstruction**

4.1. Introduction

Andaman Islands are located on the eastern side of the Bay of Bengal in the northern Indian Ocean. The Andaman islands separate the Andaman Sea from the Bay of Bengal. The Bay of Bengal and the Andaman Sea receive large fluxes of freshwater during monsoon season in the form of rainfall and riverine discharge which is reflected in the reduction in sea surface salinity of the region (Rao and Sivakumar 2003). This freshwater flux also results in surface water stratification (Thadathil et al. 2007). Long term records of these sea surface characteristics can be helpful in understanding past monsoonal variation. Corals growing in the Andaman region are suitable archive to record such changes in the past sea surface characteristic. However, there are limited information available about the proxy records of Andaman corals. Rixen et al. (2011) had analysed stable isotopic composition of a *Porites* coral from the Southern Andaman region and reported strong seasonality in the $\delta^{18}\text{O}$ and $\delta^{13}\text{C}$ record of the analysed coral. They suggested that the coral sampling site was influenced by Arabian Sea High Salinity Water during summer monsoon period via summer monsoon current.

The $\delta^{18}\text{O}$ records of corals are commonly used for understanding past SST changes and also to establish the chronology of coral proxy records. The annual cyclicity of the SST recorded by $\delta^{18}\text{O}$ values can be robustly used to identify year and season in a coral proxy records. This is done with the assumption that coral $\delta^{18}\text{O}$ values mainly represents the SST changes in the region. But for regions influenced by high rainfall or freshwater fluxes, surface seawater $\delta^{18}\text{O}$ values also varies. As both rainwater and riverine freshwater have relatively lower $\delta^{18}\text{O}$ value, their contribution would reduce $\delta^{18}\text{O}$ of surface seawater. These variabilities in seawater $\delta^{18}\text{O}$ value also get embedded in the coral $\delta^{18}\text{O}$ records. Therefore, coral $\delta^{18}\text{O}$ records from region influenced by freshwater flux may not mimic seasonal SST changes, and could be unsuitable for assigning chronology to coral proxy records. In such cases, Sr/Ca proves to be a better representative of SST changes, which is not influenced by seawater $\delta^{18}\text{O}$ value (salinity) changes. Sr/Ca ratio in carbonate (aragonite) skeleton of hermatypic corals show temperature dependent partition coefficient between seawater and coral carbonate (Marshall and McCulloch 2002). This temperature dependence of the partition coefficient of Sr/Ca ratio makes it a good proxy for past sea surface temperature. Additionally, variability of Sr/Ca in seawater is far less than that of seawater $\delta^{18}\text{O}$ value which makes Sr/Ca a relatively 'cleaner' proxy for SST (Correge 2006). Therefore, Sr/Ca record is more appropriate proxy for assigning a reliable chronology to coral dataset. The paired Sr/Ca and $\delta^{18}\text{O}$ records can be effectively used to derive seawater $\delta^{18}\text{O}$ values, which is useful for understanding the variation in sea

surface conditions in the region. Landfall island is situated in the northern Andaman Sea close to the Irrawaddy delta. Irrawaddy is one of the major river system with annual freshwater discharge of $411 \pm 53 \text{ km}^3$ (Ramaswamy et al. 2008). As the Landfall Island is close to the Irrawaddy river mouth, it is expected to be influenced by the freshwater discharge of the river. Thus, for Landfall coral, Sr/Ca measurements were carried out along with $\delta^{18}\text{O}$ measurements. This paired measurement of $\delta^{18}\text{O}$ and Sr/Ca helped in assigning robust chronology and deriving valuable information about seawater $\delta^{18}\text{O}$ changes of the region.

The chronology of the Landfall coral was established for the top 65 mm based on Sr/Ca record by interpolating data points on monthly scale between the anchor points. The anchor points were fixed to the month of SST maxima and minima in the Andaman Sea. The Andaman Sea shows double peak of SST high and low every year. Thus, SST maxima around May and October were tied to Sr/Ca minima. SST minima occurring around January and August were tied to Sr/Ca maxima. The rest of the data in top 65 mm of coral were linearly interpolated between these four tie points on monthly scale. As samples below 65 mm were sub-sampled at relatively lower resolution, they were interpolated on bimonthly scale. The monthly resolution of Sr/Ca and $\delta^{18}\text{O}$ data of top 65 mm were converted to bimonthly scale and it was observed that bimonthly maxima and minima of Sr/Ca matches that of $\delta^{18}\text{O}$ values. These maxima and minima corresponds to January-February and May-June months respectively. Thus, for chronology of samples below 65 mm, $\delta^{18}\text{O}$ maxima and minima were tied to months of January-February and May-June respectively. Remaining data points were interpolated between these anchor points.

4.2. The Growth Rate of Landfall Coral

The Landfall coral data spans 69 years between 1948-2017. The average growth rate of the Landfall *Porites* coral between 1948-2017 period was $9.4 \pm 2.4 \text{ mm/yr}$ (Figure 4.1). This growth rate is slightly lower when compared to the growth rate of 11.9 mm/yr for *Porites* coral from the Port Blair analysed by Rixen et al. (2011). However, the growth rate of Landfall Island *Porites* coral falls within the observed range of growth rate of *Porites* coral from the Andaman Sea (Scoffin et al. 1992). A long term decreasing trend in the growth rate of the Landfall coral is observed. A general decreased growth rate is observed after 1998. The mean growth rate between 1949-1998 was $10.1 \pm 2.3 \text{ mm/yr}$, which decreased by 22 % to a mean of $7.9 \pm 1.8 \text{ mm/yr}$ between 1999-2017. De'ath et al. (2009) had reported decrease in calcification rate of *Porites* coral mainly due to decline in growth rate since 1990 in the Great Barrier Reef,

Australia. Ahmad et al. (2014) observed up to 15 % decrease in calcification rate in a *Porites* coral from the Lakshadweep Islands since 1996. The Kadmat coral discussed in previous chapter also showed a decreasing growth rate towards present. The decline in coral growth rate from these two distant islands indicates that the environmental stress responsible for this decline might not be local but regional. The observed reduction in coral growth rates from the Andaman and Lakshadweep islands could be related to the thermal stress induced on these corals due to warming of the Indian Ocean. Various studies have shown and discussed the warming of the Indian Ocean in last few decades (Alory et al. 2007, Swapna et al. 2014, Roxy et al. 2014). Swapna et al. (2014) observed that since 1960s the Indian Ocean SST is warming at rate of 0.15 °C per decade and 0.06 °C per decade for monsoon and non-monsoon months. Marshal and Clode (2004) had suggested that temperature affects the fundamental calcification process in corals and observed that calcification rates reduces as SST approaches seasonal maxima. Bleaching of corals is also observed when warmer than average SST condition prevail in a region. Brown et al. (1996) reported bleaching in corals from the Andaman Sea during period of elevated maximum seasonal SST in the region. Tanzil et al (2009) had shown decline in growth rates of corals from the Andaman Sea and linked it to rise in the SST of the region. Arora et al. (2019) suggested high thermal stress on coral from the Andaman and Lakshadweep islands due to elevated SST increase, causing mass bleaching events in these regions. However, ocean acidification could also be a reason for decline in coral growth rate (Manzello 2010). More investigation is required to identify the factor behind the observed reduction in growth rate of *Porites* corals in the Andaman and Lakshadweep islands.

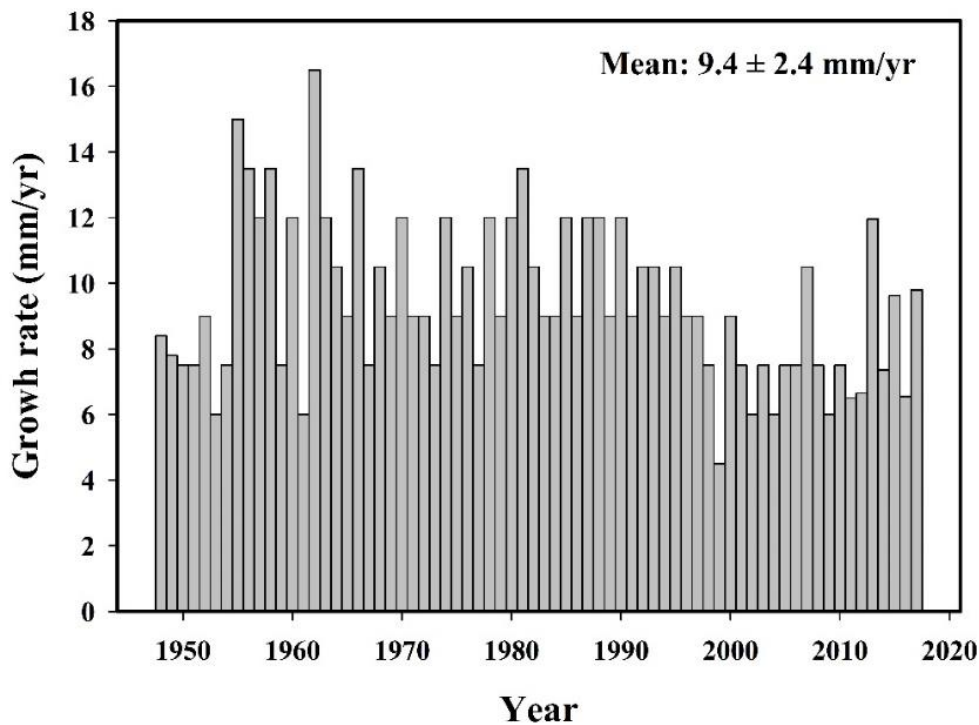


Figure 4.1: Growth rate of Landfall coral between 1949-2017

4.3. 2012-2017: Monthly Records

The top 65 mm length record of the Landfall coral corresponds to the 5 year period between 2012 to 2017. The coral samples for this interval were measured for Sr/Ca, $\delta^{18}\text{O}$ and $\delta^{13}\text{C}$ values. All the three proxies show seasonal variations. Sr/Ca and $\delta^{18}\text{O}$ values show a linear correlation ($R = 0.48$, $p < 0.001$) with each other. This correlation is observed because both vary as a function of SST. It is also observed that $\delta^{13}\text{C}$ values show distinct seasonal depletion each year. These geochemical and isotopic records are analysed in the following sections.

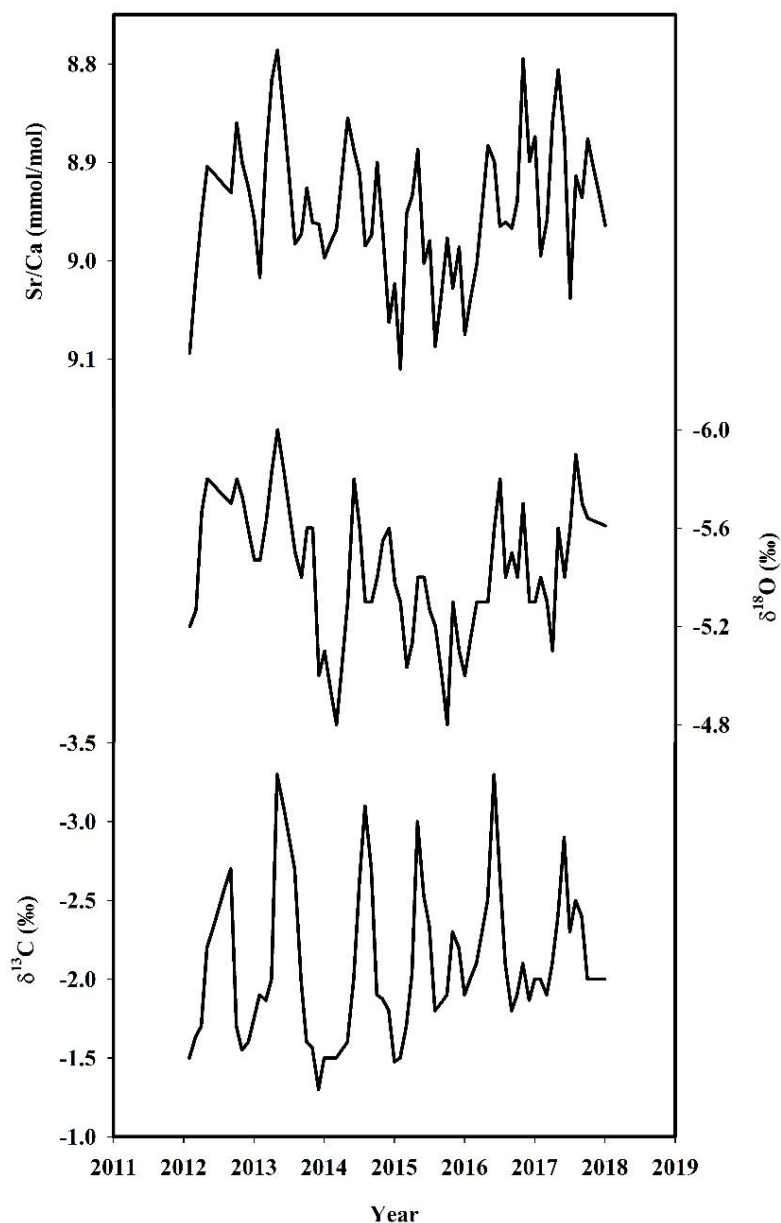


Figure 4.2: Geochemical records of the Landfall coral showing seasonality in Sr/Ca, $\delta^{18}\text{O}$ and $\delta^{13}\text{C}$ values between 2012-2017

4.3.1. Paired Sr/Ca and $\delta^{18}\text{O}$ Record

The annual bands between 2012-2017 from the Landfall coral were analysed for their Sr/Ca ratio and stable oxygen and carbon isotopic composition. The Sr/Ca ratio in these six year band ranges from 8.78 to 9.11 mmol mol⁻¹ with mean value of 8.95 ± 0.07 mmol mol⁻¹. The monthly Sr/Ca values show two maxima and two minima every year (Figure 4.2). Highest Sr/Ca value is observed during the month of February 2015 and lowest value in the month of May 2013. Average seasonality of the Landfall coral Sr/Ca values is 0.19 mmol mol⁻¹, which translates to 3.2 °C using general Sr/Ca-SST relationship (-0.06 mmol mol⁻¹ °C⁻¹) for *Porites* coral (Corrège

2006). The seasonality of 3 °C (ERSSTv5) for mean SST for the period 2012-2017 is comparable to that derived from coral Sr/Ca value, suggesting that Sr/Ca values of Landfall coral records the SST variations of the region.

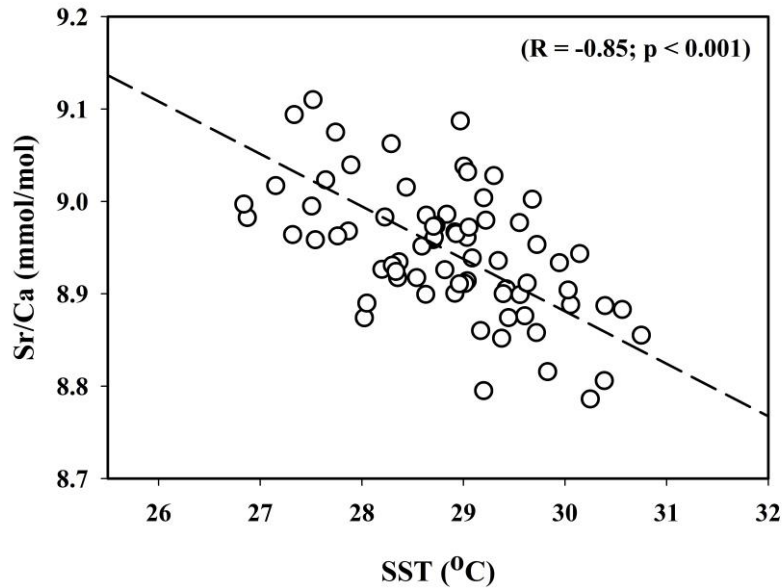


Figure 4.3: Linear correlation between the Landfall coral Sr/Ca values and sea surface temperature of the region

The monthly Landfall coral Sr/Ca values show a significant negative correlation with SST values of the region (Figure 4.3). Following correlation is obtained between seasonal extreme values of Landfall coral Sr/Ca values and SST values,

$$\text{Sr/Ca} = [(-0.057) \times \text{SST}] + 10.585 \quad (R = -0.85, p < 0.001) \quad (1)$$

The slope of the Landfall coral Sr/Ca-SST relation ($-0.057 \text{ mmol mol}^{-1} \text{ } ^\circ\text{C}^{-1}$) is within the range of -0.04 to $-0.08 \text{ mmol mol}^{-1} \text{ } ^\circ\text{C}^{-1}$ observed by others (Smith et al. 1979, Shen et al. 1996, Quinn and Sampson 2002, Fallon et al. 2003, Corrège 2006, Murty et al. 2018). Table 4.1 lists Sr/Ca-SST relation obtained for *Porites* from other Indian Ocean region (Heiss et al. 1997, Marshall and McCulloch 2001, Felis et al. 2004, Zinke et al. 2004, Pfeiffer et al. 2009, Sagar et al. 2016, Watanabe et al. 2017) and the Landfall coral Sr/Ca-SST relation is comparable to these equations.

Table 4.1: Sr/Ca-SST calibration obtained for *Porites* corals from the Indian Ocean region

Study	Location	Slope (m)	Intercept (c)	R²	Source of SST
Heiss et al. 1997	La Reunion	-0.061	10.577	0.84	COADS
Marshall and McCulloch 2001	Xmas Island	-0.0593	10.375	0.69	IGOSS
Felis et al. 2004	Eliat, Red Sea	-0.0597	10.781	0.78	Local SST
Zinke et al. 2004	Madagascar	-0.05	10.348	0.89	GISST
Pfeiffer et al. 2009	Chagos	-0.077	10.94	0.49	ERSST
Sagar et al. 2016	Lakshadweep	-0.104	12.08	0.73	ERSST
Watanabe et al. 2017	Oman	-0.044	10.46	0.90	AVHRR
This study	Andaman	-0.057	10.585	0.72	ERSST

It is observed that slope and intercept of the Sr/Ca-SST relation of the Indian Ocean corals show linear relation (Figure 4.4). Marshal and McCulloch (2002) also reported such spread in the Sr/Ca calibrations of different corals. They suggested that the observed linear relationship between intercept and slope of the Sr/Ca-SST relation could help validate the obtained calibration. However, the reason for such linear correlation was not given, and it was suggested that linear spread show that coral from different regions respond to the local environment (Marshal and McCulloch 2002). D’Olivo et al. (2018) explained the linear relationship between the intercept and slope of Sr/Ca-SST relation mathematically. They suggested that correlation results due to narrow range of Sr/Ca and SST data, which falls within a constrained area located far from zero on both axis. The Sr/Ca-SST relation of Landfall coral falls along the linear spread of slope-intercept relation of Indian Ocean corals, which validates the derived correlation equation.

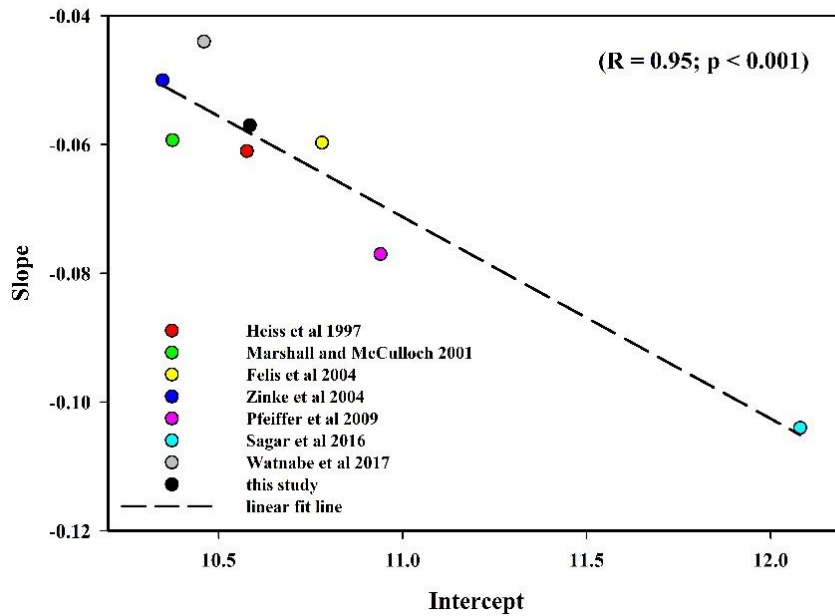


Figure 4.4: Linear correlation between slope and intercept of Sr/Ca-SST relation of *Porites* corals from Indian Ocean

A significant correlation between the Landfall coral Sr/Ca value and SST suggests that Sr/Ca in *Porites* corals from the Andaman can be potentially used as a paleothermometer for the region. Based on the observed slope ($-0.057 \text{ mmol mol}^{-1} \text{ }^{\circ}\text{C}^{-1}$), SST seasonality explains 89 % of the coral Sr/Ca seasonality. The Sr/Ca values also show dual oscillation nature of SST variability observed in the Andaman region (Rengarajan and Marichamy 1972). This further affirms that seasonality of SST in Andaman is recorded in coral Sr/Ca values. Using obtained Sr/Ca-SST relation, monthly SST values were calculated. For accuracy, observed and calculated SST were compared. The difference between monthly maxima and minima of observed and calculated SST ranges between -1.4 to $1.6 \text{ }^{\circ}\text{C}$. For monthly values, the difference ranged between -2.3 to $2.6 \text{ }^{\circ}\text{C}$. The root mean square residual (RMSR) for reconstructed monthly SST values was $1.0 \text{ }^{\circ}\text{C}$ (Figure 4.5). The RMSR value for reconstructed minima and maxima was $1.1 \text{ }^{\circ}\text{C}$ and $0.8 \text{ }^{\circ}\text{C}$ respectively, indicating that warmest months reflect SST more accurately than coolest months.

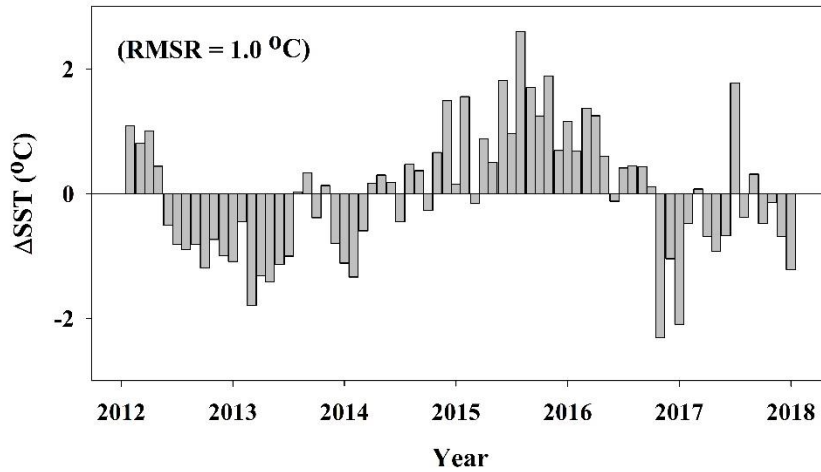


Figure 4.5: Difference between observed monthly SST and reconstructed monthly SST using coral Sr/Ca values

The oxygen isotopic composition of Landfall coral shows seasonal variability ranging between -4.8 to -6.0 ‰ (Figure 4.2). The mean coral $\delta^{18}\text{O}$ value is -5.4 ± 0.3 ‰ between 2012-2017. When seasonal extremes of the Landfall coral $\delta^{18}\text{O}$ value and SST values were compared following correlation was observed,

$$\delta^{18}\text{O} = [(-0.08) \times \text{SST}] - 3.26 \quad (R = -0.25, p < 0.03) \quad (2)$$

The weak correlation and low slope value suggests that apart from SST, $\delta^{18}\text{O}$ of seawater also has contribution to the coral $\delta^{18}\text{O}$ values. The Bay of Bengal and Andaman Sea receives large flux of freshwater annually (Delaygue et al. 2001, Rao and Sivakumar 2003, Sengupta et al. 2006, Achyutan et al. 2013). The river runoff, precipitation and evaporation together drives the $\delta^{18}\text{O}$ of seawater in this region. During pre-monsoon period between March-May, the river discharge in the region is low, and evaporation is high due to rise in SST. This leads to increase in both salinity and $\delta^{18}\text{O}$ of seawater in the region during pre-monsoon period. Whereas, due to increase river runoff during summer monsoon period, salinity and $\delta^{18}\text{O}$ of seawater decreases (Achyutan et al. 2013). Thus, the SST and the seawater $\delta^{18}\text{O}$ value of the region should have contrasting influence on coral $\delta^{18}\text{O}$ values. This contrasting influence explains the lower slope of coral $\delta^{18}\text{O}$ -SST correlation compared to general range of $0.18 - 0.23$ ‰°C⁻¹, and suggests that $\delta^{18}\text{O}$ of seawater plays a crucial role in driving the coral $\delta^{18}\text{O}$ changes in this region. This also implies that coral $\delta^{18}\text{O}$ values alone from the Andaman region may not provide good estimates of SST changes. To reconstruct SST variability using Andaman coral $\delta^{18}\text{O}$ values, seawater $\delta^{18}\text{O}$ variability of the region is required. But, seawater $\delta^{18}\text{O}$ observations from the Andaman region is scarce. Nevertheless, the same can be obtained from coral $\delta^{18}\text{O}$ values.

Paired Sr/Ca and $\delta^{18}\text{O}$ values of a coral can be used to reconstruct $\delta^{18}\text{O}$ value of seawater (McCulloch et al. 1994, Gagan et al. 1998). This pairing approach is used to reconstruct $\delta^{18}\text{O}$ of seawater from Sr/Ca and $\delta^{18}\text{O}$ data of the Landfall coral.

Different methods have been employed to obtain $\delta^{18}\text{O}$ of seawater using paired Sr/Ca and $\delta^{18}\text{O}$ coral data (McCulloch et al. 1994, Gagan et al. 1998, Ren et al. 2003, Cahyarini et al. 2008, Bolton et al. 2014). Using the observed coral $\delta^{18}\text{O}$ -SST correlation to convert coral $\delta^{18}\text{O}$ values to temperature unit, and then subtracting it from coral Sr/Ca derived temperature can result in spurious seawater $\delta^{18}\text{O}$ values (Cahyarini et al. 2008). The slope and intercept of coral $\delta^{18}\text{O}$ -SST correlation can be modified by seawater $\delta^{18}\text{O}$ values of the region. The covarying SST and SSS can reduce the seasonality of coral $\delta^{18}\text{O}$ values, and subsequently the slope of coral $\delta^{18}\text{O}$ -SST relation. The intercept of coral $\delta^{18}\text{O}$ -SST correlation includes components of both SST and SSS. Centering method suggested by Cahyarini et al. (2008) removes the intercept value of coral $\delta^{18}\text{O}$ (Sr/Ca)-SST correlation for seawater $\delta^{18}\text{O}$ calculation. Removing intercept will center the linear regression by omitting the mean value of the variable. Centering is done by normalizing the data to its mean value. This method states that variation in coral $\delta^{18}\text{O}$ value relative to its mean can be defined as the sum of $\delta^{18}\text{O}_{\text{SST}}$ relative to mean $\delta^{18}\text{O}_{\text{SST}}$ and $\delta^{18}\text{O}_{\text{sw}}$ relative to mean $\delta^{18}\text{O}_{\text{sw}}$, where $\delta^{18}\text{O}_{\text{SST}}$ is SST contribution to coral $\delta^{18}\text{O}$ value and $\delta^{18}\text{O}_{\text{sw}}$ is seawater $\delta^{18}\text{O}$ contribution to coral $\delta^{18}\text{O}$ value (Cahyarini et al 2008). Thus, coral $\delta^{18}\text{O}$ relative to its mean can be represented as

$$\Delta\delta^{18}\text{O}_{\text{coral}} = \Delta\delta^{18}\text{O}_{\text{SST}} + \Delta\delta^{18}\text{O}_{\text{sw}} \quad (3)$$

Mean centered SST contribution to coral $\delta^{18}\text{O}$ value ($\Delta\delta^{18}\text{O}_{\text{SST}}$) can be estimated using regression slope of coral $\delta^{18}\text{O}$ vs SST, regression slope of coral Sr/Ca vs SST and coral mean centered Sr/Ca values. The centering method allows use of known slope of coral $\delta^{18}\text{O}$ -SST relationship for calculating seawater $\delta^{18}\text{O}$ value of regions, where SST covaries with SSS and seawater $\delta^{18}\text{O}$ value. Andaman is one such region where monthly SST and SSS variations show similar trend (Rengarajan and Marichamy 1972). Therefore, centering method was applied to obtain seawater $\delta^{18}\text{O}$ values recorded by the Landfall coral. The formula used to calculate seawater $\delta^{18}\text{O}$ value is,

$$\Delta\delta^{18}\text{O}_{\text{sw}} = \Delta\delta^{18}\text{O}_{\text{coral}} - [(\gamma/\beta) \times \Delta\text{Sr/Ca}] \quad (4)$$

where $\Delta\delta^{18}\text{O}_{\text{sw}}$, $\Delta\delta^{18}\text{O}_{\text{coral}}$ and $\Delta\text{Sr/Ca}$ are mean centered values of seawater $\delta^{18}\text{O}$, coral $\delta^{18}\text{O}$ and coral Sr/Ca ratio. γ and β are regression slope of coral $\delta^{18}\text{O}$ -SST and Sr/Ca-SST respectively. The value of γ used here is general slope of coral $\delta^{18}\text{O}$ -SST relation ($-0.18 \text{‰}^{\circ}\text{C}^{-1}$)

¹), as correlation slope of the Landfall coral $\delta^{18}\text{O}$ -SST is too low ($-0.08 \text{ ‰}^\circ\text{C}^{-1}$). The β value used is ($-0.057 \text{ mmol mol}^{-1} \text{ }^\circ\text{C}^{-1}$) the slope obtained for the Landfall coral Sr/Ca-SST correlation. The error associated with $\Delta\delta^{18}\text{O}_{\text{sw}}$ is calculated by using following equation,

$$\sigma_{\Delta\delta_{\text{sw}}}^2 = \sigma_{\delta_{\text{coral}}}^2 + [(\gamma/\beta)^2 \times \sigma_{\text{Sr/Ca}}^2] \quad (5)$$

where $\sigma_{\Delta\delta_{\text{sw}}}$ is error in calculated $\Delta\delta^{18}\text{O}_{\text{sw}}$ values, $\sigma_{\delta_{\text{coral}}}$ is error in coral $\delta^{18}\text{O}$ measurement and $\sigma_{\text{Sr/Ca}}$ is error in coral Sr/Ca measurement.

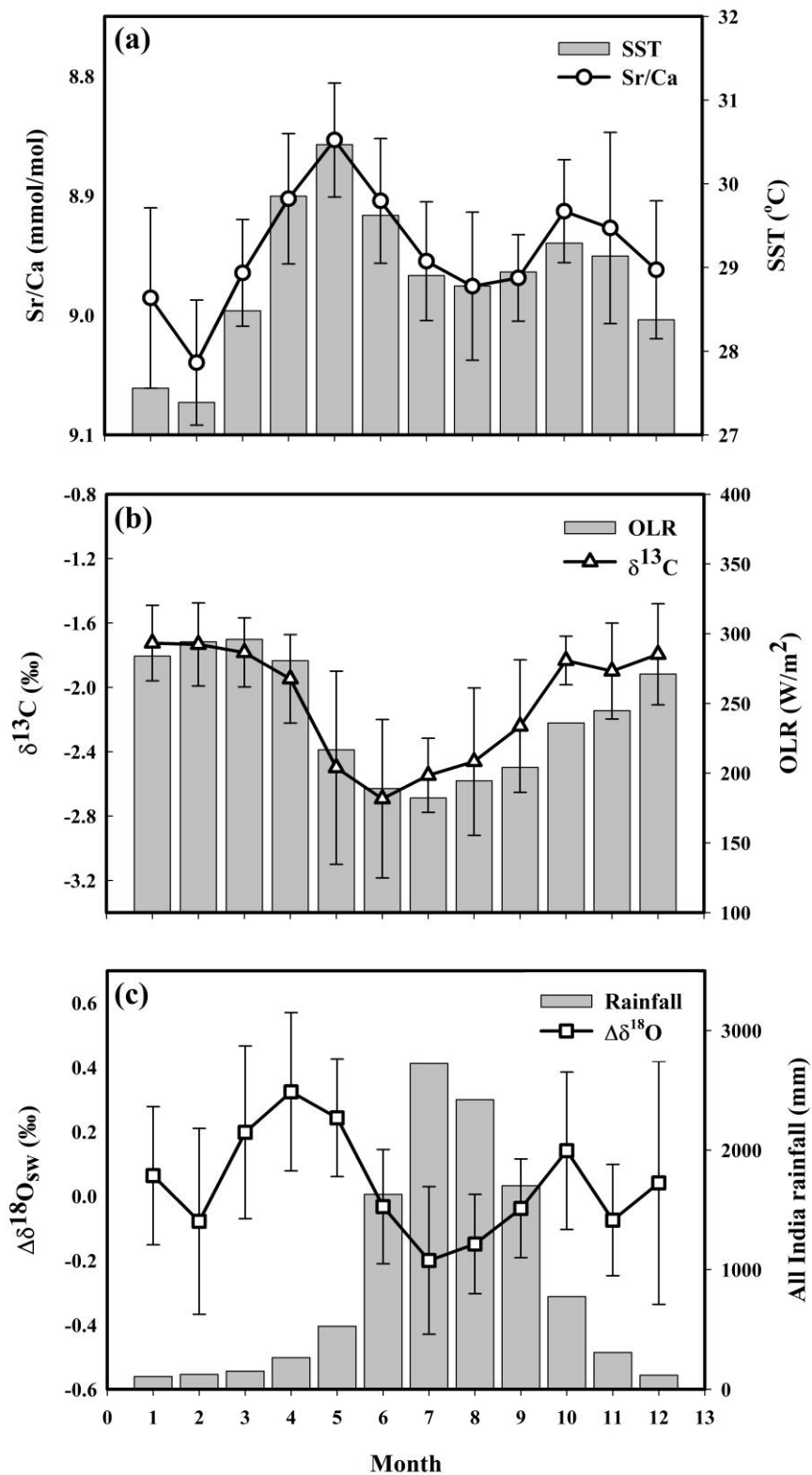


Figure 4.6: (a) Mean monthly values of sea surface temperature (SST) and Sr/Ca ratio of Landfall coral, (b) mean monthly values of outgoing longwave radiation (OLR) and $\delta^{13}\text{C}$ of Landfall coral, (c) mean monthly values of All India Rainfall and reconstructed $\Delta\delta^{18}\text{O}_{\text{sw}}$

4.3.2. Seawater $\delta^{18}\text{O}$ Variability in Andaman

Using paired Sr/Ca and $\delta^{18}\text{O}$ values of corals, $\Delta\delta^{18}\text{O}_{\text{sw}}$ values were obtained. The $\Delta\delta^{18}\text{O}_{\text{sw}}$ values obtained from the Landfall coral ranges between -0.5 to 0.6 ‰ between 2012-2017. The peak of mean monthly $\Delta\delta^{18}\text{O}_{\text{sw}}$ values is around April-May, months which have high SST values (Figure 4.6). During these months, the Andaman receives low rainfall compared to monsoon period, and evaporation is maximum. These together can result in the increase of $\Delta\delta^{18}\text{O}_{\text{sw}}$ values during this period. The minima of $\Delta\delta^{18}\text{O}_{\text{sw}}$ is around July-August month, unlike SST minima which is around January-February. This is because during July-August (monsoon) period, Andaman receives maximum rainfall (Kumar et al. 2012). As precipitation and river discharge reaches maximum during this season and SST reduces, the $\Delta\delta^{18}\text{O}_{\text{sw}}$ value reaches its minima in the region. The seasonality of calculated average monthly $\Delta\delta^{18}\text{O}_{\text{sw}}$ data between 2012-2017 is 0.52‰. As Landfall Island is closer to the Irrawaddy delta, the seasonal freshwater discharge can result in such variation in $\delta^{18}\text{O}$ of seawater in the region. Rengarajan and Marichamy (1972) had observed monthly salinity variation of about 3.1 in Andaman over the year. Using the slope of 0.15 ‰ per salinity unit (Sengupta et al. 2013), the salinity range observed in Andaman should amount to 0.47 ‰, which is comparable to the seasonality of $\Delta\delta^{18}\text{O}_{\text{sw}}$ (0.52 ‰) recorded by the Landfall coral. Using equation (4), error in coral $\delta^{18}\text{O}$ and Sr/Ca measurement of 0.1 ‰ and 0.02 mmol mol⁻¹ respectively yields an error of 0.12 ‰ in $\Delta\delta^{18}\text{O}_{\text{sw}}$ values. The error in reconstructed $\Delta\delta^{18}\text{O}_{\text{sw}}$ values is lower than seasonal variability of $\Delta\delta^{18}\text{O}_{\text{sw}}$ in Andaman. Thus, the seasonal cycle of $\Delta\delta^{18}\text{O}_{\text{sw}}$ near Landfall can be determined using paired Sr/Ca and $\delta^{18}\text{O}$ data of *Porites* from the region. Average monthly $\Delta\delta^{18}\text{O}_{\text{sw}}$ values show maximum in April, which agrees with observed monthly SSS high around April near Port Blair, Andaman (Rengarajan and Marichamy 1972). This high is followed by low $\Delta\delta^{18}\text{O}_{\text{sw}}$ period during monsoon, when high precipitation and river discharge reduces SSS in the region. Indian summer monsoon rainfall brings major freshwater flux in the region in the form of precipitation and riverine discharge. This flux of freshwater during monsoon season decreases the salinity and $\delta^{18}\text{O}$ value of seawater. Therefore, seasons with intense summer monsoon rainfall should be reflected in $\Delta\delta^{18}\text{O}_{\text{sw}}$ recorded by the coral.

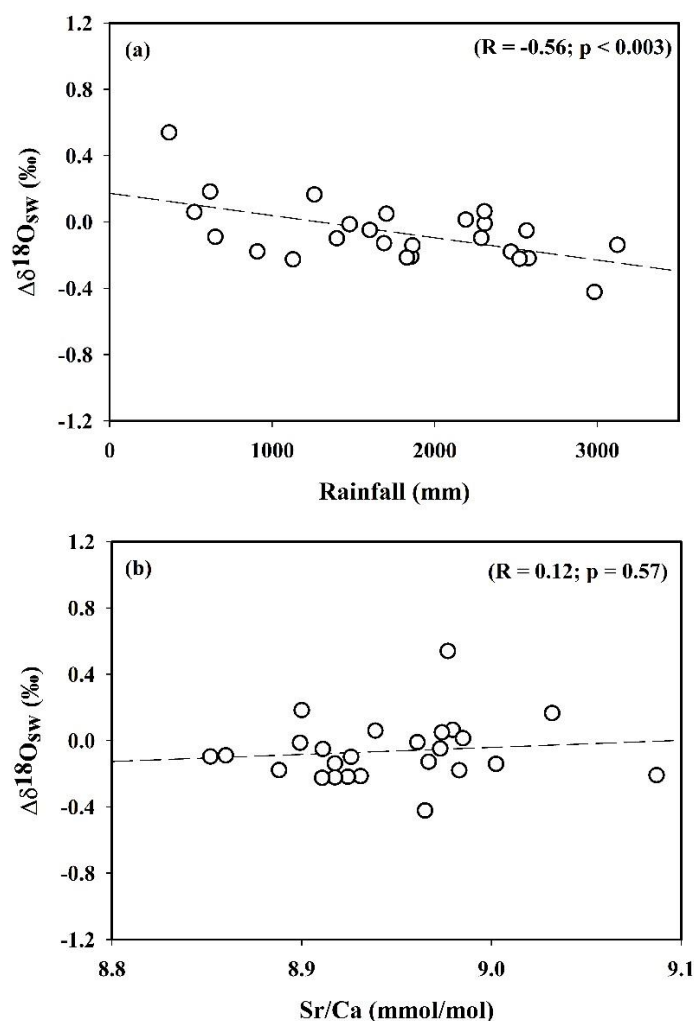


Figure 4.7: Correlation of reconstructed $\Delta\delta^{18}\text{O}_{\text{sw}}$ with (a) rainfall and (b) coral Sr/Ca ratio for time period between June and October

Figure 4.7 shows correlation of $\Delta\delta^{18}\text{O}_{\text{sw}}$ with rainfall and coral Sr/Ca values during monsoon period (June-October). The all India rainfall value and $\Delta\delta^{18}\text{O}_{\text{sw}}$ values show significant correlation ($R = 0.56$, $p < 0.003$), but no significant correlation is observed between $\Delta\delta^{18}\text{O}_{\text{sw}}$ and Sr/Ca values. This suggests that rainfall influences surface waters oxygen isotopic composition during this season. Rainfall and related riverine flux has lower $\delta^{18}\text{O}$ value as compared to seawater. The freshwater input to the northern Bay of Bengal and Andaman Sea decreases the oxygen isotopic values of surface seawater. During period of enhanced monsoon rainfall more riverine discharge to the northern Bay of Bengal and Andaman Sea could result in increased depletion of surface water $\delta^{18}\text{O}$ value. Insignificant correlation of $\Delta\delta^{18}\text{O}_{\text{sw}}$ with Sr/Ca values (proxy of temperature) suggests that surface water temperature does not effect surface water oxygen isotopic composition during this period. It is perhaps because riverine discharge and rainfall dominate during monsoon period essentially changes the isotopic

composition of the seawater. $\Delta\delta^{18}\text{O}_{\text{sw}}$ values for period between November and May were also correlated with rainfall and coral Sr/Ca (Figure 4.8). Interestingly, during this period $\Delta\delta^{18}\text{O}_{\text{sw}}$ values do not show significant correlation with rainfall. A significant correlation ($R = 0.48$, $p < 0.002$) with Sr/Ca values was observed. This implies that during the November to May period, surface water temperature regulates the surface water oxygen isotopic composition of the region but not the rainfall. The significant correlation between rainfall and $\Delta\delta^{18}\text{O}_{\text{sw}}$ during monsoon period (June-October) suggests that by reconstructing $\Delta\delta^{18}\text{O}_{\text{sw}}$ from *Porites* coral of the study area, qualitative reconstruction of past seasonal monsoon rainfall can be obtained. The obtained $\Delta\delta^{18}\text{O}_{\text{sw}}$ values can also be used to obtain $\delta^{18}\text{O}$ -SST relation for the region.

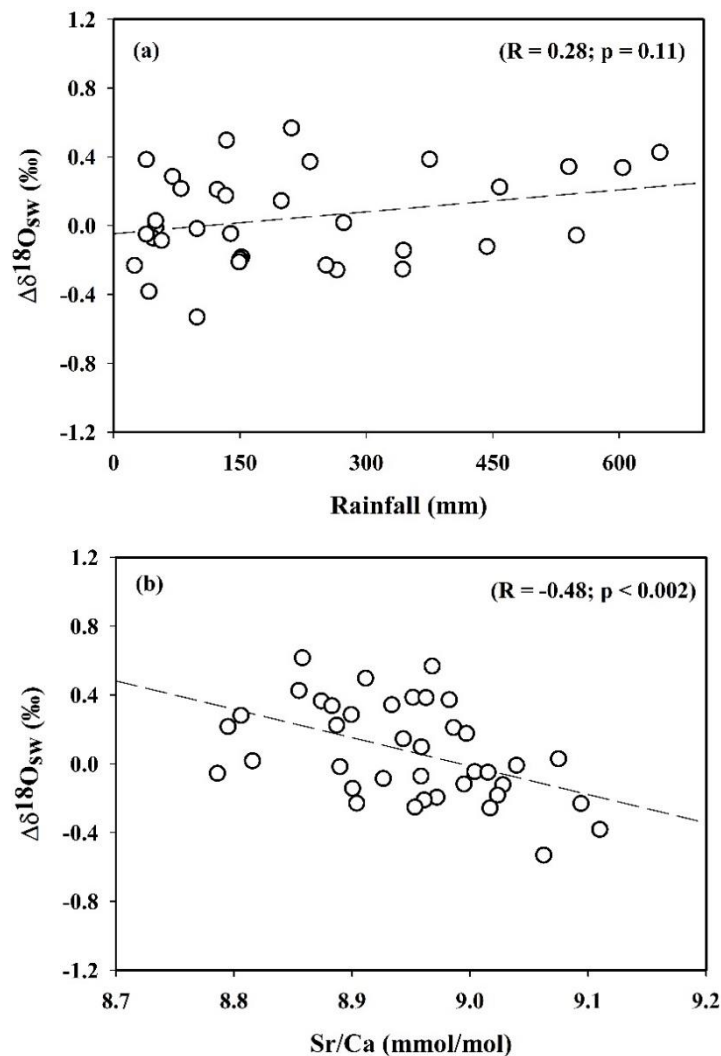


Figure 4.8: Correlation of reconstructed $\Delta\delta^{18}\text{O}_{\text{sw}}$ with (a) rainfall and (b) coral Sr/Ca ratio for time period between November and May

4.3.3. $\delta^{13}\text{C}$ Variability in Landfall Coral

The $\delta^{13}\text{C}$ value of the Landfall coral shows a good seasonality, with prominent depletion around monsoon season. The coral $\delta^{13}\text{C}$ values varies between -1.3 to -3.3 ‰ with mean value of -2.1 ± 0.5 ‰. Seasonal depletion of around 1 ‰ in $\delta^{13}\text{C}$ values is observed each year, and most depleted values occur between May to August. Unlike $\delta^{18}\text{O}$, coral $\delta^{13}\text{C}$ composition is influenced by both kinetic and metabolic effects. Kinetic effect leads to enrichment of lighter isotopes of carbon and oxygen during hydration and hydroxylation of CO_2 in corals (McConnaughy 1989b). Metabolic effect further alters coral $\delta^{13}\text{C}$ composition due to processes like photosynthesis and respiration in corals. Photosynthesis carried out by symbiotic algae in hermatypic corals greatly influences coral $\delta^{13}\text{C}$ values. Photosynthesis preferentially takes lighter carbon isotope and leaves the internal DIC pool enriched in heavier carbon isotope (Swart 1983, McConnaughy 1989a, 1989b). Apart from photosynthesis other factors like $\delta^{13}\text{C}$ value of seawater, respiration of corals, feeding habit or mass spawning of corals can also influence coral $\delta^{13}\text{C}$ values (Gagan et al. 1994, Felis et al. 1998, Grottoli and Wellington 1999, Rosenfeld et al. 2003, Dassie et al. 2013, Gagan et al. 2015).

Like $\delta^{18}\text{O}$ value, the monsoon also appears to be modulating carbon isotope of the Landfall coral. The distinct depletion of coral $\delta^{13}\text{C}$ values during monsoon period both at monthly and bimonthly scale implies that the environmental and or physiological factors affecting carbon isotope of the Landfall coral is related to monsoon in the region. Physiological factors like photosynthesis and respiration in corals have contrasting influence on coral $\delta^{13}\text{C}$ value. However, in coral $\delta^{13}\text{C}$ value, enrichment due to photosynthesis is much larger than depletion by respiration in corals (McConnaughy, 1989b). Feeding of zooplanktons with lower $\delta^{13}\text{C}$ value also affects the coral $\delta^{13}\text{C}$ values (Grottoli and Wellington 1999). In Andaman, increase in planktonic organisms is observed during colder months (Rengarajan and Marichamy 1972), implying that the coral $\delta^{13}\text{C}$ values should be lower during winter months. But depleted $\delta^{13}\text{C}$ values in Landfall coral occur during summer monsoon period, negating zooplankton feeding of coral as reason for observed $\delta^{13}\text{C}$ value depletion in Landfall coral. Additionally, light availability for corals generally play significant role in modulating corals $\delta^{13}\text{C}$ values. As symbiont zooxanthellae in corals fixes ^{12}C during photosynthesis, it leaves corals internal DIC pool enriched in ^{13}C leading to increase in skeletal $\delta^{13}\text{C}$ values.

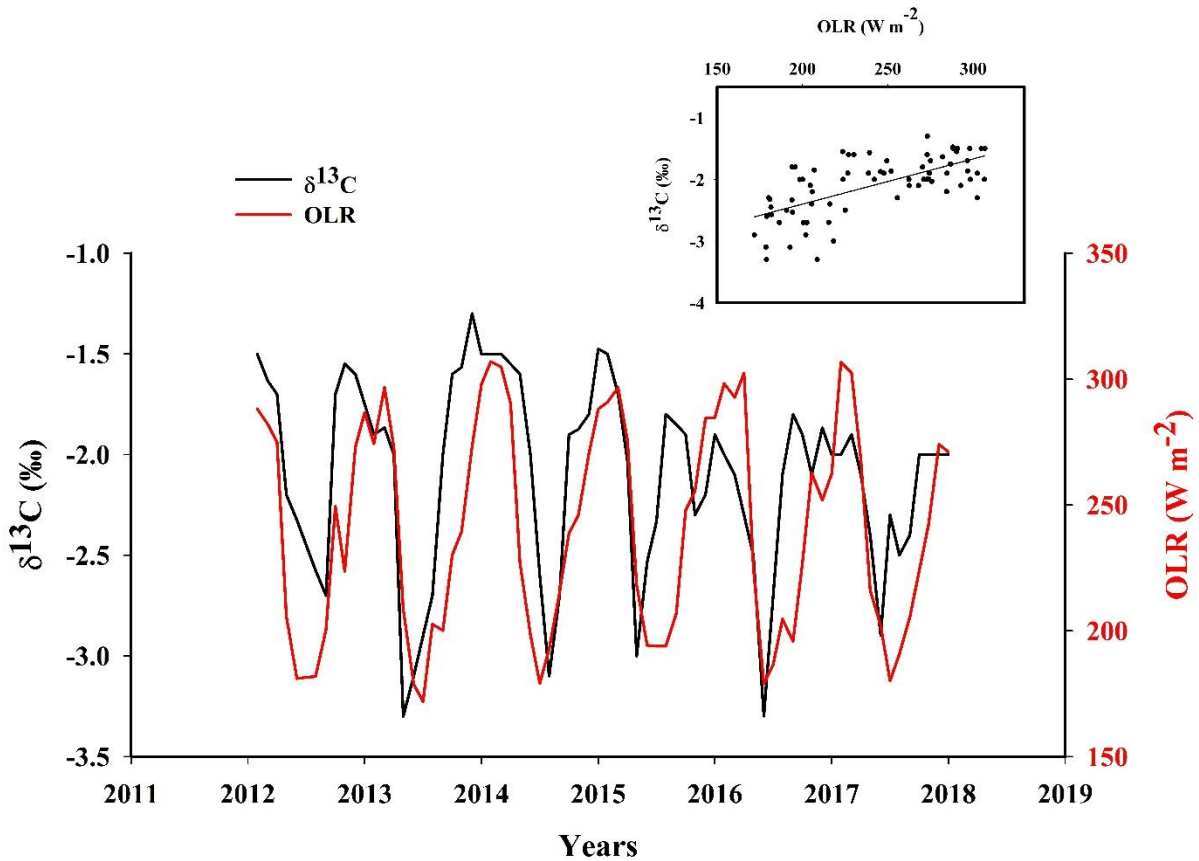


Figure 4.9: Monthly $\delta^{13}\text{C}$ values of the Landfall coral and outgoing longwave radiation (OLR) values over the region. (inset: correlation plot between monthly $\delta^{13}\text{C}$ values and outgoing longwave radiation)

To investigate the influence of photosynthetic activity on the Landfall coral carbon isotope, $\delta^{13}\text{C}$ values were compared with OLR (Outgoing Longwave Radiation) values, which indicates the cloud cover over the region. Figure 4.9 show the monthly OLR variation along with Landfall coral $\delta^{13}\text{C}$ values, where it can be observed that coral $\delta^{13}\text{C}$ value depletes when OLR is low and vice versa. Monthly OLR values show significant correlation with $\delta^{13}\text{C}$ values ($R = 0.66$, $p < 0.001$). The positive correlation between OLR and $\delta^{13}\text{C}$ value implies that coral $\delta^{13}\text{C}$ values record seasonal variation in photosynthetic activity of corals due to change in light availability during monsoon season. The difference between $\delta^{13}\text{C}$ values of monsoon and non-monsoon period can be used as support for chronology proxy in *Porites* corals from the region. In absence of coral Sr/Ca records, $\delta^{13}\text{C}$ values can be useful in identifying monsoon and non-monsoon period in coral annual density bands in this region.

4.4. 1949-2011: Bimonthly Records

Landfall coral samples between 1949-2011 were analysed for stable oxygen and carbon isotopic composition at bimonthly resolution. Both oxygen and carbon isotope data show

seasonal variations (Figure 4.10). The bimonthly $\delta^{18}\text{O}$ value ranges between -4.9 to -6.3 ‰ for the period 1949-2011 with a mean of -5.5 ± 0.2 ‰. The bimonthly $\delta^{13}\text{C}$ data has a mean of -1.7 ± 0.6 ‰ and varies between -0.5 to -3.6 ‰. The bimonthly $\delta^{18}\text{O}$ and $\delta^{13}\text{C}$ values between 1949-2011 show a weak positive correlation ($R = 0.43$; $p < 0.001$), also observed for the monthly values between 2012-2017 ($R = 0.41$; $p < 0.001$). A distinct depletion in bimonthly $\delta^{13}\text{C}$ value during late 1950s is also observed (Figure 4.10). However, such depletion is not observed in the contemporaneous $\delta^{18}\text{O}$ values, which suggests that some metabolic process could have resulted in such depletion.

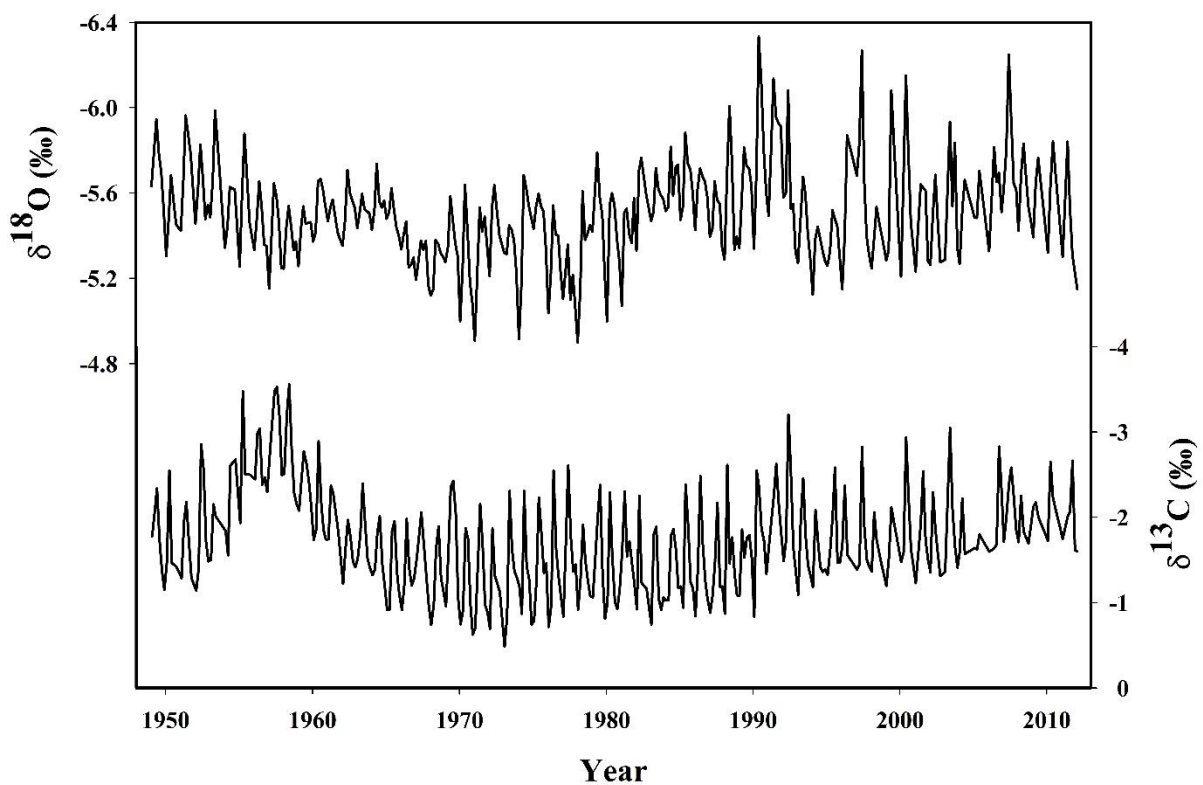


Figure 4.10: Bimonthly $\delta^{18}\text{O}$ and $\delta^{13}\text{C}$ record of the Landfall coral between 1949-2011

The monthly record of Landfall coral between 2012-2017 showed that seawater $\delta^{18}\text{O}$ change influences the coral $\delta^{18}\text{O}$ -SST relationship in the region. Therefore, to obtain a reliable coral $\delta^{18}\text{O}$ -SST relationship, information of seawater $\delta^{18}\text{O}$ variability is important. The earlier derived mean monthly $\Delta\delta^{18}\text{O}_{\text{sw}}$ values were converted to mean bimonthly values by averaging two consecutive month values. It is assumed that the calculated mean bimonthly $\Delta\delta^{18}\text{O}_{\text{sw}}$ values represent average seawater $\delta^{18}\text{O}$ seasonality of the region. These values were deducted from the bimonthly $\Delta\delta^{18}\text{O}_{\text{coral}}$ values (mean centered) to obtain the temperature component of corals oxygen isotope ($\Delta\delta^{18}\text{O}_{\text{SST}}$). The obtained $\Delta\delta^{18}\text{O}_{\text{SST}}$ values show good correlation with

bimonthly SST variability (Figure 4.11) and by correlating extreme values following correlation is obtained,

$$(\Delta\delta^{18}\text{O}_c - \Delta\delta^{18}\text{O}_{sw}) = [(-0.19) \times \Delta\text{SST}] - 0.09 \quad (5)$$

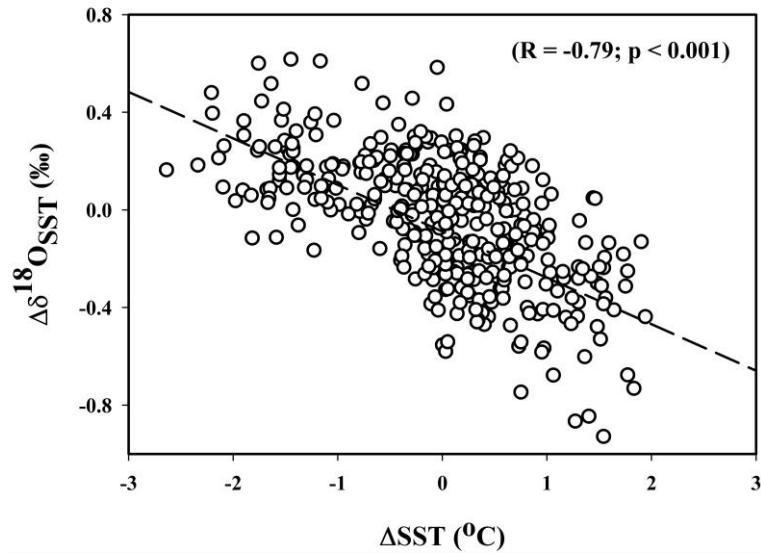


Figure 4.11: Linear correlation between SST variability and temperature component of Landfall $\delta^{18}\text{O}$ values between 1949-2011

The obtained slope of correlation between Landfall coral $\delta^{18}\text{O}$ and SST is $-0.19 \text{ } \text{‰}^{\circ}\text{C}^{-1}$, which is well within the range of slope reported for $\delta^{18}\text{O}$ -SST relationship of *Porites* corals. This implies that the obtained mean $\Delta\delta^{18}\text{O}_{\text{coral}}$ values are appropriate representative of seawater $\delta^{18}\text{O}$ seasonality. In absence of in-situ measured seawater $\delta^{18}\text{O}$ values, the calculated mean $\Delta\delta^{18}\text{O}_{sw}$ values can be used to derive past SST variability from coral $\delta^{18}\text{O}$ values of the region. The Landfall coral $\delta^{18}\text{O}$ values between 1949-2011 was analysed for interannual or decadal variability. It is found that 10 year running mean values of coral $\delta^{18}\text{O}$ value shows a cyclicity which follows the variability of 10 year running mean of ONI (Ocean Nino Index) (Figure 4.12).

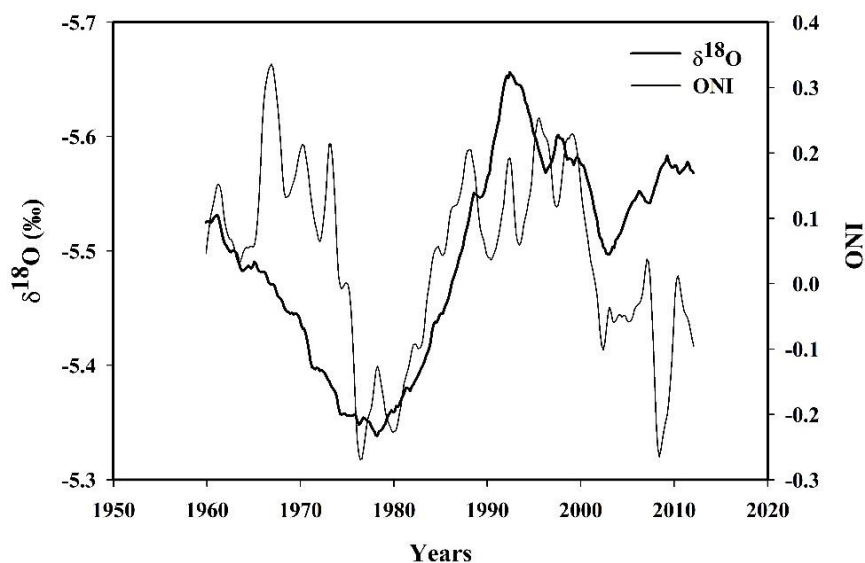


Figure 4.12: Ten year running mean values of coral $\delta^{18}\text{O}$ and ONI (Ocean Niño Index) values

With increasing (decrease) ONI the decrease (increase) in $\delta^{18}\text{O}$ value, suggests comparatively warm or fresh sea surface conditions in the Andaman, when east central tropical Pacific was relatively warmer and vice versa. This possibly suggests that on long time scale, SST condition in NINO 3.4 region (5°N - 5°S , 120° - 170°W) in Pacific influences the sea surface conditions in the Andaman region. Corals from the eastern and equatorial Indian Ocean have shown ENSO driven interannual and decadal climate variability (Charles et al. 1997, Cole et al. 2000, Pfeiffer et al. 2004). Ahmad et al. (2011) reported that coral from the Lakshadweep islands in the north western Indian Ocean also recorded ENSO like periodicity. The covarying oxygen isotopic record of Landfall coral and ONI running mean value suggests that north eastern Indian Ocean might be influenced by the SST variability in the east central tropical Pacific region.

4.5. Annual Oxygen Isotope Variations in Landfall and Kadmat Coral

The bimonthly values of oxygen isotope of Landfall and Kadmat corals were converted to annual values by averaging the six data points of each year. The annual $\delta^{18}\text{O}$ values of Landfall coral show a small decreasing trend between 1948-2017. It is observed that annual $\delta^{18}\text{O}$ values show relatively higher values between 1955-1982, which indicates cooler or less saline sea surface conditions. When annual $\delta^{18}\text{O}$ values of Kadmat coral and Landfall corals were compared, it is observed that both show a decreasing trend between overlapping time period of 1978-2013 (Figure 4.13). Which suggests that both regions in the northern Indian Ocean experienced relative warming or freshening of surface seawater during this period. The annual $\delta^{18}\text{O}$ values of Kadmat coral and Landfall corals also show a weak but significant positive

correlation ($R = 0.39$, $p < 0.02$) with each other. A correlation between annual proxy records of these corals situated in two different basins indicate that a large scale process might be influencing these corals.

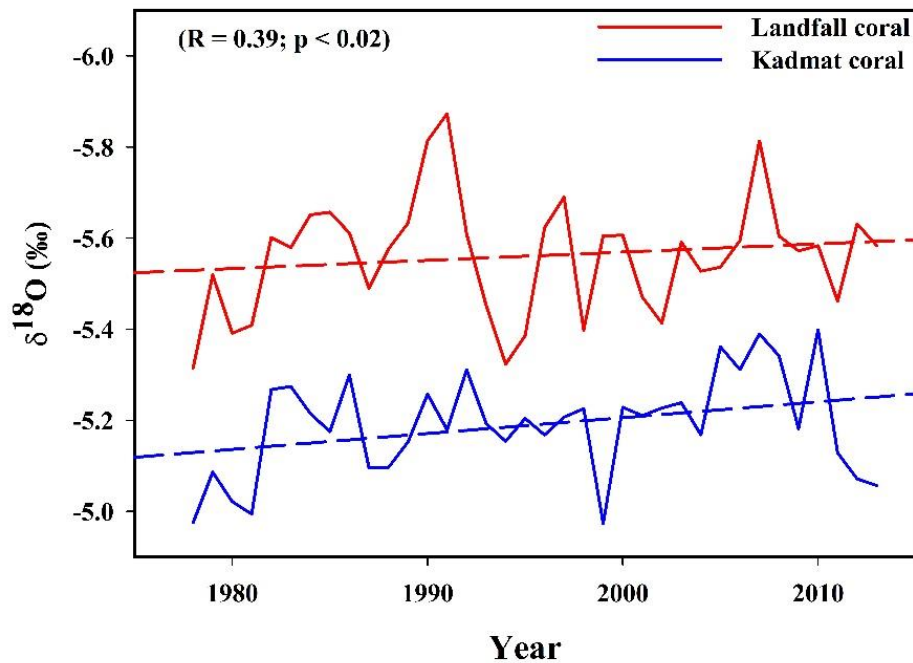


Figure 4.13: A long term depleting trend in annual $\delta^{18}\text{O}$ values of Landfall and Kadmat coral

Based on the above discussion, the observations made using geochemical proxies demonstrate that *Porites* corals from the Andaman region can record useful climatic parameters like sea surface temperature, monsoon rainfall and cloud cover. Sr/Ca of Landfall coral faithfully records the sea surface temperature variability. Coral $\delta^{18}\text{O}$ value can also be used to estimate sea surface temperature variability using obtained mean monthly $\Delta\delta^{18}\text{O}_{\text{sw}}$ variability. However, use of mean monthly $\Delta\delta^{18}\text{O}_{\text{sw}}$ value ignores the interannual changes in seawater $\delta^{18}\text{O}$ values, which can reduce the accuracy of the estimated SST variability. Reconstructed $\Delta\delta^{18}\text{O}_{\text{sw}}$ values from the Andaman corals could provide information about summer monsoon rainfall. Further, the Landfall coral record also shows that SST variability in Pacific region influences the sea surface condition in the Andaman Sea. As it is observed that Andaman coral can potentially provide crucial information about past climatic conditions, more coral records from the region going back in history should be explored to better understand the past monsoon and climate variability.

4.6. Inferences

The Sr/Ca ratio of Landfall coral show good correlation with SST, whereas, coral $\delta^{18}\text{O}$ values show a relatively weak correlation with a low slope suggesting significant contribution of seawater $\delta^{18}\text{O}$ variation in the Landfall coral $\delta^{18}\text{O}$ variability. Therefore, in absence of information about seawater $\delta^{18}\text{O}$ changes, Sr/Ca ratio appears to be a better proxy for SST reconstruction in the Andaman region. Using paired Sr/Ca and $\delta^{18}\text{O}$ values, $\Delta\delta^{18}\text{O}_{\text{sw}}$ was reconstructed. The reconstructed monthly $\Delta\delta^{18}\text{O}_{\text{sw}}$ values from the Andaman region show influence of both SST and rainfall. The obtained correlation between seasonal rainfall and $\Delta\delta^{18}\text{O}_{\text{sw}}$ values suggests that Andaman coral derived $\Delta\delta^{18}\text{O}_{\text{sw}}$ values could also be used for qualitative reconstruction of past monsoon rainfall. The Landfall coral $\delta^{18}\text{O}$ values show good correlation with SST when corrected for seawater $\delta^{18}\text{O}$ changes. Landfall coral $\delta^{18}\text{O}$ values show comparatively warm or fresh sea surface conditions during time period when east central tropical Pacific is relatively warmer, suggesting long term SST changes in Nino region of Pacific possibly influences the sea surface conditions in the Andaman region. Landfall coral $\delta^{13}\text{C}$ values record the seasonal change in photosynthesis caused by change in light availability during monsoon period.

Chapter-5
Marine Reservoir Correction and Air-sea CO₂
Exchange Rates Based on Radiocarbon Records
from Kadmat and Landfall Corals

5.1. Introduction

Radiocarbon is one of the naturally occurring radioisotopes of carbon. It is produced in the atmosphere by the interaction of cosmic ray produced thermal neutrons and nitrogen atoms. The ^{14}C atoms reacts immediately after it is formed in the atmosphere to either directly form $^{14}\text{CO}_2$ molecules or form ^{14}CO which further oxidises to $^{14}\text{CO}_2$ (Alves et al 2018). The $^{14}\text{CO}_2$ gets distributed in the atmosphere along with CO_2 and follows pathways of stable carbon isotopes as their chemical properties are identical. The natural production of radiocarbon has almost remained constant for several thousands of years. During early 1950s and 1960s, apart from the natural production, artificial radiocarbon (bomb carbon) was introduced in the atmosphere due to nuclear testing carried out in the upper atmosphere. This increased the atmospheric radiocarbon levels to almost double than its natural production. Figure 5.1 shows increase in the atmospheric radiocarbon level during early 1950s, with its peak around mid-1960 and subsequent decrease due to exchange between atmosphere and other carbon reservoirs. ^{14}C in the atmosphere reaches the ocean mainly through air-sea CO_2 exchange process (Alves et al. 2018; Bhushan et al. 2000; Dutta and Bhushan 2012).

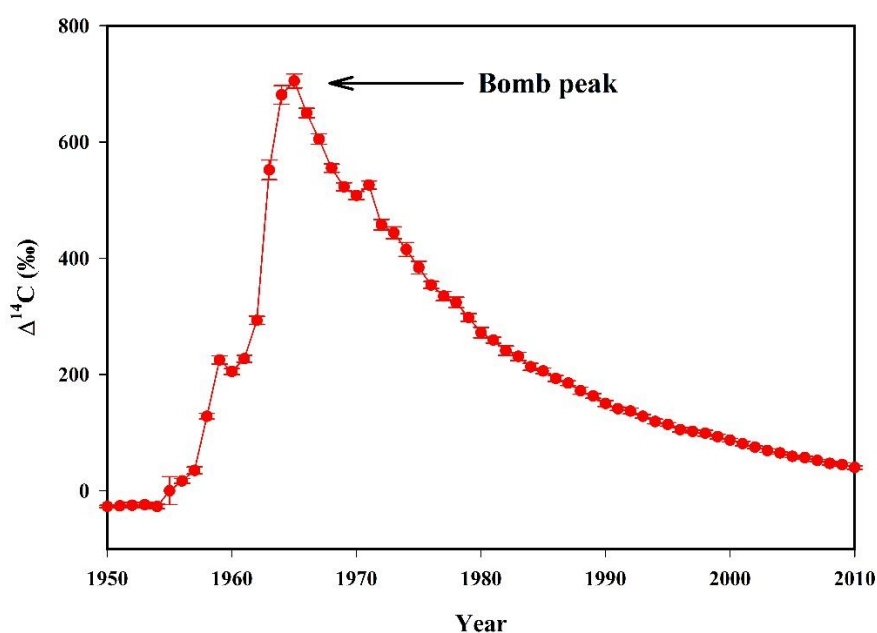


Figure 5.1: Atmospheric radiocarbon values from the northern hemisphere (Hua et al. 2013), showing bomb radiocarbon peak

The radiocarbon concentration in surface seawater shows both spatial and temporal variation, which can be very resourceful in understanding various natural processes occurring in the atmosphere, ocean and at ocean-atmosphere interface. The bomb radiocarbon spike in the

natural system as a result of nuclear testing has been effectively used as a potential tracer to study ocean circulation and air-sea CO₂ exchange processes. Corals from shallow marine regions incorporate signatures of surface seawater radiocarbon as a function of time with high resolution. The radiocarbon signature embedded in coral provides information about natural processes affecting the surface waters of a region (Druffel 2002). Cember (1989) based on studies of bomb radiocarbon in corals observed a CO₂ invasion flux of 8 mol m⁻² yr⁻¹ for the Red Sea in the northern Indian Ocean. Chakraborty et al. (1994) analysed a coral from Gulf of Kutch for radiocarbon and obtained an air-sea CO₂ exchange rate of 11-12 mol m⁻² yr⁻¹ for the region. The surface seawater radiocarbon concentrations are much lower than those observed in the atmosphere due to reservoir effect and thus are dampened. This reservoir effect need to be corrected in radiocarbon dating of any marine species. However, there are no pre-bomb surface seawater radiocarbon measurements available for any part of the world ocean. The pre-bomb period coral radiocarbon records thus can provide crucial information about the oceanography and reservoir age of the region, where coral are growing. In this chapter, two *Porites* corals, one each from the Arabian Sea (Kadmat coral) and the Andaman Sea (Landfall coral) have been investigated for their radiocarbon distribution to understand oceanography, air-sea CO₂ exchange rates and reservoir age corrections of the region

5.2. $\Delta^{14}\text{C}$ Values of Kadmat and Landfall Coral

The *Porites* corals from the Lakshadweep islands (Kadmat coral) and the Andaman islands (Landfall coral) were analysed for their radiocarbon concentration using AMS technique. AGE3 (Automated Graphitization System) was used to graphitize the coral samples and standard. Graphitized samples of corals and standards were prepared into the targets for radiocarbon measurements in AMS. In the AMS instrument ¹⁴C/¹²C ratios were measured along with the ¹³C/¹²C ratio. Then age corrected $\Delta^{14}\text{C}$ values of Kadmat and Landfall corals samples were calculated. Kadmat coral isotopic record span 1977-2014 and Landfall coral span 1948-2018. The coral radiocarbon values provide the surface water DIC radiocarbon concentration of the Arabian Sea and the Andaman Sea for the respective year of coral growth. These coral radiocarbon records show typical bomb radiocarbon trend as observed globally in corals and surface seawater.

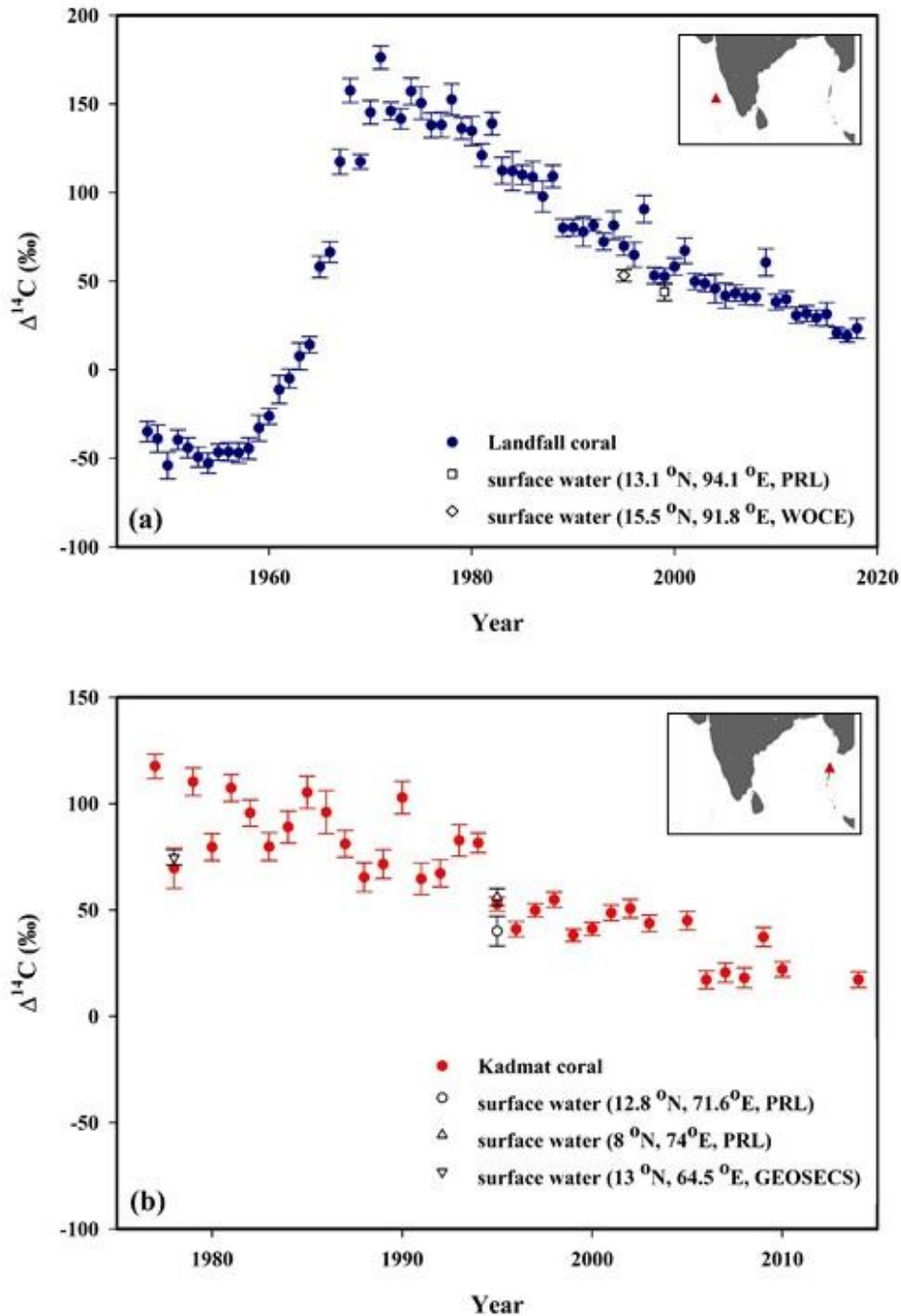


Figure 5.2: $\Delta^{14}\text{C}$ values of (a) Landfall and (b) Kadmat coral along with surface water $\Delta^{14}\text{C}$ values measured during GEOSECS, WOCE and PRL expeditions. (insets: map showing coral site in the Indian Ocean)

The Landfall coral record shows sharp increase in $\Delta^{14}\text{C}$ during 1960s reaching maxima in early 1970s due to bomb radiocarbon in the atmosphere, and then post mid-1970s a steady decreasing trend is observed. As Kadmat coral record begins from late 1970s, a distinct peak is not observed but decreasing trend towards present is noted. This decrease results mainly due to decreasing radiocarbon concentration in the atmosphere. The surface water DIC $\Delta^{14}\text{C}$ value

from the region close to coral sampling sites have been analysed by other investigators during different oceanographic expeditions between 1977-1999 (GEOSECS, WOCE, PRL). Figure 5.2 shows that the surface water $\Delta^{14}\text{C}$ values measured in coral from Landfall in the Andaman Sea (Figure 5.2a) and Kadmat in the Arabian Sea (Figure 5.2b) along with surface water radiocarbon measurement during GEOSECS (Stuiver and Ostlund, 1983), PRL (Bhushan et al. 2000; Dutta and Bhushan 2012) and WOCE (Gordon and Olson, 2020) expeditions. The radiocarbon values measured in surface waters and coral show good agreement, implying that corals faithfully record the surface water radiocarbon concentrations. The atmospheric history of radiocarbon concentration is based on data from Hua et al. (2013). Based on radiocarbon gradient in the troposphere between 1955 and 1960s, the atmosphere was divided in several zones. The northern hemispheric atmosphere was separated into three zones, among which NH (northern hemisphere) zone 3 lies between mean summer position of ITCZ and equator (Hua et al. 2013). As sample locations are situated in the northern Indian Ocean, radiocarbon values of NH zone 3 were considered for atmospheric radiocarbon record.

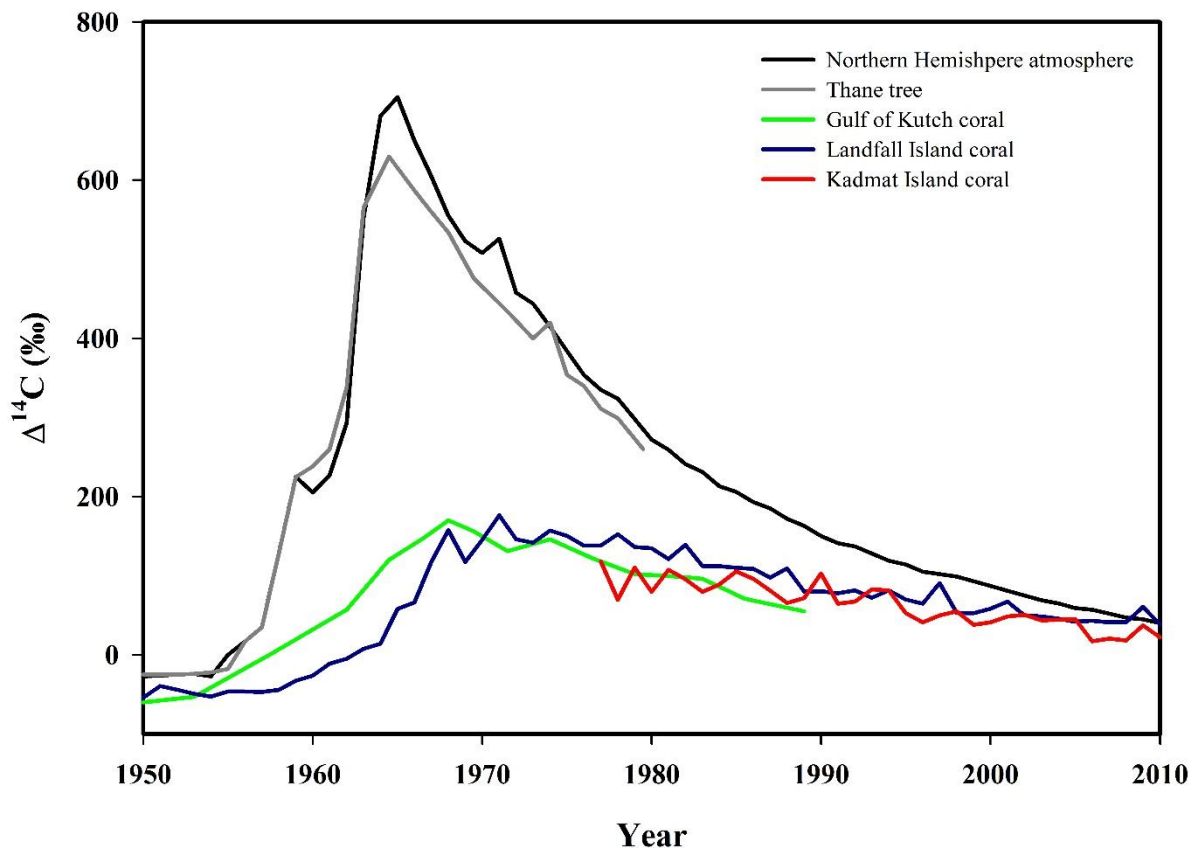


Figure 5.3: $\Delta^{14}\text{C}$ values of Kadmat coral, Landfall coral, Gulf of Kutch coral (Chakraborty et al. 1994), Thane tree ring (Chakraborty 1993) and northern hemisphere atmosphere (Hua et al. 2013)

Figure 5.3 shows radiocarbon values of Kadmat and Landfall coral along with that of northern hemisphere atmosphere zone 3 (Hua et al. 2013), the Thane tree ring and the Gulf of Kutch coral (Chakraborty et al. 1994) for comparison. The peak of radiocarbon concentration in atmosphere is around 1965. Thane tree ring shows peak value during 1964-1965 period. The thane tree ring, however, shows lower radiocarbon peak value (630 ‰) as compared to the peak value (705 ‰) of the northern hemisphere zone 3. This depletion in Thane tree ring data has been attributed to industrial input from the neighbouring regions (Chakraborty et al. 2008). The Gulf of Kutch and the Landfall coral show peak radiocarbon value of 170 ‰ and 176 ‰ respectively. The radiocarbon peak in surface ocean has been recorded during 1968 in the Gulf of Kutch coral (Chakraborty et al. 1994). In the Landfall coral from the Andaman Sea records radiocarbon peak during 1971. Chakraborty (1993) had observed that the peak in the Gulf of Kutch coral radiocarbon values arrives earlier than coral records from other oceanic region indicating higher air-sea CO_2 exchange rate in the region. The difference in air-sea CO_2

exchange rate over the Gulf of Kutch and the Andaman Sea could be the plausible reason for this difference in radiocarbon peak.

5.3. Coral records from the Indian Ocean

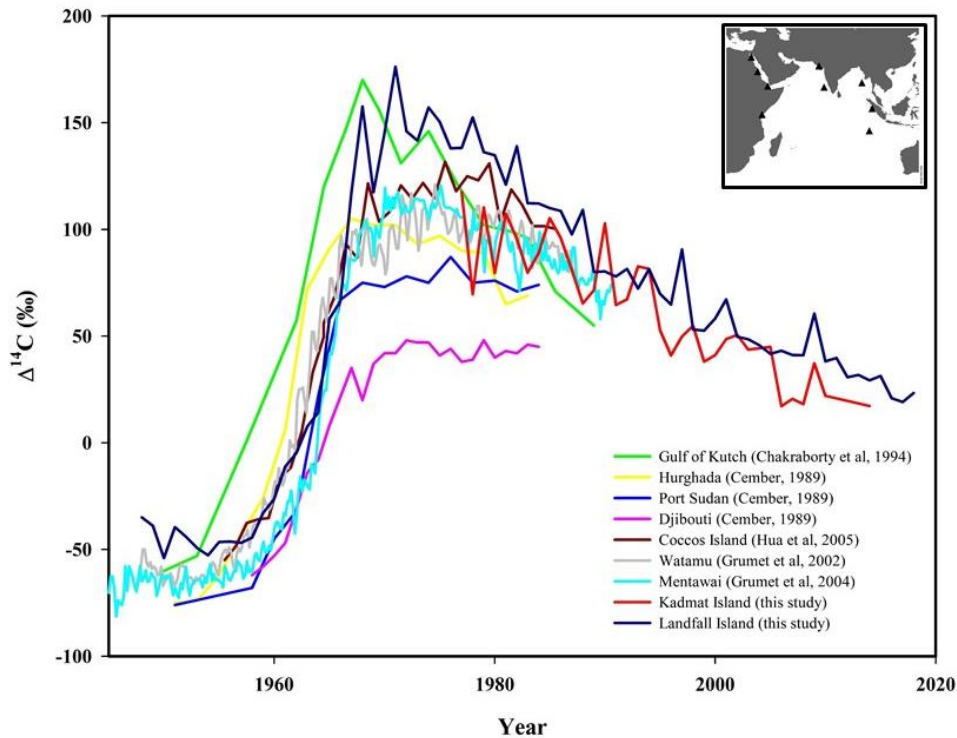


Figure 5.4: Coral radiocarbon records from the Indian Ocean (inset: map of coral sites in the Indian Ocean)

Figure 5.4 shows the bomb radiocarbon record of several coral samples studied from the Indian Ocean (Cember 1989, Chakraborty et al. 1994, Grumet et al. 2002, Grumet et al. 2004, Hua et al. 2005). The highest $\Delta^{14}\text{C}$ value observed (176 ‰) among Indian Ocean corals is from the Landfall coral. The Landfall Island is situated in the northern Andaman Sea, which receives very high freshwater flux majorly from Irrawaddy and Salween river (Ramaswamy et al. 2013). High radiocarbon value recorded in the Landfall coral suggests riverine contribution with enriched radiocarbon freshwaters to the region. The Landfall coral also shows radiocarbon peak value relatively earlier than most of the corals from the Indian Ocean, which implies stratification of upper ocean in the region. This is in accordance with the observed stratification in the Bay of Bengal (Thadathil et al. 2007). The Kadmat coral radiocarbon values are relatively lower than the Landfall coral record, but comparable to the radiocarbon record of coral from Watamu, Kenya for overlapping time period. The relatively depleted radiocarbon values

recorded in Watamu coral has been attributed to contribution from upwelling in Somali and Oman coast (Grumet et al. 2002). The comparable radiocarbon values from the Kadmat coral suggests that vertical mixing of subsurface water could be depleting the radiocarbon values of the surface water. This is also supported by the observation of SST cooling in the Lakshadweep during monsoon months due to vertical mixing of subsurface waters. The comparison of post bomb annual radiocarbon value of the Kadmat and Landfall coral shows large variability in the Kadmat coral values as compared to the Landfall coral values. The Kadmat coral $\Delta^{14}\text{C}$ exhibit changes up to 40 ‰ from one year to another, whereas year to year changes in the Landfall coral $\Delta^{14}\text{C}$ record is lower. This implies that surface water in the Andaman region is well stratified, whereas in the Lakshadweep region there is mixing of subsurface depleted waters. The coral radiocarbon records thus reflect contrasting oceanographic scenario between these basins in the northern Indian Ocean due to their varying hydrological conditions. Monsoon related upwelling and fresh water flux has played prominent role in regulating surface water characteristics in the northern Indian Ocean and thus the surface water radiocarbon composition.

5.4. Marine Reservoir Age Correction for the Andaman Basin

Radiocarbon concentration of dissolved inorganic carbon in surface seawater depends on ^{14}C concentration of the atmosphere and oceanic sub-surface waters. Since ocean sub-surface waters remain isolated from the atmosphere for hundreds of years before shoaling up, its ^{14}C concentration is generally lower than that of the atmosphere. Combination of air-sea CO_2 exchange, vertical mixing and upwelling reduces the ^{14}C activity of the surface ocean reservoir as compared to that of the atmosphere, leading to reservoir effect (Stuiver and Polach 1977, Alves et al. 2018). This causes an offset between radiocarbon age of marine samples and corresponding atmospheric age, and this offset is called the reservoir age (R) (Stuiver and Braziunas 1993). The varying intensity of air-sea CO_2 exchange, upwelling and horizontal or lateral advection, results in different reservoir ages of surface ocean across the globe. Variation of regional R from the global average R value is called reservoir effect correction (ΔR). Global average R value for the ocean is obtained from marine calibration curve (e.g. MARINE13, Reimer et al. 2013). The global average R value is the radiocarbon age corresponding to calendar year of sample growth or collection, on the marine calibration curve. Mathematically, subtracting this global average R value from measured radiocarbon age of marine sample yields ΔR (Stuiver and Braziunas 1993, Reimer and Reimer 2017, Alves et al. 2018). ΔR values are applied to radiocarbon age of marine samples before calibration to correct for local reservoir

effect. As reservoir age varies due to ocean circulation, upwelling and fresh water flux, apart from information on reservoir age correction it also helps towards understanding the oceanography of the region. In the northern Indian Ocean, ΔR values observed for the Bay of Bengal region are lower as compared to the Arabian Sea (Dutta et al. 2001). Intense upwelling in the Arabian Sea due to winds associated with monsoon leads to higher ΔR values (Southon et al. 2002), whereas relatively lower ΔR values in the Bay of Bengal (Dutta et al. 2001) is due to highly stratified surface water as a result of enormous freshwater flux, which impedes vertical mixing (Thadathil et al. 2007, Sijinkumar et al. 2016). The Andaman basin situated on the eastern side of the Bay of Bengal receives large amount of freshwater from rivers. Several scientific investigations in the Andaman region used radiocarbon ages focusing on diverse subjects like past monsoonal variability (Rashid et al. 2007, Achyutan et al. 2014, Ali et al. 2015, Ota et al. 2017, Kumar et al. 2018, Bhushan et al. 2019b), past salinity changes (Sijinkumar et al. 2016), deformational history of Andaman Islands (Rajendran et al. 2008, Kunz et al. 2010, Awasthi et al. 2013), past volcanic activity (Awasthi et al. 2010), past sea level changes (Scheffers et al. 2012), past tsunami deposits (Jankaew et al. 2008) and archeological history (Cooper 1993) of the region. Most of these studies needed reservoir age correction for the radiocarbon dates for the Andaman basin. However, with limited reservoir age estimates available from the region (Dutta et al. 2001, Southon et al. 2002), reservoir age from the surrounding regions were used for correction. In order to constrain the reservoir effect and understand the oceanography of the region, more pre-bomb radiocarbon values from this region are required. Corals are good marine archive recording the past ^{14}C changes in DIC of seawater (Druffel and Linick 1978; Hideshima et al. 2001; Grumet et al. 2002; Dang et al. 2004; Druffel et al. 2008). In this study, annually banded *Porites* coral core from the Landfall Island in the northern Andaman has been analyzed for its radiocarbon composition. The Landfall coral extends back to pre-bomb period upto year 1948. The pre-bomb radiocarbon value between 1948-1951 obtained from the Landfall coral has been used to estimate the reservoir age for the northern Andaman basin.

5.5. Landfall Corals Radiocarbon Record between 1948-1951

Results of radiocarbon measurement from the Landfall Coral are summarized in Table 5.1, where $\Delta^{14}\text{C}$ (‰) and radiocarbon age (yr BP) were calculated using measured $^{14}\text{C}/^{12}\text{C}$ and $^{13}\text{C}/^{12}\text{C}$ ratios. The results have been reported following conventions of Stuiver and Polach (1977). Calculated $\Delta^{14}\text{C}$ are corrected for fractionation and age between year of measurement and year of coral band growth. The dilution of ^{14}C values in the atmosphere and the ocean due

to addition fossil fuel derived CO₂ devoid of ¹⁴C, is known as the Suess effect. As samples belong to 20th century, Suess correction of $-9 \pm 3 \text{ ‰}$ is applied only to $\Delta^{14}\text{C}$ values of corals (Southon et al. 2002), however, radiocarbon age and reservoir age correction (ΔR) are based on non-Suess corrected $\Delta^{14}\text{C}$ values. Dutta et al. (2001) and Southon et al. (2002) did not use Suess corrected $\Delta^{14}\text{C}$ value to calculate the ΔR values. Although, Southon et al. (2002) reported Suess corrected $\Delta^{14}\text{C}$ values, but the ΔR values were calculated without Suess correction. Thus, to maintain uniformity and ease for comparison, ΔR values were calculated without Suess correction. Model ¹⁴C age is derived from MARINE13 calibration curve, which uses IntCal13 curve and ocean-atmosphere box diffusion model to obtain global marine surface ocean curve for 0 to 10.5 cal kBP (Reimer et al. 2013). The model ¹⁴C age used here for period 1948-1951 is $469 \pm 23 \text{ yr BP}$. Reservoir age correction (ΔR) values are calculated by subtracting model ¹⁴C age from conventional radiocarbon age of the coral samples (see Appendix C).

Table 5.1: Results of ^{14}C analysis in Landfall coral skeleton between 1948-1951

Year (AD)	$\Delta^{14}\text{C}$ (‰)	$\Delta^{14}\text{C}$ (Suess corrected) (‰)	Radiocarbon age (yr BP)	Model ^{14}C age (yr BP)	ΔR (yr)
1948	-38 ± 8	-29 ± 9	313 ± 67	469 ± 23	-156 ± 71
1948	-32 ± 8	-23 ± 9	263 ± 66	469 ± 23	-206 ± 70
1949	-39 ± 8	-30 ± 9	321 ± 67	469 ± 23	-148 ± 71
1950	-54 ± 8	-45 ± 9	446 ± 68	469 ± 23	-23 ± 72
1951	-41 ± 8	-32 ± 9	335 ± 67	469 ± 23	-134 ± 71
1951	-38 ± 8	-29 ± 9	310 ± 67	469 ± 23	-159 ± 71
Average	-40	-31	331		-138
Std dev	7	7	61		61

Errors quoted for $\Delta^{14}\text{C}$, radiocarbon age and ΔR are one sigma. The $\Delta^{14}\text{C}$ value for the Landfall coral sample ranges from -32 ‰ to -54 ‰ with mean value of -40 ± 7 ‰ (mean \pm SD, n=6) between 1948-1951. The Suess-corrected $\Delta^{14}\text{C}$ value averages around -31 ± 7 ‰. Between 1948-1951, ΔR value recorded by the Landfall coral ranges between -23 to -206 yr. The χ^2 test was carried out to check whether the variability in coral ΔR value is consistent with the standard measurement errors (Mangerud et al. 2006). It is observed that $\chi^2/(n-1)$ value is less than 1 suggesting that variance in ΔR is mainly due to measurement uncertainty. The observed changes in radiocarbon values of coral could result from local oceanographic conditions. Reservoir correction, calculated using MARINE13 derived model age, for Chilika lake in the northern Bay of Bengal (Dutta et al. 2001) equals to -61 ± 61 yrs. As it is the only reservoir correction value available from the region, it is assumed to be representative of the northern Bay of Bengal. This value is lower than the Landfall coral ΔR value of -23 ± 76 yrs for the year 1950, suggesting lateral mixing of surface waters from the northern Bay of Bengal may not result in such change in ΔR value. This suggests that the observed variation in coral radiocarbon values could have resulted from either vertical mixing or lateral transport from the southern Andaman region. The mean ΔR value of Landfall coral is calculated to be -138 ± 61 yr. In absence of any other ΔR value reported from the northern Andaman, the obtained mean value of -138 ± 61 yr can be applied to radiocarbon dates for the northern Andaman region for reservoir age correction. Previously, Dutta et al. (2001) and Southon et al. (2002) had reported radiocarbon values of bivalve (*Asaphis deflavata*) and gastropod (*Thais sp*) shell from the

Andaman region. Since there are no other coral based ΔR value reported from the region, these mollusk ΔR values are compared with coral derived ΔR value in this study. Bivalve shell from the Stewart Sound in the northern Andaman gave $\Delta^{14}C$ value of $-55 \pm 4 \text{ ‰}$ (Dutta et al. 2001), and gastropod shell from the Nicobar Island showed $\Delta^{14}C$ value of $-53.6 \pm 7.7 \text{ ‰}$ (Southon et al. 2002). The $\Delta^{14}C$ values from Landfall coral are higher compared to these samples from Stewart Sound and Nicobar Island samples.

Table 5.2: Reservoir age correction (ΔR) values of pre-bomb marine samples from the Andaman Basin

	Sample	Site	Location	Year of collection /growth	$\Delta^{14}C$ (‰)	Radiocarbon age (yr BP)	Model ^{14}C age (yr BP)	ΔR (^{14}C yr)
This study	<i>Porites</i> sp. (c)	Landfall Island	13° 39' N, 93° 02' E	1948-1951	-40 ± 7	331 ± 61	469 ± 23	-138 ± 61
Dutta et al. 2001	<i>Asaphis deflavata</i> (b)	Stewart Sound	13° 01' N, 92° 58' E	1935	-55 ± 4	469 ± 40	457 ± 23	12 ± 46
Southon et al. 2002	<i>Thais</i> sp. (g)	Nicobar Islands	9° N, 94° E	1913	-53.6 ± 7.7	478 ± 65	448 ± 23	30 ± 69

(b=bivalve, c=coral, g=gastropod)

The ΔR values calculated from the reported $\Delta^{14}C$ of bivalve and gastropod shells from the Stewart Sound and Nicobar Island is 12 ± 46 and 30 ± 69 yrs respectively (Table 5.2). Both these values are much higher than ΔR value of the Landfall coral. It is interesting to note that even the highest ΔR value recorded by Landfall coral is lower than ΔR of bivalve and gastropod shells from Stewart Sound and Nicobar Island. The model ages used for reservoir age calculation for each sample is different as the year of growth or collection for these samples varies from 1913 to 1951. The model age ranges from 448 to 469 yr BP. The observed differences in ΔR value of samples are result of either species specific ^{14}C activity or oceanic processes like upwelling and circulation or both.

Feeding habits and habitats of mollusk can have effects on their radiocarbon records. Species dependent ^{14}C activity can result in variable ΔR values for the same region (Dye 1994, Forman and Polyak 1997, Hogg et al. 1998, Petchey et al. 2012). Bivalves can be suspension feeders or deposit feeders. Some bivalves engage in deposit feeding depending on their local conditions (Petchey et al. 2004). Thus, bivalves feeding on detritus of old limestone can result in high

radiocarbon ages. Petchey et al. (2004) analysed marine shells from the Coral Sea and the Solomon Sea region, and they found mollusk (*Asaphis violascens*) collected from area dominated by calcareous bedrock yielded high ΔR values. Unlike bivalves, *Thais sp* is a carnivorous predator. The radiocarbon content of these gastropod may not represent seawater DIC ^{14}C content, as their radiocarbon content depends on the carbon reservoir of their prey (Hua 2015). Lindauer et al. (2017) had also observed influence of food resource and habitat on the ΔR of bivalve and gastropod from the Gulf of Oman region. Therefore, enriched values in mollusk (*Asaphis deflavata*, *Thais sp*) from the Andaman could be due to species specific ^{14}C activity. Apart from species difference, the sample location can also be possible reason behind observed differences in ΔR value from the Andaman region. The Landfall Island is located in the northern part of Andaman archipelago, which receives large flux of fresh riverine water. Salinity in the Andaman basin increases southwards (Babu et al. 1976) and reservoir age correction also shows increasing value as one move to locations further south in the Andaman basin away from freshwater region. During winters, southern Andaman sea is influenced by flows from the Malacca strait originating from the South China Sea (Raju et al. 1981). The average ΔR value reported for the South China Sea is -3 ± 50 yrs (Dang et al. 2004). During summer monsoon, Southwest Monsoon Current flows eastward south of Sri Lanka to bring saltier Arabian Sea waters into the Bay of Bengal (Schott et al. 2009). Southon et al. (2002) reported ΔR values of 127 yr for the Sri Lankan region. During the same period (summer), southern Andaman (around ten degree channel) receives strong influx of surface currents from the Bay of Bengal (Kiran 2017), which could bring ΔR enriched waters to the southern Andaman. These surface currents in summer and winter season could lead to the observed high ΔR values in the southern Andaman. Whereas, the northern Andaman region receives freshwater flux from rivers causing stratification of surface waters, which inhibits vertical mixing and contributes to the lower reservoir age of the region. By comparing previously reported ΔR values with the Landfall coral, it is observed that there exists significantly large variation in ΔR values from the Andaman Sea derived from coral and mollusk shells (Dutta et al. 2001, Southon et al. 2002) (Figure 5.5). Reservoir age correction values from the northern Andaman Sea and the Bay of Bengal are lower when compared to the southern Andaman Sea. These variations in reservoir age corrections need to be accounted while correcting radiocarbon dates of marine samples for reservoir age of the region.

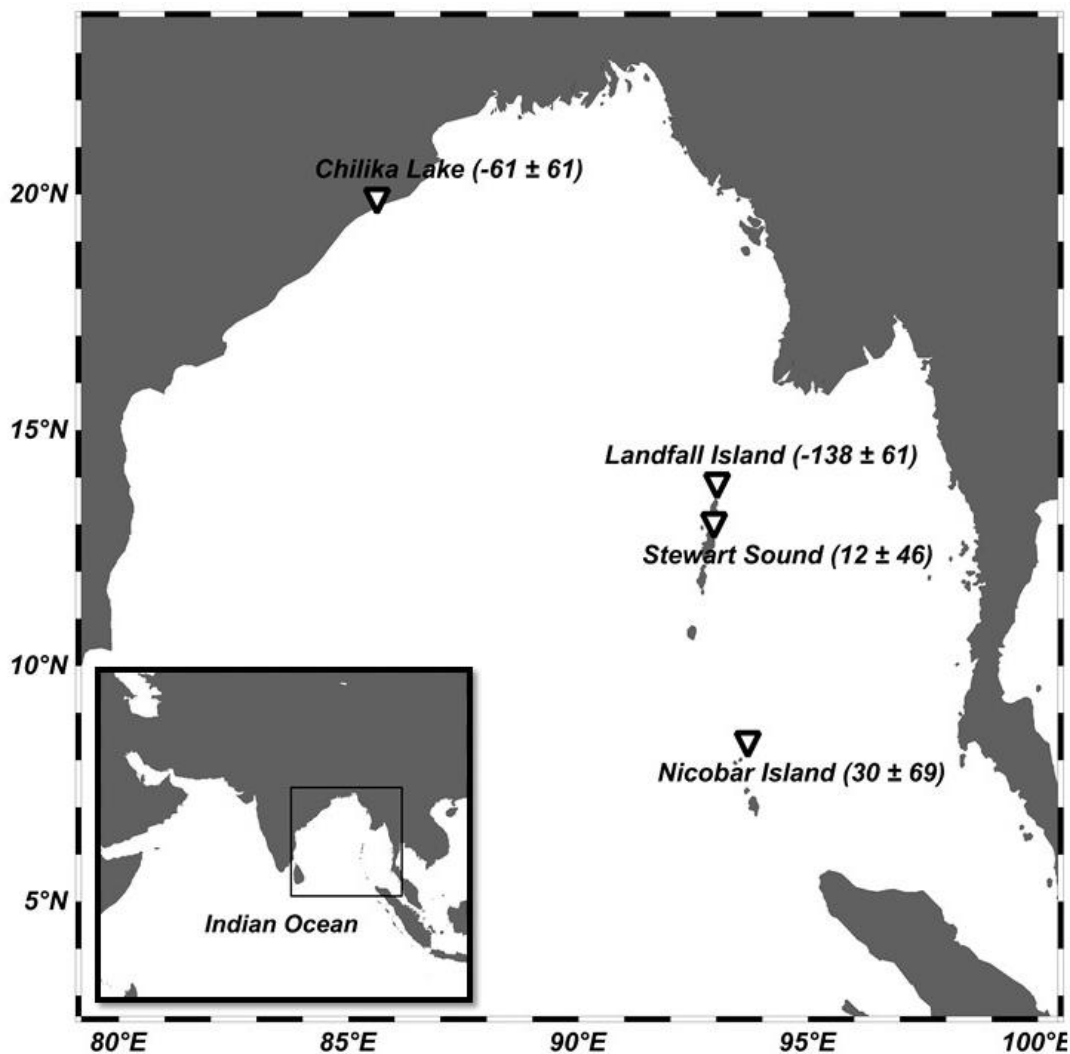


Figure 5.5: Map of north-eastern Indian Ocean with reservoir age correction values from Landfall Island (this study), Chilika lake, Stewart sound (Dutta et al. 2001) and Nicobar Island (Southon et al. 2002) (Inset: Study location marked by rectangle in northern Indian Ocean)

5.6. Air-Sea CO₂ Exchange Rates over the Indian Ocean based on Corals

The Indian Ocean has been known to be a sink of CO₂ (Louanchi et al. 1996, Sabine et al. 2000, Takahashi et al. 2009). However, CO₂ flux in the northern Indian Ocean is found to be from sea to air (Bates et al. 2006, Takahashi et al. 2009). Using the bomb radiocarbon, Dutta and Bhushan (2012) estimated net CO₂ flux from the northern Indian Ocean around 104 Tg C yr⁻¹. Louanchi et al. (1996) had estimated a CO₂ flux rate of 169 Tg C yr⁻¹ for the Indian Ocean between 10° S – 18° N. For area between 10° S- 10° N in the Indian Ocean, Bates et al. (2006) calculated net CO₂ flux of 180 Tg C yr⁻¹. The Arabian Sea has been shown to be a perennial source of CO₂ (Sarma 2003), whereas Bay of Bengal has been observed to be a sink of CO₂ (Kumar et al. 1996; Dutta and Bhushan 2012). Bates et al. (2006) observed both Arabian Sea

and the Bay of Bengal to be source of CO₂. Bhushan et al. (2000) constrained CO₂ evasion rates from the Arabian Sea between 50-180 Tg C yr⁻¹. Sarma et al. (2003) estimated CO₂ emission of 90 Tg C yr⁻¹, and Bates et al. (2006) estimated flux of 64 Tg C yr⁻¹ for the Arabian Sea. Coral radiocarbon records from the northern Indian Ocean region can be useful in constraining the air-sea CO₂ exchange rates and CO₂ fluxes over the region (Bhushan et al. 2000, Dutta and Bhushan 2012). However, due to limited coral radiocarbon records from the northern Indian Ocean, more coral records are required to better constrain the air-sea CO₂ exchange rates and surface water movements over the region.

In view of limited coral records from the Arabian Sea and the Bay of Bengal, *Porites* coral from Lakshadweep and Andaman Islands were analysed for their radiocarbon composition. Temporal variations in these coral radiocarbon values has been analysed. Based on these coral and atmospheric radiocarbon values, air-sea CO₂ exchange rate over the Lakshadweep and Andaman region has been estimated. Air-sea CO₂ exchange rates across the northern Indian Ocean is related to the wind speed of the region. The CO₂ exchange rates are used to constrain the CO₂ fluxes over this region. This study adds up to understanding of spatial variation in carbon fluxes over the northern Indian Ocean. Large variability exists in the air-sea CO₂ exchange rates over the northern Indian Ocean which is related to the variability of wind speed over the region.

Radiocarbon based air-sea CO₂ exchange rates can be obtained by following relationship given by Stuiver (1980) modified for the northern Indian Ocean by Dutta & Bhushan (2012),

$$Q_{14} = (1.24 \times 10^{-15}) \times F_{12} \times \int_0^t (\Delta^{14}C_{atm} - \Delta^{14}C_{mix} - 60) dt \quad (1)$$

Where, Q₁₄ is the bomb radiocarbon inventory and F₁₂ is the air-sea CO₂ exchange rate. Δ¹⁴C_{atm} and Δ¹⁴C_{mix} is radiocarbon values of atmosphere and mixed layer respectively. However, this air-sea CO₂ exchange rate estimation has assumption that net bomb radiocarbon inventory of ocean is dependent on the integrated atmosphere-ocean Δ¹⁴C gradient and air-sea CO₂ exchange rate. It is also assumed that variations in bomb radiocarbon inventory is due to air-sea CO₂ exchange only and the CO₂ invasion and evasion rates between atmosphere and sea has remained same. Equation (1) requires time integrated coral radiocarbon value from beginning of bomb radiocarbon in corals. The Landfall coral Δ¹⁴C values, northern atmospheric Δ¹⁴C values and bomb radiocarbon inventory from location near to the coral site (Dutta and Bhushan 2012) yields F₁₂ value of 8.8 ± 1.3 mol m⁻² yr⁻¹. The Kadmat coral record starts from 1977, which is much later than start of bomb radiocarbon in coral records from the Arabian

Sea (Chakraborty et al. 1994). To derive air-sea CO₂ exchange rates from coral records like the Kadmat coral, equation (1) was further modified as follows (described in Appendix D),

$$Q_{14}^{t_2} - Q_{14}^{t_1} = (1.24 \times 10^{-15}) \times F_{12} \times \int_{t_1}^{t_2} (\Delta^{14}C_{atm} - \Delta^{14}C_{mix} - 60) dt \quad (2)$$

Equation (2) requires difference between bomb radiocarbon inventory between time t₁ and t₂ to calculate F₁₂. Dutta & Bhushan (2012) had calculated bomb radiocarbon inventory in the Arabian Sea during 1994-1999. They had also reoccupied few GEOSECS stations in the Arabian Sea and calculated the change in the bomb radiocarbon inventory since GEOSECS for these stations (Dutta and Bhushan 2012). They calculated average difference of bomb radiocarbon inventory in two decades between GEOSECS and PRL expeditions to be 1.1 × 10⁹ atoms cm⁻². Using this value along with time integrated radiocarbon variation in atmosphere and the Kadmat coral between 1977-1999 in equation (2), air-sea CO₂ exchange rate (F₁₂) of 13.4 ± 2.1 mol m⁻² yr⁻¹ was obtained.

5.7. Air-Sea CO₂ Exchange Rate and Wind Speed

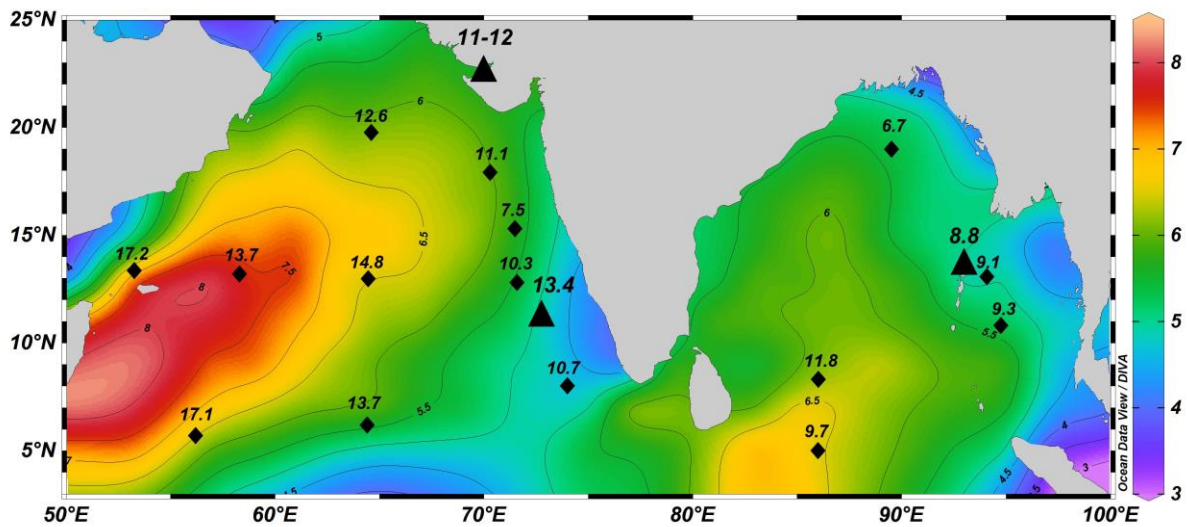


Figure 5.6: Air-sea CO₂ exchange rates in the northern Indian Ocean along with colour contours of average wind speed (m s⁻¹) (COADS, Slutz et al. 1985). ▲ represents coral based air-sea CO₂ exchange rates (mol m⁻² yr⁻¹) from this study and Chakraborty et al. (1994). ♦ represents CO₂ air-sea exchange rates (mol m⁻² yr⁻¹) estimated by Dutta and Bhushan (2012)

Earlier investigations from the Arabian Sea and the Bay of Bengal regions on CO₂ air-sea exchange rate reported range from 7-18 mol m⁻² yr⁻¹ and 6-12 mol m⁻² yr⁻¹ respectively (Bhushan et al. 2000, Dutta and Bhushan 2012). Though, these studies on air-sea CO₂ exchange rates were based on the bomb-radiocarbon inventory penetration in the water column, the

calculated CO₂ air-sea exchange rate values has been derived using time integrated radiocarbon values of surface ocean from the region using coral samples from the Arabian Sea and the Bay of Bengal. There seems to be good agreement in the mean CO₂ air-sea exchange rate calculated both for the Arabian Sea and the Bay of Bengal either derived from bomb-radiocarbon inventory of water column or corals (Chakraborty et al. 1994, Dutta and Bhushan 2012). Figure 5.6 shows the CO₂ air-sea exchange rates from various locations in the northern Indian Ocean both from water column and coral studies. High air-sea CO₂ exchange rates are observed in the western Arabian Sea, where wind speed is generally higher than other locations. However, Bay of Bengal shows relatively lower air-sea CO₂ exchange rates where wind speed is relatively lower. Although wind does not control gas transfer directly, but it influences most of the boundary layer processes and therefore on global scale wind speed is considered as the main forcing factor for gas transfer (Wanninkhof 2014). Using coral radiocarbon values, Cember et al. (1989) calculated air-sea CO₂ exchange rate in the Red Sea to be 8 mol m⁻² yr⁻¹ where mean wind speed is 4.7 m s⁻¹. The exchange rate calculated from Landfall coral is 8.8 ± 1.3 mol m⁻² yr⁻¹, close to the value reported by Cember et al. (1989) and the wind speed of the region is also similar. In the northern Arabian Sea, Chakraborty et al. (1994) estimated air-sea CO₂ exchange rate of about 11-12 mol m⁻² yr⁻¹, based on radiocarbon values of coral from the Gulf of Kutch. The air-sea CO₂ exchange rate calculated for Kadmat coral is 13.4 ± 2.1 mol m⁻² yr⁻¹, comparable to that estimated for the Gulf of Kutch, but wind speed is little lower in Lakshadweep as compared to the Gulf of Kutch. Earlier investigations reported empirical relationship between wind speed and gas transfer velocity (Liss and Merlivat 1986, Wanninkhof and McGillis 1999, Wanninkhof 2014). All the CO₂ exchange rates estimated either using bomb-radiocarbon in the northern Indian Ocean are plotted as a function of wind speed over the region (Figure 5.7). The bomb-radiocarbon based air-sea CO₂ exchange rate estimates does not agree well with the wind speed based cubic polynomial fit by Wanninkhof and McGillis (1999). But the estimated CO₂ air-sea exchange rates follow the trend of quadratic equation between wind speed and exchange rate by Wanninkhof (2014). This suggests that wind speed mainly influences the CO₂ air-sea exchange rates, which governs the net amount of bomb carbon going into the northern Indian Ocean and quadratic relation with wind speed provides better estimates of CO₂ exchange rates as compared to the cubic relation with wind speed. Figure 5.6 and Figure 5.7 show that regions with comparable wind speed show different exchange rates, which does not match with the empirical relation estimate. Dutta and Bhushan (2012) had observed that in some cases calculated air-sea CO₂ exchange rate could be anomalously different from empirical wind speed relationship. They suggested that lateral advection of ¹⁴C-enriched waters

to the region could lead to overestimation of CO₂ exchange rates. This deviation from the polynomial relation could also be due to some other factors like chemical enhancement of CO₂ exchange (Wanninkof and Knox 1996).

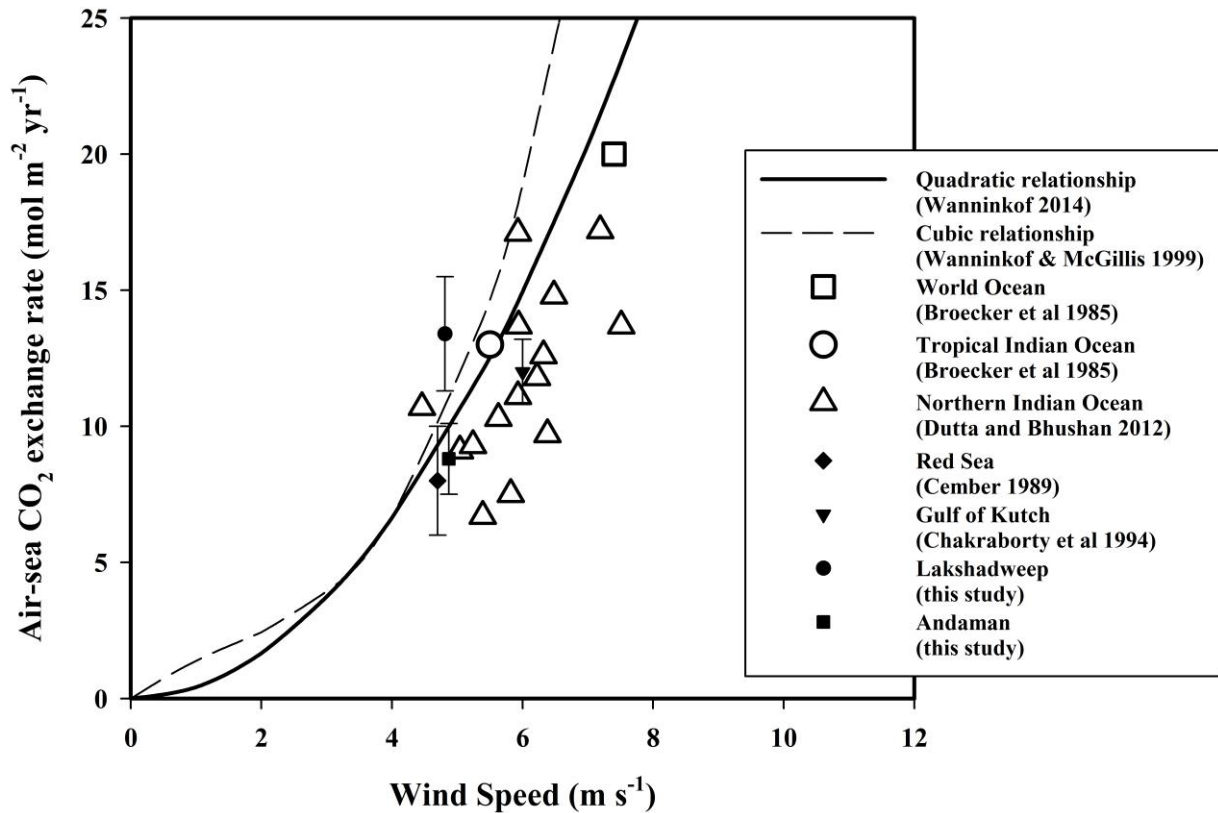


Figure 5.7: Relationship between air-sea CO₂ exchange rate and wind speed. Air-sea CO₂ exchange rates were calculated from gas transfer velocity (or piston velocity) using equation (1) in Druffel et al. (1989). Lines represent empirically derived relationship between wind speed and air-sea CO₂ exchange rates. Datapoints are bomb radiocarbon based estimates of air-sea CO₂ exchanges rates in northern Indian ocean region along with tropical Indian ocean and world ocean values

5.8. Air-Sea CO₂ Exchange Rate and surface water chemistry

Apart from wind speed, chemical property of seawater also plays an important role in air-sea exchange rate. CO₂ air-sea exchange requires molecular diffusion of CO₂ across boundary layer at air-sea interface driven by the CO₂ gradient in that layer. This exchange rate can be increased by chemical enhancement significantly at lower wind speed (Wanninkhof and Knox 1996, Kuss and Schneider 2004). Annual sea surface salinity values show maxima in the Arabian Sea, whereas the Bay of Bengal shows minima due to differences in hydrological forcing (Rao and Sivakumar 2003). River discharge and rainfall exceeds evaporation in the Bay of Bengal almost throughout the year leading to lower salinity in the region. Here, we have compared surface ocean carbonate chemistry of the northern Indian Ocean with radiocarbon based air-sea CO₂ exchange rates. Alkalinity, DIC and pCO₂ data were obtained from Takahashi et al (2014) dataset. The Arabian Sea region also shows relatively higher alkalinity and DIC values as compared to the Bay of Bengal region (Figure 8). The surface water chemistry of the two basins in the northern Indian Ocean is different. It is observed that the CO₂ exchange rate over the northern Indian Ocean show significant positive correlation with pCO₂ ($R^2 = 0.66$, $p < 0.005$), alkalinity ($R^2 = 0.34$, $p < 0.02$) and DIC ($R^2 = 0.36$, $p < 0.01$). This suggests that region with higher air-sea CO₂ exchange rates corresponds to the region where pCO₂, alkalinity and DIC is high. The salinity, alkalinity and DIC of the Bay of Bengal are relatively lower due to the freshwater influx which inhibits the vertical mixing or upwelling in the basin. Such scenario can also cause reduction in the surface water pCO₂ in the Bay of Bengal region. Kumar et al (1996) had suggested that thermohaline stratification along with biological production can lead to the reduction in pCO₂ of the Bay region. Whereas, the Arabian Sea experiences vertical mixing and upwelling which can increase the pCO₂, alkalinity and DIC of the region. This is also supported by the observation that excess CO₂ and bomb-14C penetrate deeper in the Arabian Sea (Dutta and Bhushan 2012). In the northern Indian Ocean the region which show CO₂ transfer from ocean to atmosphere also show high CO₂ transfer rates. Such scenario makes the northern Indian Ocean overall as source of atmospheric CO₂ as also observed in model based study by Louanchi et al (1996).

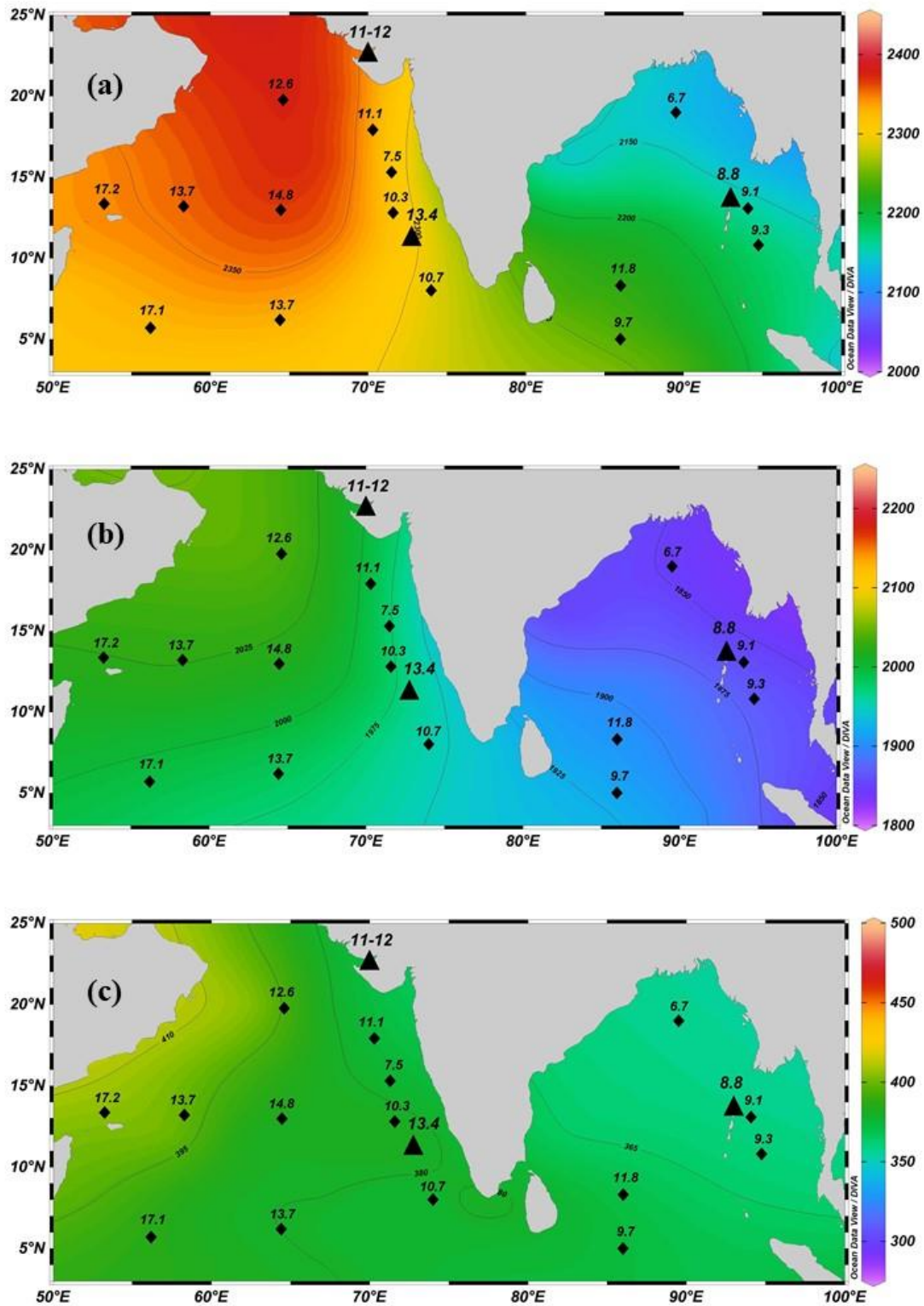


Figure 5.8: Colour contours of (a) Alkalinity ($\mu\text{Eq kg}^{-1}$), (b) Total carbon or DIC ($\mu\text{mol kg}^{-1}$), (c) $p\text{CO}_{2\text{sw}}$ of seawater (μatm) over the northern Indian Ocean (Takahashi et al 2014) along with the air-sea CO₂ exchange rates. ▲ represents coral based CO₂ air-sea exchange rates ($\text{mol m}^{-2} \text{yr}^{-1}$) from this study and Chakraborty et al (1994). ◆ represents CO₂ air-sea exchange rates ($\text{mol m}^{-2} \text{yr}^{-1}$) estimated by Dutta and Bhushan (2012).

5.9. Estimation of Net CO₂ Flux

The ocean is a large reservoir of CO₂ as compared to the atmosphere. The surface ocean Dissolved Inorganic Carbon inventory is about 1200 Gt C compared to the atmospheric inventory of 748 Gt C (Alves et al. 2018). The ocean reservoir stores about 50 times more dissolve inorganic carbon in comparison to the atmosphere (Alves et al. 2018). The ocean behaves as a sink for anthropogenic CO₂ emissions. Takahashi et al. (2009) provided net global ocean uptake flux of CO₂ to be around -2.0 ± 1.0 Pg C yr⁻¹. However, this uptake rate can vary from one region to another. Assessing the air-sea CO₂ fluxes and studying its temporal and spatial changes can improve our understanding of carbon cycling over a region. Difference between partial pressure of CO₂ in ocean and atmosphere drives the net transfer of CO₂ across the surface ocean. Using air-sea CO₂ exchange rate value, the net transfer of CO₂ across surface ocean can be determined by the following equation,

$$F = F_{12} \times \frac{\Delta pCO_2}{pCO_{2\ air}} \quad (3)$$

where, F is net CO₂ flux between air and sea. pCO_{2 air} is the partial pressure of CO₂ in the atmosphere and ΔpCO₂ is the difference of CO₂ partial pressure in surface ocean and atmosphere. If the value of F is positive, it means CO₂ flux is from ocean to atmosphere and vice versa. Generally, tropical oceans show positive ΔpCO₂ values with little seasonality implying that they are source region for CO₂ throughout the year (Takahashi et al. 2009). Sarma et al. (1998) had observed that the central and eastern Arabian Sea acts as source of CO₂ in almost every season. The ΔpCO₂ values for a 4° × 5° grid near Lakshadweep and Andaman coral sites were obtained from the gridded ΔpCO₂ values of Takahashi et al. (2009). The ΔpCO₂ values were 23.1 μatm and -3.5 μatm respectively for Lakshadweep and northern Andaman region. Following Dutta and Bhushan (2012), the net CO₂ flux for the Lakshadweep region was estimated to be 0.9 ± 0.1 mol m⁻² yr⁻¹ and for the Andaman region it was -0.1 ± 0.01 mol m⁻² yr⁻¹. This implies that the Lakshadweep region acts as a source of CO₂, whereas the northern Andaman region is a sink for CO₂. Based on the area of about 0.24×10^6 km² for the 4° × 5° grids, net regional CO₂ flux over the Lakshadweep Sea and the northern Andaman Sea was determined (Table 5.3). The Lakshadweep region show net regional CO₂ flux of 2.5 ± 0.4 Tg C yr⁻¹, while the northern Andaman region shows value of -0.3 ± 0.04 Tg C yr⁻¹. Sarma (2003) reported that the eastern Arabian Sea region releases annual CO₂ flux of about 8.21 Tg C yr⁻¹. The calculated net CO₂ flux value for the Lakshadweep region shows good agreement with this estimate. Bates et al. (2006) observed that the Indian Ocean is a source of CO₂ with total flux

of $237 \pm 132 \text{ Tg C yr}^{-1}$. Takahashi et al. (2009) also reported that the Indian Ocean north of 14° S is a source of CO_2 . However, they showed that the southern Indian Ocean is significant sink for CO_2 , which is in agreement with Louanchi et al. (1996) observation showing Indian Ocean between $20^\circ - 50^\circ \text{ S}$ as main sink of CO_2 . Monsoon plays an important role in pCO_2 dynamics of northern Indian Ocean region. Upwelling during monsoon bring high- pCO_2 carbon rich subsurface water to the surface increasing pCO_2 , which is reduced by biological productivity (Sabine et al. 2000). Monsoon causes strong upwelling in the Arabian Sea, whereas large freshwater discharge in the northern Bay of Bengal leads to surface stratification. These condition can produce contrasting net CO_2 flux in these two basins. Sarma et al. (2003) showed that the Arabian Sea is perennial source of CO_2 and pCO_2 in the region shows large variability due to monsoon induced seasonal upwelling and related biological processes. Dutta and Bhushan (2012) had estimated net CO_2 flux of 69 Tg C yr^{-1} for the Arabian Sea. The area of Lakshadweep region for which the CO_2 flux is calculated in this study is about 5 % of the Arabian Sea area, and it contributes almost 4 % of the net CO_2 flux from the Arabian Sea. Northern Andaman region, located on the eastern side of the southern Bay of Bengal, is a sink for CO_2 although the overall southern Bay of Bengal is a source of CO_2 (Dutta and Bhushan, 2012). Kumar et al. (1996) had observed that the northern Bay of Bengal is a sink of atmospheric CO_2 and suggested that moderately high new production and strong stratification as a result of river discharge in the region could lower the pCO_2 in surface waters. As the northern Andaman region is proximal to major rivers like Irrawaddy and Salween, it suggests that comparable biological pumping and surface stratification exists, which could explain the air to sea flux of CO_2 in this region. Thus, monsoon induced upwelling in the Arabian Sea and surface stratification in the Bay of Bengal are supposedly the causative mechanism for the observed contrast in net CO_2 flux from the Lakshadweep and the Andaman region.

Table 5.3: Air to sea CO_2 net flux estimates based on coral radiocarbon record from the northern Indian Ocean region

Region	ΔpCO_2 (μatm)	Mean air-sea CO_2 exchange rate ($\text{mol m}^{-2} \text{ yr}^{-1}$)	Net regional flux of CO_2 (Tg C yr^{-1})
Lakshadweep Sea ($10^\circ\text{-}14^\circ \text{ N}$, $70^\circ\text{-}75^\circ \text{ E}$)	23.128	13.4 ± 2.1	2.5 ± 0.4
Northern Andaman Sea ($10^\circ\text{-}14^\circ \text{ N}$, $90^\circ\text{-}95^\circ \text{ E}$)	-3.513	8.8 ± 1.3	-0.3 ± 0.04

Coral radiocarbon based air-sea CO₂ exchange rate thus provides important insight on the CO₂ fluxes over the study area. The air-sea CO₂ exchange rate over northern Indian Ocean show significant correlation with the wind speed. Measurements are required with more spatial coverage to improve understanding of CO₂ fluxes in the northern Indian Ocean.

5.10. Inferences

The radiocarbon record from the Landfall coral shows presence of stratification in the Andaman Sea region, whereas Kadmat coral radiocarbon record suggests influence of vertical mixing of subsurface waters in the region. The Landfall radiocarbon record extend up to year 1948 and provide pre-bomb radiocarbon values of DIC of surface water. The pre-bomb $\Delta^{14}\text{C}$ values of Landfall coral for the period 1948-1951 varies between -32 to -54 ‰. The mean ΔR value obtained from the Landfall coral is -138 ± 61 yr, which is lowest reported for the northern Indian Ocean. The ΔR values reported from the Andaman basin shows large variations, wherein southern Andaman ΔR value is higher than that of the northern Andaman and Bay of Bengal. As the northern Andaman basin receives more freshwater flux as compared to the southern Andaman, such differences in reservoir age could be observed. However, difference in ΔR values due to species dependent ¹⁴C variability cannot be ruled out. The coral radiocarbon record based air-sea CO₂ exchange rate over the Lakshadweep region is calculated to be 13.4 ± 2.1 mol m⁻² yr⁻¹, whereas for the northern Andaman region it is found to be 8.8 ± 1.3 mol m⁻² yr⁻¹. It is observed that air-sea CO₂ exchange rate over northern Indian Ocean follow a quadratic relation with the wind speed. The calculated net regional CO₂ flux from the Lakshadweep region is about 2.5 Tg C yr⁻¹ and for northern Andaman region it is -0.3 Tg C yr⁻¹. This implies that Lakshadweep region is a source of CO₂ whereas northern Andaman region is a sink for CO₂.

Chapter-6

Summary and Conclusion

6.1. Summary and Conclusion

This research work aims to investigate, reconstruct, and understand past changes in climate and sea surface conditions using geochemical proxies from corals from the northern Indian Ocean. Towards this, two coral cores, one each from the Lakshadweep and the Andaman islands, were analysed for their stable oxygen and carbon isotopes, radiocarbon, and Sr/Ca ratios. Both the Lakshadweep and Andaman regions are influenced by Indian monsoon during the summer season, however, these regions experience different sea surface conditions during the summer monsoon period. The Lakshadweep region experiences monsoon induced vertical mixing in the surface waters, which in turn changes the SST of the region. In contrast, the Andaman region receives large freshwater flux resulting from monsoonal rainfall and related riverine discharge, which stratifies the surface water column, inhibiting the vertical mixing in the region. A large number of coral colonies including massive type corals like *Porites* are found abundant in these regions. Specimens of these corals can record changes in climate patterns and sea-surface conditions in their geochemical properties. In a nutshell, based on geochemical analyses of Kadmat (Lakshadweep) and Landfall (Andaman) corals, following are the findings of the present research work:

- Both corals from the Kadmat and Landfall islands show alternating high- and low-density banding in the x-radiograph of their skeleton, suggesting seasonality in the deposition of their skeletal carbonate. The Kadmat coral showed an average growth rate of 14.7 ± 4.8 mm/year between 1977-2014. The Landfall coral has an average growth rate of 9.4 ± 2.4 mm/yr between 1948-2017. Both the Kadmat and Landfall corals show decline in their growth rates towards the present, which could be related to warming of the northern India Ocean.
- The Kadmat coral proxy record spans a timeframe of 37 years captured between 1977-2014. The mean $\delta^{18}\text{O}$ value of Kadmat coral is $-5.2 \pm 0.2\text{‰}$. On comparing the observed mean $\delta^{18}\text{O}$ value with reported mean $\delta^{18}\text{O}$ values of other *Porites* coral and giant clam (*Tridacna Maximus*) of Lakshadweep, it is observed that the *Porites* corals from the Lakshadweep islands exhibit inter colony variability in their $\delta^{18}\text{O}$ values. Thus, additional information is required about the disequilibrium offset to reconstruct past SST based on fossil Lakshadweep corals $\delta^{18}\text{O}$ records. The oxygen isotopic records from the Lakshadweep corals thus should be carefully interpreted for paleoclimatic studies.

- Kadmat coral $\delta^{18}\text{O}$ values were used to reconstruct high-resolution seawater $\delta^{18}\text{O}$ record. On a seasonal scale, the lowest mean $\delta^{18}\text{O}_{\text{sw}}$ value is obtained during the winter months of January-February, in agreement with freshening of Lakshadweep surface waters during the same season. In the absence of long term in-situ seawater $\delta^{18}\text{O}$ measurements, the coral-based $\delta^{18}\text{O}_{\text{sw}}$ can be useful for $\delta^{18}\text{O}$ -SST calibration and SST reconstruction purposes. The four-year running mean value of derived $\delta^{18}\text{O}_{\text{sw}}$ shows periods of depletion coinciding with periods of enhanced All India Rainfall intensity (four-year running mean). This observation suggests that the Lakshadweep corals can efficiently record rainfall signatures in their isotopic trends and can be used to identify periods of enhanced rainfall.
- Since inter colony variability exists in $\delta^{18}\text{O}$ values of Lakshadweep corals, correlating mean centered monthly $\delta^{18}\text{O}$ values and SST values can provide a reliable $\delta^{18}\text{O}$ -SST relation. The calibration equation derived from such correlation can be used to reconstruct past SST variability. By using the available $\delta^{18}\text{O}$ records from Lakshadweep corals and Kadmat coral derived $\delta^{18}\text{O}_{\text{sw}}$ values a calibration equation was obtained. It was observed that Lakshadweep coral $\delta^{18}\text{O}$ values corresponding to monsoon months record the regional SST variations more robustly as compared to $\delta^{18}\text{O}$ values of summer months.
- The Sr/Ca ratios of the Landfall coral shows a good correlation with SST, yielding a Sr/Ca-SST calibration equation. In contrast, coral $\delta^{18}\text{O}$ values show a relatively weak correlation with SST yielding a shallow slope suggesting a significant contribution of seawater $\delta^{18}\text{O}$ variation in the Landfall coral $\delta^{18}\text{O}$ variability. In the absence of information about seawater $\delta^{18}\text{O}$ changes, Sr/Ca ratio appears to be a better proxy for SST reconstruction in the Andaman region.
- Using the paired Sr/Ca and $\delta^{18}\text{O}$ measurements in Landfall coral, seawater $\delta^{18}\text{O}$ values were reconstructed for the region. It was found that both SST and rainfall influence the monthly seawater $\delta^{18}\text{O}$ values. The obtained correlation between seasonal rainfall and $\Delta\delta^{18}\text{O}_{\text{sw}}$ values suggests that Andaman coral derived $\Delta\delta^{18}\text{O}_{\text{sw}}$ values can also be used for qualitative reconstruction of past monsoon rainfall.
- The Landfall coral $\delta^{18}\text{O}$ values show a good correlation with SST but only after correcting for seawater $\delta^{18}\text{O}$ value changes. It was found that the Landfall coral derived seawater $\delta^{18}\text{O}$ values show comparatively warm or fresh sea surface conditions during relatively warmer phase in east central tropical Pacific. This observation might suggest

that long term SST changes in Nino region of the Pacific Ocean influence the sea surface conditions in the Andaman region.

- $\delta^{13}\text{C}$ values of both Kadmat and Landfall coral show seasonality. Kadmat coral $\delta^{13}\text{C}$ record show depletion during the monsoon period. It was observed that the $\delta^{13}\text{C}$ variability in Kadmat coral is not only modulated by photosynthesis, but some other processes that contribute to the observed $\delta^{13}\text{C}$ variability. In contrast, Landfall coral $\delta^{13}\text{C}$ values record the seasonal changes in photosynthesis is possibly caused by changes in light availability.
- The radiocarbon record of Kadmat coral shows relatively lower $\Delta^{14}\text{C}$ values compared to the Landfall coral radiocarbon record for the contemporary period. This observation suggests the influence of upwelled waters in the Lakshadweep region. The Landfall coral records the highest $\Delta^{14}\text{C}$ values in the Indian Ocean region, and the post-bomb $\Delta^{14}\text{C}$ values also show less variability compared to the Kadmat coral. This observation indicates that the waters near the Landfall region are stratified, with dampened vertical mixing. The present-day surface water radiocarbon concentrations in the Arabian and Andaman seas can be different in two basins due to various oceanic processes.
- Based on coral radiocarbon values, the obtained air-sea CO_2 exchange rates were calculated to be: (i) $13.4 \pm 2.1 \text{ mol m}^{-2} \text{ yr}^{-1}$ for the Lakshadweep region, and (ii) $8.8 \pm 1.3 \text{ mol m}^{-2} \text{ yr}^{-1}$ for the northern Andaman region. Further, It was found that the air-sea CO_2 exchange rates over the northern Indian Ocean follow a quadratic relationship with the wind speed. The calculated net regional CO_2 flux from the Lakshadweep region is about 2.5 Tg C yr^{-1} , and for the northern Andaman region, it is $-0.3 \text{ Tg C yr}^{-1}$. These observations suggest that the Lakshadweep region is a net source of CO_2 , whereas the northern Andaman region is a sink for atmospheric CO_2 . These observations suggest that despite the Arabian Sea and Andaman Sea being contemporary basins in the northern Indian Ocean, they have different CO_2 sequestration rates.
- The Landfall coral radiocarbon record extends up to the year 1948. Thus, it provides pre-bomb radiocarbon values of surface water DIC. The pre-bomb values for the period 1948-1951 vary between -32 to -54‰. The mean reservoir age correction value (ΔR) obtained for this period from the Landfall coral is $-138 \pm 61 \text{ yr}$, which is lowest reported for the northern Indian Ocean. The ΔR values reported from the Andaman basin shows significant variations, with southern Andaman showing relatively elevated ΔR values than the northern Andaman and Bay of Bengal. As the northern Andaman basin

receives relatively more freshwater flux as compared to the southern Andaman, such differences in reservoir age results due to the local oceanic processes governing these regions. However, differences in ΔR values due to species-dependent ^{14}C variability cannot be ruled out. This study reports the reservoir age corrections for the northern Andaman region. This new reservoir age correction data can be a valuable contribution to the global reservoir age inventory of the oceans, and can help in correction of radiocarbon ages from this region.

6.2. Future Scope of the Study

This work has investigated the geochemical and isotope proxies in corals from Indian coral reefs to explore their ability to provide information about past climate variations and sea surface conditions. The obtained results show that these corals have potential to provide information about past SST and monsoonal rainfall changes. This premise provides further encouragement to study the geochemical and isotopic proxies in fossil corals from these regions to understand past climatic and oceanic conditions. The past coral records, especially from warmer conditions than present-day, are of particular interest. Such records can be instrumental in predicting climatic and oceanic conditions in the contemporary warming world.

Studying past monsoon variations is essential for understanding the dynamic nature of monsoon. Paired Sr/Ca and $\delta^{18}\text{O}$ studies in longer coral cores extended to prolonged durations from these regions can be very helpful in understanding past monsoon/climate variations and associated sea surface condition changes. It has been observed that the reconstructed Andaman seawater $\delta^{18}\text{O}$ values are influenced by monsoon rainfall. Extended Andaman seawater $\delta^{18}\text{O}$ records can help us understand past monsoon rainfall variations over a longer timescale. The reconstructed Lakshadweep seawater $\delta^{18}\text{O}$ values can also help to identify enhanced rainfall periods on an interannual scale. The stable carbon isotope record of the Lakshadweep coral suggests that photosynthesis might not be the primary factor modulating their $\delta^{13}\text{C}$ values. A more detailed investigation is required to quantify controlling factor behind $\delta^{13}\text{C}$ variations in Lakshadweep corals. This will help in understanding the seasonality observed in these records.

Based on radiocarbon records of corals, air-sea CO_2 exchange rates over the Lakshadweep and Andaman seas were estimated. Coral radiocarbon records from other reefs can provide valuable information to understand the variation in air-sea CO_2 exchange rates on regional to global scale. High resolution (seasonal) radiocarbon records from these corals can help to better understand seasonal upwelling or surface circulation changes in the region. The pre-bomb

radiocarbon records from corals in the northern Indian Ocean can provide much better constraints on marine reservoir ages. This is necessary for accurate radiocarbon dating of marine samples in the region. Pre-bomb coral radiocarbon records from these corals can also provide information about the degree of Suess effect over the northern Indian Ocean.

Appendix A

Calculation of pMC and $\Delta^{14}\text{C}$ values from raw data obtained from AMS:

AMS measures isotopes of carbon (^{12}C , ^{13}C , and ^{14}C) in the samples. This provides us with $^{14}\text{C}/^{12}\text{C}$, $^{14}\text{C}/^{13}\text{C}$ and $^{13}\text{C}/^{12}\text{C}$ ratios in the sample. Specific activity (A) of sample and standard are required to calculate pMC and $\Delta^{14}\text{C}$ values in a sample (Stuiver and Polach 1977). Specific activity is related to the fraction of ^{14}C in total carbon atoms (Donahue et al. 1990) and can be represented as follows,

$$A = \frac{^{14}\text{C}}{^{12}\text{C}}$$

This ratio is measured for sample, process blank, primary standard and secondary standard. Process blank is a material which has no radiocarbon atom left in it and that has been processed (graphitization) following same procedure as that of samples. Primary standard is the Oxalic acid standards (Ox I and Ox II) against which the activity of a material is calculated for its radiocarbon concentration. Primary standard provides the radiocarbon reference value with respect to which all radiocarbon data are reported. Secondary standard are inter-comparison exercise samples, whose radiocarbon values with respect to primary standard value is known with a consensus.

Activity of samples and standards are corrected for the process blank activity. The resultant activity is then normalised for ^{13}C fractionation (Stuiver 1983, Donahue et al. 1990) by following equations,

$$A_{SN} = A_S \times \left\{ \frac{1 - \frac{25}{1000}}{\delta^{13}\text{C}} \right\}^2$$

$$A_{ON} = 0.95 \times A_{OXI} \times \left\{ \frac{1 - \frac{19}{1000}}{\delta^{13}\text{C}} \right\}^2$$

$$A_{ON} = 0.7459 \times A_{OXII} \times \left\{ \frac{1 - \frac{25}{1000}}{\delta^{13}\text{C}} \right\}^2$$

Where, A_S is the activity of the sample, A_{OXI} is the activity of Old oxalic acid (Ox I) and A_{OXII} is the activity of New oxalic acid (Ox II). The resultant activity of samples and standards are then used to calculate pMC and $\Delta^{14}\text{C}$ values using following equations as mentioned earlier

$$pMC = \frac{A_{SN}}{A_{ON}} \times 100$$

$$\Delta^{14}\text{C} = \left(\frac{A_{SN} e^{\lambda c(1950-x)}}{A_{ON}} - 1 \right) \times 1000$$

Appendix B

Calculation for obtaining $\Delta\delta^{18}\text{O}$ and $\Delta\text{Sr}/\text{Ca}$ (mean centered value):

Mean centered value is calculated by removing (subtracting) mean value from each measured value of a parameter. Mathematically it can be represented as follows,

$$\Delta x = (x_i - \bar{x})$$

Where, x_i is the measured value of a parameter and \bar{x} is the mean of all measured values. $\Delta\delta^{18}\text{O}_{\text{coral}}$, $\Delta\delta^{18}\text{O}_{\text{sw}}$ and $\Delta\text{Sr}/\text{Ca}$ values are calculated by using this formula in following form,

$$\Delta\delta^{18}\text{O}_{\text{coral}} = (\delta^{18}\text{O}_{\text{coral}_i} - \overline{\delta^{18}\text{O}})$$

$$\Delta\delta^{18}\text{O}_{\text{sw}} = (\delta^{18}\text{O}_{\text{sw}_i} - \overline{\delta^{18}\text{O}})$$

$$\Delta\text{Sr}/\text{Ca} = (\text{Sr}/\text{Ca}_i - \overline{\text{Sr}/\text{Ca}})$$

Appendix C

Determination of reservoir age correction value (ΔR):

Ocean is a huge reservoir of carbon and it mixes slowly compared to atmosphere. Thus ocean has lower ^{14}C concentration compared to atmosphere, which leads to the reservoir effect in the ^{14}C based ages of marine samples. To accurately radiocarbon date marine sample, information about reservoir age correction value is required. ΔR can be calculated using known age pre-bomb marine surface samples (Reimer and Reimer 2017) using following equation,

$$\Delta R = t_{14c} - t_{marine13}$$

Where, t_{14c} is the measured radiocarbon age of the pre-bomb marine surface sample. $t_{marine13}$ is the radiocarbon age determined from known age (calendar year) of the pre-bomb marine surface sample using MARINE13 calibration curve (Figure 6.1). Marine calibration curve gives the global average marine reservoir age value. The difference of measured radiocarbon age from the global average marine reservoir age value is ΔR .

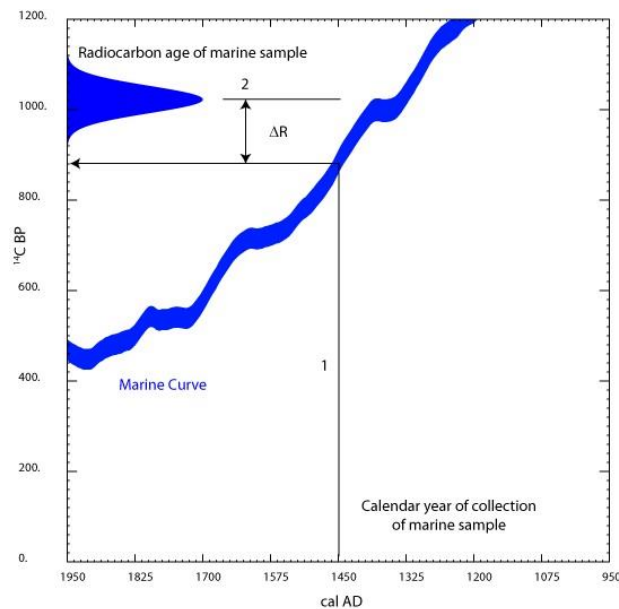


Figure 6.1: Plot showing calculation of ΔR values in two steps using measured radiocarbon age and known age of the pre-bomb surface marine samples (<http://calib.org/deltar>). Step 1 (represented by line 1) is determining ^{14}C age corresponding to the known age of the pre-bomb marine sample using marine calibration curve. Step 2 (represented by line 2) is subtracting the marine calibration curve based ^{14}C age from the measured ^{14}C age of the pre-bomb marine sample

Appendix D

Determination of air-sea CO₂ exchange rate using radiocarbon inventory change:

Following equation was given by Stuiver (1980) to determine air-sea CO₂ exchange rate, where total amount of bomb ¹⁴C transferred to the ocean is proportional to the air-sea CO₂ exchange rate and time integrated Δ¹⁴C values of atmosphere and surface ocean.

$$Q_{14} = k \times F_{12} \times \int_0^t (\Delta^{14}C_{air} - \Delta^{14}C_{mix} - 60) dt$$

Where k is a constant that accounts for fractionation factor for ocean-atmosphere transfer and normalization of ¹⁴C activity to δ¹³C value of -25 ‰. The value of constant k is 1.24 × 10⁻¹⁵. Q₁₄ is the bomb radiocarbon inventory of the ocean and F₁₂ is the air-sea CO₂ exchange rate. Δ¹⁴C_{air} and Δ¹⁴C_{mix} are radiocarbon values of atmosphere and coral respectively. Following Dutta and Bhushan (2012), 1954 is considered as the initial year (t=0) of bomb ¹⁴C penetration in to the ocean and a steady state difference of -60 ‰ between atmosphere and the northern Indian Ocean is assumed.

Equation a, for time t₁ since onset of input of bomb ¹⁴C to the ocean (t=0)

$$Q_{14}^{t_1} = k \times F_{12} \times \int_0^{t_1} (\Delta^{14}C_{air} - \Delta^{14}C_{mix} - 60) dt$$

Equation b, for time t₂ since onset of input of bomb ¹⁴C to the ocean (t=0)

$$Q_{14}^{t_2} = k \times F_{12} \times \int_0^{t_2} (\Delta^{14}C_{air} - \Delta^{14}C_{mix} - 60) dt$$

Using Equation a and b

$$Q_{14}^{t_2} - Q_{14}^{t_1} = k \times F_{12} \times \left[\int_0^{t_2} (\Delta^{14}C_{air} - \Delta^{14}C_{mix} - 60) dt - \int_0^{t_1} (\Delta^{14}C_{air} - \Delta^{14}C_{mix} - 60) dt \right]$$

$$Q_{14}^{t_2} - Q_{14}^{t_1} = k \times F_{12} \times \left[\int_{t_1}^{t_2} (\Delta^{14}C_{air}) dt - \int_{t_1}^{t_2} (\Delta^{14}C_{mix}) dt - \int_{t_1}^{t_2} 60 dt \right]$$

$$Q_{14}^{t_2} - Q_{14}^{t_1} = k \times F_{12} \times \left[\int_{t_1}^{t_2} (\Delta^{14}C_{air} - \Delta^{14}C_{mix} - 60) dt \right]$$

The above determined equation can provide air-sea CO₂ exchange rates if we have the information about change in radiocarbon inventory in the ocean. The derived equation was used to calculate air-sea CO₂ exchange rate from Kadmat coral record

Geochemical and isotopic data

Table 6.1: Stable Isotopic composition of Kadmat coral

Sr No.	Year	$\delta^{13}\text{C}$ (‰)	$\delta^{18}\text{O}$ (‰)	Anchor points
1	2014.67	-2.0	-4.9	*
2	2014.50	-1.8	-5.1	
3	2014.33	-1.4	-5.3	*
4	2014.17	-1.5	-5.3	
5	2014.00	-1.7	-5.1	
6	2013.83	-1.5	-5.1	
7	2013.67	-1.3	-5.3	
8	2013.50	-2.2	-4.7	*
9	2013.33	-1.5	-5.2	*
10	2013.17	-1.6	-5.1	
11	2013.00	-1.8	-5.0	
12	2012.83	-1.9	-5.0	
13	2012.67	-2.1	-4.9	
14	2012.50	-2.2	-4.8	*
15	2012.33	-1.5	-5.4	*
16	2012.17	-2.3	-5.1	
17	2012.00	-1.5	-5.0	
18	2011.83	-1.1	-5.2	
19	2011.67	-1.7	-4.6	*
20	2011.50	-1.8	-4.9	
21	2011.33	-1.1	-5.6	*
22	2011.17	-1.6	-5.3	
23	2011.00	-1.2	-5.6	
24	2010.83	-0.8	-5.5	
25	2010.67	-1.5	-5.2	*
26	2010.50	-1.3	-5.3	
27	2010.33	-1.3	-6.1	*
28	2010.17	-1.1	-5.3	
29	2010.00	-0.9	-5.4	
30	2009.83	-0.6	-5.3	
31	2009.67	-0.8	-5.2	
32	2009.50	-1.4	-5.0	*
33	2009.33	-1.0	-5.4	*
34	2009.17	-1.0	-5.3	
35	2009.00	-1.8	-5.1	
36	2008.83	-2.1	-5.1	
37	2008.67	-2.2	-5.2	
38	2008.50	-2.1	-5.1	*
39	2008.33	-1.1	-5.6	*
40	2008.17	-1.3	-5.4	
41	2008.00	-1.4	-5.4	
42	2007.83	-1.7	-5.3	
43	2007.67	-1.9	-5.2	*
44	2007.50	-1.6	-5.4	
45	2007.33	-0.6	-5.7	*

46	2007.17	-1.0	-5.5	
47	2007.00	-1.3	-5.3	
48	2006.83	-1.6	-5.1	
49	2006.67	-1.8	-5.2	
50	2006.50	-1.9	-5.1	*
51	2006.33	-0.7	-5.6	*
52	2006.17	-1.1	-5.3	
53	2006.00	-1.2	-5.2	
54	2005.83	-1.4	-5.2	
55	2005.67	-1.8	-5.1	*
56	2005.50	-1.9	-5.3	
57	2005.33	-1.9	-5.8	*
58	2005.17	-1.9	-5.6	
59	2005.00	-1.8	-5.4	
60	2004.83	-1.8	-5.3	
61	2004.67	-1.8	-5.1	
62	2004.50	-1.8	-4.9	*
63	2004.33	-1.9	-5.4	*
64	2004.17	-1.4	-5.3	
65	2004.00	-1.9	-5.3	
66	2003.83	-2.0	-5.1	
67	2003.67	-1.8	-4.9	*
68	2003.50	-2.1	-5.2	
69	2003.33	-1.8	-5.6	*
70	2003.17	-2.0	-5.4	
71	2003.00	-1.7	-5.3	
72	2002.83	-2.1	-5.3	
73	2002.67	-1.9	-5.0	*
74	2002.50	-1.7	-5.2	
75	2002.33	-1.1	-5.5	*
76	2002.17	-1.4	-5.2	
77	2002.00	-2.1	-5.3	
78	2001.83	-1.9	-5.2	
79	2001.67	-1.5	-5.2	
80	2001.50	-1.7	-5.0	*
81	2001.33	-1.8	-5.4	*
82	2001.17	-1.4	-5.2	
83	2001.00	-1.2	-5.2	
84	2000.83	-1.3	-5.3	
85	2000.67	-1.3	-5.2	
86	2000.50	-1.4	-5.0	*
87	2000.33	-1.1	-5.5	*
88	2000.17	-1.4	-5.2	
89	2000.00	-1.3	-5.1	
90	1999.83	-1.1	-5.1	
91	1999.67	-0.3	-4.5	*
92	1999.50	-0.3	-4.8	
93	1999.33	-0.9	-5.3	*
94	1999.17	-1.7	-5.2	
95	1999.00	-1.4	-5.1	

96	1998.83	-1.3	-5.0	
97	1998.67	-1.5	-5.0	*
98	1998.50	-1.2	-5.4	
99	1998.33	-1.4	-5.4	*
100	1998.17	-1.4	-5.3	
101	1998.00	-1.5	-5.1	
102	1997.83	-1.8	-5.0	
103	1997.67	-1.8	-4.9	*
104	1997.50	-0.8	-5.5	
105	1997.33	-1.4	-5.5	*
106	1997.17	-1.3	-5.5	
107	1997.00	-1.5	-4.9	
108	1996.83	-1.6	-5.1	
109	1996.67	-1.9	-4.9	*
110	1996.50	-1.0	-5.3	
111	1996.33	-1.3	-5.4	*
112	1996.17	-1.3	-5.2	
113	1996.00	-1.3	-5.2	
114	1995.83	-1.4	-5.1	
115	1995.67	-1.7	-4.9	*
116	1995.50	-1.7	-5.4	
117	1995.33	-1.4	-5.6	*
118	1995.17	-1.3	-5.2	
119	1995.00	-1.5	-5.1	
120	1994.83	-1.7	-5.1	
121	1994.67	-1.2	-4.9	*
122	1994.50	-1.7	-5.0	
123	1994.33	-0.7	-5.4	*
124	1994.17	-1.6	-5.2	
125	1994.00	-1.3	-5.1	
126	1993.83	-1.6	-5.4	
127	1993.67	-2.0	-5.0	*
128	1993.50	-0.9	-5.3	
129	1993.33	-1.7	-5.6	*
130	1993.17	-1.4	-5.0	
131	1993.00	-1.4	-5.2	
132	1992.83	-1.6	-5.3	
133	1992.67	-1.6	-5.0	*
134	1992.50	-0.9	-5.3	
135	1992.33	-1.5	-5.6	*
136	1992.17	-1.5	-5.3	
137	1992.00	-1.4	-5.3	
138	1991.83	-2.1	-5.2	
139	1991.67	-1.6	-4.8	*
140	1991.50	-1.1	-5.5	
141	1991.33	-1.4	-5.7	*
142	1991.17	-1.6	-4.9	
143	1991.00	-1.9	-5.2	
144	1990.83	-1.4	-5.3	
145	1990.67	-2.0	-5.0	*

146	1990.50	-1.6	-5.3	
147	1990.33	-1.1	-5.6	*
148	1990.17	-1.6	-5.2	
149	1990.00	-1.5	-5.3	
150	1989.83	-1.8	-4.9	
151	1989.67	-1.9	-5.0	
152	1989.50	-2.0	-4.9	*
153	1989.33	-0.9	-5.5	*
154	1989.17	-1.1	-5.2	
155	1989.00	-1.0	-5.1	
156	1988.83	-2.1	-5.0	
157	1988.67	-1.8	-5.0	
158	1988.50	-2.1	-4.8	*
159	1988.33	-0.6	-5.4	*
160	1988.17	-1.1	-5.2	
161	1988.00	-1.5	-5.2	
162	1987.83	-1.4	-4.9	
163	1987.67	-1.9	-4.8	*
164	1987.50	-1.7	-4.9	
165	1987.33	-0.8	-5.6	*
166	1987.17	-1.3	-5.1	
167	1987.00	-1.9	-5.0	
168	1986.83	-1.6	-5.0	
169	1986.67	-1.4	-4.9	*
170	1986.50	-1.8	-5.4	
171	1986.33	-1.2	-5.7	*
172	1986.17	-1.3	-5.4	
173	1986.00	-1.6	-5.4	
174	1985.83	-1.3	-5.2	
175	1985.67	-1.7	-5.2	
176	1985.50	-1.5	-4.9	*
177	1985.33	-0.5	-5.4	*
178	1985.17	-1.0	-5.4	
179	1985.00	-1.0	-5.2	
180	1984.83	-0.9	-5.3	
181	1984.67	-1.7	-5.0	*
182	1984.50	-1.0	-5.1	
183	1984.33	-0.9	-5.4	*
184	1984.17	-1.1	-5.2	
185	1984.00	-1.5	-5.3	
186	1983.83	-1.8	-5.2	
187	1983.67	-1.3	-4.8	*
188	1983.50	-1.3	-5.2	
189	1983.33	-0.9	-5.6	*
190	1983.17	-0.7	-5.4	
191	1983.00	-1.0	-5.2	
192	1982.83	-0.9	-5.1	
193	1982.67	-1.2	-5.1	*
194	1982.50	-0.6	-5.2	
195	1982.33	-0.4	-5.6	*

196	1982.17	-1.1	-5.4	
197	1982.00	-1.4	-5.2	
198	1981.83	-1.7	-5.0	
199	1981.67	-1.7	-4.9	
200	1981.50	-1.4	-4.7	*
201	1981.33	-0.7	-5.3	*
202	1981.17	-1.4	-5.1	
203	1981.00	-1.8	-4.9	
204	1980.83	-1.2	-5.1	
205	1980.67	-1.5	-4.8	*
206	1980.50	-1.5	-4.9	
207	1980.33	-0.7	-5.2	*
208	1980.17	-0.9	-5.2	
209	1980.00	-1.2	-5.1	
210	1979.83	-1.3	-5.0	
211	1979.67	-1.4	-4.8	*
212	1979.50	-2.3	-5.1	
213	1979.33	-2.2	-5.4	*
214	1979.17	-1.2	-5.1	
215	1979.00	-1.5	-5.1	
216	1978.83	-1.8	-5.0	
217	1978.67	-1.7	-4.8	*
218	1978.50	-1.4	-5.1	
219	1978.33	-1.0	-5.2	*
220	1978.17	-1.2	-4.9	
221	1978.00	-1.3	-4.8	
222	1977.83	-1.5	-4.9	
223	1977.67	-1.7	-4.7	*
224	1977.50	-1.6	-4.7	
225	1977.33	-1.5	-5.1	*

Table 6.2: Sr/Ca ratios and stable isotopic composition of top 65 mm of Landfall coral

Sr. No.	Year	Sr/Ca (mmol/mol)	$\delta^{13}\text{C}$ (‰)	$\delta^{18}\text{O}$ (‰)	Anchor points
1	2018.00	8.96	-2.0	-5.6	*
2	2017.92	8.93	-2.0	-5.6	
3	2017.83	8.91	-2.0	-5.6	
4	2017.75	8.88	-2.0	-5.6	*
5	2017.67	8.94	-2.4	-5.7	
6	2017.58	8.91	-2.5	-5.9	
7	2017.50	9.04	-2.3	-5.6	*
8	2017.42	8.87	-2.9	-5.4	
9	2017.33	8.81	-2.4	-5.6	*
10	2017.25	8.86	-2.1	-5.1	
11	2017.17	8.96	-1.9	-5.3	
12	2017.08	9.00	-2.0	-5.4	*
13	2017.00	8.87	-2.0	-5.3	

14	2016.92	8.90	-1.9	-5.3	
15	2016.83	8.80	-2.1	-5.7	*
16	2016.75	8.94	-1.9	-5.4	
17	2016.67	8.97	-1.8	-5.5	*
18	2016.58	8.96	-2.1	-5.4	
19	2016.50	8.97	-2.7	-5.8	
20	2016.42	8.90	-3.3	-5.6	
21	2016.33	8.88	-2.5	-5.3	*
22	2016.25	8.94	-2.3	-5.3	
23	2016.17	9.00	-2.1	-5.3	
24	2016.08	9.04	-2.0	-5.2	
25	2016.00	9.08	-1.9	-5.0	*
26	2015.92	8.99	-2.2	-5.1	
27	2015.83	9.03	-2.3	-5.3	
28	2015.75	8.98	-1.9	-4.8	*
29	2015.67	9.03	-1.9	-5.0	
30	2015.58	9.09	-1.8	-5.2	*
31	2015.50	8.98	-2.3	-5.3	
32	2015.42	9.00	-2.5	-5.4	
33	2015.33	8.89	-3.0	-5.4	*
34	2015.25	8.93	-2.0	-5.1	
35	2015.17	8.95	-1.7	-5.0	
36	2015.08	9.11	-1.5	-5.3	*
37	2015.00	9.02	-1.5	-5.4	
38	2014.92	9.06	-1.8	-5.6	
39	2014.83	8.97	-1.9	-5.6	
40	2014.75	8.90	-1.9	-5.4	*
41	2014.67	8.97	-2.7	-5.3	
42	2014.58	8.99	-3.1	-5.3	*
43	2014.50	8.91	-2.6	-5.6	
44	2014.42	8.89	-2.0	-5.8	
45	2014.33	8.86	-1.6	-5.3	*
46	2014.25	8.91	-1.6	-5.1	
47	2014.17	8.97	-1.5	-4.8	
48	2014.08	8.98	-1.5	-4.9	
49	2014.00	9.00	-1.5	-5.1	*
50	2013.92	8.96	-1.3	-5.0	
51	2013.83	8.96	-1.6	-5.6	
52	2013.75	8.93	-1.6	-5.6	*
53	2013.67	8.97	-2.0	-5.4	
54	2013.58	8.98	-2.7	-5.5	*
55	2013.50	8.92	-2.9	-5.7	
56	2013.42	8.85	-3.1	-5.8	
57	2013.33	8.79	-3.3	-6.0	*
58	2013.25	8.82	-2.0	-5.8	
59	2013.17	8.89	-1.9	-5.6	
60	2013.08	9.02	-1.9	-5.5	*
61	2013.00	8.96	-1.8	-5.5	
62	2012.92	8.93	-1.6	-5.6	
63	2012.83	8.90	-1.5	-5.7	

64	2012.75	8.86	-1.7	-5.8	*
65	2012.67	8.93	-2.7	-5.7	*
66	2012.58	8.92	-2.6	-5.7	
67	2012.50	8.92	-2.5	-5.8	
68	2012.42	8.91	-2.3	-5.8	
69	2012.33	8.90	-2.2	-5.8	*
70	2012.25	8.95	-1.7	-5.7	
71	2012.17	9.02	-1.6	-5.3	
72	2012.08	9.09	-1.5	-5.2	*

Table 6.3: Stable isotopic composition of Landfall coral below the top 65 mm

Sr No.	Year	$\delta^{13}\text{C}$ (‰)	$\delta^{18}\text{O}$ (‰)	Anchor points
1	2011.92	-1.6	-5.2	
2	2011.75	-2.7	-5.3	
3	2011.58	-2.1	-5.5	
4	2011.42	-2.0	-5.8	*
5	2011.25	-1.9	-5.6	
6	2011.08	-1.7	-5.3	*
7	2010.92	-1.9	-5.4	
8	2010.75	-2.0	-5.6	
9	2010.58	-2.1	-5.7	
10	2010.42	-2.2	-5.8	*
11	2010.25	-2.7	-5.6	
12	2010.08	-1.7	-5.3	*
13	2009.92	-1.8	-5.4	
14	2009.75	-1.9	-5.5	
15	2009.58	-1.9	-5.7	
16	2009.42	-2.0	-5.8	*
17	2009.25	-2.2	-5.6	
18	2009.08	-2.1	-5.4	*
19	2008.92	-1.9	-5.5	
20	2008.75	-1.7	-5.5	
21	2008.58	-1.8	-5.7	
22	2008.42	-1.8	-5.8	*
23	2008.25	-2.3	-5.7	
24	2008.08	-1.7	-5.4	*
25	2007.92	-1.9	-5.6	
26	2007.75	-2.3	-5.6	
27	2007.58	-2.6	-5.9	
28	2007.42	-2.4	-6.2	*
29	2007.25	-2.0	-5.8	
30	2007.08	-1.7	-5.6	*
31	2006.92	-2.3	-5.5	
32	2006.75	-2.8	-5.7	
33	2006.58	-1.7	-5.7	
34	2006.42	-1.6	-5.8	*
35	2006.25	-1.6	-5.6	

36	2006.08	-1.6	-5.3	*
37	2005.92	-1.6	-5.4	
38	2005.75	-1.7	-5.5	
39	2005.58	-1.7	-5.6	
40	2005.42	-1.8	-5.7	*
41	2005.25	-1.6	-5.5	
42	2005.08	-1.6	-5.5	*
43	2004.92	-1.6	-5.5	
44	2004.75	-1.6	-5.6	
45	2004.58	-1.6	-5.6	
46	2004.42	-1.6	-5.7	*
47	2004.25	-2.2	-5.5	
48	2004.08	-1.6	-5.3	*
49	2003.92	-1.4	-5.3	
50	2003.75	-1.7	-5.8	
51	2003.58	-2.1	-5.5	
52	2003.42	-3.0	-5.9	*
53	2003.25	-2.2	-5.6	
54	2003.08	-1.4	-5.3	*
55	2002.92	-1.3	-5.3	
56	2002.75	-1.3	-5.3	
57	2002.58	-1.6	-5.5	
58	2002.42	-1.9	-5.7	*
59	2002.25	-2.3	-5.5	
60	2002.08	-1.4	-5.3	*
61	2001.92	-1.5	-5.3	
62	2001.75	-1.7	-5.6	
63	2001.58	-2.5	-5.6	
64	2001.42	-1.9	-5.6	*
65	2001.25	-1.6	-5.4	
66	2001.08	-1.2	-5.2	*
67	2000.92	-1.4	-5.3	
68	2000.75	-1.6	-5.5	
69	2000.58	-2.3	-5.8	
70	2000.42	-2.9	-6.2	*
71	2000.25	-1.6	-5.7	
72	2000.08	-1.5	-5.2	*
73	1999.92	-1.6	-5.4	
74	1999.75	-1.8	-5.6	
75	1999.58	-2.0	-5.9	
76	1999.42	-2.1	-6.1	*
77	1999.25	-1.5	-5.3	
78	1999.08	-1.2	-5.3	*
79	1998.92	-1.3	-5.3	
80	1998.75	-1.4	-5.4	
81	1998.58	-1.6	-5.5	
82	1998.42	-1.7	-5.5	*
83	1998.25	-2.1	-5.4	
84	1998.08	-1.4	-5.2	*
85	1997.92	-1.4	-5.3	

86	1997.75	-1.5	-5.4	
87	1997.58	-1.9	-5.7	
88	1997.42	-2.8	-6.3	*
89	1997.25	-1.4	-5.8	
90	1997.08	-1.4	-5.7	*
91	1996.92	-1.4	-5.7	
92	1996.75	-1.5	-5.8	
93	1996.58	-1.5	-5.8	
94	1996.42	-1.6	-5.9	*
95	1996.25	-2.4	-5.4	
96	1996.08	-1.7	-5.1	*
97	1995.92	-1.5	-5.3	
98	1995.75	-1.5	-5.4	
99	1995.58	-2.6	-5.5	
100	1995.42	-2.0	-5.5	*
101	1995.25	-1.6	-5.3	
102	1995.08	-1.3	-5.3	*
103	1994.92	-1.4	-5.3	
104	1994.75	-1.4	-5.3	
105	1994.58	-1.4	-5.4	
106	1994.42	-1.7	-5.4	*
107	1994.25	-2.1	-5.4	
108	1994.08	-1.2	-5.1	*
109	1993.92	-1.3	-5.3	
110	1993.75	-1.4	-5.4	
111	1993.58	-1.8	-5.6	
112	1993.42	-2.5	-5.7	*
113	1993.25	-2.0	-5.5	
114	1993.08	-1.1	-5.3	*
115	1992.91	-1.4	-5.3	
116	1992.75	-1.6	-5.5	
117	1992.58	-2.5	-5.5	
118	1992.41	-3.2	-6.1	*
119	1992.25	-1.7	-5.6	
120	1992.08	-1.5	-5.6	*
121	1991.91	-1.8	-5.9	
122	1991.75	-2.2	-5.9	
123	1991.58	-2.6	-6.0	
124	1991.41	-2.2	-6.1	*
125	1991.25	-2.0	-5.8	
126	1991.08	-1.7	-5.5	*
127	1990.91	-1.3	-5.6	
128	1990.75	-1.7	-5.8	
129	1990.58	-1.9	-6.1	
130	1990.41	-2.3	-6.3	*
131	1990.25	-2.5	-5.7	
132	1990.08	-0.8	-5.3	*
133	1989.91	-1.5	-5.6	
134	1989.75	-1.8	-5.7	
135	1989.58	-1.8	-5.7	

136	1989.41	-1.5	-5.8	*
137	1989.25	-1.9	-5.6	
138	1989.08	-1.1	-5.3	*
139	1988.91	-1.1	-5.4	
140	1988.75	-1.3	-5.3	
141	1988.58	-1.8	-5.7	
142	1988.41	-1.5	-6.0	*
143	1988.25	-2.6	-5.7	
144	1988.08	-0.9	-5.3	*
145	1987.91	-1.2	-5.3	
146	1987.75	-1.2	-5.5	
147	1987.58	-2.2	-5.6	
148	1987.41	-1.5	-5.7	*
149	1987.25	-1.1	-5.4	
150	1987.08	-0.9	-5.4	*
151	1986.91	-1.0	-5.6	
152	1986.75	-1.3	-5.7	
153	1986.58	-1.7	-5.7	
154	1986.41	-2.5	-5.7	*
155	1986.25	-1.4	-5.6	
156	1986.08	-0.8	-5.4	*
157	1985.91	-1.2	-5.6	
158	1985.75	-1.2	-5.7	
159	1985.58	-1.9	-5.7	
160	1985.41	-2.4	-5.9	*
161	1985.25	-0.9	-5.5	
162	1985.08	-1.2	-5.5	*
163	1984.91	-1.2	-5.7	
164	1984.75	-1.6	-5.7	
165	1984.58	-1.9	-5.6	
166	1984.41	-1.8	-5.8	*
167	1984.25	-1.0	-5.5	
168	1984.08	-1.0	-5.5	*
169	1983.91	-1.1	-5.6	
170	1983.75	-0.9	-5.6	
171	1983.58	-1.0	-5.6	
172	1983.41	-1.9	-5.7	*
173	1983.25	-1.8	-5.5	
174	1983.08	-0.7	-5.5	*
175	1982.91	-1.0	-5.5	
176	1982.75	-1.2	-5.6	
177	1982.58	-1.2	-5.7	
178	1982.41	-1.2	-5.8	*
179	1982.25	-2.3	-5.7	
180	1982.08	-0.9	-5.3	*
181	1981.91	-1.2	-5.6	
182	1981.75	-1.5	-5.4	
183	1981.58	-1.7	-5.4	
184	1981.41	-1.5	-5.5	*
185	1981.25	-2.3	-5.5	

186	1981.08	-1.6	-5.1	*
187	1980.91	-1.1	-5.3	
188	1980.75	-0.9	-5.4	
189	1980.58	-1.0	-5.5	
190	1980.41	-1.6	-5.6	*
191	1980.25	-2.3	-5.5	
192	1980.08	-1.0	-5.0	*
193	1979.91	-0.8	-5.2	
194	1979.75	-1.3	-5.5	
195	1979.58	-2.4	-5.6	
196	1979.41	-2.0	-5.8	*
197	1979.25	-1.5	-5.6	
198	1979.08	-1.1	-5.4	*
199	1978.91	-1.1	-5.4	
200	1978.75	-1.3	-5.4	
201	1978.58	-1.5	-5.4	
202	1978.41	-1.9	-5.6	*
203	1978.25	-1.3	-5.1	
204	1978.08	-0.9	-4.9	*
205	1977.91	-1.4	-5.1	
206	1977.75	-1.4	-5.2	
207	1977.58	-1.8	-5.1	
208	1977.41	-2.6	-5.4	*
209	1977.25	-1.7	-5.2	
210	1977.08	-0.8	-5.1	*
211	1976.91	-1.1	-5.2	
212	1976.75	-1.3	-5.4	
213	1976.58	-1.6	-5.4	
214	1976.41	-2.5	-5.5	*
215	1976.25	-1.0	-5.2	
216	1976.08	-0.7	-5.0	*
217	1975.91	-1.5	-5.3	
218	1975.75	-1.3	-5.5	
219	1975.58	-1.8	-5.5	
220	1975.41	-2.2	-5.6	*
221	1975.25	-1.3	-5.5	
222	1975.08	-0.8	-5.4	*
223	1974.91	-0.7	-5.5	
224	1974.75	-1.3	-5.5	
225	1974.58	-1.4	-5.6	
226	1974.41	-2.3	-5.7	*
227	1974.25	-0.9	-5.2	
228	1974.08	-1.2	-4.9	*
229	1973.91	-1.3	-5.2	
230	1973.75	-1.4	-5.4	
231	1973.58	-1.6	-5.4	
232	1973.41	-2.3	-5.4	*
233	1973.25	-0.8	-5.3	
234	1973.08	-0.5	-5.3	*
235	1972.91	-0.8	-5.4	

236	1972.75	-1.1	-5.4	
237	1972.58	-1.2	-5.5	
238	1972.41	-1.3	-5.6	*
239	1972.25	-1.9	-5.5	
240	1972.08	-0.7	-5.2	*
241	1971.91	-0.9	-5.4	
242	1971.75	-1.0	-5.5	
243	1971.58	-1.7	-5.4	
244	1971.41	-2.2	-5.5	*
245	1971.25	-1.4	-5.2	
246	1971.08	-0.7	-4.9	*
247	1970.91	-0.6	-5.1	
248	1970.75	-1.0	-5.2	
249	1970.58	-1.8	-5.4	
250	1970.41	-1.9	-5.6	*
251	1970.25	-0.9	-5.2	
252	1970.08	-0.7	-5.0	*
253	1969.91	-1.1	-5.3	
254	1969.75	-2.0	-5.4	
255	1969.58	-2.4	-5.5	
256	1969.41	-2.4	-5.6	*
257	1969.25	-1.6	-5.3	
258	1969.08	-1.0	-5.3	*
259	1968.91	-1.1	-5.3	
260	1968.75	-1.3	-5.3	
261	1968.58	-1.9	-5.4	
262	1968.41	-1.6	-5.4	*
263	1968.25	-1.0	-5.1	
264	1968.08	-0.7	-5.1	*
265	1967.91	-1.0	-5.2	
266	1967.75	-1.3	-5.4	
267	1967.58	-1.7	-5.3	
268	1967.41	-2.1	-5.4	*
269	1967.25	-1.8	-5.3	
270	1967.08	-1.5	-5.2	*
271	1966.91	-1.3	-5.3	
272	1966.75	-1.2	-5.3	
273	1966.58	-1.4	-5.3	
274	1966.41	-2.0	-5.5	*
275	1966.25	-1.2	-5.4	
276	1966.08	-0.9	-5.3	*
277	1965.91	-1.1	-5.4	
278	1965.75	-1.3	-5.4	
279	1965.58	-2.0	-5.5	
280	1965.41	-1.8	-5.6	*
281	1965.25	-0.9	-5.5	
282	1965.08	-0.9	-5.5	*
283	1964.91	-1.2	-5.6	
284	1964.75	-1.4	-5.5	
285	1964.58	-2.0	-5.6	

286	1964.41	-1.8	-5.7	*
287	1964.25	-1.4	-5.5	
288	1964.08	-1.3	-5.4	*
289	1963.91	-1.4	-5.5	
290	1963.75	-1.5	-5.5	
291	1963.58	-1.9	-5.5	
292	1963.41	-2.4	-5.6	*
293	1963.25	-1.8	-5.5	
294	1963.08	-1.5	-5.4	*
295	1962.91	-1.4	-5.5	
296	1962.75	-1.5	-5.6	
297	1962.58	-1.8	-5.6	
298	1962.41	-2.0	-5.7	*
299	1962.25	-1.6	-5.5	
300	1962.08	-1.2	-5.4	*
301	1961.91	-1.5	-5.4	
302	1961.75	-1.8	-5.4	
303	1961.58	-2.1	-5.5	
304	1961.41	-2.3	-5.6	*
305	1961.25	-2.4	-5.5	
306	1961.08	-1.7	-5.5	*
307	1960.91	-1.7	-5.5	
308	1960.75	-1.9	-5.6	
309	1960.58	-2.2	-5.7	
310	1960.41	-2.9	-5.7	*
311	1960.25	-1.9	-5.4	
312	1960.08	-1.7	-5.4	*
313	1959.91	-2.1	-5.5	
314	1959.75	-2.4	-5.5	
315	1959.58	-2.6	-5.5	
316	1959.41	-2.8	-5.5	*
317	1959.25	-2.5	-5.4	
318	1959.08	-2.1	-5.3	*
319	1958.91	-2.2	-5.4	
320	1958.75	-2.3	-5.3	
321	1958.58	-2.8	-5.4	
322	1958.41	-3.6	-5.5	*
323	1958.25	-3.2	-5.4	
324	1958.08	-2.5	-5.2	*
325	1957.91	-2.5	-5.2	
326	1957.75	-3.2	-5.5	
327	1957.58	-3.5	-5.6	
328	1957.41	-3.5	-5.6	*
329	1957.25	-3.1	-5.4	
330	1957.08	-2.7	-5.2	*
331	1956.91	-2.3	-5.4	
332	1956.75	-2.5	-5.4	
333	1956.58	-2.4	-5.5	
334	1956.41	-3.0	-5.7	*
335	1956.25	-3.0	-5.5	

336	1956.08	-2.4	-5.3	*
337	1955.91	-2.5	-5.4	
338	1955.75	-2.5	-5.5	
339	1955.58	-2.5	-5.7	
340	1955.41	-2.5	-5.9	*
341	1955.25	-3.5	-5.6	
342	1955.08	-1.9	-5.3	*
343	1954.91	-2.3	-5.4	
344	1954.75	-2.7	-5.6	
345	1954.58	-2.6	-5.6	
346	1954.41	-2.6	-5.6	*
347	1954.25	-1.6	-5.4	
348	1954.08	-1.8	-5.3	*
349	1953.91	-1.9	-5.5	
350	1953.75	-1.9	-5.7	
351	1953.58	-2.0	-5.8	
352	1953.41	-2.0	-6.0	*
353	1953.25	-2.2	-5.7	
354	1953.08	-1.5	-5.5	*
355	1952.91	-1.5	-5.5	
356	1952.75	-1.7	-5.5	
357	1952.58	-2.6	-5.7	
358	1952.41	-2.9	-5.8	*
359	1952.25	-1.4	-5.6	
360	1952.08	-1.1	-5.5	*
361	1951.91	-1.2	-5.6	
362	1951.75	-1.3	-5.8	
363	1951.58	-1.7	-5.9	
364	1951.41	-2.2	-6.0	*
365	1951.25	-2.0	-5.7	
366	1951.08	-1.3	-5.4	*
367	1950.91	-1.4	-5.4	
368	1950.75	-1.4	-5.5	
369	1950.58	-1.4	-5.6	
370	1950.41	-1.5	-5.7	*
371	1950.25	-2.5	-5.5	
372	1950.08	-1.5	-5.3	*
373	1949.91	-1.1	-5.5	
374	1949.75	-1.4	-5.7	
375	1949.58	-1.7	-5.8	
376	1949.41	-2.3	-5.9	*
377	1949.25	-2.1	-5.8	
378	1949.08	-1.8	-5.6	*
379	1948.91	-1.5	-5.7	
380	1948.75	-1.2	-5.8	
381	1948.58	-1.5	-5.8	
382	1948.41	-1.4	-5.9	*
383	1948.25	-1.8	-5.8	
384	1948.08	-2.1	-5.6	*

Table 6.4: Radiocarbon values of Kadmat coral samples

Sr. No.	Year	$\Delta^{14}\text{C} \pm \sigma$ (‰)
1	2014	17 \pm 4
2	2010	22 \pm 4
3	2009	37 \pm 5
4	2008	18 \pm 5
5	2007	21 \pm 5
6	2006	17 \pm 4
7	2005	45 \pm 4
8	2003	44 \pm 4
9	2002	51 \pm 4
10	2001	49 \pm 4
11	2000	41 \pm 3
12	1999	38 \pm 3
13	1998	55 \pm 4
14	1997	50 \pm 3
15	1996	41 \pm 4
16	1995	53 \pm 3
17	1994	81 \pm 5
18	1993	83 \pm 7
19	1992	67 \pm 6
20	1991	65 \pm 7
21	1990	103 \pm 8
22	1989	72 \pm 7
23	1988	65 \pm 7
24	1987	81 \pm 6
25	1986	96 \pm 10
26	1985	105 \pm 8
27	1984	89 \pm 8
28	1983	80 \pm 7
29	1982	96 \pm 6
30	1981	107 \pm 6
31	1980	80 \pm 6
32	1979	110 \pm 7
33	1978	70 \pm 9
34	1977	118 \pm 6

Table 6.5: Radiocarbon values of Landfall coral samples

Sr. No.	Year	$\Delta^{14}\text{C} \pm \sigma$ (‰)
1	2018	23 \pm 6
2	2017	19 \pm 4
3	2016	21 \pm 3
4	2015	31 \pm 7
5	2014	29 \pm 4
6	2013	32 \pm 4
7	2012	31 \pm 5

8	2011	40 ± 5
9	2010	38 ± 4
10	2009	61 ± 8
11	2008	41 ± 5
12	2007	41 ± 5
13	2006	43 ± 5
14	2005	42 ± 7
15	2004	46 ± 8
16	2003	49 ± 5
17	2002	50 ± 5
18	2001	67 ± 7
19	2000	58 ± 5
20	1999	53 ± 5
21	1998	53 ± 5
22	1997	91 ± 8
23	1996	65 ± 7
24	1995	70 ± 5
25	1994	81 ± 8
26	1993	72 ± 5
27	1992	82 ± 3
28	1991	78 ± 8
29	1990	80 ± 5
30	1989	80 ± 5
31	1988	109 ± 6
32	1987	98 ± 9
33	1986	109 ± 9
34	1985	110 ± 5
35	1984	112 ± 11
36	1983	112 ± 7
37	1982	139 ± 6
38	1981	121 ± 6
39	1980	135 ± 8
40	1979	136 ± 6
41	1978	152 ± 9
42	1977	138 ± 7
43	1976	138 ± 7
44	1975	150 ± 9
45	1974	157 ± 7
46	1973	142 ± 6
47	1972	146 ± 5
48	1971	176 ± 7
49	1970	145 ± 7
50	1969	117 ± 4
51	1968	158 ± 7
52	1967	117 ± 7
53	1966	66 ± 6
54	1965	58 ± 6
55	1964	14 ± 5
56	1963	8 ± 8
57	1962	-5 ± 5

58	1961	-11 ± 8
59	1960	-26 ± 4
60	1959	-33 ± 7
61	1958	-44 ± 6
62	1957	-47 ± 6
63	1956	-46 ± 5
64	1955	-46 ± 5
65	1954	-53 ± 6
66	1953	-49 ± 6
67	1952	-44 ± 6
68	1951	-40 ± 6
69	1950	-54 ± 8
70	1949	-39 ± 8
71	1948	-35 ± 6

References

- Abram NJ, Gagan MK, Cole JE, et al., (2008). Recent intensification of tropical climate variability in the Indian Ocean. *Nat Geosci* 1:849–853. <https://doi.org/10.1038/ngeo357>
- Abram NJ, Gagan MK, McCulloch MT, et al., (2003). Coral reef death during the 1997 Indian Ocean Dipole linked to Indonesian wildfires. *Science* (80-) 301:952–955. <https://doi.org/10.1126/science.1083841>
- Achyuthan, H., Nagasundaram, M., Gourlan, A.T., Eastoe, C., Ahmad, S.M. and Padmakumari, V.M., (2014). Mid-Holocene Indian Summer Monsoon variability off the Andaman Islands, Bay of Bengal. *Quaternary International*, 349, pp.232-244.
- Achyuthan, H., Deshpande, R.D., Rao, M.S., Kumar, B., Nallathambi, T., Kumar, K.S., Ramesh, R., Ramachandran, P., Maurya, A.S. and Gupta, S.K., (2013). Stable isotopes and salinity in the surface waters of the Bay of Bengal: implications for water dynamics and palaeoclimate. *Marine Chemistry*, 149, pp.51-62.
- Ahmad SM, Farnaaz S, Sagar N, et al. (2014) Oxygen isotopic evidence for decrease in calcification rate of *Porites* coral from the Lakshadweep Island. *Quat Int* 349:22–28. <https://doi.org/10.1016/j.quaint.2014.04.053>
- Ahmad SM, Padmakumari VM, Raza W, et al. (2011) High-resolution carbon and oxygen isotope records from a scleractinian (*Porites*) coral of Lakshadweep Archipelago. *Quat Int* 238:107–114. <https://doi.org/10.1016/j.quaint.2009.11.020>
- Ali, S., Hathorne, E.C., Frank, M., Gebregiorgis, D., Statterger, K., Stumpf, R., Kutterolf, S., Johnson, J.E. and Giosan, L., (2015). South Asian monsoon history over the past 60 kyr recorded by radiogenic isotopes and clay mineral assemblages in the Andaman Sea. *Geochemistry, Geophysics, Geosystems*, 16(2), pp.505-521.
- Allison N, Finch AA, (2004). High-resolution Sr/Ca records in modern *Porites lobata* corals: Effects of skeletal extension rate and architecture. *Geochemistry, Geophys Geosystems* 5:. <https://doi.org/10.1029/2004GC000696>
- Allison, N., Tudhope, A.W. and Fallick, A.E., (1996). Factors influencing the stable carbon and oxygen isotopic composition of *Porites lutea* coral skeletons from Phuket, South Thailand. *Coral Reefs*, 15(1), pp.43-57.
- Alory, G., Wijffels, S. and Meyers, G., (2007). Observed temperature trends in the Indian Ocean over 1960–1999 and associated mechanisms. *Geophysical Research Letters*, 34(2).
- Alves EQ, Macario K, Ascough P, Bronk Ramsey C, (2018). The Worldwide Marine Radiocarbon Reservoir Effect: Definitions, Mechanisms, and Prospects. *Rev Geophys* 56:278–305. <https://doi.org/10.1002/2017RG000588>
- Arora, M., Chaudhury, N.R., Gujrati, A. and Patel, R.C., (2019). Bleaching stress on Indian coral reef regions during mass coral bleaching years using NOAA OISST data. *Current Science*, 117(2), p.242.
- Awasthi, N., Ray, J.S., Laskar, A.H., Kumar, A., Sudhakar, M., Bhutani, R., Sheth, H.C. and Yadava, M.G., (2010). Major ash eruptions of Barren Island volcano (Andaman Sea) during the past 72 kyr: clues from a sediment core record. *Bulletin of Volcanology*, 72(9),

pp.1131-1136.

- Awasthi, N., Ray, J.S., Laskar, A.H. and Yadava, M.G., (2013). Chronology of major terrace forming events in the Andaman Islands during the last 40 kyr. *Journal of the Geological Society of India*, 82(1), pp.59-66.
- Babu, V.R. and Sastry, J.S., (1976). Hydrography of the Andaman Sea during late winter. *Indian Journal of Marine Sciences*, 5, pp.179-189.
- Bahuguna, A., Chaudhury, R.N., Bhattji, N. and Navalgund, R.R., (2013). Spatial inventory and ecological status of coral reefs of the Central Indian Ocean using Resourcesat-1. *Indian Journal of Geo-Marine Sciences*, 42(6), pp. 684-696.
- Barnes DJ, Lough JM, (1993). On the nature and causes of density banding in massive coral skeletons. *J Exp Mar Bio Ecol* 167:91–108. [https://doi.org/10.1016/0022-0981\(93\)90186-R](https://doi.org/10.1016/0022-0981(93)90186-R)
- Bates, N.R., Pequignet, A.C. and Sabine, C.L., (2006). Ocean carbon cycling in the Indian Ocean: 1. Spatiotemporal variability of inorganic carbon and air-sea CO₂ gas exchange. *Global Biogeochemical Cycles*, 20(3).
- Beck JW, Edwards RL, Ito E, et al., (1992). Sea-surface temperature from coral skeletal strontium/calcium ratios. *Science*, 257:644–647. <https://doi.org/10.1126/science.257.5070.644>
- Bhushan, R., Somayajulu, B.L.K., Chakraborty, S. and Krishnaswami, S., (2000). Radiocarbon in the Arabian Sea water column: Temporal variations in bomb ¹⁴C inventory since the GEOSECS and CO₂ air-sea exchange rates. *Journal of Geophysical Research: Oceans*, 105(C6), pp.14273-14282.
- Bhushan, R., Yadava, M.G., Shah, M.S. and Raj, H., (2019a). Performance of a new 1MV AMS facility (AURiS) at PRL, Ahmedabad, India. *Nuclear Instruments and Methods in Physics Research Section B: Beam Interactions with Materials and Atoms*, 439, pp.76-79
- Bhushan, R., Yadava, M.G., Shah, M.S., Banerji, U.S., Raj, H., Shah, C. and Dabhi, A.J., (2019b). First results from the PRL accelerator mass spectrometer. *Current Science (Bangalore)*, 116(3), pp.361-363.
- Boaretto, E., Bryant, C., Carmi, I., Cook, G., Gulliksen, S., Harkness, D., Heinemeier, J., McClure, J., McGee, E., Naysmith, P. and Possnert, G., (2002). Summary findings of the fourth international radiocarbon intercomparison (FIRI)(1998–2001). *Journal of Quaternary Science: Published for the Quaternary Research Association*, 17(7), pp.633-637.
- Bolton, A., Goodkin, N.F., Hughen, K., Ostermann, D.R., Vo, S.T. and Phan, H.K., (2014). Paired *Porites* coral Sr/Ca and δ¹⁸O from the western South China Sea: Proxy calibration of sea surface temperature and precipitation. *Palaeogeography, Palaeoclimatology, Palaeoecology*, 410, pp.233-243.
- Broecker, W.S., Peng, T.H., Ostlund, G. and Stuiver, M., (1985). The distribution of bomb radiocarbon in the ocean. *Journal of Geophysical Research: Oceans*, 90(C4), pp.6953-6970.
- Brown, B.E., Dunne, R.P. and Chansang, H., (1996). Coral bleaching relative to elevated seawater temperature in the Andaman Sea (Indian Ocean) over the last 50 years. *Coral Reefs*, 15(3), pp.151-152.

- Cahyarini, S.Y., Pfeiffer, M., Timm, O., Dullo, W.C. and Schönberg, D.G., (2008). Reconstructing seawater $\delta^{18}\text{O}$ from paired coral $\delta^{18}\text{O}$ and Sr/Ca ratios: Methods, error analysis and problems, with examples from Tahiti (French Polynesia) and Timor (Indonesia). *Geochimica et Cosmochimica Acta*, 72(12), pp.2841-2853.
- Cember, R., (1989). Bomb radiocarbon in the Red Sea: A medium-scale gas exchange experiment. *Journal of Geophysical Research: Oceans*, 94(C2), pp.2111-2123.
- Chakraborty S., (1993). Environmental significance of isotope and trace elemental variations in banded corals, Ph.D. thesis, Maharaja Sayajirao Univ., Baroda, India.
- Chakraborty S., (2020) Potential of reef building corals to study the past Indian monsoon rainfall variability. *Current Science*, Vol. 119, No. 2. 10.18520/cs/v119/i2/273-281
- Chakraborty, S., Dutta, K., Bhattacharyya, A., Nigam, M., Schuur, E.A. and Shah, S.K., (2008). Atmospheric ^{14}C variability recorded in tree rings from Peninsular India: implications for fossil fuel CO_2 emission and atmospheric transport. *Radiocarbon*, 50(3), pp.321-330.
- Chakraborty S, Ramesh R, (1993). Monsoon-induced sea surface temperature changes recorded in Indian corals. *Terra Nov* 5:545–551. <https://doi.org/10.1111/j.1365-3121.1993.tb00303.x>
- Chakraborty S, Ramesh R (1997) Environmental significance of carbon and oxygen isotope ratios of banded corals from Lakshadweep, India. *Quat Int* 37:55–65. [https://doi.org/10.1016/1040-6182\(96\)00028-6](https://doi.org/10.1016/1040-6182(96)00028-6)
- Chakraborty, S., Ramesh, R. and Krishnaswami, S., (1994). Air-sea exchange of CO_2 in the Gulf of Kutch, northern Arabian Sea based on bomb-carbon in corals and tree rings. *Proceedings of the Indian Academy of Sciences-Earth and Planetary Sciences*, 103(2), pp.329-340.
- Chakraborty S., Tiwari Y.K., Deb Burman P.K., Baidya Roy S., Valsala V., (2020). Observations and Modeling of GHG Concentrations and Fluxes Over India. In: Krishnan R., Sanjay J., Gnanaseelan C., Mujumdar M., Kulkarni A., Chakraborty S. (eds) *Assessment of Climate Change over the Indian Region*. Springer, Singapore. <https://doi.org/10.1007/978-981-15-4327-2>.
- Chamizo, E., López-Gutiérrez, J.M., Ruiz-Gómez, A., Santos, F.J., García-León, M., Maden, C. and Alfimov, V., (2008). Status of the compact 1 MV AMS facility at the Centro Nacional de Aceleradores (Spain). *Nuclear Instruments and Methods in Physics Research Section B: Beam Interactions with Materials and Atoms*, 266(10), pp.2217-2220.
- Charles CD, Hunter DE, Fairbanks RG, (1997). Interaction between the ENSO and the Asian monsoon in a coral record of tropical climate. *Science* (80-) 277:925–928. <https://doi.org/10.1126/science.277.5328.925>
- Cole, J.E., Dunbar, R.B., McClanahan, T.R. and Muthiga, N.A., (2000). Tropical Pacific forcing of decadal SST variability in the western Indian Ocean over the past two centuries. *Science*, 287(5453), pp.617-619.
- Cole, J.E. and Fairbanks, R.G., (1990). The Southern Oscillation recorded in the $\delta^{18}\text{O}$ of corals from Tarawa Atoll. *Paleoceanography*, 5(5), pp.669-683.
- Cooper, Z., (1993). The origins of the Andaman Islanders: local myth and archaeological evidence. *Antiquity*, 67(255), pp.394-399.

- Corrège, T., (2006). Sea surface temperature and salinity reconstruction from coral geochemical tracers. *Palaeogeography, Palaeoclimatology, Palaeoecology*, 232(2-4), pp.408-428
- Corrège, T., Delcroix, T., Récy, J., Beck, W., Cabioch, G. and Le Cornec, F., (2000). Evidence for stronger El Niño-Southern Oscillation (ENSO) events in a mid-Holocene massive coral. *Paleoceanography*, 15(4), pp.465-470.
- Corrège, T., Gagan, M.K., Beck, J.W., Burr, G.S., Cabioch, G. and Le Cornec, F., (2004). Interdecadal variation in the extent of South Pacific tropical waters during the Younger Dryas event. *Nature*, 428(6986), pp.927-929.
- Damassa, T.D., Cole, J.E., Barnett, H.R., Ault, T.R. and McClanahan, T.R., (2006). Enhanced multidecadal climate variability in the seventeenth century from coral isotope records in the western Indian Ocean. *Paleoceanography*, 21(2).
- Dassié EP, Lemley GM, Linsley BK, (2013). The Suess effect in Fiji coral $\delta^{13}\text{C}$ and its potential as a tracer of anthropogenic CO_2 uptake. *Palaeogeogr Palaeoclimatol Palaeoecol* 370:30–40. <https://doi.org/10.1016/j.palaeo.2012.11.012>
- Dang, P.X., Mitsuguchi, T., Kitagawa, H., Shibata, Y. and Kobayashi, T., (2004). Marine reservoir correction in the south of Vietnam estimated from an annually-banded coral. *Radiocarbon*, 46(2), pp.657-660.
- De'ath, G., Lough, J.M. and Fabricius, K.E., (2009). Declining coral calcification on the Great Barrier Reef. *Science*, 323(5910), pp.116-119.
- Delaygue, G., Bard, E., Rollion, C., Jouzel, J., Stiévenard, M., Duplessy, J.C. and Ganssen, G., (2001). Oxygen isotope/salinity relationship in the northern Indian Ocean. *Journal of Geophysical Research: Oceans*, 106(C3), pp.4565-4574.
- DeLong KL, Flannery JA, Maupin CR, et al., (2011), A coral Sr/Ca calibration and replication study of two massive corals from the gulf of mexico. *Palaeogeogr Palaeoclimatol Palaeoecol* 307:117–128. <https://doi.org/10.1016/j.palaeo.2011.05.005>
- Deshpande, R.D., Muraleedharan, P.M., Singh, R.L., Kumar, B., Rao, M.S., Dave, M., Sivakumar, K.U. and Gupta, S.K., (2013). Spatio-temporal distributions of $\delta^{18}\text{O}$, δD and salinity in the Arabian Sea: Identifying processes and controls. *Marine Chemistry*, 157, pp.144-161.
- De Villiers S, Shen GT, Nelson BK, (1994). The Sr Ca-temperature relationship in coralline aragonite: Influence of variability in (Sr Ca)seawater and skeletal growth parameters. *Geochim Cosmochim Acta* 58:197–208. [https://doi.org/10.1016/0016-7037\(94\)90457-X](https://doi.org/10.1016/0016-7037(94)90457-X)
- D'Olivo, J.P., Sinclair, D.J., Rankenburg, K. and McCulloch, M.T., (2018). A universal multi-trace element calibration for reconstructing sea surface temperatures from long-lived *Porites* corals: Removing 'vital-effects'. *Geochimica et Cosmochimica Acta*, 239, pp.109-135.
- Donahue, D.J., Linick, T.W. and Jull, A.T., (1990). Isotope-ratio and background corrections for accelerator mass spectrometry radiocarbon measurements. *Radiocarbon*, 32(2), pp.135-142.
- Druffel, E.R., (1989). Decade time scale variability of ventilation in the North Atlantic: High-precision measurements of bomb radiocarbon in banded corals. *Journal of Geophysical Research: Oceans*, 94(C3), pp.3271-3285.

- Druffel ERM, (1997). Geochemistry of corals: Proxies of past ocean chemistry, ocean circulation, and climate. *Proc Natl Acad Sci* 94:8354–8361. <https://doi.org/10.1073/pnas.94.16.8354>
- Druffel ERM, (2002). Radiocarbon in Corals: Records of the Carbon Cycle, Surface Circulation and Climate. *Oceanography* 15:122–127. <https://doi.org/10.5670/oceanog.2002.43>
- Druffel, E.R. and Griffin, S., (1993). Large variations of surface ocean radiocarbon: evidence of circulation changes in the southwestern Pacific. *Journal of Geophysical Research: Oceans*, 98(C11), pp.20249-20259.
- Druffel, E.R., Griffin, S., Beupré, S.R. and Dunbar, R.B., (2007). Oceanic climate and circulation changes during the past four centuries from radiocarbon in corals. *Geophysical Research Letters*, 34(9).
- Druffel, E.M. and Linick, T.W., (1978). Radiocarbon in annual coral rings of Florida. *Geophysical Research Letters*, 5(11), pp.913-916.
- Druffel, E.R., Robinson, L.F., Griffin, S., Halley, R.B., Southon, J.R. and Adkins, J.F., (2008). Low reservoir ages for the surface ocean from mid-Holocene Florida corals. *Paleoceanography*, 23(2).
- Druffel, E.M. and Suess, H.E., (1983). On the radiocarbon record in banded corals: exchange parameters and net transport of $^{14}\text{CO}_2$ between atmosphere and surface ocean. *Journal of Geophysical Research: Oceans*, 88(C2), pp.1271-1280.
- Dutta K, Bhushan R, (2012). Radiocarbon in the Northern Indian Ocean two decades after GEOSECS. *Global Biogeochem Cycles* 26:1–14. <https://doi.org/10.1029/2010GB004027>
- Dutta K, Bhushan R, Somayajulu B, (2001). ΔR correction values for the northern Indian Ocean. *Radiocarbon*. 43(2A):483-8.
- Dye, T., (1994). Apparent ages of marine shells: implications for archaeological dating in Hawai'i. *Radiocarbon*, 36(1), pp.51-57.
- Epstein, S., Buchsbaum, R., Lowenstam, H. and Urey, H.C., (1951). Carbonate-water isotopic temperature scale. *Geological Society of America Bulletin*, 62(4), pp.417-426.
- Epstein S, Buchsbaum R, Lowenstam HA, Urey HC, (1953). Revised carbonate-water isotopic temperature scale. *Bull Geol Soc Am* 64:1315–1326
- Fairbanks RG, Dodge RE, (1979). Annual periodicity of the $^{18}\text{O}/^{16}\text{O}$ and $^{13}\text{C}/^{12}\text{C}$ ratios in the coral *Montastrea annularis*. *Geochim Cosmochim Acta* 43:1009–1020. [https://doi.org/10.1016/0016-7037\(79\)90090-5](https://doi.org/10.1016/0016-7037(79)90090-5)
- Fallon, S.J., McCulloch, M.T. and Alibert, C., (2003). Examining water temperature proxies in *Porites* corals from the Great Barrier Reef: a cross-shelf comparison. *Coral Reefs*, 22(4), pp.389-404.
- Felis, T., Lohmann, G., Kuhnert, H., Lorenz, S.J., Scholz, D., Pätzold, J., Al-Rousan, S.A. and Al-Moghrabi, S.M., (2004). Increased seasonality in Middle East temperatures during the last interglacial period. *Nature*, 429(6988), pp.164-168.
- Felis T, Pätzold J, Loya Y, (2003). Mean oxygen-isotope signatures in *Porites spp.* corals: Inter-colony variability and correction for extension-rate effects. *Coral Reefs* 22:328–336.

<https://doi.org/10.1007/s00338-003-0324-3>

- Felis, T., Pätzold, J., Loya, Y., Fine, M., Nawar, A.H. and Wefer, G., (2000). A coral oxygen isotope record from the northern Red Sea documenting NAO, ENSO, and North Pacific teleconnections on Middle East climate variability since the year 1750. *Paleoceanography*, 15(6), pp.679-694.
- Felis, T., Pätzold, J., Loya, Y. and Wefer, G., (1998). Vertical water mass mixing and plankton blooms recorded in skeletal stable carbon isotopes of a Red Sea coral. *Journal of Geophysical Research: Oceans*, 103(C13), pp.30731-30739.
- Forman, S.L. and Polyak, L., (1997). Radiocarbon content of pre-bomb marine mollusks and variations in the ^{14}C Reservoir age for coastal areas of the Barents and Kara Seas, Russia. *Geophysical Research Letters*, 24(8), pp.885-888.
- Gagan MK, Ayliffe LK, Hopley D, et al., (1998). Temperature and surface-ocean water balance of the mid-Holocene tropical western Pacific. *Science* (80-) 279:1014–1017. <https://doi.org/10.1126/science.279.5353.1014>
- Gagan MK, Chivas AR, Isdale PJ, (1994). High-resolution isotopic records from corals using ocean temperature and mass-spawning chronometers. *Earth Planet Sci Lett* 121:549–558. [https://doi.org/10.1016/0012-821X\(94\)90090-6](https://doi.org/10.1016/0012-821X(94)90090-6)
- Gagan, M.K., Sosdian, S.M., Scott-Gagan, H., Sieh, K., Hantoro, W.S., Natawidjaja, D.H., Briggs, R.W., Suwargadi, B.W. and Rifai, H., (2015). Coral $^{13}\text{C}/^{12}\text{C}$ records of vertical seafloor displacement during megathrust earthquakes west of Sumatra. *Earth and Planetary Science Letters*, 432, pp.461-471.
- Good SA, Martin MJ, Rayner NA, (2013). EN4: Quality controlled ocean temperature and salinity profiles and monthly objective analyses with uncertainty estimates. *J Geophys Res Ocean* 118:6704–6716
- Gopalakrishna, V.V., Johnson, Z., Salgaonkar, G., Nisha, K., Rajan, C.K. and Rao, R.R., (2005). Observed variability of sea surface salinity and thermal inversions in the Lakshadweep Sea during contrast monsoons. *Geophysical research letters*, 32(18).
- Gordon AL and Olson DB, (2020). Bottle data from Cruise I09N, exchange version. Accessed from CCHDO https://cchdo.ucsd.edu/cruise/316N145_6. Access date 2020-04-08.
- Grottoli, A.G. and Eakin, C.M., (2007). A review of modern coral $\delta^{18}\text{O}$ and $\Delta^{14}\text{C}$ proxy records. *Earth-Science Reviews*, 81(1-2), pp.67-91.
- Grottoli AG, Rodrigues LJ, Palardy JE, (2006). Heterotrophic plasticity and resilience in bleached corals. *Nature* 440:1186–1189. <https://doi.org/10.1038/nature04565>
- Grottoli AG, Wellington GM, (1999). Effect of light and zooplankton on skeletal $\delta^{13}\text{C}$ values in the eastern Pacific corals *Pavona clavus* and *Pavona gigantea*. *Coral Reefs* 18:29–41. <https://doi.org/10.1007/s003380050150>
- Grumet NS, Abram NJ, Beck JW, et al., (2004). Coral radiocarbon records of Indian Ocean water mass mixing and wind-induced upwelling along the coast of Sumatra, Indonesia. *J Geophys Res C Ocean* 109:1–15. <https://doi.org/10.1029/2003JC002087>
- Grumet, N.S., Guilderson, T.P. and Dunbar, R.B., (2002). Pre-bomb radiocarbon variability inferred from a Kenyan coral record. *Radiocarbon*, 44(2), pp.581-590.

- Guilderson TP, Fallon S, Moore MD, et al., (2009). Seasonally resolved surface water $\Delta^{14}\text{C}$ variability in the Lombok Strait: A coralline perspective. *J Geophys Res Ocean* 114:1–9. <https://doi.org/10.1029/2008JC004876>
- Heiss, G. A., G. F. Camoin, A. Eisenhauer, D. Wischow, W.-Chr. Dullo, and B. Hansen (1997). Stable isotope and Sr/Ca—Signals in the corals from the Indian Ocean, *Prox. 8th Int. Coral Reef Sym.*, 2, 1713–1718
- Hideshima, S., Matsumoto, E., Abe, O. and Kitagawa, H., (2001). Northwest Pacific marine reservoir correction estimated from annually banded coral from Ishigaki Island, southern Japan. *Radiocarbon*, 43(2A), pp.473-476.
- Hogg, A.G., Higham, T.F. and Dahm, J., (1997). ^{14}C dating of modern marine and estuarine shellfish. *Radiocarbon*, 40(2), pp.975-984.
- Hua, Q., (2015). Radiocarbon dating of marine carbonates. In: Rink, W.J., and Thompson, J. (Eds.), *Encyclopedia of Scientific Dating Methods*. Earth Sciences Series, Springer, Netherlands, p.676-679.
- Hua Q, Barbetti M, Jacobsen GE, et al. (2000). Bomb radiocarbon in annual tree rings from Thailand and Australia. *Nucl Instruments Methods Phys Res Sect B Beam Interact with Mater Atoms* 172:359–365. [https://doi.org/10.1016/S0168-583X\(00\)00147-6](https://doi.org/10.1016/S0168-583X(00)00147-6)
- Hua, Q., Barbetti, M. and Rakowski, A.Z., (2013). Atmospheric radiocarbon for the period 1950–2010. *Radiocarbon*, 55(4), pp.2059-2072.
- Hua Q, Woodroffe CD, Smithers SG, et al. (2005). Radiocarbon in corals from the Cocos (Keeling) Islands and implications for Indian Ocean circulation. *Geophys Res Lett* 32:1–4. <https://doi.org/10.1029/2005GL023882>
- Hudson JH, Shinn EA, Halley RB, Lidz B, (1976). Sclerochronology: A tool for interpreting past environments. *Geology* 4:361–364. [https://doi.org/10.1130/0091-7613\(1976\)4<361:SATFIP>2.0.CO;2](https://doi.org/10.1130/0091-7613(1976)4<361:SATFIP>2.0.CO;2)
- Jacob, S.A.W., Suter, M. and Synal, H.A., (2000). Ion beam interaction with stripper gas—Key for AMS at sub MeV. *Nuclear Instruments and Methods in Physics Research Section B: Beam Interactions with Materials and Atoms*, 172(1-4), pp.235-241.
- James, P.S.B.R., (2011). Lakshadweep: Islands of ecological fragility, environmental sensitivity and anthropogenic vulnerability. *Journal of Coastal Environment*, 2(1), pp.9-25.
- Jankaew, K., Atwater, B.F., Sawai, Y., Choowong, M., Charoentitirat, T., Martin, M.E. and Prendergast, A., (2008). Medieval forewarning of the 2004 Indian Ocean tsunami in Thailand. *Nature*, 455(7217), pp.1228-1231.
- Key RM, (2001). Radiocarbon. *Encycl Ocean Sci* 75:2338–2353. <https://doi.org/10.1006/rwos.2001.0162>
- Kim S-T, O’Neil JR, (1997). Equilibrium and nonequilibrium oxygen isotope effects in synthetic carbonates. *Geochim Cosmochim Acta* 61:3461–3475. [https://doi.org/10.1016/S0016-7037\(97\)00169-5](https://doi.org/10.1016/S0016-7037(97)00169-5)
- Kinsman DJJ, Holland HD, (1969). The co-precipitation of cations with CaCO_3 , -IV . The co-precipitation of Sr^{2+} with aragonite between 16°C and 96°C. *Geochim Cosmochim Acta* 33:1–17

- Kiran, S.R., (2017). General circulation and principal wave modes in Andaman Sea from observations. *Indian Journal of Science and Technology*, 10(24), pp.1-11.
- Klein, M.G., Mous, D.J.W. and Gott dang, A., (2006). A compact 1 MV multi-element AMS system. *Nuclear Instruments and Methods in Physics Research Section B: Beam Interactions with Materials and Atoms*, 249(1-2), pp.764-767.
- M. Klein, D.J.W. Mous, A. Gott dang, Fast and accurate sequential injection AMS with gated faraday cup current measurement, *Radiocarbon*. 46 (2004) 77–82. doi:10.1017/S0033822200039370.
- Kotov, S. and Pälke, H., (2018). QAnalySeries-a cross-platform time series tuning and analysis tool. *AGUFM*, 2018, pp.PP53D-1230.
- Knutson DW, Buddemeier RW, Smith S V., Url S, (1972). Coral Chronometers : Seasonal Growth Bands in Reef Corals *Coral Chronometers : Seasonal Growth Bands in Reef Corals*. *Science* (80-) 177:270–272
- Krishnan, R., Sanjay, J., Gnanaseelan, C., Mujumdar, M., Kulkarni, A. and Chakraborty, S., (2020). Assessment of Climate Change over the Indian Region: A Report of the Ministry of Earth Sciences (MoES), Government of India.
- Kumar, M.D., Naqvi, S.W.A., George, M.D. and Jayakumar, D.A., (1996). A sink for atmospheric carbon dioxide in the northeast Indian Ocean. *Journal of Geophysical Research: Oceans*, 101(C8), pp.18121-18125
- Kumar, N., Yadav, B.P., Tyagi, A. and Jaswal, A.K., (2012). Trend and spatial distribution of rainfall & rainy days over Andaman & Nicobar Islands. *Natural hazards*, 63(2), pp.575-587.
- Kumar, P.K., Band, S.T., Ramesh, R. and Awasthi, N., (2018). Monsoon variability and upper ocean stratification during the last ~66 ka over the Andaman Sea: Inferences from the $\delta^{18}\text{O}$ records of planktonic foraminifera. *Quaternary International*, 479, pp.12-18.
- Kunz, A., Frechen, M., Ramesh, R. and Urban, B., (2010). Revealing the coastal event-history of the Andaman Islands (Bay of Bengal) during the Holocene using radiocarbon and OSL dating. *International Journal of Earth Sciences*, 99(8), pp.1741-1761.
- Kuss, J. and Schneider, B., (2004). Chemical enhancement of the CO_2 gas exchange at a smooth seawater surface. *Marine Chemistry*, 91(1-4), pp.165-174.
- Le Bec N, Juillet-Leclerc A, Corrège T, et al. (2000). A coral $\delta^{18}\text{O}$ record of ENSO driven sea surface salinity variability in Fiji (south-western tropical Pacific). *Geophys Res Lett* 27:3897–3900. <https://doi.org/10.1029/2000GL011843>
- Le Cornec, F. and Corregge, T., (1997). Determination of uranium to calcium and strontium to calcium ratios in corals by inductively coupled plasma mass spectrometry. *Journal of Analytical Atomic Spectrometry*, 12(9), pp.969-973.
- Lee, H.T., Gruber, A., Ellingson, R.G. and Laszlo, I., (2007). Development of the HIRS outgoing longwave radiation climate dataset. *Journal of atmospheric and oceanic technology*, 24(12), pp.2029-2047.
- Levy O, Rosenfeld M, Yam R, Shemesh A (2006). Heterogeneity of coral skeletons isotopic compositions during the 1998 bleaching event. *Limnol Oceanogr* 51:1142–1148

- Lindauer, S., Santos, G.M., Steinhof, A., Yousif, E., Phillips, C., Jasim, S.A., Uerpmann, H.P. and Hinderer, M., (2017). The local marine reservoir effect at Kalba (UAE) between the Neolithic and Bronze Age: An indicator of sea level and climate changes. *Quaternary Geochronology*, 42, pp.105-116.
- Linsley BK, Messier RG, Dunbar RB, (1999). Assessing between-colony oxygen isotope variability in the coral *Porites lobata* at Clipperton Atoll. *Coral Reefs* 18:13–27. <https://doi.org/10.1007/s003380050148>
- Linsley BK, Wellington GM, Schrag DP, (2000). Decadal sea surface temperature variability in the subtropical south pacific from 1726 to 1997 A.D. *Science* (80-) 290:1145–1148. <https://doi.org/10.1126/science.290.5494.1145>
- Liss, P.S. and Merlivat, L., (1986). Air-sea gas exchange rates: Introduction and synthesis. In *The role of air-sea exchange in geochemical cycling* (pp. 113-127). Springer, Dordrecht.
- Louanchi, F., Metzl, N. and Poisson, A., (1996). Modelling the monthly sea surface fCO₂ fields in the Indian Ocean. *Marine Chemistry*, 55(3-4), pp.265-279.
- Lough, J.M., (2010). Climate records from corals. *Wiley interdisciplinary reviews: climate change*, 1(3), pp.318-331
- Lough, J.M. and Barnes, D.J., (2000). Environmental controls on growth of the massive coral *Porites*. *Journal of experimental marine biology and ecology*, 245(2), pp.225-243.
- Mangerud, J., Bondevik, S., Gulliksen, S., Hufthammer, A.K. and Høisæter, T., (2006). Marine ¹⁴C reservoir ages for 19th century whales and molluscs from the North Atlantic. *Quaternary Science Reviews*, 25(23-24), pp.3228-3245.
- Manzello, D.P., (2010). Coral growth with thermal stress and ocean acidification: lessons from the eastern tropical Pacific. *Coral reefs*, 29(3), pp.749-758.
- Marshall, A.T. and Clode, P., (2004). Calcification rate and the effect of temperature in a zooxanthellate and an azooxanthellate scleractinian reef coral. *Coral reefs*, 23(2), pp.218-224.
- Marshall JF, McCulloch MT, (2001). Evidence of El Nino and the Indian Ocean Dipole from Sr / Ca derived SSTs for modern corals at Christmas Island, eastern Indian Ocean. *Geophys Res Letfers* 28:3453–3456
- Marshall JF, McCulloch MT, (2002). An assessment of the Sr/Ca ratio in shallow water hermatypic corals as a proxy for sea surface temperature. *Geochim Cosmochim Acta* 66:3263–3280. [https://doi.org/10.1016/S0016-7037\(02\)00926-2](https://doi.org/10.1016/S0016-7037(02)00926-2)
- McConnaughey T, (1989a). ¹³C and ¹⁸O isotopic disequilibrium in biological carbonates: I. Patterns. *Geochim Cosmochim Acta* 53:151–162. [https://doi.org/10.1016/0016-7037\(89\)90282-2](https://doi.org/10.1016/0016-7037(89)90282-2)
- McConnaughey T, (1989b). ¹³C and ¹⁸O isotopic disequilibrium in biological carbonates: II. In vitro simulation of kinetic isotope effects. *Geochim Cosmochim Acta* 53:151–162. [https://doi.org/10.1016/0016-7037\(89\)90282-2](https://doi.org/10.1016/0016-7037(89)90282-2)
- McConnaughey TA, Burdett J, Whelan JF, Paull CK, (1997). Carbon isotopes in biological carbonates: Respiration and photosynthesis. *Geochim Cosmochim Acta* 61:611–622. [https://doi.org/10.1016/S0016-7037\(96\)00361-4](https://doi.org/10.1016/S0016-7037(96)00361-4)

- McCulloch MT, D'Olivo JP, Falter J, et al., (2017). Coral calcification in a changing World and the interactive dynamics of pH and DIC upregulation. *Nat Commun* 8:1–8. <https://doi.org/10.1038/ncomms15686>
- McCulloch, M., Fallon, S., Wyndham, T., Hendy, E., Lough, J. and Barnes, D., (2003). Coral record of increased sediment flux to the inner Great Barrier Reef since European settlement. *Nature*, 421(6924), pp.727-730.
- McCulloch, M.T., Gagan, M.K., Mortimer, G.E., Chivas, A.R. and Isdale, P.J., (1994). A high-resolution Sr/Ca and $\delta^{18}\text{O}$ coral record from the Great Barrier Reef, Australia, and the 1982–1983 El Niño. *Geochimica et Cosmochimica Acta*, 58(12), pp.2747-2754.
- Mitsuguchi, T., Matsumoto, E., Abe, O., Uchida, T. and Isdale, P.J., (1996). Mg/Ca thermometry in coral skeletons. *Science*, 274(5289), pp.961-963.
- Morimoto M, Abe O, Kayanne H, et al., (2002). Salinity records for the 1997-98 El Niño from Western Pacific corals. *Geophys Res Lett* 29:35-1-35-4. <https://doi.org/10.1029/2001GL013521>
- Muley, E.V., Venkataraman, K., Alfred, J.R.B. and Wafar, M.V.M., (2000). Status of coral reefs of India. In *Proceedings of the Ninth International Coral Reef Symposium, Bali, 23-27 October 2000*, (Vol. 2, pp. 847-853).
- Murphy, J.O., Lawson, E.M., Fink, D., Hotchkis, M.A.C., Hua, Q., Jacobsen, G.E., Smith, A.M. and Tuniz, C., (1997). ^{14}C AMS measurements of the bomb pulse in N-and S-Hemisphere tropical trees. *Nuclear Instruments and Methods in Physics Research Section B: Beam Interactions with Materials and Atoms*, 123(1-4), pp.447-450.
- Murty, S.A., Bernstein, W.N., Ossolinski, J.E., Davis, R.S., Goodkin, N.F. and Hughen, K.A., (2018). Spatial and temporal robustness of Sr/Ca-SST calibrations in Red Sea corals: Evidence for influence of mean annual temperature on calibration slopes. *Paleoceanography and Paleoclimatology*, 33(5), pp.443-456.
- Nakamura N, Kayanne H, Iijima H, et al., (2011). Footprints of IOD and ENSO in the Kenyan coral record. *Geophys Res Lett* 38:3–7. <https://doi.org/10.1029/2011GL049877>
- Ota, Y., Kawahata, H., Murayama, M., Inoue, M., Yokoyama, Y., Miyairi, Y., Aung, T., Hossain, H.Z., Suzuki, A., Kitamura, A. and Moe, K.T., (2017). Effects of intensification of the Indian Summer Monsoon on northern Andaman Sea sediments during the past 700 years. *Journal of Quaternary Science*, 32(4), pp.528-539.
- Paul, M.R. and Ramamirtham, C.P., (1963). Hydrography of the Laccadives offshore waters- A study of the winter conditions. *Journal of the Marine Biological Association of India*, 5(2), pp.159-169
- Petchey, F., Phelan, M. and White, J.P., (2004). New ΔR values for the southwest Pacific Ocean. *Radiocarbon*, 46(2), pp.1005-1014.
- Petchey, F., Ulm, S., David, B., McNiven, I.J., Asmussen, B., Tomkins, H., Richards, T., Rowe, C., Leavesley, M., Mandui, H. and Stanisc, J., (2012). ^{14}C marine reservoir variability in herbivores and deposit-feeding gastropods from an open coastline, Papua New Guinea. *Radiocarbon*, 54(3-4), pp.967-978.
- Pfeiffer M, Dullo WC (2006) Monsoon-induced cooling of the western equatorial Indian Ocean as recorded in coral oxygen isotope records from the Seychelles covering the period of 1840-1994 *AD. Quat Sci Rev* 25:993–1009.

<https://doi.org/10.1016/j.quascirev.2005.11.005>

- Pfeiffer, M., Dullo, W.C. and Eisenhauer, A., (2004). Variability of the Intertropical Convergence Zone recorded in coral isotopic records from the central Indian Ocean (Chagos Archipelago). *Quaternary Research*, 61(3), pp.245-255
- Pfeiffer M, Dullo WC, Zinke J, Garbe-Schönberg D, (2009). Three monthly coral Sr/Ca records from the Chagos Archipelago covering the period of 1950-1995 A.D.: Reproducibility and implications for quantitative reconstructions of sea surface temperature variations. *Int J Earth Sci* 98:53–66. <https://doi.org/10.1007/s00531-008-0326-z>
- Pillai C S G., (1996). Coral reefs of India: Their conservation and management. In: *Marine Biodiversity conservation and Management* (Ed. Menon N G and Pillai C S G). CMFRI pp. 16–31
- Pillai, C.G., (2010). A review of the status of corals and coral reefs of India. *Indian Journal of Animal Sciences*, 80(4 (Supp)), pp.53-56.
- Pillai, C.S.G. and Jasmine, S., (1989). The coral fauna of Lakshadweep. *CMFRI Bulletin Marine living resources of the union territory of Lakshadweep An Indicative Survey With Suggestions For Development*, 43, pp.179-195.
- Quinn, T.M. and Sampson, D.E., (2002). A multiproxy approach to reconstructing sea surface conditions using coral skeleton geochemistry. *Paleoceanography*, 17(4), pp.14-1.
- Rajan, R. S., (2013). Reconstruction of past sea surface temperature around Lakshadweep Islands using oxygen isotopes from scleractinian corals. PhD Thesis, Osmania University, Hyderabad, India.
- Rajendran, K., Rajendran, C.P., Earnest, A., Prasad, G.R., Dutta, K., Ray, D.K. and Anu, R., (2008). Age estimates of coastal terraces in the Andaman and Nicobar Islands and their tectonic implications. *Tectonophysics*, 455(1-4), pp.53-60.
- Raju, D.V., Gouveia, A.D. and Murty, C.S., (1981). Some physical characteristics of Andaman Sea waters during winter. *Indian Journal of Marine Sciences*, 10, pp.211-218.
- Ramaswamy, V., Gaye, B., Shirodkar, P.V., Rao, P.S., Chivas, A.R., Wheeler, D. and Thwin, S., (2008). Distribution and sources of organic carbon, nitrogen and their isotopic signatures in sediments from the Ayeyarwady (Irrawaddy) continental shelf, northern Andaman Sea. *Marine Chemistry*, 111(3-4), pp.137-150.
- Rashid, H., Flower, B.P., Poore, R.Z. and Quinn, T.M., (2007). A ~ 25 ka Indian Ocean monsoon variability record from the Andaman Sea. *Quaternary Science Reviews*, 26(19-21), pp.2586-2597.
- Rao, R.R. and Sivakumar, R., (2003). Seasonal variability of sea surface salinity and salt budget of the mixed layer of the north Indian Ocean. *Journal of Geophysical Research: Oceans*, 108(C1), pp.9-1.
- Reimer, P.J., Bard, E., Bayliss, A., Beck, J.W., Blackwell, P.G., Ramsey, C.B., Buck, C.E., Cheng, H., Edwards, R.L., Friedrich, M. and Grootes, P.M., (2013). IntCal13 and Marine13 radiocarbon age calibration curves 0–50,000 years cal BP. *Radiocarbon*, 55(4), pp.1869-1887.
- Reimer RW, Reimer PJ, (2017). An Online Application for ΔR Calculation. *Radiocarbon* 59:1623–1627. <https://doi.org/10.1017/RDC.2016.117>

- Ren, L., Linsley, B.K., Wellington, G.M., Schrag, D.P. and Hoegh-Guldberg, O., (2003). Deconvolving the $\delta^{18}\text{O}$ seawater component from subseasonal coral $\delta^{18}\text{O}$ and Sr/Ca at Rarotonga in the southwestern subtropical Pacific for the period 1726 to 1997. *Geochimica et Cosmochimica Acta*, 67(9), pp.1609-1621.
- Rengarajan, K. and Marichamy, R., (1972). Seasonal changes in the temperature, salinity And plankton volume at Port Blair, Andaman. *Indian Journal of Fisheries*, 19(1&2), pp.60-69.
- Rixen T, Ramachandran P, Lehnhoff L, et al., (2011). Impact of monsoon-driven surface ocean processes on a coral off Port Blair on the Andaman Islands and their link to North Atlantic climate variations. *Glob Planet Change* 75:1–13. <https://doi.org/10.1016/j.gloplacha.2010.09.005>
- Rosenfeld M, Yam R, Shemesh A, Loya Y, (2003). Implication of water depth on stable isotope composition and skeletal density banding patterns in a *Porites lutea* colony: Results from a long-term translocation experiment. *Coral Reefs* 22:337–345. <https://doi.org/10.1007/s00338-003-0333-2>
- Roxy, M.K., Ritika, K., Terray, P. and Masson, S., (2014). The curious case of Indian Ocean warming. *Journal of Climate*, 27(22), pp.8501-8509.
- Rozanski, K., Stichler, W., Gonfiantini, R., Scott, E.M., Beukens, R.P., Kromer, B. and Van Der Plicht, J., (1992). The IAEA 14 C intercomparison exercise 1990. *Radiocarbon*, 34(3), pp.506-519.
- Sabine, C.L., Wanninkhof, R., Key, R.M., Goyet, C. and Millero, F.J., (2000). Seasonal CO₂ fluxes in the tropical and subtropical Indian Ocean. *Marine Chemistry*, 72(1), pp.33-53.
- Sagar, N., Hetzinger, S., Pfeiffer, M., Masood Ahmad, S., Dullo, W.C. and Garbe-Schönberg, D., (2016). High-resolution Sr/Ca ratios in a *Porites lutea* coral from Lakshadweep Archipelago, southeast Arabian Sea: An example from a region experiencing steady rise in the reef temperature. *Journal of Geophysical Research: Oceans*, 121(1), pp.252-266.
- Sarma, V.V.S.S., (2003). Monthly variability in surface pCO₂ and net air-sea CO₂ flux in the Arabian Sea. *Journal of Geophysical Research: Oceans*, 108(C8).
- Sarma, V.V.S.S., Kumar, M.D. and George, M.D., (1998). The central and eastern Arabian Sea as a perennial source of atmospheric carbon dioxide. *Tellus B: Chemical and Physical Meteorology*, 50(2), pp.179-184.
- Scheffers, A., Brill, D., Kelletat, D., Brückner, H., Scheffers, S. and Fox, K., (2012). Holocene sea levels along the Andaman Sea coast of Thailand. *The Holocene*, 22(10), pp.1169-1180.
- Schott, F.A., Xie, S.P. and McCreary Jr, J.P., (2009). Indian Ocean circulation and climate variability. *Reviews of Geophysics*, 47(1).
- Schrag, D.P., (1999). Rapid analysis of high-precision Sr/Ca ratios in corals and other marine carbonates. *Paleoceanography*, 14(2), pp.97-102.
- Scoffin, T.P., Tudhope, A.W., Brown, B.E., Chansang, H. and Cheeney, R.F., (1992). Patterns and possible environmental controls of skeletogenesis of *Porites lutea*, South Thailand. *Coral Reefs*, 11(1), pp.1-11.
- Scott, E.M., Cook, G.T. and Naysmith, P., (2010). The Fifth International Radiocarbon Intercomparison (VIRI): an assessment of laboratory performance in stage 3.

- Radiocarbon, 52(3), pp.859-865.
- Sengupta, D., Bharath Raj, G.N. and Shenoi, S.S.C., (2006). Surface freshwater from Bay of Bengal runoff and Indonesian Throughflow in the tropical Indian Ocean. *Geophysical Research Letters*, 33(22).
- Sengupta, S., Parekh, A., Chakraborty, S., Ravi Kumar, K. and Bose, T., (2013). Vertical variation of oxygen isotope in Bay of Bengal and its relationships with water masses. *Journal of Geophysical Research: Oceans*, 118(12), pp.6411-6424.
- Shankar, D., Vinayachandran, P.N. and Unnikrishnan, A.S., (2002). The monsoon currents in the north Indian Ocean. *Progress in oceanography*, 52(1), pp.63-120.
- Shen CC, Lee T, Chen CY, et al., (1996). The calibration of D[Sr/Ca] versus sea surface temperature relationship for *Porites* corals. *Geochim Cosmochim Acta* 60:3849–3858. [https://doi.org/10.1016/0016-7037\(96\)00205-0](https://doi.org/10.1016/0016-7037(96)00205-0)
- Shen, G.T., Cole, J.E., Lea, D.W., Linn, L.J., McConnaughey, T.A. and Fairbanks, R.G., (1992). Surface ocean variability at Galapagos from 1936–1982: calibration of geochemical tracers in corals. *Paleoceanography*, 7(5), pp.563-588.
- Shenoi, S.S.C., Shankar, D. and Shetye, S.R., (1999). On the sea surface temperature high in the Lakshadweep Sea before the onset of the southwest monsoon. *Journal of Geophysical Research: Oceans*, 104(C7), pp.15703-15712.
- Shimamura, M., Oba, T., Xu, G., Lu, B., Wang, L., Murayama, M., Toyoda, K. and Winter, A., (2005). Fidelity of $\delta^{18}\text{O}$ as a proxy for sea surface temperature: Influence of variable coral growth rates on the coral *Porites lutea* from Hainan Island, China. *Geochemistry, Geophysics, Geosystems*, 6(9).
- Sijinkumar AV, Clemens S, Nath BN, Prell W, Benshila R, Lengaigne M. (2016). $\delta^{18}\text{O}$ and salinity variability from the Last Glacial Maximum to Recent in the Bay of Bengal and Andaman Sea. *Quaternary Science Reviews*. 135:79-91.
- Slutz, R.J., Lubker, S.J., Hiscox, J.D., Woodruff, S.D., Jenne, R.L., Joseph, D.H., Steurer, P.M. and Elms, J.D., (1985). Comprehensive ocean-atmosphere data set: Release 1. Boulder, Colo.[NOAA and NCDC].
- Smith S V., Buddemeier RW, Redalje RC, Houck JE (1979) Strontium-calcium thermometry in coral skeletons. *Science* (80-) 204:404–407. <https://doi.org/10.1126/science.204.4391.404>
- Southon J, Kashgarian M, Fontugne M, Metivier B, Yim WW. (2002). Marine reservoir corrections for the Indian Ocean and Southeast Asia. *Radiocarbon*. 44(1):167-80.
- Sreekesh S, (2016). Rainfall variation in Lakshadweep Islands. *Indian Journal of Geo Marine Sciences*, 45 (11): 1603-1609.
- Stuiver, M., (1980). ^{14}C distribution in the Atlantic Ocean. *Journal of Geophysical Research: Oceans*, 85(C5), pp.2711-2718.
- Stuiver, M., (1983). International agreements and the use of the new oxalic acid standard. *Radiocarbon*, 25(2), pp.793-795.
- Stuiver M, Braziunas TF, (1993). Modeling atmospheric ^{14}C influences and ^{14}C ages of marine samples to 10 000 BC

- Stuiver, M. and Östlund, H.G., (1983). GEOSECS Indian Ocean and Mediterranean radiocarbon. *Radiocarbon*, 25(1), pp.1-29.
- Stuiver M, Polach HA, (1977). Reporting of ^{14}C data. *Radiocarbon* 19:355–363. <https://doi.org/10.1016/j.forsciint.2010.11.013>
- Sun, D., Su, R., McConnaughey, T.A. and Bloemendal, J., (2008). Variability of skeletal growth and $\delta^{13}\text{C}$ in massive corals from the South China Sea: Effects of photosynthesis, respiration and human activities. *Chemical Geology*, 255(3-4), pp.414-425.
- Suresh, V. R., & Mathew, K. J. (1993). Skeletal extension of staghorn coral *Acropora formosa* in relation to environment at Kavaratti atoll (Lakshadweep). *Indian J. Mar. Sci.*, 22(3), 176-179.
- Suzuki, A., Hibino, K., Iwase, A. and Kawahata, H., (2005). Intercolony variability of skeletal oxygen and carbon isotope signatures of cultured *Porites* corals: Temperature-controlled experiments. *Geochimica et Cosmochimica Acta*, 69(18), pp.4453-4462.
- Suzuki, A., Yukino, I. and Kawahata, H., (1999). Temperature-skeletal $\delta^{18}\text{O}$ relationship of *Porites australiensis* from Ishigaki Island, the Ryukyus, Japan. *Geochemical Journal*, 33(6), pp.419-428.
- Swapna, P., Krishnan, R. and Wallace, J.M., (2014). Indian Ocean and monsoon coupled interactions in a warming environment. *Climate dynamics*, 42(9-10), pp.2439-2454.
- Swart PK, (1983). Carbon and oxygen isotope fractionation in scleractinian corals: a review. *Earth-science Rev* 19:51–80
- Synal H., (2009). New and Improved AMS Facilities, Physics (College. Park. Md).
- Takahashi, T., S. C. Sutherland, D. W. Chipman, J. G. Goddard, T. Newberger and C. Sweeney. (2014). Climatological Distributions of pH, pCO₂, Total CO₂, Alkalinity, and CaCO₃ Saturation in the Global Surface Ocean. ORNL/CDIAC-160, NDP-094. Carbon Dioxide Information Analysis Center, Oak Ridge National Laboratory, U.S. Department of Energy, Oak Ridge, Tennessee. doi: 10.3334/CDIAC/OTG.NDP094
- Takahashi, T., Sutherland, S. C., Wanninkhof, R., Sweeney, C., Feely, R. A., Chipman, D. W., Hales, B., Friederich, G., Chavez, F., et al., (2009). Climatological mean and decadal changes in surface ocean pCO₂, and net sea-air CO₂ flux over the global oceans. *Deep-Sea Res. II*, 554-577. doi: 10.1016/j.dsr2.2008.12.009.
- Tanzil, J.T.I., Brown, B.E., Tudhope, A.W. and Dunne, R.P., 2009. Decline in skeletal growth of the coral *Porites lutea* from the Andaman Sea, South Thailand between 1984 and 2005. *Coral reefs*, 28(2), pp.519-528.
- Thadathil, P., Muraleedharan, P.M., Rao, R.R., Somayajulu, Y.K., Reddy, G.V. and Revichandran, C., (2007). Observed seasonal variability of barrier layer in the Bay of Bengal. *Journal of Geophysical Research: Oceans*, 112(C2).
- Tudhope, A.W., Chilcott, C.P., McCulloch, M.T., Cook, E.R., Chappell, J., Ellam, R.M., Lea, D.W., Lough, J.M. and Shimmield, G.B., (2001). Variability in the El Niño-Southern Oscillation through a glacial-interglacial cycle. *Science*, 291(5508), pp.1511-1517.
- Tudhope, A.W., Lea, D.W., Shimmield, G.B., Chilcott, C.P. and Head, S., (1996). Monsoon climate and Arabian Sea coastal upwelling recorded in massive corals from southern Oman. *Palaios*, 11(4), pp.347-361.

- Urey, H.C., (1947). The thermodynamic properties of isotopic substances. *Journal of the Chemical Society (Resumed)*, pp.562-581.
- Varkey M J, Das V K and Ramaraju D V (1979). Physical characteristics of the Laccadive Sea (Lakshadweep). *Indian Journal of Marine Sciences*, 8 203–210
- Wacker, L., Fülöp, R.H., Hajdas, I., Molnár, M. and Rethemeyer, J., (2013). A novel approach to process carbonate samples for radiocarbon measurements with helium carrier gas. *Nuclear Instruments and Methods in Physics Research Section B: Beam Interactions with Materials and Atoms*, 294, pp.214-217.
- Wacker, L., Němec, M. and Bourquin, J., (2010). A revolutionary graphitisation system: fully automated, compact and simple. *Nuclear Instruments and Methods in Physics Research Section B: Beam Interactions with Materials and Atoms*, 268(7-8), pp.931-934.
- Wanninkhof, R., (2014). Relationship between wind speed and gas exchange over the ocean revisited. *Limnology and Oceanography: Methods*, 12(6), pp.351-362.
- Wanninkhof, R. and Knox, M., (1996). Chemical enhancement of CO₂ exchange in natural waters. *Limnology and Oceanography*, 41(4), pp.689-697.
- Wanninkhof, R. and McGillis, W.R., (1999). A cubic relationship between air-sea CO₂ exchange and wind speed. *Geophysical Research Letters*, 26(13), pp.1889-1892.
- Watanabe, T.K., Watanabe, T., Yamazaki, A., Pfeiffer, M., Garbe-Schönberg, D. and Claereboudt, M.R., (2017). Past summer upwelling events in the Gulf of Oman derived from a coral geochemical record. *Scientific reports*, 7(1), pp.1-7.
- Watanabe, T., Winter, A. and Oba, T., (2001). Seasonal changes in sea surface temperature and salinity during the Little Ice Age in the Caribbean Sea deduced from Mg/Ca and ¹⁸O/¹⁶O ratios in corals. *Marine Geology*, 173(1-4), pp.21-35.
- Weber, J.N., (1973). Incorporation of strontium into reef coral skeletal carbonate. *Geochimica et Cosmochimica Acta*, 37(9), pp.2173-2190.
- Weber JN, Woodhead PMJ, (1972). Temperature dependence of oxygen-18 concentration in reef coral carbonates. *J Geophys Res* 77:463–473. <https://doi.org/10.1029/JC077i003p00463>
- Wei G, McCulloch MT, Mortimer G, et al., (2009). Evidence for ocean acidification in the Great Barrier Reef of Australia. *Geochim Cosmochim Acta* 73:2332–2346. <https://doi.org/10.1016/j.gca.2009.02.009>
- Wei, G., Sun, M., Li, X. and Nie, B., (2000). Mg/Ca, Sr/Ca and U/Ca ratios of a *Porites* coral from Sanya Bay, Hainan Island, South China Sea and their relationships to sea surface temperature. *Palaeogeography, Palaeoclimatology, Palaeoecology*, 162(1-2), pp.59-74.
- Wellington, G.M., Dunbar, R.B. and Merlen, G., (1996). Calibration of stable oxygen isotope signatures in Galapagos corals. *Paleoceanography*, 11(4), pp.467-480.
- Wu HC, Dissard D, Douville E, et al., (2018). Surface ocean pH variations since 1689 CE and recent ocean acidification in the tropical South Pacific. *Nat Commun* 9:. <https://doi.org/10.1038/s41467-018-04922-1>
- Zinke, J., Dullo, W.C., Heiss, G.A. and Eisenhauer, A., (2004). ENSO and Indian Ocean subtropical dipole variability is recorded in a coral record off southwest Madagascar for

the period 1659 to 1995. *Earth and Planetary Science Letters*, 228(1-2), pp.177-194.

Zweng, M. M., J. R. Reagan, D. Seidov, T. P. Boyer, R. A. Locarnini, H. E. Garcia, A. V. Mishonov, O. K. Baranova, K. Weathers, C. R. Paver, and I. Smolyar, (2018). *World Ocean Atlas 2018, Volume 2: Salinity*. A. Mishonov Technical Ed.; NOAA Atlas NESDIS 82, 50 pp.

List of Publications

Thesis related publications:

1. **Raj, H.**, Bhushan, R., Muruganantham, M., Nambiar, R., Dabhi, A.J.,
Marine Reservoir Age Correction for the Andaman Basin
Radiocarbon (2020) (Accepted)
2. Bhushan, R., Yadava, M.G., Shah, M.S. and **Raj, H.**,
Performance of a new IMV AMS facility (AURiS) at PRL, Ahmedabad, India
Nuclear Instruments and Methods in Physics Research Section B: Beam Interactions
with Materials and Atoms, 439, pp.76-79. (2019)
3. Bhushan, R., Yadava, M.G., Shah, M.S., Banerji, U.S., **Raj, H.**, Shah, C. and Dabhi,
A.J.,
First results from the PRL accelerator mass spectrometer
Current Science, 116(3), pp.361-363. (2019)
4. **Raj, H.**, and Bhushan, R.,
*Air-sea CO₂ exchange rate over the northern Indian Ocean based on coral
radiocarbon records*
(under review) (2020)
5. **Raj, H.**, Bhushan, R., R., Kumar, S., Banerji, U., Shah, C., Verma, S.,
Monsoon signature in Porites from the northern Indian Ocean
(under review) (2020)
6. **Raj, H.**, Bhushan, Sudheer, A.K.,
*Paired Sr/Ca and stable isotopic measurements in Landfall coral from the northern
Indian Ocean and its significance*
(under preparation)

Other publications:

1. Sengupta, T., Deshpande Mukherjee, A., Bhushan, R., Ram, F., Bera, M.K., **Raj, H.**,
Dabhi, A.J., Bisht, R.S., Rawat, Y.S., Bhattacharya, S.K. and Juyal, N.,
*Did the Harappan settlement of Dholavira (India) collapse during the onset of
Meghalayan stage drought?*
Journal of Quaternary Science, 35(3), pp.382-395. (2020)